The effects of Tumour necrosis factor-alpha and Interleukin-1-beta on intracellular calcium handling and contractility in sheep ventricular myocytes

Natasha Elise Hadgraft

School of Environment and Life Sciences

University of Salford

Supervisor: Dr David Greensmith

Submitted in partial fulfilment of the requirements of the Degree of Doctor of Philosophy

April 2019

List of contents

List of figures

List of tables

ACKNOWLEDGEMENTS

I am grateful for all the guidance, training and support offered by my supervisor, Dr David Greensmith

Many thanks to the Trafford / Dibb laboratories of the University of Manchester, for provision of sheep ventricular myocytes and use of the experimental models

I would like to thank my parents, Liesl and Andrew Hadgraft, and my Grandma Fletcher for on-going love and support

Last but by no means least, I would also like to thank Robert Forshaw, who has always believed in me

University of Salford MANCHESTER

Research, Innovation and A
Engagement Ethical Approv

Research Centres Support T
G0.3 Joule House
University of Salford
M5 4WT

T +44(0)161 295 5278

www.salford.ac.uk/

19 August 2016

Dear Natasha,

RE: ETHICS APPLICATION ST16/115 – A clinically relevant investigation to determine a cellular basis for cardiac dysfunction in sepsis

Based on the information you provided, I am pleased to inform you that your application ST 16/115 has been approved.

If there are any changes to the project and/ or its methodology, please inform the Panel as soon as possible by contacting S&T-ResearchEthics@salford.ac.uk

Yours sincerely,

Prof Mohammed Arif
Chair of the Science & Technology Research Ethics Panel
Professor of Sustainability and Process Management,
School of Built Environment
University of Salford
Maxwell Building, The Crescent
Greater Manchester, UK M5 4WT
Phone: + 44 161 295 6829
Email: m.arif@salford.ac.uk

Abbreviations

ADP	adenosine diphosphate
AKI	acute kidney injury
ANOVA	analysis of variance
ATP	adenosine triphosphate
AV	atrioventricular
BDM	2,3-butanedione monoxime
BP	band-pass
BSA	bovine serum albumin
CaM	calmodulin
CaMKII	calcium/calmodulin-dependent protein kinase II
cAMP	cyclic adenosine monophosphate
CCD	charge-coupled device
$[Ca^{2+}]_i$	intracellular calcium
CICR	calcium-induced calcium release
CLP	cecal ligation and puncture
CRT	cardiac resynchronization therapy
DAMPs	danger-associated molecular patterns
DIC	disseminated intravascular coagulation
DHPR	dihydropyridine receptor
ECC	excitation-contraction coupling
ECM	extracellular matrix
EF	ejection fraction
HCN	hyperpolarization-activated cyclic nucleotide–gated
HF	heart failure

HIV	human immunodeficiency virus
I_{CaL}	L-type Ca^{2+} current
IFN	interferon
IL	interleukin
IL-1β	interleukin-1-beta
LED	light emitting diode
LP	long-pass
LTCC	L-type Ca^{2+} channel
LV	left ventricular
MI	myocardial infarction
NAC	N-acetyl-L-cysteine
NCX	sodium-calcium exchanger
NHS	National Health Service
NOS	nitric oxide synthase
Nox	NADPH oxidase
NS	not significant
NT	normal Tyrodes
PAMPs	pathogen associated molecular patterns
PBS	phosphate buffered saline
PKA	protein kinase A
PKC	protein kinase C
PLN	phospholamban
PMCA	plasma membrane Ca^{2+} ATPase
PMT	photo multiplier tube
P_o	open probability
RC	rate constant
ROS	reactive oxygen species

RyR	ryanodine receptor
SAD	sepsis-associated delirium
SAE	sepsis-associated encephalopathy
SAN	sinoatrial node
SERCA	sarcoplasmic/endoplasmic reticulum calcium ATPase
SR	sarcoplasmic reticulum
SS	steady state
TGF	transforming growth factor
Tn	troponin
TNF-α	tumour necrosis factor-alpha
Tm	tropomyosin
TnC	troponin C
TnI	troponin I
TnT	troponin T
t-tubules	transverse tubules

Abstract

Proinflammatory cytokines such as TNF-α and IL-1β are implicated in the pathogenesis of inflammatory disease states such as sepsis. In sepsis, myocardial depression is a leading cause of death. To design novel therapeutic targets, it is essential that we understand how these cytokines mediate the cellular basis of this cardiac dysfunction. Previous studies, including Greensmith and Nirmalan (2013), demonstrate that perturbed intracellular calcium handling and contractility can account for many aspects of myocardial depression. However, many of these studies suffer important limitations in that (A) small mammal models were used in which the translational relevance is questionable and (B) it remains unclear how proinflammatory cytokines affect certain key aspects of cellular function. To address this, we re-characterised the effects of TNF-α and IL-1β on intracellular calcium handling using a large animal model then investigated their effects on the ryanodine receptor (RyR) and myofilament sensitivity to calcium.

Sheep ventricular myocytes were used for all experiments. All procedures used accord with the Animals (Scientific Procedures) Act, UK, 1986 and Directive 2010/63/EU of the European Parliament. Intracellular calcium and contractility dynamics were measured by epi-fluorescent photometry and video sarcomere detection respectively. In all experiments, cells were separately exposed to 50 ng/ml TNF-α and IL-1β acutely. When required, cells were excited using field stimulation at a rate of 0.5 Hz. To indicate changes to RyR properties, intracellular Ca^{2+} waves were facilitated using 0.3 mM Ouabain and 5 mM Ca^{2+}. SR Ca^{2+} content was estimated using the amplitude of 10 mM caffeine-evoked Ca^{2+} transients.

TNF-α and IL-1β decreased SR Ca^{2+} content by 27 and 41 % respectively accounting for a 17 and 24 % decrease of systolic calcium. Only with TNF-α did this reduction in systolic Ca^{2+} translate to reduced systolic shortening (20 %). We observed no negative effect on the rate of systolic or caffeine-evoked Ca^{2+} decay. TNF-α and IL-1β decreased Ca^{2+} wave amplitude by 46 and 34 % and increased frequency by 38 and 28 %. Both cytokines reduced SR Ca^{2+} threshold for waves. In saponin-permeabilised cells the degree of sarcomere shortening over equivalent calcium ranges was attenuated.

These findings confirm that in sheep, TNF-α and IL-1β decrease SR Ca^{2+} content leading to reduced systolic Ca^{2+}. The increase of Ca^{2+} wave frequency and decrease of amplitude suggests both cytokines increase ryanodine receptor open probability; confirmed by a decreased SR Ca^{2+} threshold for waves. So while the reduction of SR Ca^{2+} content does not appear to be SERCA-dependent increased RyR leak may contribute. The loss of contractile response to increased Ca^{2+} suggests that both cytokines reduce myofilament Ca^{2+} sensitivity. These findings advance our understanding of cytokine-mediated cardiac intracellular Ca^{2+} dysregulation and provide additional cellular substrates for myocardial depression in sepsis.

Chapter 1

General introduction

1.1 Sepsis

Sepsis is the inflammatory response to systemic infection. In a localised infection, leukocytes congregate at the site of infection and the production of cytokines at this site increases. This local inflammatory response is necessary to mediate the immune response against the infection. In sepsis, the increased cytokine production is elevated further, generating a *cytokine storm*, which is widespread across the body. Instead of aiding the immune response, inflammation becomes an additional burden and can induce multiple organ dysfunction, including heart failure. In severe cases, sepsis can lead to death. Even in those who survive sepsis, some forms of organ dysfunction can be permanent (A. Kumar et al., 1996).

1.1.1 The burden of sepsis

Fleischmann et al. (2016) used reports of hospital-treated sepsis acquired between 2005 and 2015 to predict the global impact of sepsis and estimated that there are 31.5 million incidences of sepsis each year. 19.4 million of these cases were deemed severe and 5.3 million led to death. However, the study acknowledged that these figures may under-represent the true global impact of sepsis due to various limitations. One limitation is lack of publications – and therefore data acquired – from lower income countries, as high-income countries only amount to 13 % of the global population. Another limitation is international classification of diseases (ICD) miscoding and differences defining of sepsis by in-hospital administrative reports, as it is believed some cases of sepsis have been overlooked or misdiagnosed. What is clear, is sepsis remains a leading cause of morbidity and mortality worldwide.

In the UK alone, current estimations indicate that approximately 260,000 cases of sepsis occur annually, resulting in 44,000 fatalities (Daniels et al., 2017). Based on these incidence figures, it was estimated that the total cost of sepsis in the United Kingdom (UK) on the National Health Service (NHS) is £11.25 billion each year. This figure includes direct costs such as hospital costs and long-term complications in survivors. Amputation, kidney

dysfunction and the impact on mental health, were estimated at approximately £1.5 billion, in addition to financial losses due to legal action and loss of productivity. Whilst the resistance or sensitivity to antibiotics does not impact the proportion of patients affected by sepsis, the burden and cost of hospitalization is greater with antibiotic resistant strains due to the additional treatment required and longer hospital stays (Zilberberg, Nathanson, Sulham, Fan, & Shorr, 2017).

1.1.2 Epidemiology of sepsis

The prevalence of sepsis within a population can be determined by the region, due to the level of exposure to pathogens. In developing countries or warmer climates where exposure to a wider variety of pathogens is possible, this increases the susceptibility to infection and sepsis in those who live there (Teparrukkul, Hantrakun, Day, West, & Limmathurotsakul, 2017; Vugia et al., 1993).

A number of host factors can impact susceptibility to development of sepsis as well as severity and mortality. Age is an important factor determining vulnerability to sepsis. Increased age in adults with sepsis is associated with increased mortality, earlier fatalities and an increased need for continued care in survivors (Martin, Mannino, & Moss, 2006). The risk of sepsis development is 13.1 fold greater in individuals over the age of 65, with a 1.54 fold increase in the likelihood of death (Liang, 2016). Martin et al. (2006) reported that over 2 decades in the United States (US), 64.9 % of hospitalised patients with sepsis were over the age of 65. The occurrence of conditions associated with sepsis development such as urinary tract infections (UTI) and pneumonia are also higher in the elderly (Liang, 2016). At any age, individuals – predominantly males – with a history of gout, frequent UTIs or renal dysfunction are also more likely to develop severe sepsis or septic shock (Lee et al., 2016).

Bacteria (see 1.1.3) already present in the genital tract in health can become pathogenic in sepsis in immunocompromised individuals or pregnant women (Kalin, Acosta, Kurinczuk, Brocklehurst, & Knight, 2015). Sepsis can encourage complications in pregnancy such as preterm birth and severe pre-eclampsia and contributes to maternal morbidity and mortality

globally. In high income countries, sepsis as a result of genital tract infection leads to 2.1 % of maternal deaths (Acosta, Bhattacharya, Tuffnell, Kurinczuk, & Knight, 2012; van Dillen, Zwart, Schutte, & van Roosmalen, 2010). Severe sepsis is the cause of ~14.4 % of maternal critical care admissions in the UK with ~10.6 % developing septic shock. The young age of the mother (under 25 years old) is a risk factor for ante- or post-natal sepsis development. Additional risk factors include obesity, delivery by caesarean section and multiple births (Acosta et al., 2012; Acosta et al., 2016).

New-borns have a high risk of infection and sepsis. This risk of late-onset sepsis development is elevated further in premature infants with a gestational age below 32 weeks and lower birth weights, especially those who require a central venous catheter (Mohseny et al., 2018; Stoll et al., 2002).

Individuals with a compromised immune system or prior health conditions are vulnerable to infection and thus sepsis. The immune system can also be suppressed by a secondary infection, as is the case in human immunodeficiency virus (HIV) positive individuals. HIV-positive individuals have an increased risk of developing sepsis, especially fungal sepsis, when compared to those who are HIV seronegative. Co-infection with HIV also increases the likelihood of a fatal outcome in those with sepsis (Vugia et al., 1993).

Surgery to treat existing conditions can increase patient vulnerability to infection. Following colorectal surgery, patients have a high predisposition for sepsis and septic shock. In this patient group, severity is higher in females and adults over the age of 65 (Sheka, Tevis, & Kennedy, 2016).

Due to the high severity and mortality of sepsis in the UK and worldwide, and the impact on vulnerable groups, it is important to increase understanding of the events that occur in sepsis, as this may further establish a clinical definition of sepsis and aid treatment, through providing novel targets for therapeutics to be used alongside those fighting the causative infection.

1.1.3 Aetiology of sepsis

It is important to note that sepsis is the *response* to infection. As such, there is no definitive causative organism and so any bacterial, fungal or viral infection can lead to sepsis. If pathogen invasion ceases to be localised and becomes systemic, so does the immune response. It is this wide-scale and overwhelming immune response that results in multi-organ failure, which shall be discussed further in section 1.1.5.

Although it is true that sepsis can develop from any pathogenic infection, sepsis is commonly associated with an acute respiratory bacterial infection, especially pneumonia-causing bacteria such as *Streptococcus pneumoniae* and *Klebsiella pneumoniae* (Opal et al., 2003). In the elderly, pneumonia-associated gram-negative bacterial sepsis is particularly prominent (Martin et al., 2006). In developing countries, sepsis caused by rarer bacterial pathogens such as *rickettsia* and *leptospira* are also found (Vugia et al., 1993).

Urinary tract infections are another common cause of sepsis. When caused by bacteria belonging to the enterobacteriaceae family – including *Escherichia coli, Klebsiella pneumonia, Klebsiella oxytoca, Enterobacter cloacae* and *Enterobacter aerogenes* – the risk of severe sepsis or septic shock development is greater. Some enterobacteriaceae can also cause pneumonia (Lee et al., 2016; Opal et al., 2003; Zilberberg et al., 2017). Post-operative UTI, resulting from early removal of the catheter following colorectal surgery, also contributes to elevated risk of bacteraemia and septic shock (Sheka et al., 2016).

In pregnant women, respiratory infections and genital tract infections are the most common causes of sepsis. There are many causes of maternal sepsis however *Streptococcus pyogenes* and *Streptococcus agalactiae* are commonly involved in progression to severe sepsis. Maternal deaths however are most commonly associated with pneumonia respiratory infections (Acosta et al., 2016; Kalin et al., 2015; van Dillen et al., 2010).

Gram-positive infections are more common in premature new-borns, particularly *Streptococcus* infection, and increases mortality of sepsis more than 2 fold (Stoll et al., 2002). In the UK, *Streptococcus agalactiae* is the highest cause of neonatal sepsis, however *Candida*

albicans infection, a yeast infection, is another major cause, especially in the form of at UTI (Kalin et al., 2015; Mohseny et al., 2018).

The type of the microorganism causing sepsis can determine patient mortality. Recorded incidence is highest for gram positive and negative bacterial sepsis (at 25.2 and 23.8 % respectively), both with a mortality of approximately 30 %, while fungal infections causing sepsis are less prevalent but have a higher mortality. Infections with *Candida* species are the predominant cause of fungal sepsis and contribute to increased mortality. *Candida* infection is opportunistic as *Candida* species are present in normal flora. The majority of the remaining invasive fungal infections are caused by *Aspergillus* species, which can also lead to sepsis, especially in immunocompromised individuals (Delaloye & Calandra, 2014).

Sepsis can also be produced by a viral infection; however, data suggests the incidence of viral infection may be lower than other causes. In addition to the systemic dysregulation which occurs in sepsis, viruses can also directly cause tissue damage. Common viral causes of sepsis include influenza viruses, enteroviruses and Herpes simplex virus (HSV). Once again, immunosuppressed individuals such as those with pre-existing conditions, neonates, the young, the elderly and pregnant women, are more susceptible to viral sepsis. Viral sepsis is also more common in South Asia, and Dengue viruses are a primary cause of viral sepsis in these tropical regions (Lin, McGinley, Drysdale, & Pollard, 2018; Shane, Sanchez, & Stoll, 2017; Teparrukkul et al., 2017; "Vaccines against influenza WHO position paper - November 2012," 2012).

As such, determining the primary cause of sepsis is as important as is its treatment. In the UK an intervention described by Daniels, Nutbeam, McNamara, and Galvin (2011) has been implemented. This requires blood cultures to be acquired and antibiotic treatment given within an hour of diagnosis to improve patient prognosis.

1.1.4 Classification of sepsis

The definition and classification of sepsis is important as this can lead to variation in reports which determine incidence and mortality. Whilst sepsis has long been known to exist, the definition and criteria for diagnosis varied considerably until the first internationally recognised definition of sepsis was provided by Bone et al. (1992). Bone et al. (1992) described sepsis as the development of systemic inflammatory response syndrome (SIRS) in response to infection. At this time the clinical diagnosis of sepsis solely required patients to meet 2 of the 4 SIRS criteria; abnormal body temperature, tachycardia (>90/min), elevated white blood cell count (>12 000/mm^3) and respiratory rate (>20/min). SIRS criteria remain important for diagnosis of sepsis however Levy et al. (2003) addressed that both tachycardia and elevated white blood cell count were also present in the absence of infection and therefore do not distinguish sepsis from other inflammatory conditions. More recently, Singer et al. (2016) highlighted improved understanding of the pathophysiology of sepsis and the preference of previous definitions to focus entirely on inflammation. Sepsis is now accepted to involve both proinflammatory and anti-inflammatory responses.

The term “severe sepsis” was coined to define sepsis with organ dysfunction. Sepsis manifests differently between patients, as such the site and magnitude of dysfunction can vary. Severe sepsis can further progress into “septic shock”, in which hypotension is induced and persists despite fluid resuscitation (Bone et al., 1992). Septic shock presents in two stages; the first stage is determined by high pulse rate, cardiac output and warm extremities. In some individuals this can progress to a hypovolemic stage, which presents as low cardiac output and cold, moist skin. Both stages result in high lactate and metabolic acidosis, further contributing to cardiac dysfunction. Patients with a high cardiac performance (cardiac index > 2.8 L/min/m^2) have a higher chance of survival, as progression to hypovolemia has been associated with increased mortality (Clowes, Vucinic, & Weidner, 1966; MacLean, Mulligan, McLean, & Duff, 1967).

Current management of sepsis in the UK implements the Sepsis 6 intervention developed by Daniels et al. (2011). Since implementation, mortality has decreased by two-fold and the average length of hospitalisation (for survivors) has reduced considerably. This intervention

prioritises medical procedures which can be used to assess the stage of sepsis and treat symptoms. These therapeutic interventions include measurement of serum lactate, as this is known to be high in septic shock it can determine sepsis severity. Oxygen is administered to allow for elevated respiratory rate and prevent metabolic acidosis. In order to manage blood pressure, urine output is monitored whilst an intravenous drip allows fluid resuscitation (Bone et al., 1992; Daniels et al., 2011; MacLean et al., 1967; Sheka et al., 2016).

1.1.5 General organ dysfunction in sepsis

As per 1.1.3, respiratory infection is a leading cause of sepsis. As such many patients with sepsis often present with acute respiratory distress syndrome (ARDS). ARDS can also be induced by non-septic lung injury such as trauma, however the risk of ARDS development and mortality are increased in sepsis-associated ARDS. The characteristics of ARDS are similar in septic and non-septic patients (Sheu et al., 2010), rapidly presenting with pulmonary oedema and severe hypoxaemia (PaO_2/F_IO_2 ratio <200). Diagnosis of ARDS involves measurement of pulmonary arterial wedge pressure (<18 mm Hg), which can be influenced in sepsis by pulmonary infiltrates and left ventricular failure, which are associated with increased left atrial pressure (Enriquez-Sarano, Rossi, Seward, Bailey, & Tajik, 1997; Wheeler & Bernard, 2007).

Acute kidney injury (AKI), a form of renal dysfunction, while not specific to sepsis, is another common manifestation. During sepsis, renal volume increases, largely attributed to oedema, by which capillary leakage and immune cell infiltration are thought to contribute (Sasaguri, Yamaguchi, Nakazono, Mizuguchi, & Irie, 2016). A reduction in blood pressure is found in approximately 80 % of sepsis-associated AKI cases, a possible result of decreased cardiac output from myocardial depression. Loss of contractility in the left ventricle results in an elevated end-diastolic ventricular volume thus cardiac preload, which can stimulate sympathetic nerve activity and release of vasoconstrictive hormones. The resulting vasoconstriction and decreased blood pressure may further contribute to AKI development, through ischemic damage and renal hypo-perfusion, leading to reduction in glomerular filtration rate and renal blood flow (Bougle & Duranteau, 2011; Wang et al., 2002).

Neurological dysfunction such as sepsis-associated encephalopathy (SAE) and sepsis-associated delirium (SAD), conditions responsible for confusion, cognitive impairment and seizures, present in a large proportion of severe sepsis patients and correspond with an increased mortality. While inflammation is thought to contribute to SAE, dysfunction can be induced by decreased blood pressure and the resulting lower cerebral perfusion. Cerebral vasoconstriction has been associated with SAE, and its presence increase the risk of SAD. The cardiovascular autoregulation required to respond to changes in blood pressure are often impaired in SAD, promoting further injury (Pierrakos et al., 2014; Schramm et al., 2012). The long-term psychological impact of sepsis on its survivors are also evident, with development of anxiety, depression and post-traumatic stress disorder-like symptoms including delusions (Jones & Griffiths, 2013).

In addition to vasoconstriction, decreased perfusion and tissue injury can also be influenced by enhanced coagulation. In response to endotoxin release in sepsis, coagulative pathways are promoted while anticoagulation is simultaneously downregulated, inducing disseminated intravascular coagulation (DIC). DIC describes thrombosis formation in small vessels across the body. This reduces blood perfusion to tissues, leading to injury and organ failure. Activation of complement-derived C5a also contributes to clot formation, by inducing aggregation of neutrophils and other leukocytes. Attempts to treat DIC with anti-coagulators to lyse clots have been dangerous, encouraging bleeding and in some cases further promoting coagulation through platelet agglutination (Hardaway, Williams, & Vasquez, 2001; Parrillo, 1989; Tsao, Ho, & Wu, 2015).

While sepsis can lead to multiple organ dysfunction as detailed above, many sepsis related deaths are due to cardiac complications.

1.1.6 Myocardial depression in sepsis

A common manifestation of cardiac dysfunction in sepsis is myocardial depression. Myocardial depression involves both diastolic and systolic dysfunction.

1.1.6.1 Diastolic dysfunction

Diastolic dysfunction in myocardial depression includes ventricular dilation and reduced compliance. This reduction in compliance means that the myocardium is less able to distend during diastole in response to increased blood flow. Systolic dysfunction takes the form of depressed contractility resulting in a reduced ejection fraction (Ognibene, Parker, Natanson, Shelhamer, & Parrillo, 1988).

Diastolic dysfunction in severe sepsis is associated with increased mortality (Clancy et al., 2017). Impaired ventricular filling is the result of diastolic dysfunction in the left ventricle. In sepsis this left ventricular dysfunction is associated with both impaired relaxation and decreased compliance (Meierhenrich, Schutz, & Gauss, 2008). Left ventricular relaxation is impaired in ~ 20 % of patients with septic shock, although this is reversible upon recovery (Bouhemad et al., 2008). Reduced diastolic compliance in sepsis can be improved by fluid resuscitation – a common practice following the diagnosis of sepsis – however this has no effect on Ca^{2+} handling mechanisms or contractility (Daniels et al., 2011; Zhong, Adams, & Rubin, 1997).

Sepsis alters the relationship between compliance and contractility, causing a downward shift in the Frank-Starling curve. Therefore any small elevation in end diastolic volume is unable to induce an increase in left ventricular performance to the same extent (Ognibene et al., 1988). Whilst end-diastolic volume increases in sepsis – possibly as a compensatory mechanism to maintain cardiac output – this is also an indicator of worsening myocardial relaxation and poor prognosis (Clancy et al., 2017).

In sepsis cardiac dysfunction can also occur in the right ventricle. As with the left ventricle, diastolic right ventricular dysfunction can take form of ventricular dilation and loss of ventricular compliance. The latter impairs the relationship between right atrial pressure and right ventricular end diastolic volume (Court, Kumar, Parrillo, & Kumar, 2002; Kimchi et al., 1984). In sepsis the right ventricular end-diastolic volume can become increased due to elevated pulmonary vascular resistance, as a result of acute lung injury. This pulmonary

vascular resistance to low cardiac output stage of septic shock and is associated with high mortality (Kimchi et al., 1984; Sibbald et al., 1978).

1.1.6.2 Systolic dysfunction

Systolic dysfunction in myocardial depression is clinically defined by the reduced left ventricular ejection fraction (LVEF). This LVEF occurs due to depressed contractility and results in a lower cardiac output and a reduction in left ventricular stroke volume. In the acute phase of sepsis LVEF is reduced to 25 %, during recovery this is restored to 50 %. With reduced LVEF the end-diastolic volume increases. In survivors of sepsis, cardiac function is fully recovered following 10 – 28 days (Ognibene et al., 1988; Parker et al., 1984; Parrillo, 1989).

Septic shock can further impair systolic function through impacting the hearts response to β-adrenergic stimulation. Archer and Black (1975) found that the effect of adrenaline application on contraction and relaxation was depressed in an endotoxin-administered model of septic shock in the heart.

Systolic dysfunction such as decreased right ventricular ejection fraction (RVEF) are found in some patients with sepsis, either alone or as a part of biventricular dysfunction. RVEF can occur during both the high and low cardiac output stages of septic shock. This right ventricular dysfunction can occur due to either direct right ventricular myocardial depression or high end right ventricular diastolic volume (Court et al., 2002; Kimchi et al., 1984).

The type of cardiac dysfunction can predict patient outcome, myocardial depression is associated with increased mortality. Some manifestations, such as left ventricular dilation and decreased ejection fraction, are more prominent in patients who go on to survive sepsis. It has been suggested that ventricular dilation helps to partially compensate for reduced ejection fraction. Survival is also higher in those presenting with an increased end diastolic volume index, resulting in a more distended ventricle during diastole and reduced compliance, whereas in non-survivors, cardiac performance is more likely to be maintained

initially, despite cardiac dysfunction. While these aspects of myocardial depression appear to facilitate survival, the decreased cardiac performance and therefore reduced cardiac output, lead to hypotension and ischemia which can contribute to dysfunction throughout the body (Court et al., 2002; Parker et al., 1984; Parker et al., 1989; Parrillo et al., 1990).

Although sepsis can induce injury in multiple organs due to infection and inflammation, the depressive effect of sepsis on the myocardium is important, as not only is it a common injury, but this can facilitate progression of damage in other organs, contributing to hypoperfusion, vasoconstriction and the resulting ischemia. Hypotension is responsible for 76 % of deaths in sepsis, contributed to by both myocardial depression and low systemic vascular resistance, with remaining deaths as a result of multiple organ dysfunction (Parrillo, 1989). Myocardial depression in sepsis is not caused by ischemia, as Cunnion, Schaer, Parker, Natanson, and Parrillo (1986) found that coronary blood circulation and oxygen supply to the myocardium is maintained.

1.1.7 Cardiac dysfunction in other inflammatory conditions

In addition to sepsis, reversible myocardial depression can occur as a result of other inflammatory conditions, such as anaphylactic shock (Raper & Fisher, 1988), or in heart failure. Mediators of myocardial depression have been identified in the blood of heart failure patients with acute renal failure. Removal of these substances through haemodialysis has been cited as a means to improve cardiac function (Blake et al., 1996). In coronary artery disease, haemodialysis is also a common treatment. Frequent use of haemodialysis can however lead to ischemic cardiomyopathy. Myocardial depression appears sporadically with regular ischemic injury. As with sepsis, myocardial depression presents with reduced LVEF, and contributes to hypotension. While myocardial depression is still reversible in these cases, prolonged myocardial injury can lead to more permanent injury such as fibrosis (Alkar, Mattsson, & Magnusson, 2018; Burton, Jefferies, Selby, & McIntyre, 2009).

Cardiac dysfunction in heart failure (HF) also shares some similarities with myocardial depression in sepsis. Chronic HF is classified by LVEF, ejection fraction (EF) is either

preserved, reduced (<40 %) or within a mid-range (40-49 %) (Tschope et al., 2019). The levels of morbidity and mortality are similar between these HF classifications (Borlaug & Paulus, 2011). HF with preserved EF presents with diastolic dysfunction, while HF with reduced EF favours systolic dysfunction (van Heerebeek et al., 2006).

In HF with preserved EF systolic left ventricular performance is normal, however relaxation is slower and diastolic stiffness is elevated. Reduced rate of relaxation contributes to decreased stroke volume, especially at higher heart rates. Passive diastolic stiffness can be induced by collagen deposition in the extracellular matrix (ECM) or up-regulation of titin. Blood pressure and end diastolic volumes are also increased in HF with preserved EF (Borlaug & Paulus, 2011).

HF with a reduced EF occurs due to reduced ventricular contractility. This leads to a decrease in stroke volume and elevated end-diastolic volume. The loss of contractility found with this form of HF is caused by an initial injury, in 2/3 of cases this injury results from coronary artery disease. Myocardial injury induces secondary responses including increased cytokine production and release of ROS and NO. HF is generally left-sided, however right-sided HF can develop (Bloom et al., 2017).

Given that myocardial depression and similar cardiac dysfunction presents in a number of conditions, it is therefore important to improve understanding of the mediators of myocardial depression.

1.1.8 Mediators of myocardial depression in sepsis

Parrillo et al. (1985) investigated a negative inotropic agent responsible for myocardial depression. The circulating myocardial depressant substance identified was a low molecular mass (10-30 KDa) macromolecule with protein characteristics. It is now accepted that the elevated presence of cytokines – especially proinflammatory cytokines – in septic serum mediates myocardial depression (Jha et al., 1993; A. Kumar et al., 1996). Reactive oxygen

species (ROS) are also known to mediate myocardial depression and contribute to cardiovascular dysfunction in septic shock (Potz, Sellke, & Abid, 2016).

1.1.8.1 Reactive oxygen species and oxidative stress

Oxidative stress occurs when production of reactive oxygen species exceeds the capacity of antioxidant enzymes. There are many forms of ROS including superoxide ($O_2^{\bullet-}$), hydrogen peroxide (H_2O_2) and nitric oxide (NO). ROS production is increased in sepsis and high ROS levels are associated with cardiovascular dysfunction including myocardial depression. (Neri, Riezzo, Pomara, Schiavone, & Turillazzi, 2016; Potz et al., 2016). Oxidative stress is also known to play a role in HF, promoting the formation of bridges within the titin molecule, limiting elasticity in HF with preserved EF (Borlaug & Paulus, 2011).

In health, ROS including NO produced by Ca^{2+}-dependent NO synthase, aid regulation of blood pressure, however when ROS levels become high leading to oxidative stress, oxidative damage is induced (Neri et al., 2016; Schulz, Nava, & Moncada, 1992). High ROS can impair blood flow reducing oxygen delivery to organs, whilst also affecting metabolism. The resulting hypoxia and decreased energy production contributes to organ damage (Potz et al., 2016).

NO synthase is the enzyme responsible for NO production. NO acts as a messenger and effector molecule. In response to infection, NO levels increase, this is thought to be a defensive mechanism against pathogens due to the bactericidal properties of NO. As such, NO synthase activation increases in septic shock (Klabunde & Coston, 1995; Neri et al., 2016; Schulz et al., 1995).

Prolonged exposure to TNF-α and IL-1β activates Ca^{2+}-independent nitric oxide synthase expression in the left ventricular wall leading to an increase in NO production. Increased NO production has been implicated in the hypotension and impaired cardiac function found in septic shock (Neri et al., 2016; Schulz et al., 1992; Schulz et al., 1995). NO synthase is not solely responsible for myocardial depression, as Klabunde and Coston (1995) found that the

use of NO synthase inhibitors did not improve left ventricular function. Additionally, whilst NO synthase is induced at higher concentrations of TNF-α, myocardial depression can occur at the lower concentrations found in septic serum. TNF-α must therefore be able to induce myocardial depression without stimulation of NO synthase (Muller-Werdan, Engelmann, & Werdan, 1998). Yokoyama et al. (1993) reflected that the reduced myocyte contractility and systolic Ca^{2+} resulting from perfusion with TNF-α was primarily due to a direct effect on Ca^{2+} handling rather than an indirect effect on protein synthesis or NO production, although the effect of TNF-α on the Ca^{2+} cycle was not further investigated.

Although this study will not be directly measuring the effects of oxidative stress on ventricular myocytes, proinflammatory cytokines have been associated with increased NO and ROS production. It stands to reason that these molecules may be involved in the effects these cytokines mediate in the heart.

1.1.8.2 Cytokines

TNF-α and IL-1β are elevated in septic serum, and increase in concentration over time (Vincent et al., 1992). Other cytokines such as interferon gamma and interleukins (-2, -4, -6, -8, -10) are also elevated in septic serum. A. Kumar et al. (1996) found that these cytokines do not produce the same magnitude of myocardial depressant effect as TNF-α and IL-1β. TNF-α is also elevated in other inflammatory conditions (Muller-Werdan et al., 1998). Alone TNF can reduce stroke volume in humans with sepsis. This was demonstrated by improved left ventricular function in patients treated with anti-TNF antibodies, although treatment only improved survival if administered early (Vincent et al., 1992). This has also been demonstrated in animal models, with TNF-α reducing the ventricular ejection fraction in dogs (Muller-Werdan et al., 1998).

In studies investigating the effect of cytokines on isolated whole heart, simultaneous TNF-α and IL-1β exposure was found to temporarily increase cardiac work, output and peak systolic pressure, prior to a substantial reduction in coronary flow and cardiac work with prolonged exposure (Schulz et al., 1995).

Previous work in rat ventricular myocytes has also determined that TNF-α and IL-1β are capable of producing myocardial injury and impairing contraction (Greensmith & Nirmalan, 2013; Radin, Holycross, Dumitrescu, Kelley, & Altschuld, 2008). These proinflammatory cytokines have been shown to synergistically induce concentration and time dependant myocardial depression (A. Kumar et al., 1996).

Another component of septic serum is histamine; an endogenous mediator of inflammation elevated on a time dependent basis in sepsis. The outcome of histamine is dependent on the receptor activated. H_3 receptor activation depresses cardiac function via adrenergic response inhibition, while activation of H_1 and H_2 receptors contributes to multiple organ dysfunction and enhanced TNF-α and IL-1β production. Histamine can therefore act as a myocardial depressant substance while up-regulating further myocardial depressant substances in the form of cytokines (Hattori et al., 2016; X. Li et al., 1998).

It is well characterised that TNF-α and IL-1β are myocardial depressant substances (Odeh, 1993; Vincent et al., 1992). The mechanism by which cytokines – particularly TNF-α and IL-1β – induce myocardial depression is not yet fully understood. Previous work by Greensmith and Nirmalan (2013) did however find that TNF-α contributes to myocardial depression through altered Ca^{2+} handling. Cytokines and their cellular effects shall be discussed further, in more detail in section 1.3. In order to understand how cytokines alter ventricular myocyte function, cell function in health must first be understood.

1.2 Excitation-contraction coupling

The mammalian heart is composed of four chambers; the right and left atrium and ventricles respectively. The contraction and subsequent relaxation of the heart occurs over 5 phases in a cardiac cycle. During atrial systole the atria contract expelling blood into ventricles, this is followed by ventricular contraction and ejection in ventricular systole releasing blood into system. During diastole the myocardium is in a state of relaxation allowing the chambers to refill with blood. Myocardial contraction is essential for cardiac function as it produces

stroke volume and regulates cardiac output, change to force of contractility alters cardiac output (Jacob, Dierberger, & Kissling, 1992).

The contraction of the whole myocardium is due to the synchronous contraction of individual myocytes from which it is formed. As such in order to understand how the myocardium contracts, we need to understand the cellular basis of contraction. Cellular contraction is dependent on excitation-contraction coupling (ECC). ECC is responsible for translating excitation of a myocyte from an action potential to cellular contraction. Several ion channels and transporters regulate ECC and will be discussed in turn below.

1.2.1 The importance of Ca^{2+}

The experiments of Ringer (1883) were the first to demonstrate that Ca^{2+} is essential for cardiac contraction. Those experiments determined that the heart was only able to contract when Ca^{2+} was present. As such, when perfused with blood or a Ca^{2+} based solution, the heart will continue to beat for hours *ex vivo*.

Ca^{2+} is an important secondary messenger involved in the regulation of multiple cellular pathways (Clapham, 2007). Ca^{2+} is required to activate myofilaments and therefore is important for contraction. In heart cells, the presence of extracellular Ca^{2+} allows the rise and fall of $[Ca^{2+}]_i$ required for cell contraction then relaxation respectively (Eisner, 2018).

During diastole intracellular Ca^{2+} ($[Ca^{2+}]_i$) remains low as Ca^{2+} is stored primarily in the sarcoplasmic reticulum (SR); an intracellular compartment. Ca^{2+} is also present in extracellular matrix (ECM). The movement of Ca^{2+} between the SR, ECM and sarcoplasm is controlled in order to regulate this contraction. The speed and effectiveness of Ca^{2+} as a signalling molecule puts it at an evolutionary advantage when compared to other signalling mechanisms such as phosphorylation (Clapham, 2007). The cyclic rise and fall of Ca^{2+} couples excitation to contraction and relaxation. This process – known as excitation-contraction coupling (ECC) – is reliant on a series of Ca^{2+} channels, pumps and exchangers. A summary diagram for ECC will be provided in Fig 1-5.

Whilst intracellular $[Ca^{2+}]_i$ regulates ECC, the majority (~99 %) of cytoplasmic Ca^{2+} is bound to buffers, these include the sarcolemma, ATPase's, contractile proteins and other ligands. Free $[Ca^{2+}]_i$ is the Ca^{2+} available to bind to myofilaments, and also fluorescent dye, as such, using fluorescence alone only free $[Ca^{2+}]_i$ is measured. Ca^{2+} buffering can be altered through change to the presence of these buffers in the cytoplasm, for example change in protein expression, and the affinity of these buffers for Ca^{2+}. A change to Ca^{2+} buffering alters the proportion of free $[Ca^{2+}]_i$ available, whilst the total cytoplasmic $[Ca^{2+}]_i$ remains the same (Smith & Eisner, 2019).

1.2.2 Excitation

The wave of excitation that ultimately excites each myocardial cell originates in the sinoatrial node (SAN). The membranes of cells within the SAN undergo spontaneous depolarisation to threshold by virtue of inward Na^+ current (I_f) from hyperpolarization-activated cyclic nucleotide–gated (HCN) channels, generating the nodal action potential (Larsson, 2010; Shinagawa, Satoh, & Noma, 2000). This wave of excitation spreads through the atrium via intermodal pathways before it is slowed for ~100 ms by the atrioventricular (AV) node in the bottom of the right atria. This allows depolarisation and thus contraction to occur in the atria, prior to the ventricles. The signal continues to propagate down through the bundle of His then along the Purkinje network, until the wave of excitation reaches cells of the ventricles. Propagation of the action potential across a sheet of myocardium is aided by coupling of myocytes to adjacent cells via gap junctions (Rohr, 2004).

Once the action potential reaches the surface membrane of ventricular myocytes it is able to propagate down sarcolemmal invaginations called transverse (t-) tubules (Fearnley, Roderick, & Bootman, 2011; Santana, Cheng, & Lederer, 2010; van Weerd & Christoffels, 2016). This takes the cells own membrane to threshold potential, therefore evoking a cellular action potential.

The ventricular action potential has 5 phases (Fig 1-1). During phase 0 rapid Na^+ influx raises the diastolic membrane potential from -90 mV to +50 mV depolarizing the membrane. Phase

1 ceases following Na^+ channel inactivation with inducing a brief repolarisation from +50 mV to +30 mV, this is called a repolarisation notch (phase 2). Depolarisation also activates voltage gated channels called L-type Ca^{2+} channels (LTCC), (which shall be discussed further in 1.2.3.1) (Fearnley et al., 2011; Rohr, 2004; Santana et al., 2010). Here, LTCC opening and the resulting Ca^{2+} influx produces the characteristic plateau (phase 3) found in cardiac myocytes (Cooper, Soeller, & Cannell, 2010; Santana et al., 2010) as Ca^{2+} influx balances K^+ efflux via K^+ channels. Following LTCC inactivation K^+ efflux dominates producing repolarisation (phase 4). This restores diastolic resting membrane potential of -90 mV, which remains constant in phase 4 until membrane depolarisation occurs again (Santana et al., 2010; W. Zhu, Varga, & Silva, 2016).

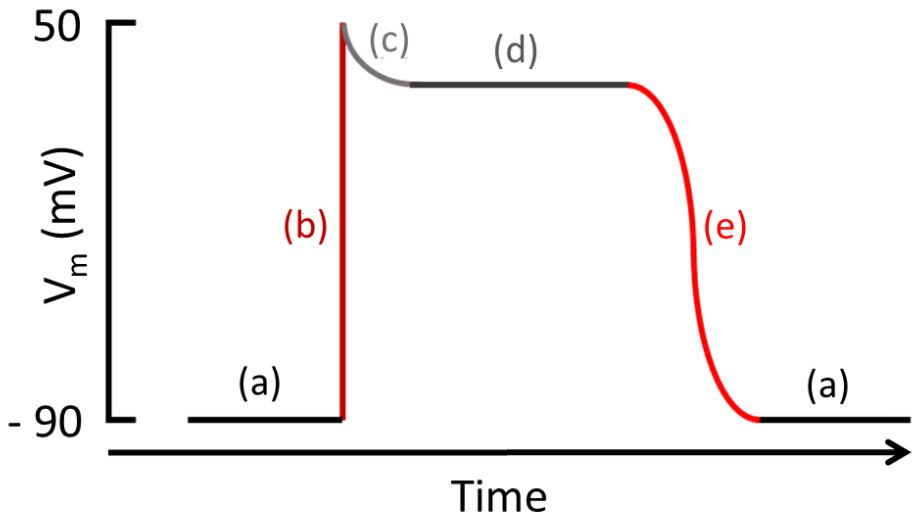

Figure 1-1. The ventricular action potential: (a) phase 0, (b) phase 1 depolarisation, (c) phase 2 notch (d) phase 3 plateau and (e) phase 4 repolarisation.

The morphology and duration of the ventricular action potential vary, but are generally much longer that of skeletal muscles, spanning ~400 ms. The duration and frequency of the action potential can impact Ca^{2+} handling mechanisms. The action potential stimulation frequency determines heart rate and is determined by the SAN action potential firing rate *in vivo* (Santana et al., 2010).

1.2.3 Sarcolemmal Ca^{2+} entry

As previously discussed, t-tubule depolarisation activates the LTCC contributing to the plateau of the action potential. This process also brings a small amount of calcium into the cell via Ca^{2+} entry and is the important first step of the Ca^{2+} cycle that produces contraction.

1.2.3.1 L-type Ca^{2+} channels

LTCC are voltage-gated channels that are selectively permeable to Ca^{2+}. Their high conductance (11-25 pS) and the fact that there exists a 10,000 fold Ca^{2+} gradient across the sarcolemma means that, when open, these channels allow Ca^{2+} entry via an electro-chemical gradient (Bean, 1989; Zahradnikova & Zahradnik, 2012).

$Ca_V1.2$ is the predominant cardiac form of LTCC. $Ca_V1.2$ is heterotetrameric and each of its 4 subunits – α1c, α2δ, β and γ – have a different role. The α1c-subunit is composed of 4 domains each with 6 transmembrane segments. Of these segments, 2 contribute to a pore formation with 0.6 nm diameter core, while the α-subunit segment acts as a voltage sensor, also known as a dihydropyridine receptor (DHPR) (Shaw & Colecraft, 2013; Zahradnikova, Zahradnik, Gyorke, & Gyorke, 1999). Both the α2δ and β subunits aid regulation of LTCC gating by altering the dependence of activation and inactivation on voltage (Buraei & Yang, 2010; Shaw & Colecraft, 2013).

LTCC are categorised by their large conductance, as oppose to T-type Ca^{2+} channels which have a lower or *tiny* conductance. LTCC also remain open for longer at ~500 ms (Nowycky, Fox, & Tsien, 1985; Treinys & Jurevicius, 2008). While T-type Ca^{2+} channels are also present in cardiac muscle, LTCC have a much larger role in Ca^{2+} influx. LTCC activity varies between cell types; the rate of activation and inactivation is 10 fold higher in cardiac myocytes when compared to that of skeletal muscle (Bean, 1989).

1.2.3.2 Voltage-dependent activation of L-type Ca^{2+} channels

In response to an action potential the membrane depolarises. As LTCC are voltage dependent, this depolarisation activates the channel permitting Ca^{2+} entry and so generating the calcium current. The voltage sensing domain (S4) is activated once the membrane potential exceeds a threshold of -40 mV. Collective activation of these domains provides pore stability when LTCC is open (Betzenhauser & Marks, 2010; Fearnley et al., 2011; W. Zhu et al., 2016). Depending on species, the optimal activation voltage is 0-10 mV resulting in the characteristic bell-shaped relationship between I_{CaL} and voltage shown in Fig 1-2. The time taken to reach peak I_{CaL} is also voltage dependent, following the same bell-shaped relationship (Pelzmann et al., 1998).

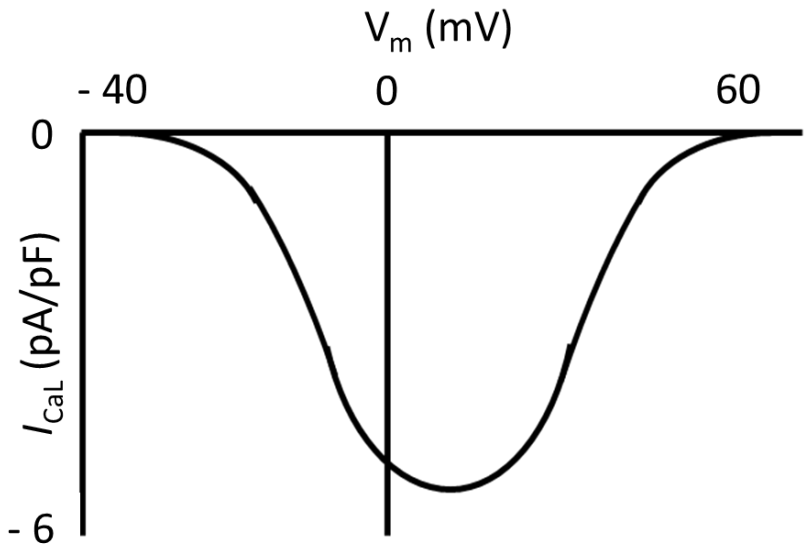

Figure 1-2. Voltage dependence of L-type Ca^{2+} current; the I-V relationship. Adapted from a figure by Pelzmann et al. (1998)

1.2.3.3 Inactivation of L-type Ca^{2+} channels

Inactivation of LTCC is dependent on $[Ca^{2+}]_i$ and voltage. The Ca^{2+} dependency of $Ca_V1.2$ accounts for 80 % of inactivation, while voltage dependent inactivation accounts for ~20 % (Lacinova & Hofmann, 2005).

Ca^{2+} dependent inactivation is mediated largely by calmodulin (CaM). CaM has 4 Ca^{2+} binding sites. At low $[Ca^{2+}]_i$ CaM is able to bind to Ca^{2+} with a high affinity, however not all 4 binding sites will be associated to Ca^{2+}. The elevated Ca^{2+} resulting from Ca^{2+} influx enables increased Ca^{2+} binding to CaM. The Ca^{2+}-associated CaM binds to an IQ motif present on the α1c-subunit of LTCC. Further Ca^{2+} influx ceases due to the subsequent inactivation of LTCC (Peterson, DeMaria, Adelman, & Yue, 1999).

Current decay contributes to voltage dependent $Ca_V1.2$ inactivation. This occurs during phase 3 of the ventricular action potential, when elevated outward K^+ drives repolarisation. The resulting reduction in the membrane potential increases the proportion of LTCC which are inactivated. Full inactivation cannot occur between -45 and 40 mV, however all LTCC are expected to be closed below 40 mV, as this is the threshold for LTCC activation (Pelzmann et al., 1998; Santana et al., 2010).

Both forms of LTCC inactivation are time dependent, following a biphasic inactivation time course of I_{CaL} with an initial fast phase followed by a slower phase of recovery. The fast phase has no dependency on membrane potential, however the slow phase is highly voltage dependent, with maximum inactivation occurring at 20 mV. At 20 mV, I_{CaL} is high and local $[Ca^{2+}]_i$ is increased rapidly, therefore Ca^{2+} dependent inactivation occurs at a faster rate than at other membrane potentials (Pelzmann et al., 1998).

Ca^{2+} influx via LTCC is not sufficient to produce contraction. It does however result in a much larger release of Ca^{2+} from the SR in a process known as calcium induced calcium releases (CICR). To understand CICR we must first understand the structural organisation of cell that permits it.

1.2.4 Sarcoplasmic reticulum

The sarcoplasmic reticulum (SR) is a specialised form of endoplasmic reticulum and the primary intercellular Ca^{2+} store. As the primary source of systolic Ca^{2+}, this reserve represents that which is required for intracellular Ca^{2+} modulation (see section 1.2.8).

1.2.5 Ca^{2+}-induced Ca^{2+}-release

Ca^{2+} influx from LTCC is not sufficient to increase global $[Ca^{2+}]_i$ enough to fully activate myofilaments. I_{CaL} can raise local $[Ca^{2+}]_i$ initiating Ca^{2+}-induced Ca^{2+}-release (CICR) from the SR. The SR Ca^{2+} release resulting from CICR is much larger than LTCC-mediated Ca^{2+} influx and leads to a much greater rise in global $[Ca^{2+}]_i$ enabling myofilament activation (Chung, Biesiadecki, Ziolo, Davis, & Janssen, 2016). The structures involved in this process shall now be discussed in further detail.

1.2.5.1 The ryanodine receptor

Ryanodine receptors (RyR) are channels responsible for SR Ca^{2+} release, playing a large role in CICR. RyR is the largest known ion channel at over 2 MDa and has a homotetrameric structure. 3 mammalian RyR isoforms exist however expression of each differs between different mammalian striated muscles and as well as parts of the body. RyR_1 is present in skeletal muscle and RyR_3 in found the brain, while RyR_2 is the cardiac form of the ryanodine receptor (Lanner, Georgiou, Joshi, & Hamilton, 2010). In the heart, CICR is more sensitive to increased $[Ca^{2+}]_i$ than skeletal muscle, suggesting RyR_2 has a greater Ca^{2+} sensitivity than other RyR isoforms (Fabiato & Fabiato, 1978).

RyR_2 is made up of 2 domains; cytoplasmic and transmembrane (Fill & Copello, 2002). The structure of these domains alters when the channel opens and closes. The cytoplasmic domain, also known as the central domain is composed of 10 sub domains. These sub-domains are collectively responsible for regulation of receptor function through binding of modulators; as such it holds multiple binding regions for Ca^{2+}, caffeine and ATP (Walpoth & Erman, 2015). Binding to these regions initiates conformational changes which increase the open probability of the channel. Both Ca^{2+} and caffeine can bind to the C-terminal while ATP has specialised binding motif. ATP is capable of activating RyR under physiological conditions and thus the ATP binding motif has been implicated in Ca^{2+} leak from the SR (Blayney et al., 2013; des Georges et al., 2016; Peng et al., 2016). The 4 homologous subunits of RyR_2 each have a Ca^{2+} binding site, thus 4 Ca^{2+} are required to bind in order to activate a single RyR.

The binding of these Ca^{2+} initiates a conformation change which opens the channel. RyR activation has a time constant of 0.07-0.27 ms (Zahradnikova et al., 1999). The remaining fifth of the protein including at least 6 α-helix transmembrane domains spans the SR lumen and membrane, forming the 3 Å wide ion conducting pore or channel domain (Fill & Copello, 2002; Lanner et al., 2010; Tunwell et al., 1996).

1.2.5.2 Organisation of excitation-contraction coupling structures

The arrangement of cellular structures including Ca^{2+} handling proteins and contractile machinery determines the efficiency of excitation-contraction coupling. Excitation reaches the inner points on the cell through t-tubules. Small structural differences exist between the arrangement of t-tubules and SR in large and small mammals. Ventricular myocytes from larger mammals have a less robust t-tubule network and lower t-tubule density than small mammals. Larger mammal myocardial t-tubules also have a wider diameter, with a t-tubule diameter of ~350 nM in humans. T-tubule density can be further impaired in cardiomyopathies and heart failure (Biesmans et al., 2011; Jayasinghe, Crossman, Soeller, & Cannell, 2012).

In addition to the involvement of SR in CICR, the SR also forms a network across the myocyte interacting with the contractile machinery. SR junctions in dyadic structures are also closely associated with myofilaments. Luminal [Ca^{2+}] varies throughout the SR with [Ca^{2+}] ~50 % higher at junctions. Ca^{2+} release is also highest at SR junctions, however this increases the magnitude and rate of Ca^{2+} release at neighbouring regions less associated with t-tubules Non-junctional SR regions primarily serve as a reservoir of Ca^{2+} (Picht et al., 2011).

1.2.5.3 The sub-cellular organisation of LTCC and RyR allows CICR

RyR are present on the SR membrane at SR junctions adjacent to t-tubules. Ca^{2+} signalling is localised to dyadic cleft in which RyR are coupled to LTCC due to their close proximity (Zahradnikova & Zahradnik, 2012). The proximity to LTCC aids RyR activation, as [Ca^{2+}]

increases locally to RyR. This amplifies Ca^{2+} signalling to promote activation of myofilaments. RyR are arranged in clusters, there are varying reports of the number of RyR within a cluster. Zahradnikova and Zahradnik (2012) suggested a cluster is composed of 40 RyR on average, while Fill and Copello (2002) suggested the number of RyR present in a cluster was between 10 and 30. RyR arrangement varies between species with human myocardium having a smaller cluster density when compared to smaller mammals (Jayasinghe et al., 2012).

The presence of dyadic junctions between the sarcolemma and terminal cisternae of the SR is beneficial to CICR. These dyadic junctions are small, narrow areas of cytoplasm, ~ 15 nm wide. These junctions provide high co-localisation of LTCC and RyR clusters (Jayasinghe et al., 2012). In cardiac muscle RyR_2 greatly outnumber the quantity of LTCC, with a single LTCC for every 5-10 RyR_2 channels (Zahradnikova & Zahradnik, 2012). Due to the contained environment, dyadic junctions allow small influxes in Ca^{2+} to rapidly increase in local $[Ca^{2+}]_i$ and activate RyR_2 (Jayasinghe et al., 2012; McDonald, Cavalie, Trautwein, & Pelzer, 1986). While individual RyR_2 have a low conductance, the association of ~ 3 RyR_2 clusters within the same dyadic cleft forms a Ca^{2+} releasing unit with a much larger net conductance (Zahradnikova & Zahradnik, 2012).

Multiple sub-populations of RyR exist based on their position in the myocyte. The majority of RyR clusters are associated with t-tubules, although this is not always the case, with 16 % of dyads forming with LTCC on the surface sarcolemma. While surface sarcolemmal dyads still have close proximity of RyR and LTCC, Ca^{2+} influx occurs at the myocytes' periphery requiring more Ca^{2+} to diffuse inward across the cell. Dyads associated with t-tubules are therefore beneficial for activation of myofilaments (Biesmans et al., 2011; Jayasinghe et al., 2012).

The association between RyR and LTCC permits CICR as the local rise in Ca^{2+} is much greater than if the same amount of Ca^{2+} had diffused across the cells. This allows small influxes of Ca^{2+} to activate the RyR.

1.2.5.4 Ca^{2+}-dependent activation of RyR

Open probability (P_o) is the likelihood that a channel – in this case RyR_2 – will be open at a single point in time. Approximately 35 -50 % of the SR Ca^{2+} content is released during systole (R. A. Bassani & Bers, 1995). Physiologically, the degree of fractional release is dependent on the two major regulators of RyR P_o; SR Ca^{2+} content and cytoplasmic [Ca^{2+}]. Free calcium in the SR lumen is able to regulate SR Ca^{2+} release via RyR and modify $[Ca^{2+}]_i$. At rest, the mammalian cardiac SR contains ~1 mM Ca^{2+}, as such Ca^{2+} release would be low (Fill & Copello, 2002; Picht et al., 2011). The dependence of RyR P_o on cytoplasmic Ca^{2+} is important in order to understand CICR, as Ca^{2+} influx via LTCC will primarily alter local $[Ca^{2+}]_i$, not SR Ca^{2+} content.

1.2.5.5 Ca^{2+} sparks

Local Ca^{2+} release from the SR can occur spontaneously when cell is at rest; these are termed Ca^{2+} sparks. A Ca^{2+} spark occurs as a result of summation of Ca^{2+} release events from 2.7-20 RyR. The spatially proximity of these RyR contributes to local net increase in Ca^{2+}. During diastole the open probability of RyR is low as $[Ca^{2+}]_i$ is also low at 50-150 nM, Ca^{2+} sparks therefore occur at a low frequency. During a single Ca^{2+} spark the local Ca^{2+} rises to 200-300 nM in approximately 10 ms. Ca^{2+} release as a result of sparks may recruit adjacent RyR within the same cluster through increasing their P_o (Betzenhauser & Marks, 2010; Zahradnikova & Zahradnik, 2012). During a Ca^{2+} spark RyR P_o decreases over the 2 s following peak P_o (Gyorke & Fill, 1993), this is attributed to rapid diffusion of Ca^{2+} away from the dyadic cleft reducing local $[Ca^{2+}]_i$ and therefore the Ca^{2+} gradient is only briefly maintained (Fill & Copello, 2002).

During systole sarcolemmal Ca^{2+} influx current driven by membrane depolarisation leads to an in increase in local $[Ca^{2+}]_i$ within dyadic clefts across the cell as a result of Ca^{2+} influx from LTCC. The elevated $[Ca^{2+}]_i$ increases RyR P_o contributing to synchronised RyR opening (Fill & Copello, 2002; Zahradnikova et al., 1999). SR Ca^{2+} release via RyR usually occurs <15 ms after membrane depolarisation (Neco et al., 2010). RyR activation requires local $[Ca^{2+}]_i$ to increase

to 0.3 – 10 µM. At steady state the range of Ca^{2+} concentrations required to activate RyR are narrower at 0.5 – 5 µM. L-type Ca^{2+} influx increases local $[Ca^{2+}]_i$ to 10-30 µM within the cleft, at these concentrations P_o is between 5-50 %. Open RyR_2 are capable of transporting 1000 µM Ca^{2+}/s (Fill & Copello, 2002; Zahradnikova et al., 1999). Ca^{2+} release from the SR during systole elevates global $[Ca^{2+}]_i$ from approximately 100 nM to 1µM (Chung et al., 2016).

1.2.5.6 Inactivation of RyR

RyR inactivation is important as it mediates cessation of SR Ca^{2+} release and therefore allows SR refilling following systole. This enables Ca^{2+} removal to decrease $[Ca^{2+}]_i$, allowing relaxation, and SR Ca^{2+} content to be sustained during diastole.

While low Ca^{2+} concentrations activate the RyR (0.3 – 10 µM), much higher Ca^{2+} concentrations (1-10 mM) bind to an inhibition site leading to Ca^{2+} dependent inactivation (Fill & Copello, 2002). Inactivation of RyR also requires dissociation of $[Ca^{2+}]_i$ from the binding sites causing the channel to close (Zahradnikova et al., 1999). Full RyR inactivation has a time constant of 5-6 ms. Decrease in local $[Ca^{2+}]_i$ aids Ca^{2+} dissociation and therefore Ca^{2+} dependent inactivation. Local $[Ca^{2+}]_i$ is reduced through Ca^{2+} removal from the cytoplasm, contributing to reduced RyR P_o. The rate of RyR inactivation is dependent on activity of Ca^{2+} removal mechanisms, although rate of Ca^{2+} decay and inactivation are not equal. Rate of RyR inactivation is 10 fold slower than rate of Ca^{2+} removal (Fill & Copello, 2002).

1.2.6 Calcium removal

The removal of calcium from the cytoplasm is important following systole to lower $[Ca^{2+}]_i$ to diastolic levels, enabling relaxation. The majority of cytoplasmic Ca^{2+} is returned to the SR via the sarcoplasmic/endoplasmic reticulum Ca^{2+}-ATPase (SERCA). Ca^{2+} efflux into the ECM occurs primarily via the sodium-calcium exchanger (NCX). Ca^{2+} uptake by SERCA is 3-4 fold faster than NCX-mediated Ca^{2+} efflux. The faster speed of Ca^{2+} uptake when compared to

Ca^{2+} extrusion explains why the majority of Ca^{2+} is taken up by SERCA during relaxation (R. A. Bassani, Bassani, & Bers, 1992). While other Ca^{2+} removal mechanisms exist, they do not contribute to the same extent as SERCA and NCX do to net Ca^{2+} removal following systole. The reduction of $[Ca^{2+}]_i$ following contraction regulates the transition between systole and diastole.

1.2.6.1 The sarcoplasmic endoplasmic reticulum Ca^{2+}-ATPase (SERCA)

Sarcoplasmic/endoplasmic reticulum Ca^{2+}-ATPase (SERCA) is a Ca^{2+} pump on the SR membrane, responsible for SR Ca^{2+} uptake. In rodents SERCA accounts for ~ 90 % of Ca^{2+} removal (Milani-Nejad & Janssen, 2014), whereas human and sheep SERCA activity is responsible for 76 and 81.5 % of Ca^{2+} removal, respectively (Dibb, Rueckschloss, Eisner, Isenberg, & Trafford, 2004; Piacentino et al., 2003).

SERCA is the primary Ca^{2+} removal mechanism responsible for lowering $[Ca^{2+}]_i$ to diastolic levels following systole. There are three SERCA isoforms of which SERCA2 is most prevalent in the heart. Of the 3 SERCA2 variants – 2a, 2b and 2c – both SERCA2a and SERCA2c are found in cardiac muscle. SERCA2a plays a large role in Ca^{2+} handling and has a high affinity to Ca^{2+} (Kranias & Hajjar, 2012). The removal of Ca^{2+} from the cytoplasm via SERCA enables relaxation of the myofilaments, whilst SR loading replenishes SR Ca^{2+} content for subsequent systolic Ca^{2+} release

At steady state, Ca^{2+} release from the SR is fractional, thus the SR is not completely emptied and remains at a higher concentration than that of cytoplasmic Ca^{2+} (R. A. Bassani & Bers, 1995). Ca^{2+} uptake into the SR therefore requires Ca^{2+} to move against a steep concentration gradient. SERCA has a high affinity binding site for ATP and uses ATP hydrolysis to enable Ca^{2+} uptake via active transport (Takenaka, Adler, & Katz, 1982). ATP hydrolysis phosphorylates SERCA2a forming a phosphoprotein. This reaction alters the structure of SERCA2a transporting the Ca^{2+} into the lumen of the SR. Reddy, Jones, Pace, and Stokes (1996) found that 2 Ca^{2+} bind to SERCA2a at once and are transported with the hydrolysis of a single ATP molecule. The maximum Ca^{2+} which can be taken up by individual SERCA in a

second is estimated to be between 10 and 15 Ca^{2+} (Levitsky, Benevolensky, Levchenko, Smirnov, & Chazov, 1981; Shigekawa, Finegan, & Katz, 1976).

The rate of Ca^{2+} uptake by SERCA is similar across the SR network with time constants between 140 – 159 ms. (Picht et al., 2011). Its important role in Ca^{2+} handling means that in the absence of SERCA2a cardiac function would cease (Kranias & Hajjar, 2012).

1.2.6.1.1 Regulation of SERCA

SERCA is always active, however the level of activity can change under different conditions, therefore altering the rate of SR Ca^{2+} uptake. Direct modulation of SERCA is typically not possible as SERCA activity is not affected by direct phosphorylation (Reddy et al., 1996). SERCA activity must therefore be modulated by another means.

The low molecular weight protein, phospholamban (PLN) is an important inhibitory accessory protein and a regulator of cardiac activity. In its monomeric inhibitory form, PLN forms a complex with SERCA2a. In this form PLN reduces the Ca^{2+} affinity of the pump, inhibiting SERCA2a function by 50 % and the reducing rate of Ca^{2+} uptake into the SR lumen by half following relaxation. The SERCA2a-PLN complex alters the rate of Ca^{2+} transport (K_{Ca}) from ~0.3 to ~1 µM. PLN does not have any effect on SR leak (Kranias & Hajjar, 2012; Reddy et al., 1996).

PLN has a hydrophobic SR membrane-bound region and a hydrophilic cytosolic domain contain sites for phosphorylation. PLN can be modulated by phosphorylation at a non-inhibitory cytoplasmic domain encouraging dissociation from SERCA2a. These dissociated PLN monomers combine to form much less active or inactive oligomers, predominantly pentamers (Kranias & Hajjar, 2012; MacLennan, Kimura, & Toyofuku, 1998). Phosphorylation prevents PLN from suppressing the rate of Ca^{2+} uptake, therefore stimulating SERCA2a activity. This phosphorylation reverses the PLN-induced Ca^{2+} affinity shift, increasing the Ca^{2+} affinity of the pump and thus rate of Ca^{2+} removal from the cytoplasm. As a result,

phosphorylation of PLN accelerates the rate of relaxation (Kranias & Hajjar, 2012; Reddy et al., 1996).

PLN is more effective at low $[Ca^{2+}]_i$, as high $[Ca^{2+}]_i$ can induce PLN dissociation from SERCA2a in the absence of phosphorylation through Ca^{2+} binding to an inhibitory transmembrane domain (MacLennan et al., 1998). Elevated $[Ca^{2+}]_i$ has a proportional positive effect on rate of Ca^{2+} uptake by the SR. In response to systolic $[Ca^{2+}]_i$ Ca^{2+} transport into the SR is 100-200 µM Ca^{2+}/s (R. A. Bassani & Bers, 1995) with a maximum rate of Ca^{2+} uptake peaks at 160 nM/min/mg (Wimsatt, Hohl, Brierley, & Altschuld, 1990). At rest $[Ca^{2+}]_i$ is low as is rate of Ca^{2+} uptake by SERCA at ~21 µM/s, this low Ca^{2+} uptake is able to account for any diastolic SR Ca^{2+} leak (R. A. Bassani & Bers, 1995). The free luminal $[Ca^{2+}]$ also plays a part is determining rate of Ca^{2+} uptake by SERCA through altering the concentration gradient (Picht et al., 2011).

Rate of ATP hydrolysis to ADP is much higher than the rate of the reverse reaction phosphorylation of ADP to ATP. While both the rate of the forward and reverse reaction are increased at higher $[Ca^{2+}]_i$, the forward reaction is increased to a greater extent (Feher, 1984). At steady state for every ~45 Ca^{2+} taken up by the SR, Ca^{2+} efflux is ~40 Ca^{2+}, with > 80 % of SR Ca^{2+} being exchanged with cytoplasmic Ca^{2+}. This results in net Ca^{2+} uptake by the SR (Feher, 1984; Takenaka et al., 1982). The reverse reaction or ATP formation is thought to be driven by Mg^{2+} due to its involvement in the release of P_i from phosphoprotein (Shigekawa et al., 1976).

1.2.6.2 The sodium-calcium exchanger (NCX)

Na^+ - Ca^{2+} exchanger (NCX) is a membrane protein responsible for the majority of Ca^{2+} efflux. Binding sites on NCX enable transport of Ca^{2+} and Na^+. Data shows that 3 Na^+ are exchanged for 1 Ca^{2+}; this 3+ charge influx and 2+ charge efflux contributes to a 1+ net increase in intracellular charge and so is electrogenic (Brini & Carafoli, 2011; Schillinger, Fiolet, Schlotthauer, & Hasenfuss, 2003).

NCX belongs to a family of 3 isoforms; NCX_1, NCX_2 and NCX_3. NCX_1 is the most abundant isoform in cardiac sarcolemma (Schillinger et al., 2003). NCX_1 is the main mechanism by which sarcolemma Ca^{2+} efflux occurs accounting for 15-35 % of Ca^{2+} removal following systole (R. A. Bassani et al., 1992; Dibb et al., 2004). The transport binding sites of NCX bind to Ca^{2+} with a low affinity aiding the rapid return of $[Ca^{2+}]_i$ to diastolic concentrations (Brini & Carafoli, 2011). Physiologically both $[Ca^{2+}]$ and $[Na^+]$ are much lower in the cytoplasm than in the ECM. During systole, $[Ca^{2+}]_i$ is ~1000-10000 fold lower than external Ca^{2+} concentrations, this creates a Ca^{2+} gradient (Miura & Kimura, 1989; Philipson, Bersohn, & Nishimoto, 1982). This drives Ca^{2+} removal, allowing relaxation to occur.

In addition to transport binding sites for Na^+ and Ca^{2+}, NCX has a high affinity Ca^{2+} regulatory binding site. This regulatory site found on the intracellular surface of NCX and is important for determining the magnitude of both Ca^{2+} influx and efflux (Levitsky, Fraysse, Leoty, Nicoll, & Philipson, 1996; Schillinger et al., 2003). Ca^{2+} influx via NCX is also possible due to reversible ion transport with an outward current resulting in Na^+ efflux (Miura & Kimura, 1989).

1.2.6.2.1 Regulation of the sodium-calcium exchanger

NCX_1 are primarily responsible for sarcolemmal Ca^{2+} efflux and if impaired cellular relaxation can be prolonged (Neco et al., 2010). NCX activity is dependent on Na^+ and Ca^{2+} binding to NCX transport binding sites. Activation of forward mode NCX activity is dependent on $[Na^+]_o$ and $[Ca^{2+}]_i$. The inward Na^+ gradient drives Ca^{2+} removal, even against its concentration gradient (Miura & Kimura, 1989).

Intracellular Ca^{2+} regulates NCX_1 activity through binding to one of 2 high Ca^{2+} affinity regulatory binding sites distinct from the Na^+ and Ca^{2+} transport binding site. A conformational change occurs to NCX once Ca^{2+} binds to this regulatory site, this reduces inhibition of Na^+ /Ca^{2+} current. $[Ca^{2+}]_i$ therefore has a concentration dependent effect on Ca^{2+} efflux, with high $[Ca^{2+}]_i$ is therefore able to stimulate Ca^{2+} efflux (Levitsky et al., 1996; Miura & Kimura, 1989).

As discussed in section 1.2.5.5, Ca^{2+} sparks can occur due to diastolic SR Ca^{2+} leak. Primarily Ca^{2+} is released from RyR however SERCA can also add to Ca^{2+} leak. Spark amplitude and duration are dependent of rate of SR Ca^{2+} release and rate of Ca^{2+} removal or diffusion away from the dyadic cleft. This diastolic rise $[Ca^{2+}]$ must either be taken up by SERCA or extruded from the cell. The sensitivity of NCX to high local $[Ca^{2+}]_i$ determines rate of Ca^{2+} removal and with that Ca^{2+} spark dynamics (Biesmans et al., 2011; Neco et al., 2010).

In addition to the primary role of NCX in Ca^{2+} extrusion, NCX are able to exchange Ca^{2+} and Na^{+} in reverse driving Ca^{2+} influx. Thomas et al. (2003) measured Ca^{2+} current from reverse-mode NCX activity at 90 mV. Ca^{2+} influx from reverse-mode NCX activity is not able to induce SR Ca^{2+} release alone but primes the dyadic cleft with a small increase in $[Ca^{2+}]_i$. When combined with the Ca^{2+} influx from LTCC in response to a cardiac action potential it increases the efficiency of CIRC and therefore magnitude of SR Ca^{2+} release, regardless of SR Ca^{2+} load. Reverse-mode NCX activity or outward current is only activated when $[Na^{+}]_i$ is high and therefore $[Na^{+}]_i$ regulates amplitude and rate of SR Ca^{2+} release through synergy between NCX and LTCC. High $[Na^{+}]_i$ enhances CICR via reverse-mode NCX activity, reducing $[Na^{+}]_i$, the now low $[Na^{+}]_i$ drives NCX activity, elevating the rate of Ca^{2+} efflux. This influence of $[Na^{+}]_i$ helps maintain the equilibrium between sarcolemma Ca^{2+} influx and efflux (Miura & Kimura, 1989; Neco et al., 2010; Ramirez, Sah, Liu, Rose, & Backx, 2011). Through altering Ca^{2+} and Na^{+} concentrations in the ECM, NCX activity can also regulate Ca^{2+} handling in neighbouring cells (Thomas et al., 2003).

Change to the membrane potential and heart rate impacts the proportions of reversed and forward NCX activity which occur throughout the cardiac cycle. This also alters the relative contribution of NCX to Ca^{2+} removal following systole. Increased duration of the action potential enhances the contribution of reversed mode NCX activity and Ca^{2+} influx, while reducing the duration of Ca^{2+} efflux via forward mode NCX activity. Increase in heart rate produces the opposite effect, prolonging the duration of forward mode NCX activity during diastole. The relative contribution of NCX to Ca^{2+} removal is higher, enhancing Ca^{2+} efflux. This reduces uptake of Ca^{2+} via SERCA and contributes to decreased SR Ca^{2+} content. The effect of increased heart rate on SR Ca^{2+} content explains why Ca^{2+} transient amplitude is

reduced with elevated frequency. This relationship can however differ between species (R. A. Bassani et al., 1992; Schillinger et al., 2003).

Intracellular pH can alter the exchange of Na^+ and Ca^{2+} via the NCX in either direction. Acidity decreases Na^+ /Ca^{2+} current, ceasing flux completely at below pH 6, while alkalosis stimulates NCX activity. This pH-dependency on NCX activity is highest at lower intracellular [Ca^{2+}] and [Na^+] and is thought to occur due to competitive binding of H^+ in the place of either Ca^{2+} or Na^+ to intracellular ion binding sites on NCX (Philipson et al., 1982).

Prolonged exposure to high $[Na^+]_i$ induce Na^+-dependent inactivation NCX_1. This enables inactivation of the exchanger once $[Ca^{2+}]_i$ has been reduced to normal diastolic levels. Increased $[Ca^{2+}]_i$ slows the rate of NCX inactivation (Hilgemann, Matsuoka, Nagel, & Collins, 1992). Exchange activity is modulated by ATP. At physiological concentrations Mg-ATP can increase the rate of recovery from Na^+-dependent inactivation and reactivation of inactivated Na^+-Ca^{2+} exchange. This pathway alters the sensitivity of NCX to Ca^{2+} encouraging Ca^{2+} efflux to lower $[Ca^{2+}]_i$. If $[Ca^{2+}]_i$ remains high during diastole this mechanism prevents Ca^{2+} overload when intracellular Na^+ is high. Ca^{2+} accumulates in the ECM in preparation for the next Ca^{2+} cycle (Collins, Somlyo, & Hilgemann, 1992; Hilgemann et al., 1992).

1.2.6.3 Other Ca^{2+} removal mechanisms

Plasma membrane Ca^{2+} ATPase (PMCA) and mitochondrial Ca^{2+} uptake are responsible for the remainder of Ca^{2+} extrusion, collectively contributing to less than 1 % of total Ca^{2+} removal from the cytoplasm in humans. PMCA and mitochondrial Ca^{2+} uptake are respectively 37 and 50 fold slower than that of NCX (R. A. Bassani et al., 1992; Piacentino et al., 2003).

PMCA is a sarcolemmal protein found in numerous cell types. It has a low activity rate and as such, a low rate of Ca^{2+} removal (Brini & Carafoli, 2011; Caride, Rega, & Garrahan, 1986). There are multiple isoforms of PMCA; PMCA1b and PMCA4b are thought to have the greatest involvement with Ca^{2+} removal in the heart (Dally et al., 2006). Despite its high

affinity for Ca^{2+}, PMCA transports Ca^{2+} at approximately 1µM/s, this low contribution Ca^{2+} efflux can be attributed to the enzyme's low capacity for Ca^{2+}. If PMCA alone was responsible for Ca^{2+} efflux relaxation would take approximately 60s (R. A. Bassani et al., 1992; Brini & Carafoli, 2011). PMCA expression is up-regulated in some cardiomyopathies, increasing beyond that of SERCA2a. In these cardiomyopathies this drives Ca^{2+} efflux, contributing to reduced SR Ca^{2+} content and Ca^{2+} transient amplitudes (Dally et al., 2006).

PMCA activity is dependent on phosphorylation by ATP (Caride et al., 1986). ATP hydrolysis is coupled to Ca^{2+} extrusion with low efficiency and therefore is dependent on the availability of ATP. 1 Ca^{2+} is transported per ATP hydrolysis with a stoichiometry transport ration of 1:1. PMCA act as a pump exchanging Ca^{2+} for H^{+} (Brini & Carafoli, 2011; Filomatori & Rega, 2003).

Phosphorylation of PMCA is Ca^{2+}-dependent; increased $[Ca^{2+}]_i$ elevates both rate and magnitude of phosphorylation by ATP. Ca^{2+} binds to the activation site on PMCA able to displace any Mg^{2+} already bound there. Mg^{2+} is not required for phosphorylation to occur, however its presence in the µM range can also accelerate the rate of phosphorylation and thus PMCA activation. Inhibition of PMCA is mediated by dephosphorylation. If Mg^{2+} were present during phosphorylation, the presence of Mg^{2+} during dephosphorylation can also increase rate of dephosphorylation up to a saturation point (Caride et al., 1986).

1.2.7 Contraction

The cyclic rise and fall of $[Ca^{2+}]_i$ produces contraction and relaxation. Ca^{2+} binds to myofilaments enabling cross bridges to form between them. Contraction occurs when these cross bridges allow myofilaments to slide past each other in parallel. As $[Ca^{2+}]_i$ increases, as does the activation of myofilaments and the resulting cellular contraction. With dissociation and removal of Ca^{2+} from the cytoplasm the contractile unit relaxes.

1.2.7.1 Myofilaments

In a mammalian left ventricular myocyte, contractile components called myofilaments make up ~54 % of the cell volume (Bossen, Sommer, & Waugh, 1981). Myofilaments are arranged in a specific parallel overlapping structure, forming contractile units called sarcomeres. The approximate length of the sarcomere at rest is 1.8 – 1.9 µm (Hanft, Korte, & McDonald, 2008; Jayasinghe et al., 2012).

The organisation of filaments within the sarcomere and their role in contraction were first identified by A. F. Huxley and Niedergerke (1954) and H. Huxley and Hanson (1954). The collective arrangement of sarcomeres leads to the overall striated appearance of the cardiac myocyte, with the alternating dark A-bands and light I-bands. At either end of the sarcomere Z-discs anchor the sarcomere to adjacent sarcomeres and structural cytoskeletal filaments. Thin actin filaments protrude from the Z-lines towards the centre of the sarcomere ending at the H-zone. Actin filaments are helical and double stranded, composed of polymerised globular actin monomers. These thin filaments run parallel to the myosin filaments overlapping over a 75 µm region (Hanft et al., 2008). The non-overlapping regions of actin make up the I-band which becomes narrower with contraction as the overlap between actin and myosin becomes larger (A. F. Huxley & Niedergerke, 1954) (see Fig 1-3).

The A-band spans the width of the myosin filament tails, in addition to the overlapping actin regions. As the length of myosin remains the same during contraction, the A-band width is constant (H. Huxley & Hanson, 1954). The tail ends of two coiled myosin heavy chains, composed of 300 monomers, make up the thick filament (Hanft et al., 2008). Myosin is arranged in a hexameric structure with two myosin light chains for each heavy chain. Globular myosin heads protrude from the myosin filament tails and are responsible cross bridge formation between the myosin and actin filaments. Myosin heads have both an actin binding domain and a site for ATP hydrolysis. In the centre of the sarcomere, myosin filaments are connected by M-protein and myomesin (Spudich, 2001; Warrick & Spudich, 1987).

Every seventh actin monomer is adhered to a troponin complex. Troponin (Tn) is comprised of 3 subunits, each with a specific function: TnC, TnI and TnT. TnC is the Ca^{2+} binding site, while TnI lowers the affinity of TnC for Ca^{2+}, with a role in inhibition. Tropomyosin (Tm) is a short helical polymer found between the actin strands. TnT binds to Tm, allowing Tn to bridge actin with Tm (Moss, Razumova, & Fitzsimons, 2004; Solaro, Moir, & Perry, 1976).

Titin is a structural protein found adhered to the Z-line. In this position titin can at as a scaffold to support myosin during contraction. Titin determines the stiffness or elasticity of the cell and therefore its ability to distend (Brady, 1991). High titin compliance increases both the length of a sarcomere and the strength of the interactions between myosin and actin. As such sarcomere length regulates myofilament sensitivity to Ca^{2+} and the maximum possible force which can be generated (K. L. Li et al., 2018). The sarcomere is able to stretch to extend up to ~2.3 µm in length with increased cardiac loading, contributing to length-induced activation of myofilaments and a stronger contractile force (Hanft et al., 2008).

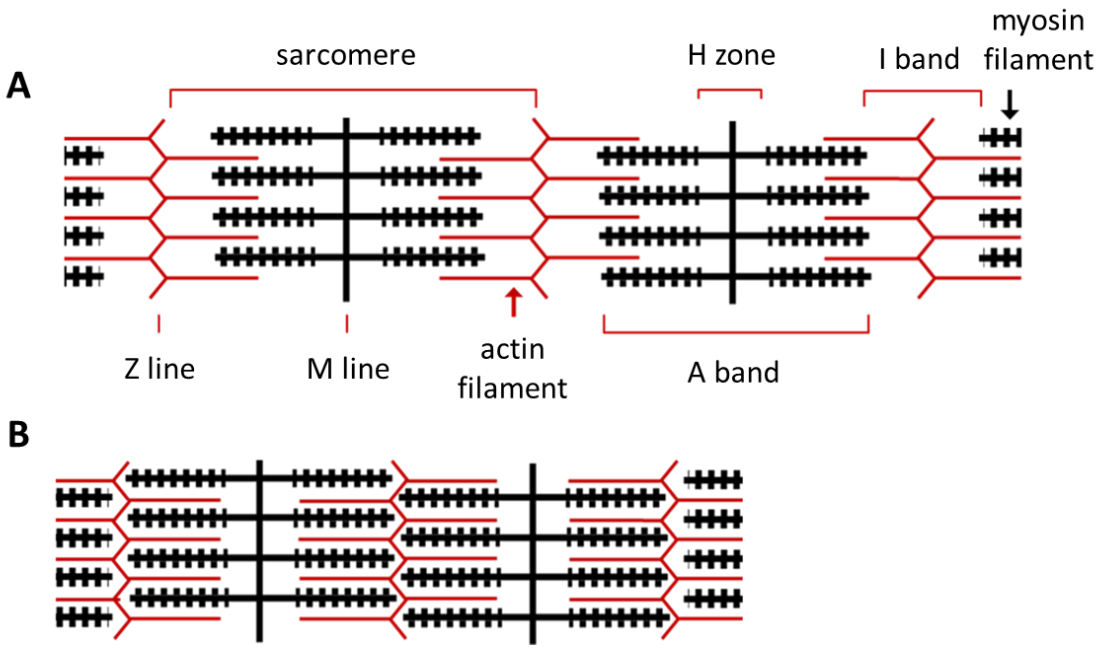

Figure 1-3. The basic arrangement of myofilaments within the sarcomere. (A) during relaxation. (B) during contraction.

1.2.7.2 Myofilament Ca^{2+} binding and cross bridge cycling

The dyadic junctions where CIRC occurs due to connections between the SR and t-tubules are also associated with the sarcomere. The regions of the SR span the 2 compartments closest to the Z-line, as such the amplitude of Ca^{2+} release is highest here. Non-junctional SR crosses the remaining compartments of the sarcomere more closely associated with the M-line. The rate of SR Ca^{2+} release is elevated with increased distance from the M-line, with Ca^{2+} release 8 ms faster at the Z-line (Picht et al., 2011).

$[Ca^{2+}]_i$ is able to regulate the level of contractile force generated by sarcomeres. At low diastolic $[Ca^{2+}]_i$ the interactions between TnI and actin, and TnT and Tm, are strong, holding tropomyosin in place. The position to tropomyosin blocks actin binding sites preventing myosin from interacting with actin, thus the number of cross bridges which are able to form are limited. Strong cross bridge formation makes it possible for some contraction to occur in the absence of Ca^{2+}, however the magnitude of contraction would be minimal (Moss et al., 2004).

Tn and Tm collectively regulate myofilament activation. The systolic rise in $[Ca^{2+}]_i$ due to CICR, increases the Ca^{2+} available to bind to TnC. Ca^{2+} binds to TnC with a low affinity inducing a conformational change in Tn. This manoeuvres Tm unblocking the actin binding site and increasing sensitivity to Ca^{2+}. This activates myofilaments enabling myosin-actin interactions (Moss et al., 2004). During contraction ~ 30 μM Ca^{2+} is bound to TnC (J. W. Bassani, Yuan, & Bers, 1995).

The myosin head has 2 domains; S1 and S2. S1 binds to actin forming the cross bridge. S1 acts as a motor; in response to phosphorylation by a single ATP molecule S1 undergoes a conformation change. This reaction adjusts the angle of the myosin head driving the power stroke. An individual power stroke results in a ~5-15 nm shortening step (Moss et al., 2004; Spudich, 2001). During maximal activation contraction of the sarcomere can shorten up to ~65 % of resting length, at this point ~30 % of cross bridges interact at once and the I-band is no longer visible (Hanft et al., 2008; H. Huxley & Hanson, 1954).

Deactivation of myofilaments requires dissociation of cross bridges and prevention of further myofilament activation through removal of Ca^{2+} from the cytoplasm (Chung et al., 2016). In addition, other factors can influence rate of deactivation. Sarcomere shortening can induce deactivation. As the sarcomere contracts the number of further strong cross bridges that can form are reduced and Ca^{2+} dissociates from TnC at a higher rate (Moss et al., 2004).

ATP availability also impacts rate of activation and deactivation of myofilaments. Just as the presence of ATP can drive the power stroke, accumulation of P_i encourages reversal of the power stroke. This accelerates cross bridge deactivation and drives relaxation (Hanft et al., 2008; Moss et al., 2004). The rate of contraction and relaxation alters when the rate of Ca^{2+} association and dissociation to TnC change by equal amounts in one direction. This does not impact the extent of sarcomere shortening unless the changes in rate are unequal (Chung et al., 2016).

1.2.7.3 Regulation of contraction

Myofilament sensitivity to Ca^{2+} is the sigmoidal relationship between the availability of Ca^{2+} to bind to TnC and the resultant force generation by the myofilaments (Fig 1-4). This relationship can shift in response to change in myofilament sensitivity to Ca^{2+}. A left shift indicates increased Ca^{2+} sensitivity, therefore a greater force will be generated with the same $[Ca^{2+}]_i$. Decreased Ca^{2+} sensitivity is denoted by right shift in relationship. With a decreased myofilament sensitivity to Ca^{2+}, a larger $[Ca^{2+}]_i$ is required to maintain a given force (Chung et al., 2016; Moss et al., 2004).

Equivalent changes in rate of association and dissociation of Ca^{2+} from TnC can alter rate of contractility. Unequal or opposite changes in rate of Ca^{2+} association and dissociation from TnC alter the ratio (k_d) between them leading to one outweighing the other, contributing to change in myofilament sensitivity to Ca^{2+}. Increased Ca^{2+} sensitivity results from either an elevated rate of association or reduced rate of dissociation. Both decrease k_d and increase

the force generated at a given $[Ca^{2+}]_i$, the former increases the rate of shortening, while the latter would slow relaxation (Chung et al., 2016).

Ca^{2+} sensitivity is altered by the availability of ATP and ADP. Elevated cytoplasmic [MgADP] increases the strength of cross bridges. As the cross bridges formed are stronger, the rate of dissociation is reduced and therefore myofilament sensitivity to Ca^{2+} is increased (Moss et al., 2004).

The pH of the cytoplasm can change under both physiological and pathological conditions and affect myofilament sensitivity to Ca^{2+}. Acidosis has a depressive effect of myofilament contractility, through decreased Ca^{2+} sensitivity. A lower pH shifts the $[Ca^{2+}]_i$ and contractile force relationship to the right, thus a greater threshold of free Ca^{2+} is required to generate the same level of contractile force, reducing the rate of contraction. The maximum force generated at saturating levels of free Ca^{2+} is limited with decreased pH. The afore mentioned effects of acidosis on SR Ca^{2+} uptake and release are thought to further exacerbate the depressive effect on myofilaments through reducing available Ca^{2+} (Fabiato & Fabiato, 1978).

1.2.8 Regulation and control of systolic Ca^{2+}

The above explains the fundamental way in which Ca^{2+} rises and falls during systole, then diastole. Normal heart function requires that this process is regulated to maintain a stable level of inotropy for a given metabolic demand. As inotropy must also adapt to meet changes in metabolic demand, the process must be controllable.

1.2.8.1 The relationship between systolic Ca^{2+} and force of contraction

The Ca^{2+} transient amplitude regulates inotropy as the rise in global $[Ca^{2+}]_i$ increases the free Ca^{2+} available to activate myofilaments. Anything that increases systolic Ca^{2+} will result in increased force of contraction. The relationship between $[Ca^{2+}]_i$ and contractile force is

sigmoidal (Fig 1-4). The binding affinity of Ca^{2+} to TnC increases as more cross bridges form, this increases the strength of subsequent cross bridge formations. The contractile force generated increases exponentially after initial myofilament activation. At higher $[Ca^{2+}]_i$ saturating levels are reached and the force of contraction cannot increase any further (Moss et al., 2004). The force of contraction is therefore highly dependent on systolic Ca^{2+}. Autoregulation prevents beat-to-beat variability in systolic Ca^{2+}, in order to maintain a steady state; this shall be discussed in section 1.2.8.3.

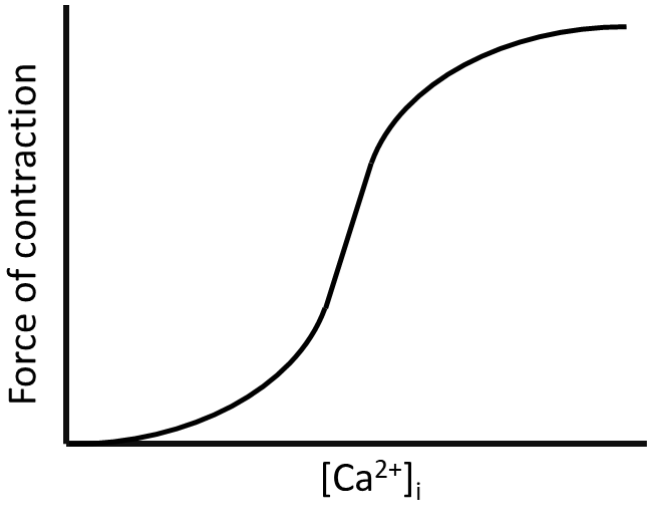

Figure 1-4. The sigmoidal relationship between free cytoplasmic Ca^{2+} concentration and force of contraction

1.2.8.2 What determines the amplitude of systolic Ca^{2+}?

The amplitude of systolic Ca^{2+} is dependent on the amount of Ca^{2+} that leaves the SR during systole. As the concentration of Ca^{2+} inside the SR is always much greater than in the cytoplasm, Ca^{2+} will flow into the cytoplasm when the RyR open during CICR (see 1.2.5.5). However, it is never the case that *all* SR Ca^{2+} is released during systole rather a fraction; termed fractional SR Ca^{2+} release.

Fractional SR Ca^{2+} release is dependent on two fundamental phenomenon. (1) the amount of Ca^{2+} stored in the SR (SR Ca^{2+} content) and (2) peak Ca^{2+} influx on I_{CaL}. For all other

parameters being equal, if either increases then so will fractional SR Ca^{2+} release thus systolic Ca^{2+}. To understand why these relationships exist, it is important to remember RyR P_o is dependent on cytoplasmic and intra-SR (luminal) Ca^{2+}.

It is convenient to consider the effect of peak I_{CaL} first. As per section 1.2.5.5, mass systolic SR Ca^{2+} release occurs as a result of summation of Ca^{2+} sparks. This is because during CICR, Ca^{2+} influx via voltage gated Ca^{2+} channels, primarily LTCC, elevates local (to the RyR) dyadic Ca^{2+} increasing RyR P_o so that enough will simultaneously open to produce mass SR Ca^{2+} release. Peak I_{CaL} represents the greatest point-in-time Ca^{2+} flux via LTCC and so the greatest increase in dyadic Ca^{2+} concentration. Increasing peak I_{CaL} means higher dyadic Ca^{2+} concentrations are reached during CICR further elevating RyR $P_{o.}$ Under these conditions, stochastically, more will happen to open simultaneously thus increasing mass SR Ca^{2+} release (Fill & Copello, 2002; Gyorke & Fill, 1993; Zahradnikova et al., 1999).

The dependence of fractional SR Ca^{2+} release on SR Ca^{2+} content is due to the fact that increasing SR Ca^{2+} also elevates RyR P_o. Compared to the time course of Ca^{2+} influx via LTCC, SR Ca^{2+} is relatively stable, so SR Ca^{2+} sets the basal RyR P_o. Increasing SR Ca^{2+} elevates that basal P_o and so pre-sensitisation such that during CICR, a *given* peak I_{CaL} results in increased simultaneous RyR opening thus mass SR Ca^{2+} release (Ching, Williams, & Sitsapesan, 2000). SR Ca^{2+} content itself is regulated by the rate of Ca^{2+} uptake. The rate of SERCA activity can therefore also impact inotropy, in addition to other Ca^{2+} dynamics, such as diastolic $[Ca^{2+}]_i$ (Kranias & Hajjar, 2012).

The dependence of fractional SR Ca^{2+} released on SR Ca^{2+} content is cubic making SR Ca^{2+} content a powerful modulator of inotropy. This also means that in the steady state, SR Ca^{2+} content must be tightly controlled via a process known as autoregulation.

1.2.8.3 Autoregulation

Autoregulation is the feedback mechanism by which SR Ca^{2+} content is modulated in order to ensure Ca^{2+} transient amplitude and the resultant inotropy are maintained at steady state.

Autoregulation is important as instability in Ca^{2+} handling can lead to beat-to-beat variations in cardiac contractility (Eisner, Choi, Diaz, O'Neill, & Trafford, 2000).

Alterations to the activity of a single component of Ca^{2+} handling cannot induce a prolonged effect on fractional SR Ca^{2+} release and thus inotropy. In the absence of a change to the Ca^{2+} trigger, alteration of RyR P_o alone has only a fleeting effect on inotropy. Increased RyR P_o elevates SR Ca^{2+} release, resulting in brief, initial increase in systolic Ca^{2+}, lasting for a single beat. The high Ca^{2+} during systole then increased forward-mode NCX activity driving a larger proportion of Ca^{2+} efflux. Due to the dependency of LTCC inactivation on $[Ca^{2+}]_{i,}$ the high Ca^{2+} during systole also increases the rate of Ca^{2+}-induced inactivation of LTCC, reducing Ca^{2+} influx (Pelzmann et al., 1998). As Ca^{2+} efflux exceeds influx, this results in reduced $[Ca^{2+}]_i$ for subsequent beats. As $[Ca^{2+}]_i$ is low, less Ca^{2+} is available for SR Ca^{2+} uptake via SERCA, leading to a decreased rate of Ca^{2+} uptake and a reduced SR Ca^{2+} content (Kranias & Hajjar, 2012). As described in section 1.2.8.2, SR Ca^{2+} content is one of the main determinants of systolic Ca^{2+}, thus a reduction in SR Ca^{2+} content and reduced I_{CaL} (or Ca^{2+} trigger) compensate for the increased RyR P_o. This allows steady state Ca^{2+} transient amplitude, and the resulting inotropy, to be restored and maintained (Eisner et al., 2000; Miura & Kimura, 1989).

If RyR P_o is reduced, SR Ca^{2+} release is reduced and thus systolic $[Ca^{2+}]_i$ is briefly reduced. $[Ca^{2+}]_i$ increases due to low NCX-mediated Ca^{2+} extrusion and a reduced rate of Ca^{2+}-dependent LTCC inactivation. High $[Na^+]_i$ resulting from the previously higher rate of NCX-mediated Ca^{2+} extrusion can also drive reverse mode NCX activity. This high $[Ca^{2+}]_i$ promotes SR Ca^{2+} uptake via SERCA and thus increases SR Ca^{2+} content. In both cases, SR Ca^{2+} content is therefore altered to compensate for the change to RyR P_o (R. A. Bassani & Bers, 1995; Eisner et al., 2000; Ramirez et al., 2011).

Though SR Ca^{2+} content and therefore inotropy are tightly regulated in the steady state, cellular inotropy must be able to adapt to meet changes to metabolic demand. β-adrenergic stimulation therefore alters the inotropic set-point which autoregulation then maintains.

1.2.8.4 Beta-adrenergic stimulation

During physiological conditions such as exercise and stress, β-adrenergic stimulation increases the production of cyclic AMP (cAMP), and therefore the activation of protein kinase A (PKA). PKA is able to phosphorylate multiple Ca^{2+} handling and regulatory proteins including PLN, LTCC and TnI. This phosphorylation increases the magnitude and force of contraction and rate of relaxation leading to sustained overall positive inotropy (Bers, 2002). As previously discussed in section 1.2.8.2, SR Ca^{2+} release, and the resulting changes to systolic Ca^{2+} and inotropy, are dependent on both I_{CaL} and SR Ca^{2+} content. Both I_{CaL} and SR Ca^{2+} content can therefore be modulated to produce a change to inotropy. Positive inotropy occurs either through direct phosphorylation of LTCC – resulting in an increase in peak I_{CaL} – or phosphorylation of PLN – the mediator of SERCA activity – increasing SR Ca^{2+} loading

LTCC is affected by β-adrenergic stimulation altering the I/V relationship. The I_{CaL} achieved at each change in membrane potential increases. This follows the same bell-curved relationship as shown in Fig 1-2, with inward Ca^{2+} current also peaking at 10 mV. β-adrenergic stimulation therefore contributes to increase Ca^{2+} influx (Pelzmann et al., 1998).

β-adrenergic stimulation requires PLN to mediate its effects on SERCA activity. cAMP-dependent phosphorylation of PLN promotes dissociation from SERCA. Ca^{2+}/calmodulin-dependent protein kinase II (CaMKII) can also act on PLN, independent of PKA. PLN dissociation increases the rate of SR Ca^{2+} uptake by SERCA, driving SR Ca^{2+} loading and rate of relaxation. The effect of phosphorylation PLN is reversible (Kranias & Hajjar, 2012; Reddy et al., 1996). PLN forms pentamers during β-adrenergic stimulation. It is the dissociation of PLN from these pentamers which enables them to reassociate with SERCA. Once the monomers are associated with SERCA, PLN returns to its inhibitory role (MacLennan et al., 1998).

RyR is also a target from phosphorylation by PKA. This alters RyR P_o producing a short-lived increase in SR Ca^{2+} release (Kranias & Hajjar, 2012). As previously mentioned the effects of RyR potentiation on inotropy are not sustainable. The impact of LTCC phosphorylation on Ca^{2+} influx would however, have the same overall effect, driving CICR (Bers, 2002).

β-adrenergic stimulation can also impact myofilament sensitivity to Ca^{2+} through phosphorylation of myofilament-associated proteins, such as Tn. This does not alter Ca^{2+} handling but can impact inotropy. In response to β-adrenergic stimulation phosphorylation of TnI regulates cardiac activity in different ways dependent on site and the degree of phosphorylation. High PKA phosphorylation of TnI improves the affinity of TnC for Ca^{2+} and increases rate of association, thus the force of contractility is increased. TnI phosphorylation can reduce the sensitivity of the myosin ATPase to Ca^{2+} encouraging Ca^{2+} dissociation and therefore rate of relaxation. This allows for a steady state of contraction and relaxation to be reached; at higher heart rates it is beneficial for new Ca^{2+} cycles to begin more rapidly (Bers, 2002; Solaro et al., 1976).

The average basal heart rate varies in different mammals however the heart rate of sheep is similar to humans when compared to smaller mammal models such as rats. On average, the human myocardium beats at approximately 72 beats per minute (BPM), this is within the range of sheep at 60 – 120 BPM. Rat myocardium beat at a much faster pace (250-493 BPM) (Milani-Nejad & Janssen, 2014). β-adrenergic stimulation acts on the SA node contributing to increased firing rate, modulated by increased SR Ca^{2+} release in pacemaker cells (Ju & Allen, 1999). At a higher heart rate relaxation time is reduced, decreasing the time for Ca^{2+} uptake by the SR. A reduction in SR Ca^{2+} loading contributes to decreased amplitude of subsequent Ca^{2+} releases at steady state (Santana et al., 2010; Schillinger et al., 2003).

1.2.8.5 Modulation of Ca^{2+} handling by physiological agents

While rapid changes in $[Ca^{2+}]_i$ are primarily responsible for regulation of RyR_2 activation and inactivation, RyR are not solely sensitive to Ca^{2+}. Other physiological agents – Mg^{2+} and ATP – have the ability to further alter P_o and modulate RyR, determining how RyR respond to change in Ca^{2+}. This impacts the rate and magnitude of SR Ca^{2+} release.

Mg^{2+} is capable of competitively binding to the non-specific high Ca^{2+} inhibition site of RyR (Fill & Copello, 2002). When compared to other RyR isoforms, RyR_2 has a reduced sensitivity to Mg^{2+}. High $[Mg^{2+}]$ at mM concentrations still have an inhibitory effect on RyR_2 decreasing

P_o (Tunwell et al., 1996; Valdivia, Kaplan, Ellis-Davies, & Lederer, 1995). Rate of RyR_2 activation is reduced with Mg^{2+} as RyR is less sensitive to elevated cytoplasmic Ca^{2+}. Mg^{2+} also impacts the decay time of P_o following Ca^{2+} release, therefore once activated the channel can remain open longer, although with Mg^{2+} inactivation can occur at a lower $[Ca^{2+}]_i$, as such inactivation is 10 fold faster in the presence of Mg^{2+} (Fill & Copello, 2002; Valdivia et al., 1995).

RyR_2 activation does not require the presence of ATP however the sensitivity of RyR to Ca^{2+} is increased when RyR is bound to ATP. RyR P_o is increased at a lower $[Ca^{2+}]_i$ with ATP and so less $[Ca^{2+}]_i$ is required to open the channel. With a higher rate of RyR activation, SR Ca^{2+} release is greater. A large majority of cytoplasmic ATP is bound to Mg^{2+}, only free ATP can bind to RyR_2 (Fill & Copello, 2002; Rousseau, Smith, Henderson, & Meissner, 1986).

Exposure to these physiological agents can alter RyR P_o, thus SR Ca^{2+} release and degree of shortening. This modulation of RyR has no long-lasting effects on inotropy (Fill & Copello, 2002).

1.2.9 Impaired regulation of Ca^{2+} handling in disease

The regulation of Ca^{2+} handling mechanisms can become dysfunctional in disease. A major systolic dysfunction in cardiomyopathies is negative inotropy due to reduced SR Ca^{2+} content. Elevated diastolic SR Ca^{2+} leak is thought to decrease SR Ca^{2+} content in heart failure. This may therefore contribute to loss of contractility (Eisner et al., 2000). SR Ca^{2+} leak can also occur as a result of acidosis due to ischemia. While pH is not a physiological trigger of RyR_2, acidosis can increase the sensitivity of RyR_2 to Ca^{2+} during relaxation, contributing to reduced diastolic SR Ca^{2+} content (Fabiato & Fabiato, 1978).

At physiological concentrations ATP is usually in excess; however impaired metabolism in disease can reduce ATP levels. SERCA is an ATPase requiring which couples ATP hydrolysis to Ca^{2+} uptake. Low [ATP] can promote less efficient, uncoupled reactions, leading to a

reduction in rate of Ca^{2+} uptake. This also contributes to negative inotropy due to a reduction in SR Ca^{2+} Content (Feher, 1984; Takenaka et al., 1982).

The loss of contractile force present in many cardiomyopathies is often still able to maintain a stroke volume due to increased end-diastolic volume (Jacob et al., 1992). This compensatory mechanism is however hindered by diastolic dysfunction such as loss of compliance (Maurer, Spevack, Burkhoff, & Kronzon, 2004).

Ca^{2+} handling instability and delayed autoregulation can lead to the occurrence of alternans. Alternans are alternating short and large Ca^{2+} transients resulting from change in beat-to-beat change in SR Ca^{2+} content (Eisner et al., 2000). Left ventricular alternans are associated with left ventricular dysfunction in cardiomyopathies, as well as in coronary artery disease and systemic hypertension (Nguyen, Cao, Tran, & Movahed, 2013).

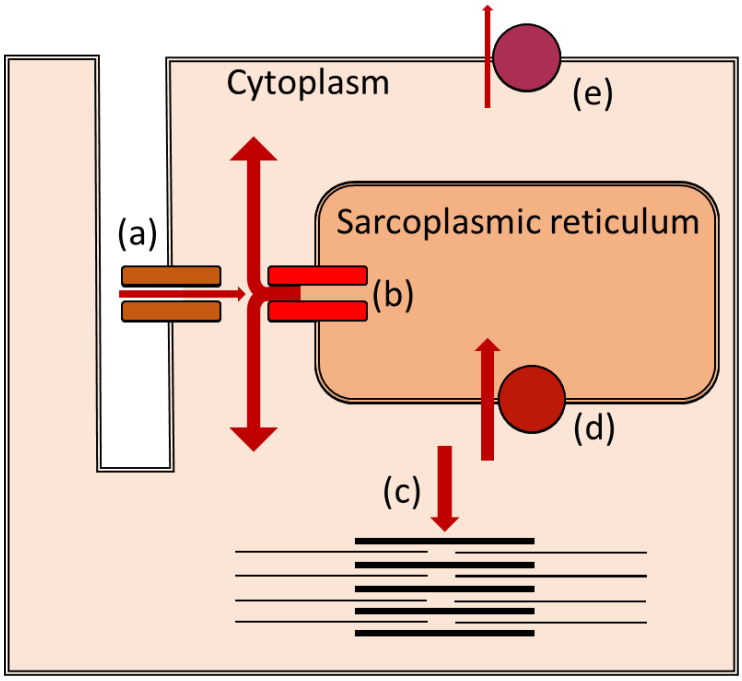

Figure 1-5. A diagram providing an overview of excitation-contraction coupling. The movement of Ca^{2+} has been indicated by red arrows (a) a ventricular action potential activates LTCC leading to a small Ca^{2+} influx. (b) the rise in local $[Ca^{2+}]_i$ leads to SR Ca^{2+} release via RyR. (c) the increase in global $[Ca^{2+}]_i$ activates myofilaments initiating contraction. (d) the majority of cytoplasmic Ca^{2+} is taken up by SERCA to replenish SR Ca^{2+} content. (e) sarcolemmal proteins, primarily NCX, remove the remaining Ca^{2+}, aiding relaxation.

1.3 Cytokines

1.3.1 What are cytokines?

Cytokines are small soluble peptides (<40 kDa) which act as cell signalling molecules mediating autocrine, paracrine or endocrine signalling. Cytokines also have an important role in modulation of the immune response, hematopoietic developmental pathways and inflammation (D. Chen, Assad-Kottner, Orrego, & Torre-Amione, 2008; Chousterman, Swirski, & Weber, 2017; Oppenheim, Matsushima, Yoshimura, Leonard, & Neta, 1989; Ozaki & Leonard, 2002).

Cytokine release is stimulated by the presence of exogenous polysaccharides or bacterial endotoxins, causing levels to be raised in response to infection, however following recovery cytokines levels reduce to the basal level in health (Dinarello, 2007). The high potency of cytokines means that only low concentrations are required to mediate an effect (D. Chen et al., 2008). These effects can be amplified by simultaneous release of different cytokines working synergistically (Oppenheim et al., 1989). The function of different cytokines can overlap due to similarity of the binding motifs on some receptors, enabling these cytokines to share a single signalling pathway (Ozaki & Leonard, 2002).

There are many different forms of cytokines, which include tumour necrosis factors, interleukins, growth factors, interferons and chemokines. The rate of production, release and the longevity of their effects differs between cytokines (Chousterman et al., 2017; Oppenheim et al., 1989).

As the biochemical structure of cytokines differs, they are each able to bind to different receptors. The majority bind only to their own cell membrane receptors in order to activate specific cell signalling pathways (Dinarello, 2007; Oppenheim et al., 1989). Some cytokines are pleiotropic; able to activate multiple signalling pathways, and therefore able to carry out various roles. This pleiotropy can be due to either activation of multiple receptors or activation of receptors capable of activating multiple pathways (D. Chen et al., 2008; Ozaki & Leonard, 2002).

1.3.2 Role of cytokines in the immune response

The primary role of cytokines is to protect the host, through preventing or fighting infection, by mediating an inflammatory or immune response. The expression of cytokines varies in response to different viral and bacterial infections, and some cytokines are present in the absence of infection. TNF-α and Interferon (IFN) -α, -β and -γ expression in the lungs are known to be protective against viral infections such as influenza, through preventing replication and viral load from increasing (Hoshino et al., 1983; Seo & Webster, 2002). IFN-γ also plays a role in prevention against bacterial infection (Sawai et al., 1999).

Proinflammatory cytokines including TNF-α, IL-6, IL-1β and IFN-γ are known to produce intracellular and extracellular ROS on a time and dose dependent basis. Cytokine induced ROS generation can occur through the mitochondria electron transport chain or by nicotinamide adenine dinucleotide phosphate (NADPH) oxidase 2 (Nox2) (Agharazii et al., 2015; D. Yang et al., 2007). ROS generation, particularly those derived from Nox2, can prevent infection and aid pathogen removal. ROS act through either direct oxidative damage to pathogens, activating other host immune responses or promotion of cell death pathways in microbes and infected host cells (Paiva & Bozza, 2014).

In health cytokines are present in serum at much lower concentrations. Changes to basal serum cytokine concentrations occur with age, with many cytokines increasing in the elderly. With increased age, various interleukins increase in serum by ~10–40 fold, while TNF-α maintains a stable concentration in serum throughout the lifespan (Scheinert et al., 2015).

1.3.3 The role of cytokines in inflammation and disease progression

While cytokines can be beneficial in fighting infection, if serum cytokine concentrations remain high following recovery from infection, this can lead to autoimmune disease. TNF-α is the dominant cytokine present in autoimmune diseases (Dinarello, 2007). Some cytokines are associated with specific disease states. IL-4, IL-13, and IL-5 which all mediate the chronic

inflammatory response involved in various allergic diseases including asthma (Ngoc, Gold, Tzianabos, Weiss, & Celedon, 2005).

Cytokines can also contribute to infectious disease pathogenesis. Duration of exposure can impact the overall effect a cytokine has on the body and whether it is negative or positive on health. IFN-γ initially prevents progression of stomach infection by *Helicobacter pylori* through decreasing the magnitude of colonisation. Prolonged exposure to IFN-γ has been shown to also contribute to the gastric inflammation and exacerbate symptoms (Sawai et al., 1999).

Many pleiotropic cytokines have both positive and negative effects, such as association with both regulation of host response and disease progression (Dinarello, 2007). Carswell et al. (1975) found that TNF-α is cytotoxic to tumour cells however more recently TNF-α was also found to promote cell growth. Similarly, proinflammatory cytokines including IL-6 are elevated in breast and pancreatic cancer, with the additional involvement of TNF-α and IL-1β in the latter. Increased IL-6 expression has been suggested to be involved in tumour progression, metastases and a poorer clinical outcome, although there is also evidence that IL-6 can mediate a tumour-suppressive host response (Farajzadeh Valilou, Keshavarz-Fathi, Silvestris, Argentiero, & Rezaei, 2018; Zhang & Adachi, 1999). Although cytokines are classified into pro- and anti-inflammatory, some cytokines, such as IL-6, have properties of both. IL-6 is primarily proinflammatory but can drive anti-inflammatory pathways by down-regulation of both TNF-α and IL-1, and up-regulation of IL-1Ra (Thakur et al., 2002).

It is not only proinflammatory cytokines which have this dual role in disease prevention and progression. The anti-inflammatory cytokine IL-10 has varying effects on tumour migration and is capable of both preventing angiogenesis and encouraging cell proliferation (L. Li et al., 2017). Similarly, IL-2 has an important role in immunity, responsible for cytotoxic T-cell production, however following organ or tissue transplantation IL-2 promotes graft-versus-host disease (Dinarello, 2007).

In order to mediate the inflammatory response, the proportions of proinflammatory or anti-inflammatory cytokines can change. When balanced each can neutralise the others' effects,

whereas if the proportion of one outweighs the other, this determines the overall inflammatory response. If this response is excessive this can bring about dysfunction. Infection or injury initially drives proinflammatory cytokine production (Thakur et al., 2002) (A. Kumar, Kumar, Paladugu, Mensing, & Parrillo, 2007). The ratio of proinflammatory cytokines such as TNF-α and IL-6, to the anti-inflammatory IL-10 can determine the overall inflammatory response. Higher TNF-α and IL-6 relative to IL-10 can indicate an excessive inflammatory response in systemic inflammation. The compensatory increased release of anti-inflammatory cytokines however, can raise concentrations beyond that of proinflammatory cytokines. This can lead to anti-inflammatory response syndrome following systemic inflammation (Jerin et al., 2003; Mannick, Rodrick, & Lederer, 2001). In infection, IL-1β levels increase, this cytokine is a very commonly involved in autoinflammatory disease. The ratio between the proinflammatory IL-1β and the competitive inhibitor IL-1Ra can determine whether a proinflammatory response is generated. The proportions of IL-1β to IL-1Ra can indicate disease severity, with excess IL-1Ra reducing severity (Dinarello, 2007; Mannick et al., 2001; Thakur et al., 2002).

The proportion of different individual cytokines expressed is important as imbalance – not solely between proinflammatory and anti-inflammatory cytokines, but also those with contrasting roles – can result in disease development. Oestrogen is known to regulate the expression of various proinflammatory cytokines to promote bone remodelling. TNF-α, IL-1β and IL-6 encourage bone resorption with a concentration dependant effect on loss of bone density. In the absence of oestrogen, the production of these cytokines is increased to beyond that of Interferon-γ (IFN-γ) and leukaemia inhibitory factor (LIF) involved in inhibition of bone resorption. In this case imbalance of cytokines leads to development of postmenopausal osteoporosis (Zheng et al., 1997).

The accumulation of ROS due to increase in ROS production by proinflammatory cytokines or reduced expression of antioxidant enzymes, leads to oxidative stress which contributes to inflammation in disease. ROS can also modulate on some downstream signalling pathways which can lead to further complications in disease (Agharazii et al., 2015; D. Yang et al., 2007). At high levels mitochondrial ROS can act on signalling pathways which further promote release of proinflammatory cytokines including TNF, IL-1β, IL-6 and IL-18,

amplifying the signal (Naik & Dixit, 2011). While ROS can be beneficial to fighting infection, some pathogens favour oxidative stress conditions (Paiva & Bozza, 2014).

1.3.4 TNF-α and IL-1β are major regulators of inflammation

Tumour necrosis factor-alpha (TNF-α) and Interleukin-1-beta (IL-1β) are proinflammatory cytokines which exert very similar effects on cells. They share important roles in both host response to an infectious stimulus and tissue repair following injury (Mann & Young, 1994; Oppenheim et al., 1989).

1.3.4.1 Tumour necrosis factor-alpha

TNF-α, also referred to as cachectin, was first identified by Carswell et al. (1975). TNF-α is sourced from macrophages, as well as non-immune cells such as endothelial cells and myocytes under some conditions. This release is induced by exposure to endotoxins and can mediate the cytotoxicity of activated macrophages. The protein structure of TNF-α is made up of 17 KDa monomers which unite to form a trimer (Blum & Miller, 2001; Eck & Sprang, 1989). TNF-α primarily interacts with a cell through binding to transmembrane receptors including the 55 kDa TNF receptor-1 (TNFR1) and 75 kDa TNF receptor-2 (TNFR2) with different effects, but is also able to bind to other receptors (Idriss & Naismith, 2000; Kelly et al., 2010; Monden et al., 2007).

1.3.4.2 Interleukin-1-beta

IL-1β, also known as cataboline, is released from a variety of cells including macrophages and monocytes. The 31 kDa inactive IL-1β precursor becomes active in response to molecules released from dead cells and pathogens, such as endotoxins (Blum & Miller, 2001; Chaudhry et al., 2013; Lopez-Castejon & Brough, 2011).

IL-1β also has multiple receptors; the type I IL-1 receptor (IL-1RI) and the type II IL-1 receptor (IL-1RII). IL-1RI is found on the surface of multiple cells, however the effect of cytokine exposure is dependent upon the target cell. IL-1β binding to IL-1RI has been associated with stress and immune responses (Oppenheim et al., 1989; Subramaniam, Stansberg, & Cunningham, 2004). IL-1RI are not in abundance, however very few interactions per cell (<10) with either IL-1α or IL-1β are required to achieve a strong signal through simultaneous activation of multiple pathways, promoting inflammation. Competitive inhibition of IL-1α and IL-1β binding to the IL-1RI by the IL-1 receptor antagonist (IL-1Ra) prevents inflammation. IL-1RII, found predominantly on immune cells, provides a negative feedback mechanism through binding and neutralising IL-1β precursor. This inhibits the activation of pathways from IL-1RI binding (Chaudhry et al., 2013; Subramaniam et al., 2004).

1.3.5 The role of cytokines in sepsis

In response to infection, pathogen associated molecular patterns (PAMPs) and bacterial endotoxins present in serum or at the site of infection promote increased cytokine production.

This cytokine recruitment is meant to help coordinate the immune response, and thus fight the infection. As infection and inflammation is systemic in sepsis, the cytokine response is overwhelming, this is known as a cytokine storm. At these concentrations, cytokines are harmful, initially promoting fever in patients and mediating direct organ dysfunction (Chaudhry et al., 2013; Markel et al., 2007).

Circulation of both proinflammatory and anti-inflammatory cytokines increases in sepsis. The main proinflammatory cytokines increased include IL-6, IL-8, IL-12, IL-18, IFN-γ, TNF-α and IL-1β. TNF-α and IL-1β responses are much greater in sepsis when compared to systemic inflammation resulting from a non-infection associated injury, both are associated with cardiac dysfunction in sepsis. Due to their ability to work synergistically, low concentrations are effective. Other proinflammatory cytokines present are responsible for recruitment of inflammatory cells, further promoting inflammation (Chaudhry et al., 2013; Jerin et al., 2003;

A. Kumar et al., 1996; Mera et al., 2011). Due to the excessive inflammation which occurs in sepsis, anti-inflammatory therapies targeting proinflammatory cytokines, particularly TNF-α and IL-1β, have been investigated as possible treatments. Anti-TNF-α has only been able to induce a modest reduction in the mortality of patients with sepsis. The results of combined anti-inflammatory therapies targeting both TNF-α and IL-1β activity is dependent on patient mortality risk, only effective in patients with a high risk of death (Eichacker et al., 2002; P. Qiu et al., 2013).

IL-10 is an important anti-inflammatory cytokine elevated in septic serum (A. Kumar et al., 1996). IL-10 is a known deactivator of cytokine synthesis, able to suppress production of proinflammatory cytokines including IL-1, IL-6, IL-8, IL-12 and TNF-α (Chaudhry et al., 2013; Mera et al., 2011). IL-4 and IL-13 release is also greater in sepsis (Fernandez et al., 2013; A. Kumar et al., 1996). IL-13 is able to inhibit cytokine expression and production including that of TNF-α. IL-4 and IL-13 have similar anti-inflammatory effects and the role of both unclear in sepsis as neither appears to be involved in host defence response against infection (Chaudhry et al., 2013).

While the concentration of many cytokines is unchanged regardless of the stage and severity of sepsis, some relative cytokine concentrations can be used as indicators of sepsis severity and prognosis. A reduction in circulating IL-6 is an indicator of good prognosis, while high IL-10 levels are associated with increased mortality (Chaudhry et al., 2013). There are conflicting reports on which stage of sepsis is indicated by high IL-10; Fernandez et al. (2013) found high IL-10 in patients with septic shock, while Mera et al. (2011) reported high levels of IL-10 in the serum of patients with less severe sepsis. Septic shock is also denoted by elevated levels of IL-6 and IL-13 (Fernandez et al., 2013).

Severe sepsis presents with low IL-2 and high IL-8 in septic serum. The persistent high levels of certain cytokines such as IL-1β, IL-6, IL-8, IL-12, IFN-γ and IL-18 correlate with elevated risk of death. IL-8 is further elevated in non-survivors (Mera et al., 2011). This large elevation in IL-8 as an indicator of death was confirmed in a larger cohort of patients with post-surgical associated sepsis by Fernandez et al. (2013).

In some patients with sepsis, death occurs from secondary causes which are not associated with hyper-inflammation. This suggests that in some individuals, defective cytokine production follows the excessive inflammatory phase in severe sepsis. This may also occur as a result of excess anti-inflammatory cytokine production, leading to compensatory anti-inflammatory response syndrome. The immunosuppression in these individuals may allow the initial infection causing sepsis to thrive and make the patient vulnerable to further infection from opportunistic pathogens (Boomer et al., 2011; Mannick et al., 2001).

1.3.5.1 The role of cytokines in myocardial depression in sepsis

Cytokines are known to be elevated in sepsis as discussed above, in section 1.3.5. This has been directly associated with myocardial depression. The diastolic and systolic features of myocardial depression were discussed in sections 1.1.6.1 and 1.1.6.2. An important aspect of myocardial depression is a reduced LVEF. In sepsis, this decrease in LVEF, and on occasion also reduced RVEF, is due to reduced myocardial contractility. This contributes to decreased cardiac output and increased end-diastolic volume (Court et al., 2002; Kimchi et al., 1984; Ognibene et al., 1988; Parker et al., 1984; Parrillo, 1989). As per section 1.1.8.2, TNF-α has been shown to reduce the ventricular ejection fraction in patients and animal models (Muller-Werdan et al., 1998; Vincent et al., 1992). TNF-α and IL-1β exposure has also been shown to induce an ultimate reduction in cardiac work and coronary flow. The latter would be expected with a reduced LVEF (Schulz et al., 1995).

Impaired relaxation and loss of compliance has also been identified in many patients with septic shock (Bouhemad et al., 2008; Meierhenrich et al., 2008). These may also be associated with TNF-α and IL-1β exposure. The known cellular effects of these cytokines, particularly altered ECC, shall be discussed further in section 1.3.7.

1.3.6 Cytokines in heart failure

Cytokines are released to aid recovery from myocardial injury, however they can also play an important role in the development and progression of heart failure due to the resulting inflammatory response (D. Chen et al., 2008; Gullestad et al., 2012; Monden et al., 2007). In both HF with both reduced and preserved EF the circulating concentrations of proinflammatory cytokines TNF-α, IL-1β and IL-6 are elevated (Gullestad et al., 2012). Heart failure with reduced EF can be induced by overexpression of these cytokines, as well as IL-2, can also induce biventricular dilatation. This cardiac depression can result in premature death (Blum & Miller, 2001; Bryant et al., 1998).

TNF-α and IL-6 contribute to the development of chronic heart failure and acute decompensated heart failure with preserved EF. While TNF-α is generally high in stable heart failure patients, IL-6 is elevated further in acutely decompensated heart failure. TNF-α and IL-6 are therefore useful biomarkers for severity and outcome (Abernethy et al., 2018; D. Chen et al., 2008).

Injury from myocardial infarction (MI) increases the risk heart failure development. ROS and danger-associated molecular patterns (DAMPs) are released due to ischemia-reperfusion injury and mechanical stress in MI. Post-MI, both ROS and DAMPs promote cytokine release including TNF-α, IL-1β and IL-6 in the myocardium (Gullestad et al., 2012; Monden et al., 2007).

Following a cardiac event such as MI, ischemia or another form of myocardial injury, TNF-α levels rise and bind to available soluble TNF receptors. The proportion of these receptors circulating changes in heart failure and can be used to determine prognosis (Gullestad et al., 2012; Kelly et al., 2010; Monden et al., 2007). TNF-α binding to TNFR1 promotes cardiac remodelling, this is a mechanism by which the heart can adapt to decreased cardiac output, as is partially accomplished in HF with preserved EF. If this fails however, the ability to provide adequate cardiac output may decrease further, as in HF with reduced EF (Mann & Young, 1994; Monden et al., 2007). Different types of cardiac remodelling occur in HF, wall thickness is increased in HF with preserved EF, while apoptosis and fibrosis are up-regulated

in HF with reduced EF (Gullestad et al., 2012). Interaction with the TNFR1 also can be detrimental to recovery, inducing reversible contractile dysfunction and dilation, particularly in the left ventricle, associated with and time and TNF-α concentration dependant reduction in systolic Ca^{2+}. This receptor also activates signalling pathways further elevating production of other proinflammatory cytokines (D. Chen et al., 2008; Kelly et al., 2010; Monden et al., 2007; Yokoyama et al., 1993). This effect on ventricular dysfunction is lessened with TNF-α bound to TNFR2, encouraging improved myocardial function, decreased apoptosis and reduced damaging cardiac remodelling, aiding both survival and recovery (Kelly et al., 2010; Monden et al., 2007).

Anti-inflammatory cytokines also have important roles in HF. IL-10 contributes to diastolic dysfunction in through promoting biventricular dilatation (Blum & Miller, 2001). The presence of transforming growth factor-β1 (TGF-β1) has both positive and negative effects on HF. TGF-β1 can prevent or reduce the cardio-depressant effect of proinflammatory cytokines, including TNF-α and IL-1β, on a dose dependent basis. TGF-β can however also encourage fibrosis and ECM remodelling (Gullestad et al., 2012; A. Kumar et al., 2007).

The dual function of proinflammatory cytokines in both supporting and worsening health, may suggest why there has been a mixed response to anti-cytokine treatments such as TNF-α and IL-1β inhibitors in treating myocarditis and systemic inflammation (Eichacker et al., 2002; Monden et al., 2007; P. Qiu et al., 2013).

1.3.7 Role of cytokines in perturbed EC coupling

Given that cytokines – especially TNF-α and IL-1β – are associated with negative inotropy and diastolic dysfunction in the whole heart, it is important to determine how these cytokines effect Ca^{2+} handling and contractility on a cellular level.

While in sepsis cardiac dysfunction can occur in both ventricles, LV dysfunction is much greater than in the RV in myocardial depression. In response to endotoxin release from pathogens in sepsis, cytokine levels and cytokine receptor expression increases in the heart.

The distribution of cytokines and their receptors in tissues varies, as such the proportion of TNF-α release is greater in the RV (Markel et al., 2007; Oppenheim et al., 1989). Markel et al. (2007) demonstrated that the RV may be more resistant to TNFR1 signalling than the LV. The TNFR1 resistance and elevated TNF-α levels and TNFR2 expression promote TNFR2 signalling, driving recovery through activation of protective signalling cascades (Monden et al., 2007).

1.3.7.1 Global [Ca^{2+}] and contractility

Greensmith and Nirmalan (2013) studied the effect of TNF-α on rat ventricular myocytes. They found that 50 ng/ml TNF-α decreased Ca^{2+} transient amplitude by 31 % and contractility by 19 %. This provides a cellular basis for systolic dysfunction in myocardial depression in sepsis. A myocardial depressant effect has also been observed in rat ventricular myocytes which were exposed to serum containing elevated proinflammatory cytokines, including both TNF-α and IL-1β. The serum induced a 20 % decrease in Ca^{2+} transient amplitude resulting in reduced myocyte shortening (Fernandez-Sada et al., 2017). While the relative decrease in Ca^{2+} transient amplitude and contractility is not to the same magnitude as found by Greensmith and Nirmalan (2013), the serum used contained a lower concentration of TNF-α, alongside other components such as leptin.

IL-1β is also proven to have a negative inotropic effect on rat ventricular myocytes. Following a 30 minute incubation with 10 ng/ml, IL-1β Ca^{2+} amplitude was reduced and contractility was depressed (Radin et al., 2008). Leptin was also high in the serum used by Fernandez-Sada et al. (2017), while leptin has a small negative inotropic effect on its own, it has been shown to interact with IL-1β preventing IL-1β induced myocardial depression (Radin et al., 2008).

TNF-α and IL-1β have been found to work synergistically in rat ventricular myocytes. With prolonged (3 hour) simultaneous application, TNF-α (0.05 ng/ml) and IL-1β (2 ng/ml) induce a 40 % decrease in Ca^{2+} transient amplitude and 46 % reduction is cell shortening (Duncan, Yang, Hopkins, Steele, & Harrison, 2010).

Less evidence has been identified which could provide a cellular basis for diastolic dysfunction in the heart. Both Greensmith and Nirmalan (2013) and Duncan et al. (2010) found no change to resting cell length, with TNF-α, or combined TNF-α and IL-1β treatment.

1.3.7.2 SR Ca^{2+} content and CICR

Negative inotropy can be caused by a reduction in Ca^{2+} influx. Both TNF-α application and prolonged (24 hour) IL-1β exposure leads to rapid inactivation of the LTCC and decreased in L-type Ca^{2+} current density, reducing Ca^{2+} influx (El Khoury, Mathieu, & Fiset, 2014; Greensmith & Nirmalan, 2013). The impact of IL-1β on LTCC was suggested to be a combination of ROS signalling and protein kinase C (PKC) activation (El Khoury et al., 2014). In both cases, the cytokine-mediated decrease in Ca^{2+} influx would also contribute to myocardial depression, through its impact on CICR.

In work by Greensmith and Nirmalan (2013) the decrease in Ca^{2+} transient amplitude was attributed to a 14 % decrease in SR Ca^{2+} content. This is contrary to work by Jha et al. (1993) who reported that SR Ca^{2+} content was unaffected in dog hearts perfused with *E.coli*-related septic serum.

There is also evidence that RyR P_o may be altered with these cytokines, which would provide a possible mechanism for decreased SR Ca^{2+} content Spontaneous Ca^{2+} release from the SR has been identified in a rat model of sepsis (X. Zhu et al., 2005). In rat myocytes Duncan et al. (2010) demonstrated that this SR Ca^{2+} leak can be induced through synergistic treatment with TNF-α and IL-1β. These cytokines increase the frequency of Ca^{2+} sparks by more than four-fold. During electric stimulation, the distribution of Ca^{2+} release was uneven across the myocyte due to depolarisation by NCX-mediated Ca^{2+} removal. IL-1β also individually increases spontaneous Ca^{2+} release from the SR in mice ventricular myocytes (Monnerat et al., 2016). While this evidence supports that cytokines, particularly TNF-α and IL-1β, cause SR Ca^{2+} leak, another study by Jha et al. (1993) found that Ca^{2+} release from the SR was not impaired by exposure to septic serum.

Proinflammatory cytokine exposure, including to TNF-α and IL-1β, does not only induce myocardial depressant effects. The impaired Ca^{2+} handling can also be a precursor for ventricular arrhythmia in those with existing medical conditions, such as in patients with sepsis, where the prevalence of ventricular arrhythmias increases (Fernandez-Sada et al., 2017; Shahreyar et al., 2018). Both TNF-α and IL-1β have been associated with increased frequency of spontaneous waves due to propagation of Ca^{2+} sparks and thus increases the likelihood of arrhythmia development (Duncan et al., 2010; Monnerat et al., 2016; Shahreyar et al., 2018).

The effects of TNF-α and IL-1β on RyR P_o shall be discussed and investigated further in chapter 5.

1.3.7.3 Ca^{2+} removal mechanisms and relaxation

Both Greensmith and Nirmalan (2013) and Duncan et al. (2010) found no recorded change in diastolic function, including rate of Ca^{2+} decay or rate of relaxation in response to application of TNF-α alone, or with IL-1β. This suggests that the combined Ca^{2+} removal mechanisms – SERCA and NCX – were unaffected by these cytokine treatments. These studies could therefore not yet provide a cellular basis to account for diastolic dysfunction also present in myocardial depression.

Fernandez-Sada et al. (2017) did find diastolic dysfunction in the form of increased Ca^{2+} decay time and subsequent myocyte relaxation in response to septic serum. It is possible that another component of the serum besides TNF-α, possibly IL-1β, may be responsible for the increased relaxation time, this warrants further investigation. Radin et al. (2008) confirmed that IL-1β could reduce rate of Ca^{2+} removal and induce prolonged relaxation. Bouhemad et al. (2008) found that in ~41 % patients with septic shock, expression of the cytokines; TNF-α, IL-8 and IL-10, and the cardiac contractile regulatory protein TnI were elevated. This was associated with reversible diastolic dysfunction through impaired LV relaxation, as well as systolic dysfunction, especially in individuals where TnI expression had increased by >50 %. This may also allude to a possible mechanism for change in myofilament

sensitivity to Ca^{2+}. While some studies have investigated the effects of these cytokines on myofilament sensitivity to Ca^{2+}, this shall be discussed further in section 5.1.3.

1.4 Main aims

While current evidence supports that TNF-α and IL-1β contribute to myocardial depression through altered Ca^{2+} handling, the reported changes to Ca^{2+} handling are variable. Many of these studies have investigated the effects of intact septic serum or the combined effects of multiple cytokines on ventricular myocytes, the numerous cytokines or other components present make it difficult to distinguish the individual effects of TNF-α and IL-1β.

Of the studies which have attempted to characterise the individual effects of these cytokines on intracellular Ca^{2+} handling, many have not used an integrative approach, for instance by not measuring the simultaneous effects of these cytokines on contractility. The majority of previous work has also been carried out in small mammal models, and as such may not be entirely representative of the condition in large mammals such as humans. This work aims to initially investigate whether the findings of Greensmith and Nirmalan (2013) are reproducible in a large mammal model. The effect of IL-1β on Ca^{2+} handling in large mammal left ventricular myocytes will also be investigated, as few studies have looked at the individual effects of IL-1β, in this way.

The 1^{st} beat increase in systolic Ca^{2+} amplitude with application of TNF-α previously acknowledged by Greensmith and Nirmalan (2013) will also be investigated further, alongside a more thorough, robust determination of the individual effects of both TNF-α and IL-1β on RyR $P_{o.}$

Whilst some work has explored the effects of these cytokines on myofilament sensitivity to Ca^{2+}, once again many used small mammal models, and very few studied the effects of IL-1β alone. As such, the effects of both cytokines on myofilament sensitivity to Ca^{2+} shall be characterised in a large mammal model. A better understanding of the impact of elevated TNF-α and IL-1β in sepsis on all aspects of ECC in ventricular cardiac myocytes may aid

treatment of myocardial depression. This may also be preventative of further damage to other organs and systems.

In heart failure, cytokines – including TNF-α – are also elevated and in some cases aspects of myocardial depression feature in heart failure patients. This study shall also investigate the effects of TNF-α in cells isolated from a large mammal heart failure model and a heart failure 5 week recovery model, and whether the magnitude of these changes differs from the young, healthy model. This could potentially indicate whether heart failure patients, or those in recovery, are more or less susceptible to the myocardial depressant effects of TNF-α. The study may also reveal if the effects of TNF-α have already been saturated due to the prior effects on Ca^{2+} handling and contractility in heart failure and possible previous exposure to high TNF-α serum concentrations.

Chapter 2

General methodology

2.1 Primary myocyte isolation and preparation

2.1.1 Animals, tissue preparation and ethics

Mid-myocardial left ventricular myocytes and tissue were isolated from young control sheep at approximately 18 months old and in good health at the University of Manchester. Other experimental ovine models used were a tachypaced induced heart failure model and a heart failure recovery model, in which tachypacy was ceased 5 weeks prior to sacrifice, to enable potential recovery to occur.

All surgical procedures involved in the development of the heart failure and heart failure recovery models were carried out under analgesia (meloxicam, 0.5 mg/kg) and anaesthesia (isoflurane, 1-4 % in oxygen). The antibiotic (enrofloxacin 2.5 mg/kg) was also administered to prevent infection. The surgical procedure involved implantation of a pacemaker in the right ventricle, this shall be discussed further in section 6.2.1.

2.1.2 Ethics

All procedures accord with the Animals (Scientific Procedures) Act, UK, 1986 and Directive 2010/63/EU of the European Parliament (Home Office, 1986). Ethical approval was also sought from both the University of Salford ethical review board. All procedures were carried out at The University of Manchester and as such were also approved by The University of Manchester Welfare and Ethical Review Board.

2.1.3 Isolation of sheep left ventricular myocytes

Sheep were given heparin (10-20 ml) intravenously and then killed by lethal injection of sodium pentobarbitone (200 mg/kg). The administration of heparin was required to prevent formation of blood clots. Cardiothoracic incisions were made to gain access to the heart and enable rapid removal. The heart was then rinsed and briefly stored in Ca^{2+} free isolation

solution (see table 2-1 for components) to remove excess blood and prevent tissue deterioration.

The ventricles were cut away from the rest of the heart to allow sole isolation of ventricular myocytes. The left ventricle was then cannulated via the coronary artery onto Langendorff apparatus, as shown in Fig 2-1. The tissue of the left ventricle was perfused with Ca^{2+} free isolation solution for 10 minutes removing blood from the tissue, and enabling control over components present during the initial heart isolation and subsequent digestion. This also serves to prevent clots and thus maximising the perfused region of the left ventricle. Flow rate of solution and pressure within tubing and circulatory vessels was regulated with a peristaltic pump (Fig 2-1).

To facilitate cell disassociation from the tissue, collagenase type I (Worthington) (0.096-0.108 mg/ml) and protease (Sigma) (~ 0.022 mg/ml) were then added to the perfusate in order to digest the collagen fibres and other extracellular matrix (ECM) proteins involved in cell adhesion. Enzyme concentration and perfusion times (typically within a range of 5-15 minutes) were adjusted to optimise cell quality and yield. Tissue digestion was determined by several observations; increased tissue translucency and viscosity of perfusate. All solutions used were preheated to 37°C in a water bath, which is within the optimal temperature window for the digestive enzymes used.

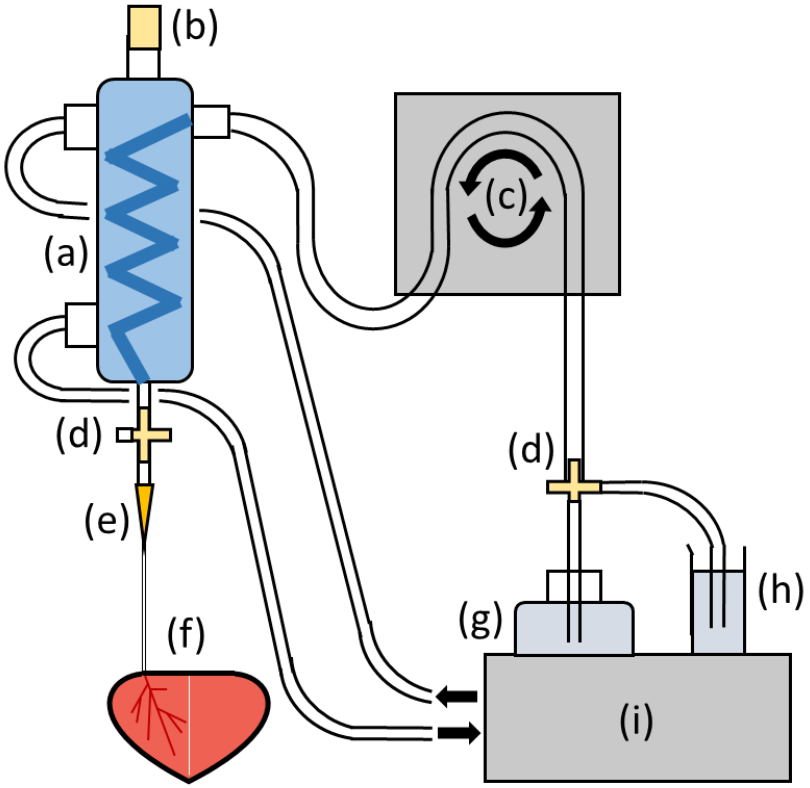

Figure 2-1. Langendorff apparatus set up for myocyte isolation. (a) heat exchanger (b) cork sealing the coil within the heat exchanger. (c) peristaltic pump. (d) multi-way taps. (e) cannula. (f) cannulated sheep ventricle. (g) Ca^{2+} free isolation solution. (h) low Ca^{2+} taurine solution. (i) water bath.

Table 2-1 – Components of the Ca^{2+} free isolation solution	
Ingredients	Concentration (mM)
BDM	10
NaCl	133
HEPES	10
Glucose	11.1
BSA	7.5
KCl	4
$MgSO_4$	1.2
NaH_2PO_4	1.2
The pH of was adjusted to 7.34 at room temperature (~22°C) through addition of either 1 M NaOH or 1 M HCl prior to volumizing.	
All components sourced from Sigma-Aldrich or Fisher	

Following digestion, the perfusate was switched to a low Ca^{2+} (0.1 mM) taurine (50 mM) containing solution for 20 minutes. This served as a wash to remove residual enzyme. As described in table 2-3, taurine supports restoration of contractile function with the reintroduction of Ca^{2+} and prevent Ca^{2+} overload. The digested area of the left ventricle was then dissected, and the epicardium and endocardium were removed. Remaining tissue was minced and agitated using a pasteur pipette in fresh taurine solution, then filtered through a net mesh (200 µm pores).

Table 2-2 – Components of the low Ca^{2+} taurine perfusion solution	
Ingredients	Concentration (mM)
BDM	10
NaCl	108
HEPES	10
Glucose	11.1
BSA	7.5
KCl	4
$MgSO_4$	1.2
NaH_2PO_4	1.2
Taurine	50
$CaCl_2$	0.1
The pH was adjusted to 7.34 at room temperature (~22°C) through addition of either 1 M NaOH or 1 M HCl prior to volumizing.	
All components sourced from Sigma-Aldrich or Fisher	

Table 2-3 – Importance of solution components to cell survival during isolation	
Component	Importance
Ca^{2+}	The absence of Ca^{2+} is known to weaken cell adhesion, promoting the release of myocytes during enzymatic digestion (Dolara, Agresti, Giotti, & Pasquini, 1973; Vendome et al., 2011; Yates & Dhalla, 1975). Ca^{2+} increases collagenase activity, therefore in its absence there is a reduced the risk of over-digestion (Head & Yankeelov, 1976). Ca^{2+} must be reintroduced promptly following digestion, as prolonged Ca^{2+} free perfusion contributes to structural damage and loss of function (Yates & Dhalla, 1975).
BDM	Cardioprotective against the effects of hypoxia and ischemia. Inhibits contraction by ~82 %, delaying hyper-contracture during myocyte isolation (Zimmermann et al., 1996). Enhances the yield of viable, Ca^{2+} tolerant cells, prevents bleb formation and slow the rate of degradation (Kivisto et al., 1995; Thum & Borlak, 2001). Not included in experimental solution due to its negative inotropic nature.
Taurine	Slows the rate of Ca^{2+} release from myocytes when perfused with Ca^{2+} free solution. Helps maintain osmotic pressure and prevents Ca^{2+} overload, promoting contractile recovery upon Ca^{2+} reperfusion (Hansen, Andersen, Birkedal, Cornett, & Wibrand, 2006; Suleiman, Rodrigo, & Chapman, 1992).
BSA	Prevents tissue damage through oedema during isolation, by maintaining colloid osmotic pressure (Suelter & DeLuca, 1983).
HEPES	Used to buffer pH. This has a higher efficiency than other traditionally used bicarbonate buffers due to its reduced influence from fluctuations in carbon dioxide from metabolism (Baicu & Taylor, 2002; Good et al., 1966).
Glucose	Provides an energy source to enable metabolism, thus extending the survival of the isolated myocytes (Locke, 1895).

2.1.4 Myocyte storage and loading with Ca^{2+} indicators

Freshly isolated cells were viewed at 40 x magnification using oil immersion. Good quality, viable cells were identified by their characteristic morphological features; a distinctive rod shape and striated structure. Dead or non-viable cells were identified by their round shape due to hyper-contracture (Kivisto et al., 1995). Cells were suspended in fresh solution, allowing them to be diluted or concentrated, dependent on the yield of viable cells.

Prior to experimentation, cells were stored at room temperature and loaded in an intermediate solution, gradually elevating the Ca^{2+} concentration to that of the experimental solution in under to prevent Ca^{2+}overload, which could result in cellular damage. In the majority of experiments the desired Ca^{2+} was 1.8 mM, and therefore cells were stored in a (50:50) taurine:Tyrodes solution (approximately 0.95 mM Ca^{2+}).

Preparation of the stock solution for the Ca^{2+} indicator, Fura-2, was carried out by a reconstituting 1 mg of desiccated Fura-2 in its cell-permeant acetoxymethyl (AM) ester form (Thermofisher) in pluronic F-127 (20 % solution in DMSO). The stock was stored in the dark at -20°C for use within the following month.

An alloquot of cells suspended in the afore-mentioned taurine:Tyrodes 1:1 storage solution (3-4 ml) were loaded with Fura-2-AM (final concentration 0.1 mM) for 10 minutes. Loading was effectively stopped by addition of excess solution. These cells were left for at least ~25 min to allow de-esterification of Fura-2. The attachment of AM ester to the Fura-2 neutralises the indicators charge allowing intracellular loading through passive diffusion across the membrane. Esterases present in the cytoplasm cleave the AM esters by hydrolysis preventing the now charged, hydrophilic fluorophore from leaving the cell in its pentacarboxylate form. Loading was ceased by diluting the cells further, thus reducing the indicator concentration (Takahashi, Camacho, Lechleiter, & Herman, 1999). Unlike some other fluorphores Fura-2-AM is fluorescent prior to cleaving of the AM, as such cells were re-suspended to remove residual Fura-2. Throughout and after loading, the vial of cells was surrounded by foil to prevent photobleaching from exposure to light.

2.2 General procedures and equipment

2.2.1 Standard experimental solution

Tyrode's solution is an isotonic solution developed by Maurice Tyrode, following the adaption of Ringer's solutions to the mammalian heart by Locke (1895). Unlike its predecessors, Tyrodes's solution contains magnesium. In the standard experimental solution (table 2-4) and all other experimental solutions used in this study, $MgCl_2$ concentration was kept constant as variability in magnesium concentration can impact Fura-2 emission intensity (Grynkiewicz, Poenie, & Tsien, 1985).

Table 2-4 – Components of standard experimental solution (Normal Tyrode's)

Ingredients	Concentration (mM)
NaCl	140
HEPES	10
Glucose	10
BSA	15
KCl	4
$MgCl_2$	1
$CaCl_2$	1.8
Probenecid (dissolved in NaOH)	2
The pH was adjusted to 7.34 at room temperature (~22°C) through addition of either 1 M NaOH or 1 M HCl prior to volumising	
All components sourced from Sigma-Aldrich, Fisher or Fluka	

Tyrode's solution was stored for up to 5 days at 4 °C, without $CaCl_2$ and glucose to reduce the risk of bacterial growth. Both were added on the day of use. While the solutions used in

myocyte isolation contained BSA to maintain colloid osmotic pressure (as described in table 2-3), a higher concentration of BSA (0.1 %, 15 mM) was added to experimental solutions to serve an additional purpose. BSA adsorption to the inner surface of tubing, through either priming tubing with BSA or addition to carrier solutions, is a traditional and effective method of preventing non-specific interactions between the surface and other proteins in solution (Suelter & DeLuca, 1983).

While Fura-2 in its penta-carboxylate form is unable to passively diffuse across the membrane, Fura-2 is an organic anion, and thus efflux can be carried out via organic anion transporters. The rate of indicator secretion of from the cell is slower at temperatures below 37 °C. While loaded cells were stored at room temperature (~22 °C) prior to use, during experiments solutions are heated to 37 °C in order to remain physiologically relevant. Through a similar mechanism the indicator can also accumulate in intracellular compartments such as vesicles and organelles, with the potential to lead to cytotoxicity. Both Fura-2 efflux and accumulation can disrupt the fluorescent signal. A known inhibitor of organic anion transport is probenecid (Di Virgilio, Steinberg, & Silverstein, 1989). Due to the low solubility of probenecid, it was first dissolved in a small volume NaOH. pH adjustment was carried out after probenecid was added to the standard experimental (Tyrode's) solution due to the alkaline nature of NaOH. As cells were loaded in taurine:Tyrode's solution 1:1, ~1 mM probenecid was present, this was advantageous as probenecid prevents clearance of Fura-2 from the cell. The de-esterification process and intracellular Ca^{2+} concentration, both at rest and when field stimulated, are unaffected by the presence of probenecid (Di Virgilio, Steinberg, Swanson, & Silverstein, 1988).

2.2.2 Preparation of cytokine solutions

Human, recombinant TNF-α and IL-1β (both obtained from Sigma-Aldrich) were reconstituted in 0.1 % BSA in phosphate-buffered saline (PBS) and stored in aliquots with a stock concentration of 100 µg/ml, at -20 °C. The BSA was added to prevent cytokine adsorption to tubing, which would otherwise result in a decreased final concentration

reaching the cell. This is especially important given the low concentrations being used of both TNF-α and IL-1β in experiments (50 ng/ml).

2.2.3 Pre-experimental preparations

Following the loading protocol, cells were allowed to settle in a cell bath for ~10 minutes. Cells were viewed again, using an epi-fluorescent inverted microscope under x 40 magnification. Immersion oil was used to improve resolution. The previously described characteristic appearance of viable myocytes was used to select cells for experimentation. Those with a granulated appearance, evidence of a disrupted membrane, or cytoskeletal damage such as blebbing, were avoided.

Through perfusion of the cell bath with experimental control solution and field stimulation, it was possible to determine whether contractile function had returned. This was especially important given their previous exposure to BDM. The flow through the bath also aided clearance of debris and dead cells. Some cells began oscillating with the reintroduction to Ca^{2+} at physiological concentrations; these cells were treated as non-viable due to their low tolerance to Ca^{2+}.

Once a viable cell had been identified, it was positioned into the centre of the window with aid of the eyepiece and the imaging provided by an Ion Optix MyoCam-S CCD camera. Blinds were used to isolate the single cell from nearby cells and debris, to ensure the signal recorded belonged solely to that cell.

2.2.4 Control of perfusion

In order for experiments to be physiologically relevant, temperature of all solutions were kept at 37°C. To mitigate bubble formation solutions were preheated using BubbleStop and the inline heating element, ThermoClamp^{TM}-1 (AutoMate Scientific). This controlled temperature of solutions to within 1 °C of 37 °C during experiments.

A ValveLink system (AutoMate Scientific) was used to control perfusion by enabling switching between solutions. Flow rate was controlled by (1) reservoir height and (2) the solution level in the reservoir. To ensure rapid solution switching the perfusion pencil was placed in close proximity to the cell of interest using a 3-dimensional axis mechanical micromanipulator (Narishige). Solution in the cell bath was removed a peristaltic pump, outflow rate was adjusted to match the rate of solution inflow to maintain a stable bath level.

2.2.5 Measurement of intracellular calcium

2.2.5.1 The fluorophores

Fura-2 is a dual excitation indicator with maximum absorption peaks at 335 and 363 nm for maximum and minimum bound Ca^{2+} respectively. When bound to Ca^{2+} and excited at either wavelength Fura-2 emits at 510 nm, described as blue emission (Takahashi et al., 1999). Through measurement of the 510 nm emitted light in response to the both excitation wavelengths, two traces can be formed from, with a positive and negative response to increased Ca^{2+} respectively. The ratio between these signals is unaffected by any loss of signal due to reduced indicator concentration or photobleaching, unlike other non-ratiometric fluorophores, such as Fluo-3. When using Fura-2 it is therefore possible to estimate intracellular Ca^{2+} concentration from these wavelength measurements. In addition to being a ratiometric indicator, Fura-2 also has a high emission intensity (Grynkiewicz et al., 1985).

2.2.5.2 Apparatus configuration

As the equipment measures relative changes in $[Ca^{2+}]$, it was important to limit light from other sources, as such the microscope was concealed in a large case with a blackout curtain covering the front, and additional lights were switched off during an experiment to reduce the noise in the emission signal.

LED light sources excited the cell at both 340 and 380 nm consecutively, alternating at a frequency of 200 Hz regulated by Multistream Pro (Cairn). These wavelengths are routinely used for excitation of Fura-2. The microscope configuration and beam-path are shown in Fig 2-2. Band-pass (BP) excitation filters for 340 and 380 nm respectively were placed in front of each of these LEDs. A 370 nm long-pass (LP) dichroic mirror allowed the 380 nm light beam to pass through, while deflecting the 340 nm light beam, causing beams to converge. 425 nm and 500 nm LP dichroic mirrors were used to redirect the converged 340 nm and 380 nm beams through the objective lens, whilst also eliminating the influence of any light from higher wavelengths. Once the cell had been excited at both 340 nm and 380 nm, emitted light at 510 nm, passed back through the objective lens and through the 500 nm LP dichroic mirror. A series of standard mirrors then deflect the emitted light. Blinds were used to isolate the cell in the field of view, preventing emitted light from the surrounding cells and solution from being processed. A final 600 nm LP dichroic mirror directs this into the photo multiplier tube (PMT). The PMT both detects and amplifies the emitted fluorescent signal. The emitted light from the 340 nm and 380 nm excitation waves length was separated into 2 traces through IonWizard fluorescent acquisition (Ion Optix) software.

A camera (Myocam) was used to allow the cell to be viewed in real-time, thus aiding with placement of the blinds and measurement of contractility (which shall be discussed further in section 2.2.6). To prevent this from interfering with the beam bath of the emitted light, white light from the microscope passed through a 700 nm LP filter, before reaching the cell. This then passed though the objective lens, converging with the emitted 510 nm light, and was redirected by the same 500 nm LP dichroic mirror and standard mirrors. As the light from the microscope light was now sole >700 nm, it was able to pass through the final 600 nm LP dichroic mirror, separating the light from the emitted light and allowing its detection by the camera.

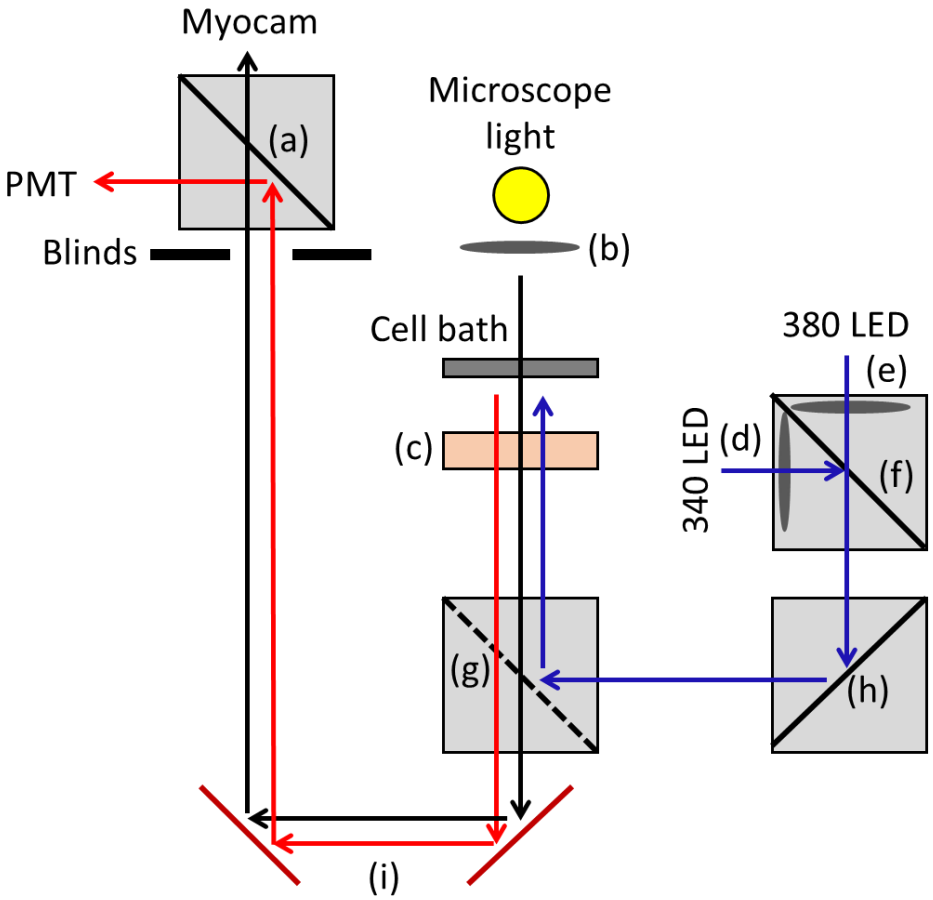

Figure 2-2. Epi-fluorescent microscope apparatus configuration. (a) 600 nm LP dichroic mirror. (b) 700 nm LP filter. (c) objective lens. (d) 340 nm BP excitation filter. (e) 380 nm BP excitation filter. (f) 370 nm LP dichroic mirror. (g) 500 nm LP dichroic mirror. (h) 425 nm LP dichroic mirror. (i) standard mirrors.

2.2.5.3 Standard settings

The emitted light signal was optimised in two ways. The gain determines magnitude of the signal amplification by the PMT, this could be adjusted however was kept fairly consistent as with increase in gain also amplifying background noise. Alternatively, the intensity of each excitation wavelength was adjusted on a cell-by-cell basis, using the dual optoled power supply (Cairn). This was a common adjustment as the uptake of indicator varied between cells. While increasing the excitation intensity will increase the light signal emitted, in excess

it will lead to photobleaching and loss of signal. Photobleaching occurs with all indicators and is proportional to light intensity and length of exposure.

2.2.6 Measurement of contractility

Changes to sarcomere length were measured as a parameter of contractility via video detection using an Ion Optix MyoCam-S high speed digital camera with a charge-coupled device (CCD). This data was acquired using the real-time by the SarcLen Sarcomere Length Acquisition Module (Ion Optix) integrated with the IonWizard 6.5 system. The myocyte was positioned to the centre of the video display and aligned so that the striations fell vertically. If necessary, image gain and offset could be altered to increase contrast to view striations clearly. A box was manually placed around a series of striations, or sarcomeres (minimum of 7), on the screen. This outlined region determined where sarcomere length was measured from and this produced a density trace. As further sarcomeres entered the identified region of interest during contraction, to reduce the impact of inconsistency at the region edges the central sarcomeres contributed more to the sarcomere length estimate. The peak produced in the density trace was used to indicate sarcomere length as sarcomeres per pixel, which was automatically converted to pixels per sarcomere by the software. A lower boundary power spectrum bar could be used to eliminate noise prior to the peak.

2.2.7 Field stimulation of ventricular myocytes

Cells were stimulated using a DS2A constant voltage isolate stimulator (Digitimer ltd). The voltage and polarity were controlled by a Constant Voltage Isolated Stimulator (model DS2A, Only the minimum voltage required to produce excitation was used; typically between 40 – 70 V, with a pulse width of 10 ms. A Train/delay generator (model DG2A, Digitimer ltd) was used to control the frequency at which cells were paced. The standard pacing frequency used was 0.5 Hz (unless otherwise stated); the pacing frequency was adjusted for specialised experiments.

2.3 Data analysis

2.3.1 Measurement of diastolic and systolic Ca^{2+}

To create a representative Ca^{2+} transient of steady state and limit the influence of any noise in the signal, 5 Ca^{2+} transients at steady state were averaged to produce a mean Ca^{2+} transient. Once exported from IonWizard (Ion Optix) software, analysis of mean Ca^{2+} transient was carried out using Ca Multi; a excel based program developed and described by Greensmith (2014). Following each experiment, the cell was moved out of the imaging window to record background signal from the surrounding medium. A trace region from this 'no cell' (F_0) state was also exported and input into the Ca Multi program. Both the 340 and 380 nm 'no cell' signals were averaged, and the resulting value was subtracted from the remaining fluorescent traces respectively. The ratio between the 340 and 380 nm wavelengths was calculated 340/380, indicating proportional change in $[Ca^{2+}]_i$ (Grynkiewicz et al., 1985). Cursors controlled via scroll bars were used to define the resting and peak fluorescent signal, from this the Ca^{2+} amplitude could be calculated (Greensmith, 2014).

2.3.2 Measurement of sarcomere shortening

In order to measure diastolic and systolic contractility, the corresponding 5 sarcomere sweeps at each steady state were averaged and exported in the same manner as described for the fluorescent data in section 2.3.1. Resting sarcomere length and peak shortening were measured using the Ca Multi program (Greensmith, 2014), which when combined allowed measurement of the amplitude of contraction (or systolic sarcomere shortening). This required used of cursors to identify the maximum or minimum sarcomere lengths, respectively, and a negative deflection was used given that the sarcomere signal moves in the opposite direction to the Ca^{2+} signal.

2.3.3 Measurement of rate of sarcomere relaxation and shortening

The rates of sarcomere relaxation and shortening were determined by the time taken to 50 % of the total incline or decline in sarcomere length respectively. This is otherwise referred to as the 50 % decay time. This was calculated through use of the excel-based program 'APD single 2010 v2'. This also required manual indication of the maximum or minimum sarcomere lengths, using cursors.

2.3.4 Measurement of rate of Ca^{2+} removal

Rate of Ca^{2+} removal was measured based on the single exponential rate constant (RC) of decay of the representative mean Ca^{2+} transient. The RC of a mean Ca^{2+} transient at steady state was termed k_{sys}, referring to systolic Ca^{2+} removal and thus the total rate of Ca^{2+} removal from the sarcoplasm via all mechanisms combined. As caffeine effectively inhibits SERCA, Ca^{2+} decay (k_{caff}) following caffeine application is primarily due to removal by NCX. Through subtracting k_{caff} from k_{sys}, the rate of SR Ca^{2+} uptake and thus SERCA activity (k_{SERCA}) can be measured. The 90-10 % of Ca^{2+} decay was measured – as described in respect to rate of relaxation in section 2.3.3 – as an alternative way of measuring the rate of change in the fluorescent signal and thus rate of Ca^{2+} removal.

2.3.5 Statistics

Following data extraction and primary analysis, raw data was compiled into an Excel (Microsoft) spreadsheet. For each parameter recorded, data was also normalised against that of the control steady state. Data were statistically analysed using SigmaPlot 12.5 (Systat Software Inc). The statistical tests used were dependent on the experiment. In the majority of experiments, a one-way ANOVA was used to compare the parameters at steady state during the control period, with cytokine treatment and during washout. A one-way ANOVA was also used to allow comparisons between the experimental models. In the experiments involving induced Ca^{2+} waves, measurements were taken from set time points, as such a

one-way repeated measures ANOVA was used to test significance. As per chapter 5, in order to compare the effects different Ca^{2+} concentrations on sarcomere length in untreated and cytokine treated cells, a two-way ANOVA was used. Any additional statistical tests used will be stated in their respective chapters. The 'n' provided refers to the total number of experiments carried out, however these cells were isolated from multiple animals. The number of animals used will also be provided in the figure legends.

Chapter 3

The effects of TNF-α and IL-1β on Ca^{2+} handling and contractility in sheep left ventricular myocytes

3.1 Introduction

As previously discussed in section 1.1.8.2, it is commonly accepted that the proinflammatory cytokines TNF-α and IL-1β are myocardial depressant substances. Both are known to have elevated serum concentrations in inflammatory conditions including sepsis (Muller-Werdan et al., 1998; Odeh, 1993; Radin et al., 2008; Vincent et al., 1992). However, the cellular basis of how TNF-α and IL-1β induce myocardial depression is not fully understood. Much evidence suggests they act by altering intracellular Ca^{2+} handling (as described in section 1.3.7), though here too, the precise mechanisms remain unclear.

Many previous studies have investigated the synergistic effect of both TNF-α and IL-1β (Duncan et al., 2010; Schulz et al., 1995), or the effect of septic serum containing TNF-α and IL-1β in addition to other cytokines (Fernandez-Sada et al., 2017; Jha et al., 1993). Common observations included loss of left ventricular contractile force and – in whole heart studies – reduced cardiac output (Jha et al., 1993; Schulz et al., 1995; Vincent et al., 1992). The effect on SR Ca^{2+} content is unclear, as Jha et al. (1993) recorded no change with septic serum, whilst Duncan et al. (2010) found evidence of increased diastolic SR Ca^{2+} release with combined TNF-α and IL-1β treatment.

While these previous studies have contributed to the understanding of the overall effect of cytokines in sepsis, they have been unable to determine the individual impact of TNF-α and IL-1β. Of those studies that have investigated the individual effects of these cytokines, many have not taken an integrative cellular approach. For example, many have only looked at certain aspects of ECC in isolation. While highly reductionist, this does not take into account the fact that ECC is a dynamic process and highly dependent on the interaction of all sub-cellular mechanisms (El Khoury et al., 2014; Trafford, Diaz, O'Neill, & Eisner, 2002).

Some limited studies have used an integrative approach to study the effect of TNF-α and IL-1β on Ca^{2+} and contractility dynamics simultaneously. Greensmith and Nirmalan (2013) performed this analysis for TNF-α and Radin et al. (2008) for IL-1β. Studies such as these *have* considerably advanced our understanding of the cellular basis of cytokine induced myocardial depression. For example, Greensmith and Nirmalan (2013) demonstrated that

TNF-α decreased SR Ca^{2+} content, leading to reduced systolic Ca^{2+} thence contractility. Interestingly, no alterations to diastolic dysfunction were observed. Radin et al. (2008) found that IL-1β also decreased cell shortening due to a reduction in systolic Ca^{2+}. While the study did not the effect of IL-1β on SR Ca^{2+} content, they demonstrated that IL-1β reduced the rate of Ca^{2+} removal and cell relaxation. However, both studies suffer the limitation that a small mammal model (rat) was used. This is important as large mammal models better represent the human condition and it is currently unknown whether in these models, these observations are reproducible. Sheep hearts are very comparable model to humans, due to their similar heart rates; 60-120 bpm in sheep and ~72 bpm in humans. Previously used models, particularly rodents, have a faster heart rate and as such have a much shorter ventricular action potential duration. Sheep and humans also have a similar proportion of Ca^{2+} handling proteins and rely on both SERCA and NCX activity for Ca^{2+} removal, unlike rodents which are more reliant on SERCA alone (Milani-Nejad & Janssen, 2014). Furthermore, certain key components of ECC were not studied; namely the RyR and myofilament sensitivity to Ca^{2+}, and so it is unclear how they are affected by TNF-α and IL-1β.

Though the effect of TNF-α and IL-1β on the ryanodine receptor and myofilament sensitivity to Ca^{2+} will be addressed specifically in chapter 4 and 5 respectively, it should be pointed out that in rat, Greensmith and Nirmalan (2013) observed a transient potentiation of systolic Ca^{2+} upon application of TNF-α. While not definitive, this may be indicative of RyR potentiation (Greensmith, Galli, Trafford, & Eisner, 2014). However, (1) Greensmith and Nirmalan (2013) did not thoroughly investigate this phenomenon (2) as this is the first reported observation of the phenomenon it is not known if it occurs in sheep.

3.1.1 What is a pathologically relevant cytokine concentration?

Previous studies have used a wide range of concentrations when investigating the effects of TNF-α and IL-1β on single myocytes or whole heart function (Amadou, Nawrocki, Best-Belpomme, Pavoine, & Pecker, 2002; Cailleret et al., 2004; Combes et al., 2002; Duncan et al., 2010; El Khoury et al., 2014; Greensmith & Nirmalan, 2013; Ing, Zang, Dzau, Webster, &

Bishopric, 1999; Kaur, Sharma, Dhingra, & Singal, 2006; Liu, Zhou, & Kennedy, 1999; Maass, White, & Horton, 2002; McTiernan et al., 1997; Y. Qiu, Liao, & Zhang, 2009; Rozanski & Witt, 1994; Schreur & Liu, 1997; Schulz et al., 1995; Skayian & Kreydiyyeh, 2006; Stamm et al., 2001; Sugishita et al., 1999; Tatsumi et al., 2000; Tsujino et al., 1994; Yokoyama et al., 1993). Mean concentrations used were 17 ± 3 ng/ml TNF-α (n=23) and 14 ± 7 ng/ml IL-1β (n=19), over a range of 0.1-50 ng/ml and 0.1-100 ng/ml respectively.

In previous data (Nirmalan et al, unpublished), plasma and intra-cardiac cytokine concentrations were measured in patients with sepsis. The latter revealed median levels of 102 pg/ml TNF-α and 48 pg/ml IL-1β at the coronary sinus, although ranges were wide; 22-1060 pg/ml and 20-420 pg/ml for TNF-α and IL-1β respectively. This does not reflect the local cytokine concentrations, which at the site of production – for example leukocytes in the heart (Neumann et al., 1995) – would be assumed to be much higher. The 50 ng/ml concentration of used for TNF-α and IL-1β in this study allowed the fundamental and individual effects of each cytokine to be determined.

3.1.2 Aims

(1) Separately characterise the effects if TNF-α and IL-1β in a sheep using an integrative approach
(2) Establish if the effects of TNF-α and IL-1β in sheep are limited to systole
(3) Ascertain whether, in sheep, there exists a temporary potentiation of systolic Ca^{2+} following application of TNF-α and IL-1β.

3.2 Methods

Left ventricular myocytes were isolated from young control sheep (aged approximately 18 months) and paced at 0.5 Hz using field stimulation (see section 2.2.7). Cells were perfused with a control solution (see section 2.2.1) until a steady state was reached at which point 50 ng/ml TNF-α or IL-1β were applied individually and changes to Ca^{2+} and contractility were

tracked to steady state. Subsequently, the reversibility of the effects of these cytokines was tested by switching back to control solution. The relative change to SR Ca^{2+} content was estimated by the amplitude of 10 mM caffeine-evoked Ca^{2+} transient (see section 2.3.4).

Unless stated as otherwise, data shown represents mean ± standard error for steady state control, cytokine then wash for a given parameter. All data for each cell were normalised to each cells' own control value, as this study measures fluorescence and not Ca^{2+} directly, normalisation allows relative change to be measured. There is a large variation in the quality of cells obtained from enzymatic digestion, normalisation also allows for baseline changes in the day-to-day quality of cells.

Data were analysed using custom written software (Greensmith, 2014) as per (section 2.3). Statistical significance ($p<0.05$) was tested using one-way analysis of variance (ANOVA) (parametric data) or ANOVA on ranks (non-parametric data). Individual comparisons between groups were tested using Dunn's, Holm-Sidak or Tukey post-hoc tests as appropriate.

3.3 Results

3.3.1 The effect of 50 ng/ml TNF-α on intracellular Ca^{2+} levels and contractility

The specimen records of Fig 3-1A and 3-1C demonstrate the effect of TNF-α on intracellular Ca^{2+} levels. The effect of TNF-α on systolic Ca^{2+} was rapid and sustained. On average, in the steady state, TNF-α irreversibly reduced Ca^{2+} transient amplitude by 16.79 ± 3.16 % ($n=28$, $p<0.05$) (Fig 3-2A). On average, diastolic Ca^{2+} decreased by 4.35 ± 1.67 % ($n=28$, $p<0.05$) (Fig 3-2C).

The effects of TNF-α on contractility are shown in the specimen records of Fig 3-1B and 3-1D. TNF-α caused a mean decrease in sarcomere amplitude of contraction by 20.31 ± 7.58 % ($n=24$, $p<0.05$) (Fig 3-2B), and a mean decrease in resting sarcomere length by 0.46 ± 0.1 % ($n=24$, $p<0.05$) was found (Fig 3-2D). With the exception of the effect on sarcomere

shortening which recovered to control levels (n=17, p>0.05), no other measured parameters reversed during washout.

The specimen record of Fig 3-1E is an example of the effect of TNF-α on rate of contractility and relaxation. TNF-α application did not change the rate of sarcomere shortening (n=22, p = 0.056) (Fig 3-2E) or the rate of relaxation (n=23, p>0.05) (Fig 3-2F). Following washout, the rate of sarcomere relaxation increased, as the 50 % decay time decreased by 18.92 ± 7.11 % (n=17, p<0.05).

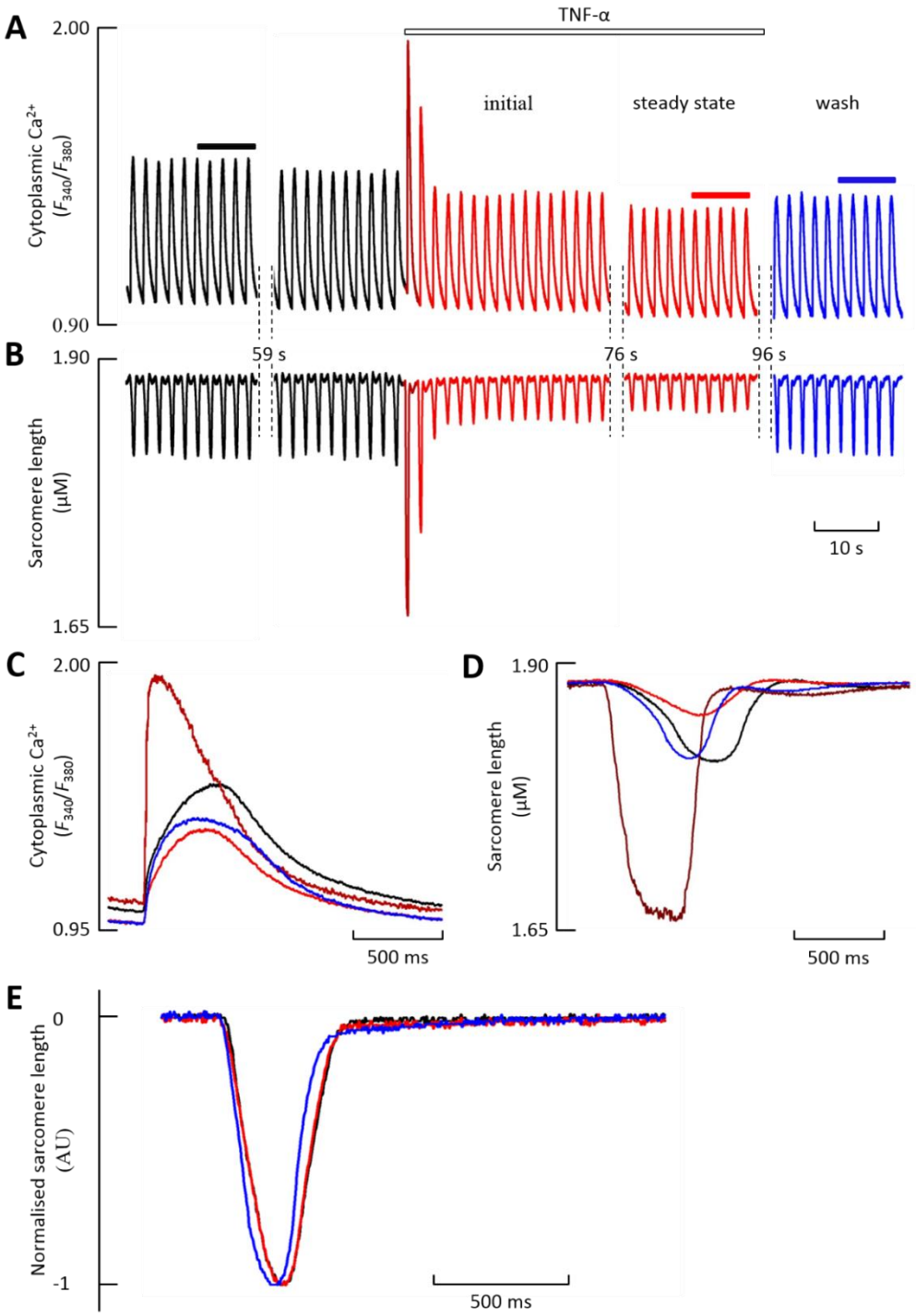

Figure 3-1. Specimen records of the effect of TNF-α on cytoplasmic Ca^{2+} and contractility in left ventricular myocytes from young control sheep. (A) specimen record showing Ca^{2+} transients. (B) specimen record showing sarcomere shortening. (C) specimen mean Ca^{2+} transients for the periods highlighted in A. (D) specimen mean sarcomere shortening traces for the periods highlighted in B. (E) specimen sarcomere shortening traces for the periods highlighted in B, with normalised diastolic and systolic levels.

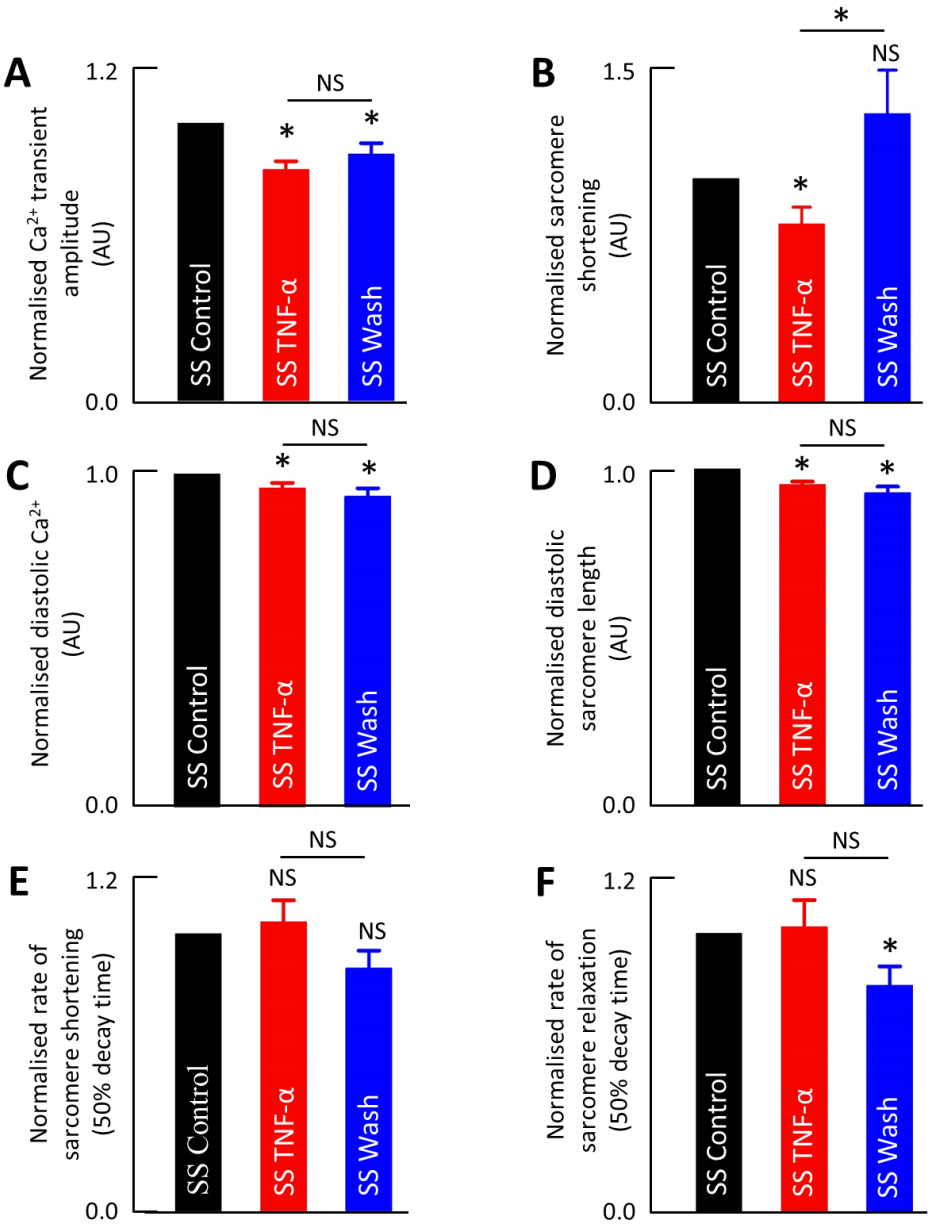

Figure 3-2. The effects of TNF-α on cytoplasmic Ca^{2+} and contractility in left ventricular myocytes from young control sheep, and washout (n = 28 cells from 10 animals). (A) mean Ca^{2+} transient amplitude. (B) mean sarcomere shortening. (C) mean diastolic Ca^{2+}. (D) mean resting sarcomere length. (E) mean 50 % sarcomere shortening time. (F) mean 50 % sarcomere relaxation time. * indicates $p < 0.05$, NS denotes non-significance ($p > 0.05$), SS = steady state.

3.3.2 The effect of 50 ng/ml IL-1β on intracellular Ca^{2+} levels and contractility

As demonstrated in the specimen traces of Fig 3-3A and 3-3C, IL-1β alters intracellular Ca^{2+} dynamics. The effect on systolic Ca^{2+} was rapid and sustained with IL-1β producing a mean decrease in Ca^{2+} transient amplitude by 23.63 ± 6.61 % (n=26, $p<0.05$), which did not reverse upon washout (Fig 3-4A).

The specimen records of 8B and 8D show an example of the effect of IL-1β on cell contractility. The magnitude of change to sarcomere shortening was unchanged by IL-1β (n=24, $p>0.05$), however following washout shortening increased on average by 146.01 ± 59.32 % (n=17, $p<0.05$) (Fig 3-4B). Whilst IL-1β did not alter diastolic Ca^{2+} (n=25, $p = 0.739$) (Fig 3-4C), resting sarcomere length was irreversibly decreased by 0.76 ± 0.2 % (n=24, $p<0.05$) (Fig 3-4D).

An example of the effect of IL-1β on rate of contractility and relaxation is demonstrated in the specimen figure of Fig 3-3E. The mean rate of sarcomere shortening (n=24, $p>0.05$) (Fig 3-4E) and relaxation (n=24, $p>0.05$) (Fig 3-4F) were not affected by IL-1β application. Following washout, the rate of both sarcomere shortening and relaxation increases, as the 50 % time taken for each decreased by 28.54 ± 10.16 % (n=17, $p<0.05$) and 50.46 ± 3.84 % (n=17, $p<0.05$).

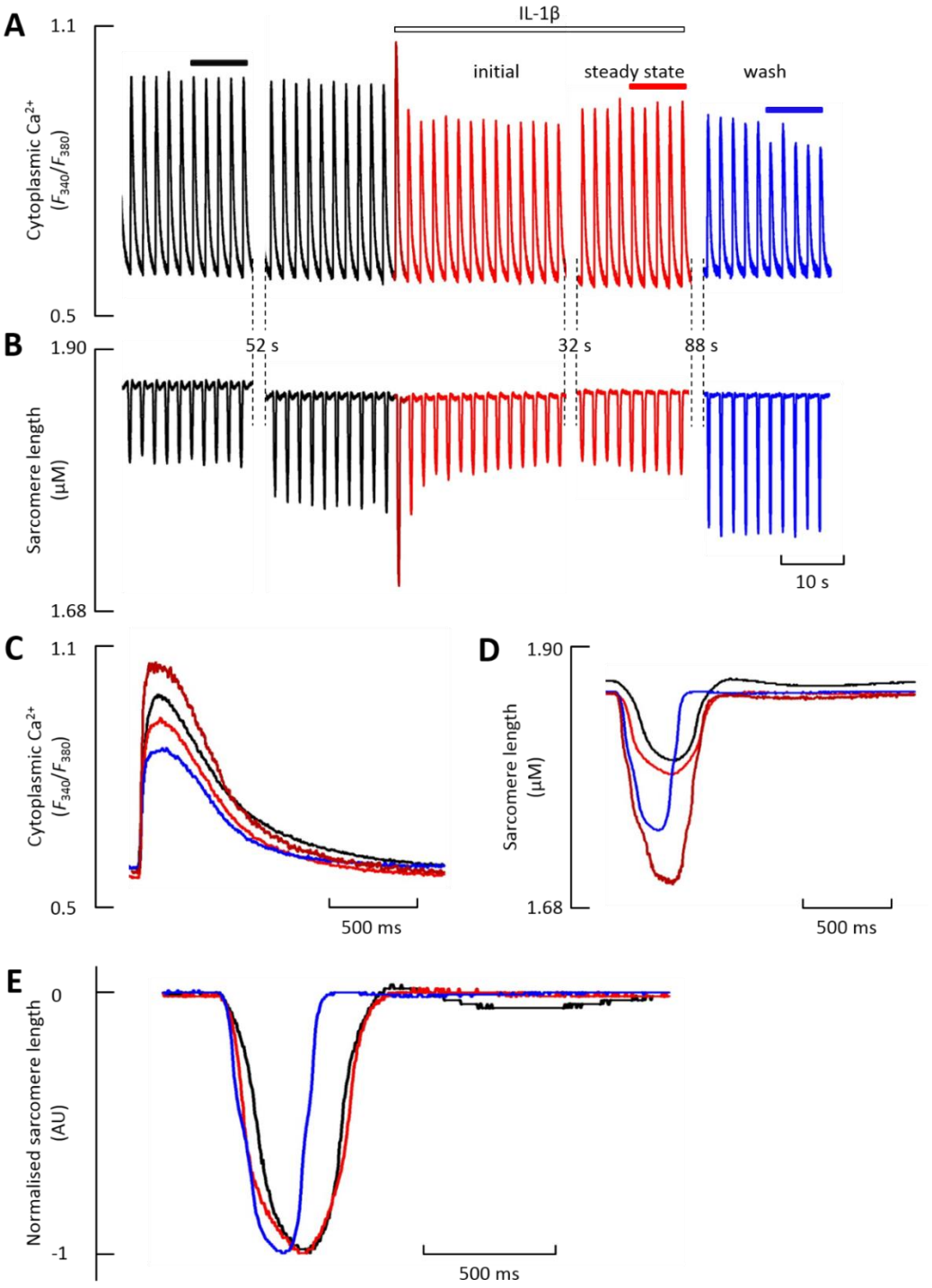

Figure 3-3. Specimen records of the effect of IL-1β on cytoplasmic Ca^{2+} and contractility in left ventricular myocytes. (A) specimen record showing Ca^{2+} transients. (B) specimen record showing sarcomere shortening. (C) specimen mean Ca^{2+} transients for the periods highlighted in A. (D) specimen mean sarcomere shortening traces for the periods highlighted in B. (E) specimen sarcomere shortening traces for the periods highlighted in B, with normalised diastolic and systolic levels.

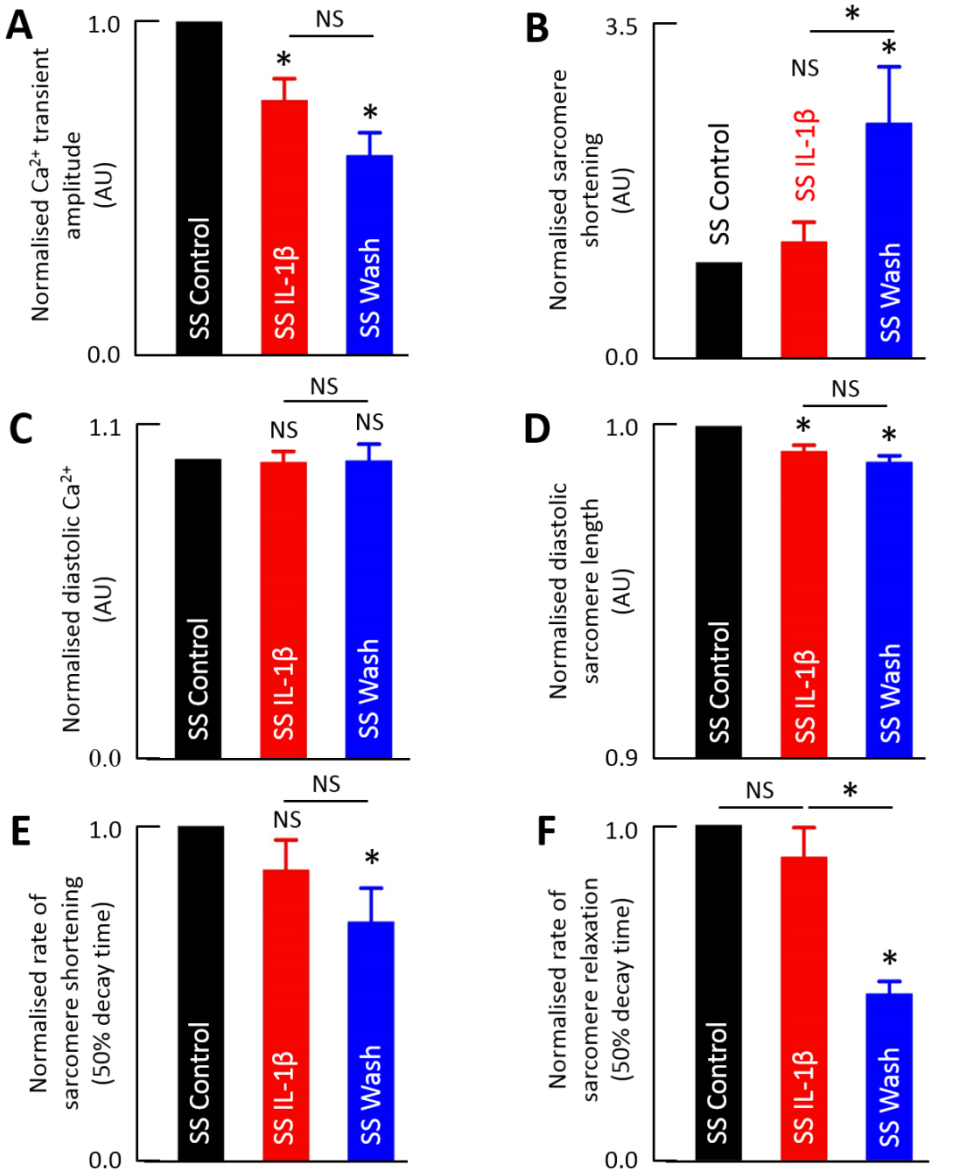

Figure 3-4. The effects of IL-1β on cytoplasmic Ca^{2+} and contractility in left ventricular myocytes, and washout (n= 29 cells from 9 animals). (A) mean Ca^{2+} transient amplitude. (B) mean sarcomere shortening. (C) mean diastolic Ca^{2+}. (D) mean resting sarcomere length. (E) mean 50 % sarcomere shortening time. (F) mean 50 % sarcomere relaxation time. * indicates $p < 0.05$, NS denotes non-significance ($p > 0.05$), SS = steady state.

3.3.3 The effect of TNF-α and IL-1β on SR Ca^{2+} content

As demonstrated by Fig 3-5, 50 ng/ml TNF-α and IL-1β decreased the caffeine evoked Ca^{2+} transient amplitude by 27.32 ± 3.41 % (n=20, $p<0.05$) and 41.39 ± 3.43 % (n=22, $p<0.05$)

respectively from control. This decrease in caffeine evoked Ca^{2+} amplitude was maintained during washout of both TNF-α (n=6, p<0.05) and IL-1β (n=18, p<0.05).

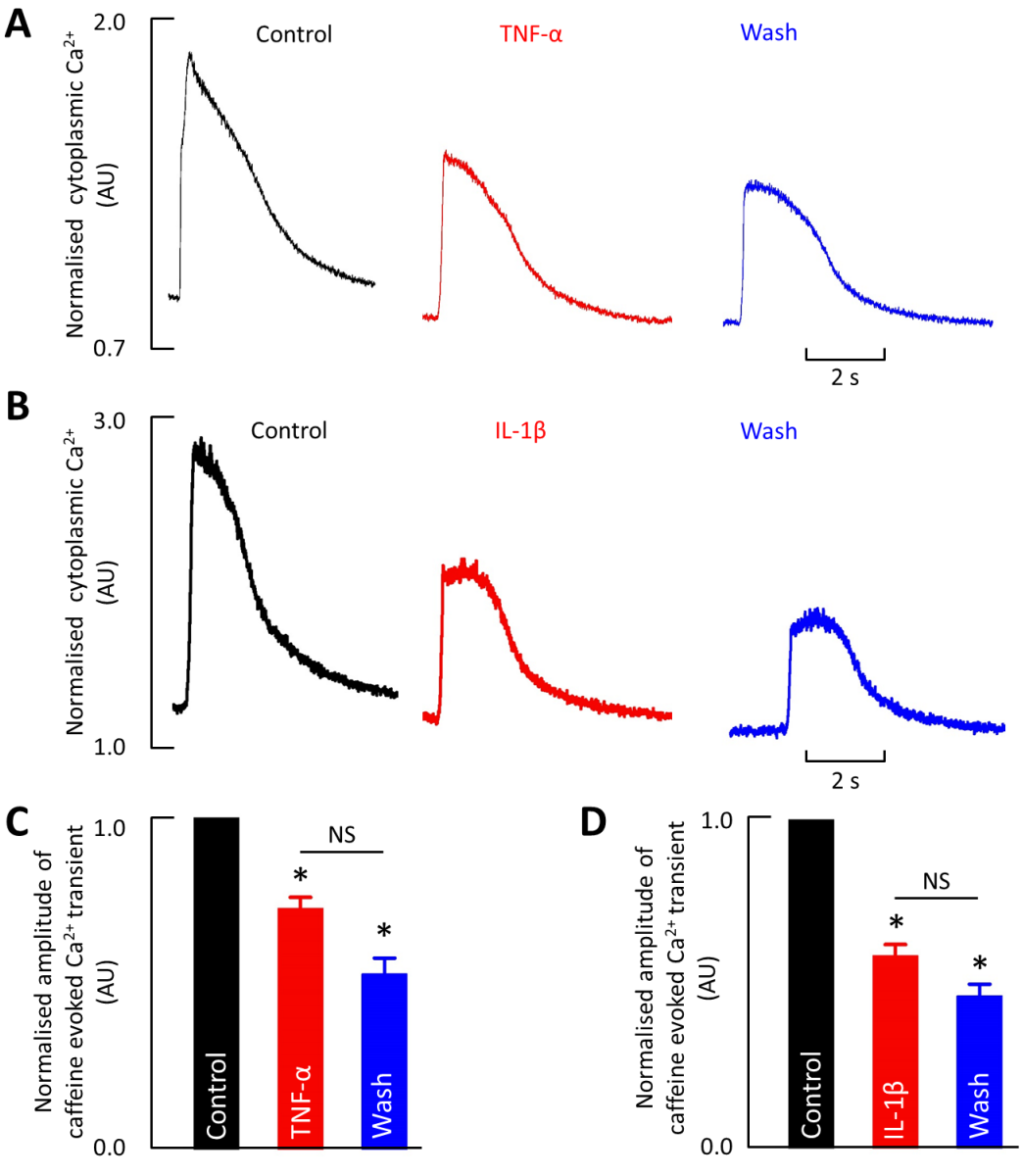

Figure 3-5. 10 mM caffeine evoked Ca^{2+} transient amplitudes in TNF-α (n= 20 cells from 7 animals) and IL-1β (n= 22 cells from 9 animals) treated cells. (A and B) specimen records for caffeine evoked Ca^{2+} transient following control, cytokine and wash steady states, for TNF-α and IL-1β respectively. (C) mean caffeine evoked Ca^{2+} transients in TNF-α treated cells. (D) mean caffeine evoked Ca^{2+} transients in IL-1β treated cells. * indicates p <0.05, NS denotes non-significance (p >0.05), SS = steady state.

3.3.4 The effect of TNF-α and IL-1β on the major Ca^{2+} removal mechanisms

The specimen record of Fig 3-6A shows an example of the effect of TNF-α on the decay phase of the systolic Ca^{2+} transient. Data have been normalised to permit direct comparability. On average, the rate constant of this decay phase (k_{sys}) was unaltered by TNF-α (n=26, p = 0.170) (Fig 3-6C). However, due to concerns over variation in the profile of the Ca^{2+} transient, the rate of systolic Ca^{2+} decay was also measured using 90 - 10 % decay time which was also unaffected by TNF-α (n=27, p = 0.242) (Fig 3-6D).

The specimen record of Fig 3-6B demonstrates the effect of TNF-α on the decay phase of the caffeine evoked Ca^{2+} transient. Data have been normalised to permit direct comparability. TNF-α did not affect the rate constant of decay of the caffeine evoked Ca^{2+} transient (k_{caff}) (n=12, p = 0.122) (Fig 3-6E). k_{SERCA} was derived by subtraction of k_{caff} from k_{sys} (see section 2.3.4) which was also unaltered by TNF-α (n=11, p>0.05) (Fig 3-6F). However, during washout k_{SERCA} increased by 91.67 ± 26.29 % (n=3, p<0.05).

Similar analysis was performed for of IL-1β and can be seen in the specimen records of Fig 3-7A and 3-7B. With IL-1β, k_{sys} increased by 24.04 ± 6.5 % (n= 26, p<0.05), increasing further to 80.54 ± 18.12 % (n= 21, p<0.05) greater than control following washout (Fig 3-7C). 90 - 10 % decay time of the Ca^{2+} transient (n=26, p>0.05) was unaltered by IL-1β, however washout produced an 11.88 ± 9.41 % decrease (n=21, p<0.05), and thus elevated rate of systolic Ca^{2+} removal following washout (Fig 3-7D).

On average IL-1β increased k_{caff} by 29.47 ± 10.55 % (n= 19, p<0.05) which was maintained during washout (n= 16, p<0.05) (Fig 3-7E). While IL-1β application did not alter the k_{SERCA} (n=19, p>0.05), following washout, k_{SERCA} increased by 78.26 ± 17.67 % (n=16, p<0.05) (Fig 3-7F).

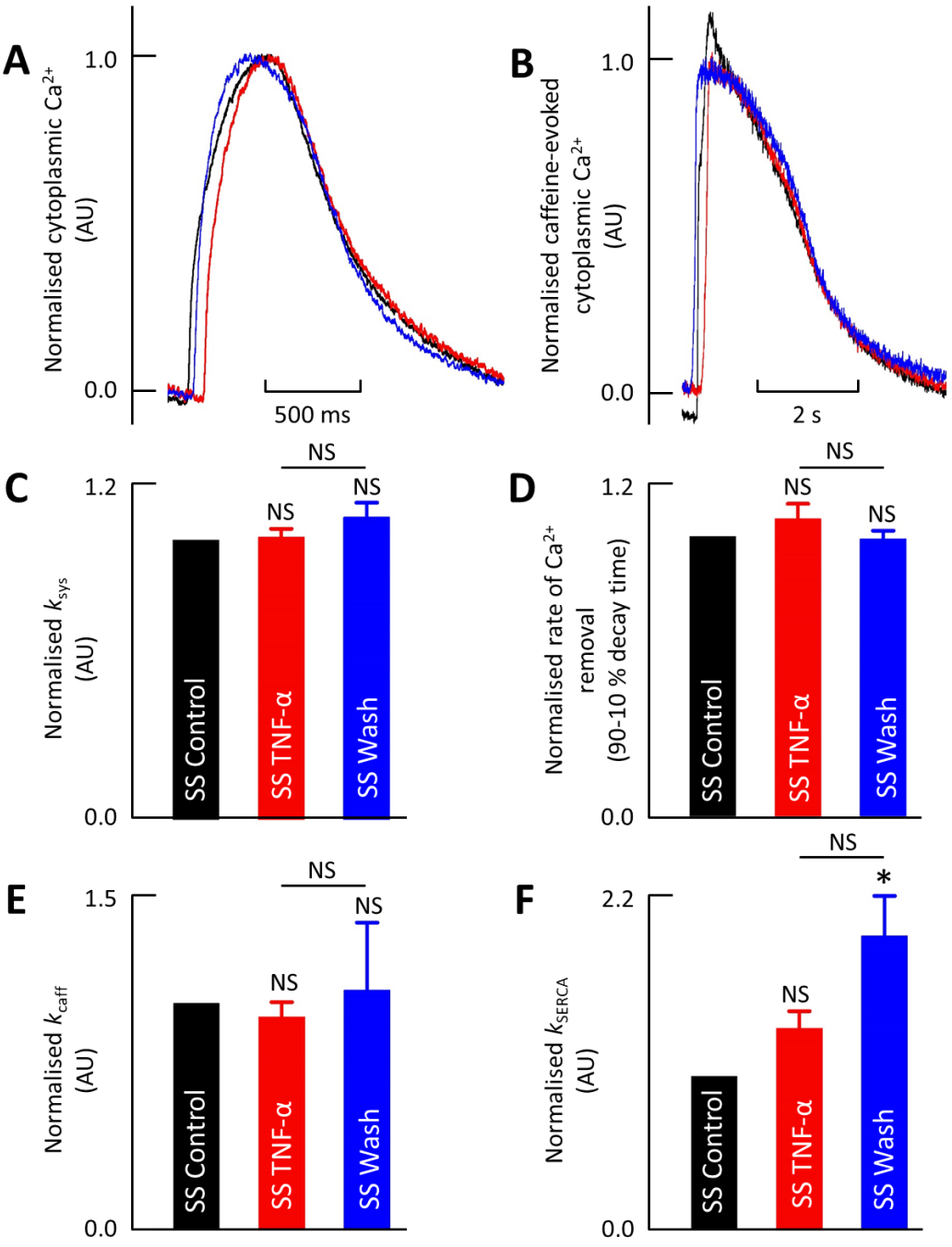

Figure 3-6. The effect of 50 ng/ml TNF-α on rate of Ca^{2+} removal (n = 26 cells from 10 animals). (A) specimen trace of Ca^{2+} transients at control, TNF-α and washout steady state, with normalised diastolic and systolic levels. (B) specimen trace of caffeine-evoked Ca^{2+} transients at control, TNF-α and washout steady state, with normalised diastolic and systolic levels. (C) mean normalised k_{sys}. (D) mean normalised 90-10 % decay time of the Ca^{2+} transient. (E) mean normalised k_{caff}. (F) mean normalised k_{SERCA}. * indicates $p < 0.05$, NS denotes non-significance ($p > 0.05$), SS = steady state.

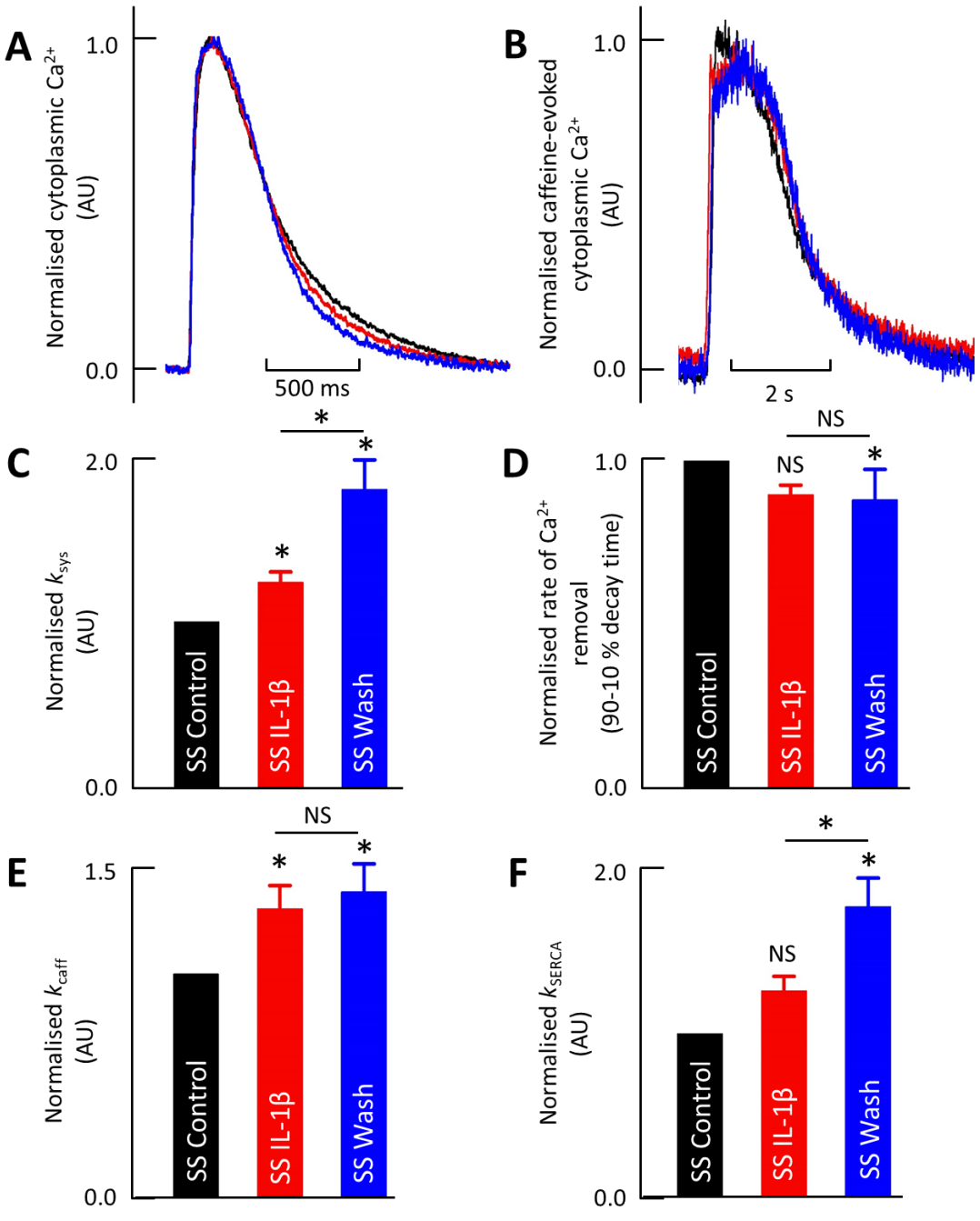

Figure 3-7. The effect of 50 ng/ml IL-1β on rate of Ca^{2+} removal (n = 26 cells from 9 animals) (A) specimen trace of Ca^{2+} transients at control, IL-1β and washout steady state, with normalised diastolic and systolic levels. (B) specimen trace of caffeine-evoked Ca^{2+} transients at control, IL-1β and washout steady state, with normalised diastolic and systolic levels. (C) mean normalised k_{sys}. (D) mean normalised 90-10 % decay time of the Ca^{2+} transient. (E) mean normalised k_{caff}. (F) mean normalised k_{SERCA}. * indicates $p < 0.05$, NS denotes non-significance ($p > 0.05$), SS = steady state.

3.3.5 The early effect of 50 ng/ml TNF-α and IL-1β on systolic Ca^{2+}

Preceding the decrease of systolic Ca^{2+} to a lower steady state (Fig 3-1 to 3-3 above), in certain cells both cytokines produced an early, short-lived potentiation of the Ca^{2+} transient amplitude lasting 1-3 beats. Potentiation was defined as a greater than 10 % increase of systolic compared to control. Potentiation was observed in 71 % of cells exposed to TNF-α and 52 % of cells exposed to IL-1β. As such, cells were sub-grouped into responders (those with an early potentiation – see Fig 3-8A and 3-8D for examples) and non-responders (those without – see Fig 3-9A and 3-9D for examples).

In responders, on average TNF-α increased the amplitude of the first beat by 57.75 ± 10.23 % ($n=20$, $p<0.05$) (Fig 3-8B). This was accompanied by a mean increase in sarcomere shortening by 348.3 ± 128.73 % ($n=15$, $p<0.05$) (Fig 3-8C). For both Ca^{2+} transient amplitude and sarcomere shortening, this initial potentiation was temporary. Cells responding to IL-1β showed a similar pattern. on average IL-1β increased the Ca^{2+} amplitude of the 1^{st} beat by 51.72 ± 12.61 % ($n=15$, $p<0.05$) (Fig 3-8E). This was accompanied by an increase in 1^{st} beat sarcomere amplitude of contraction by 215.25 ± 46.42 % ($n=14$, $p<0.05$) (Fig 3-8F). For both Ca^{2+} transient amplitude and sarcomere shortening, this initial potentiation was temporary.

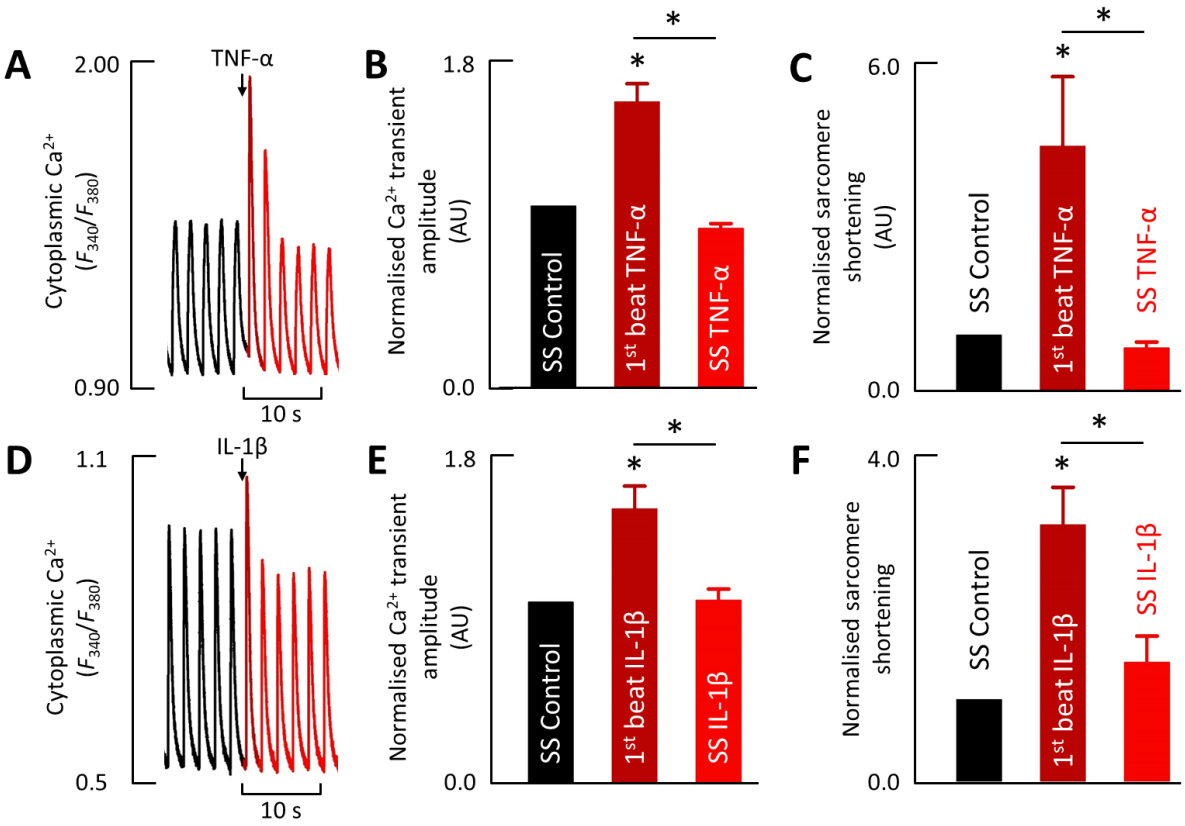

Figure 3-8. The effect of 50 ng/ml TNF-α (n = 20 cells from 7 animals) and IL-1β (n = 15 cells from 8 animals) on the 1st beat Ca^{2+} transient amplitude and contractility of cells showing signs of RyR potentiation (A) specimen record showing Ca^{2+} transients, immediately prior to [black], during [dark red] and following [red] 1st beat application of TNF-α. (B) mean normalised Ca^{2+} transient amplitude with 1st beat application of TNF-α. (C) mean normalised sarcomere shortening with 1st beat application of TNF-α. (D) specimen record showing Ca^{2+} transients with1st beat application of IL-1β, as labelled in A. (E) mean normalised Ca^{2+} transient amplitude with 1st beat application of IL-1β. (F) mean normalised sarcomere shortening with 1st beat application of IL-1β. * indicates $p < 0.05$, NS denotes non-significance ($p > 0.05$), SS = steady state.

In TNF-α non-responders, the 1st beat Ca^{2+} transient amplitude (n=8, $p>0.05$) did not differ from control, however Ca^{2+} transient amplitude had reduced by 29.09 ± 7.52 % (n=7, $p<0.05$) once steady state had been reached in TNF-α (Fig 3-9B). The 1st beat magnitude of sarcomere shortening was unchanged (n=7, $p>0.05$) with TNF-α, while a 15.77 ± 5.97 % (n=7, $p<0.05$) reduction was found at steady state (Fig 3-9C).

In IL-1β non-responders treated cells, a mean decrease in Ca^{2+} transient amplitude by 24.07 ± 5.22 % (n=14, p<0.05) was found. Ca^{2+} transient amplitude decreased further to 47.7 ± 4.45 % (n=12, p<0.05) of control at steady state (Fig 3-9E). The 1st beat magnitude of sarcomere shortening increased by 112.81 ± 76.27 % (n=13, p<0.05) with IL-1β (Fig 3-9F). Sarcomere shortening was restored to control levels at IL-1β steady state (n=11, p<0.05).

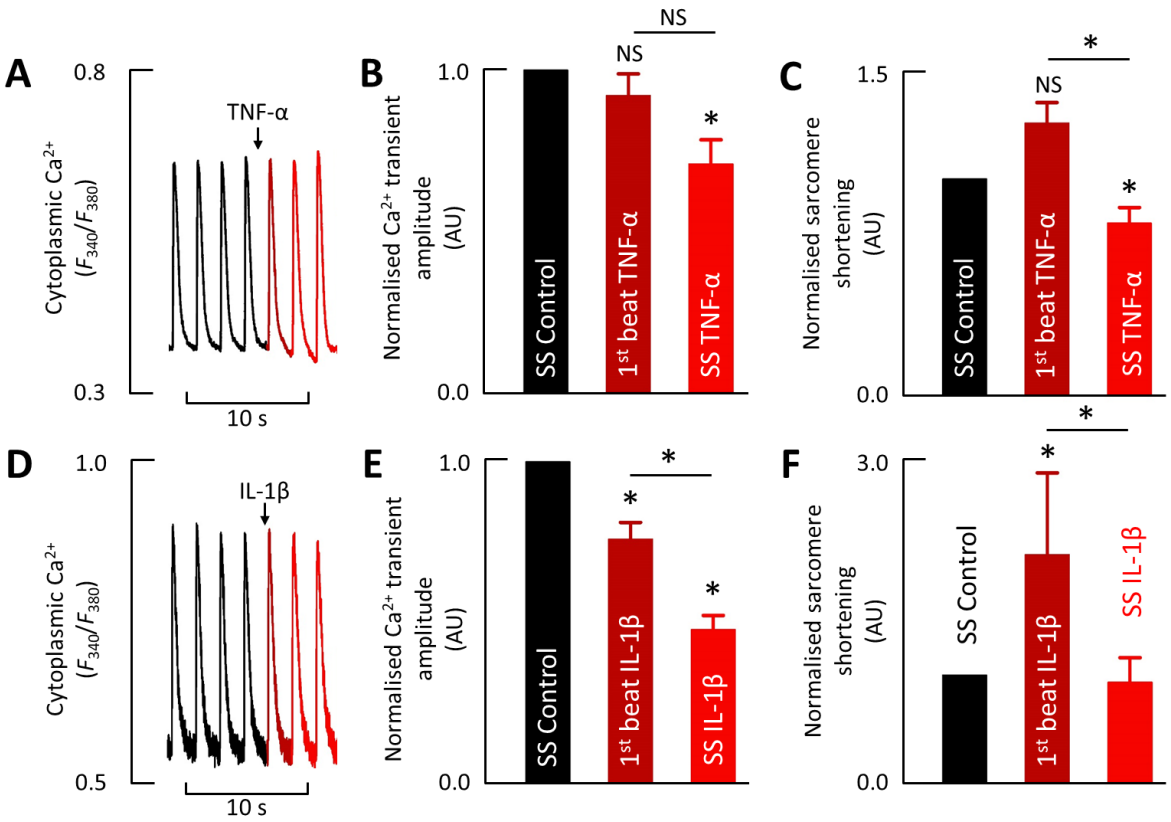

Figure 3-9. The effect of 50 ng/ml TNF-α (n = 8 cells from 6 animals) and IL-1β (n = 14 cells from 7 animals) on the 1st beat Ca^{2+} transient amplitude and contractility of cells without signs of RyR potentiation (A) specimen record showing Ca^{2+} transients, immediately prior to [black], during [dark red] and following [red] 1st beat application of TNF-α. (B) mean normalised Ca^{2+} transient amplitude with 1st beat application of TNF-α. (C) mean normalised sarcomere shortening with 1st beat application of TNF-α. (D) specimen record showing Ca^{2+} transients with 1st beat application of IL-1β, as labelled in A. (E) mean normalised Ca^{2+} transient amplitude with 1st beat application of IL-1β. (F) mean normalised sarcomere shortening with 1st beat application of IL-1β. * indicates p <0.05, NS denotes non-significance (p >0.05), SS = steady state.

To determine whether the observed phenomenon was influenced by switching between the lines, the experiment was repeated using control solution. A small, initial increase in Ca^{2+} transient amplitude by 8.12 ± 2.7 % (n=10, p<0.05) was identified following switching of the lines (Fig 3-10).

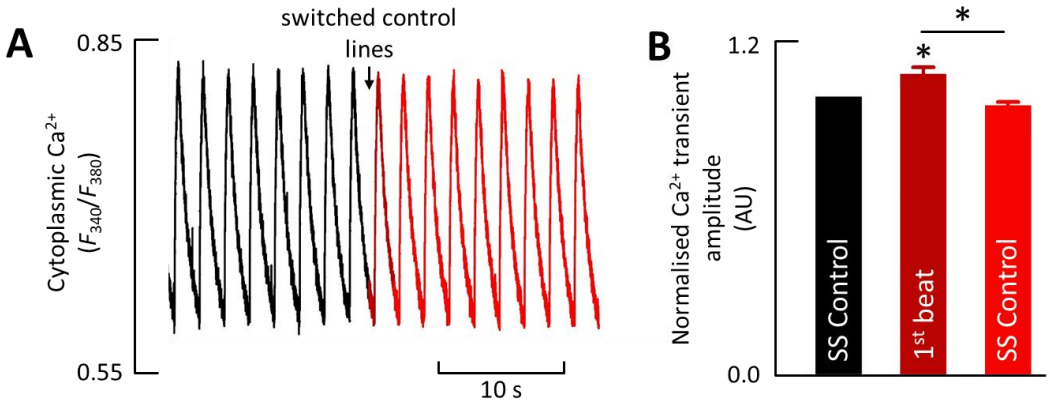

Figure 3-10. The effect of switching lines between control solutions on 1st beat and steady state Ca^{2+} amplitude (n = 10 cells from 3 animals). (A) specimen record showing Ca^{2+} transients, immediately prior to [black], during [dark red] and following [red] switching to a different control solution line (B) mean normalised Ca^{2+} transient amplitude. * indicates p <0.05, NS denotes non-significance (p >0.05), SS = steady state.

3.4 Discussion

3.4.1 Does acute exposure to 50 ng/ml TNF-α and IL-1β alter Ca^{2+} handling and contractility in a large mammal model?

TNF-α irreversibly reduced Ca^{2+} transient amplitude by 16.79 ± 3.16 % (Fig 3-2A), this corresponded with a decrease in sarcomere shortening by 20.31 ± 7.58 % (Fig 3-2B). This was to be expected as there is generally a positive relationship between $[Ca^{2+}]_i$ and cell shortening, as Ca^{2+} is required to bind to myofilaments to initiate contraction. As the same TNF-α concentration (50 ng/ml) was used by Greensmith and Nirmalan (2013) in rat myocytes, inducing similar reductions in both Ca^{2+} transient amplitude and contractility, this work confirms that the effect on systolic dysfunction is the same in a large mammal model.

As demonstrated in the specimens of Fig 3-1A and 3-1B, the onset of the depressive effect on both systolic Ca^{2+} and shortening observed was rapid, after only ~3 beats. This also agrees with the findings of Greensmith and Nirmalan (2013) which recorded both an initial and sustained reduction in systolic Ca^{2+} in rat myocytes.

IL-1β also irreversibly decreases Ca^{2+} transient amplitude by 23.63 ± 6.61 % (Fig 3-4A). Despite this reduction in Ca^{2+} transient amplitude, IL-1β had no significant effect on sarcomere shortening (Fig 3-4B). Given that the change with washout was large (a 146.01 ± 59.32 % increase), this may have masked any smaller changes to shortening with the cytokine alone.

Contrary to previous studies, including work by Greensmith and Nirmalan (2013) and Duncan et al. (2010), there was evidence of diastolic dysfunction with both TNF-α and IL-1β. TNF-α induced irreversible decreases in both diastolic Ca^{2+} by 4.35 ± 1.67 % and resting cell length by 0.46 ± 0.1 % (Fig 3-2C and 3-2D). IL-1β application was shown in Fig 3-4D, to induce a reduction in resting cell length by 0.76 ± 0.2 %, whilst no change to diastolic Ca^{2+} was recorded (Fig 3-4C). Given the magnitude of change to resting cell length with IL-1β, it is likely that and any change to diastolic Ca^{2+} would also be small. Therefore, the method used may not have been sensitive enough to detect a change.

No changes were recorded to the rate of relaxation with TNF-α (Fig 3-2F). As demonstrated in the specimen shown in Fig 3-1E, during washout 50 % time of sarcomere relaxation were decreased by 18.92 ± 7.11 %. The 91.67 ± 26.29 % increase in k_{SERCA} also found during TNF-α washout (Fig 3-6F), could account for the increased rate of sarcomere relaxation due to an elevated rate of SR Ca^{2+} uptake.

IL-1β did not affect the rate of relaxation (Fig 3-4F). This contradicts the increased rate of relaxation found by Radin et al. (2008) with IL-1β in rat. As the exposure time in this study was shorter, it is possible that an effect on relaxation had yet to become significant, that with prolonged exposure a change to relaxation may be detected. As shown in the specimen of Fig 3-3E, during washout 50 % time of sarcomere relaxation were decreased by 50.46 ± 3.84 %, this coincides with 80.54 ± 54 %, 29.47 ± 10.55 % and 78.26 ± 17.67 % increases in

k_{sys}, k_{caff} and k_{SERCA} respectively, while 90 – 10 % decay time of the Ca^{2+} transient decreased by 11.88 ± 9.41 % (Fig 3-7). All these measurements indicate an increase in rate of Ca^{2+} removal from control and cytokine steady state, which could account for the increased rate of sarcomere relaxation.

3.4.2 How do both 50 ng/ml TNF-α and IL-1β reduce Ca^{2+} transient amplitude?

The amplitude of systolic Ca^{2+} is dependent on many factors. In terms of inotropic control, there are two primary regulators (1) the amount of Ca^{2+} contained in the SR and (2) the amplitude of the on I_{CaL} (see section 1.2.8.2). Of the two, SR Ca^{2+} content is the more influential (Bers, 2002; Eisner, 2018). As such, in order to provide the basis of a pathological change to inotropy, it is logical to begin by ascertaining if SR Ca^{2+} is altered.

In young control sheep, TNF-α reduced SR Ca^{2+} content to 72.68 % of control (see Fig 3-5A and 3-5C). As the relationship between SR Ca^{2+} content and Ca^{2+} transient amplitude is cubic (Trafford, Diaz, Sibbring, & Eisner, 2000), it is possible to calculate the expected reduction in Ca^{2+} transient amplitude. As $(0.7268)^3$ = 0.3839, Ca^{2+} amplitude would be expected to decrease to 38.39 % of control, when in fact it only decreased to 83.21 %. IL-1β produced a 41.39 % reduction in SR Ca^{2+} content to 53.61 % of control (see Fig 3-5B and 3-5D). Given that $(0.5361)^3$ = 0.1541, therefore an 84.59 % decrease in Ca^{2+} transient amplitude to 15.41 % of control would be predicted, however IL-1β only reduced Ca^{2+} transient amplitude to 76.37 % of control.

Some caution must be used when interpreting the precise relationship and so apparent attenuated decrease of systolic Ca^{2+}. SR Ca^{2+} content was estimated using the amplitude of the caffeine-evoked Ca^{2+} transient, which can be independently affected by intracellular Ca^{2+} buffering. As the effects of TNF-α and IL-1β on Ca^{2+} buffering are unknown, it cannot be ruled out that such an effect may independently affect the amplitude of the caffeine evoked Ca^{2+} transient in these experiments (Trafford, Diaz, & Eisner, 1999). The decrease observed is considerable (27 and 41 % by TNF-α and IL-1β respectively), and therefore it is highly unlikely that altered Ca^{2+} buffering could account for this alone. It is much more likely that the

majority of this change is due a considerably reduced release of SR Ca^{2+} content resulting from a depletion of SR Ca^{2+} (J. W. Bassani et al., 1995). As such, at least qualitatively, the decrease of systolic Ca^{2+} produced by both cytokines *can* be explained by a decrease of SR Ca^{2+}. This is corroborated by the fact that in rat Greensmith and Nirmalan (2013) observed a decrease of SR Ca^{2+} when measured quantitively by integration of caffeine-evoked sodium currents – a method that measures total rather than only free Ca^{2+} and so is not affected by altered Ca^{2+} buffering (Varro, Negretti, Hester, & Eisner, 1993).

As previously mentioned I_{CaL} is also known to regulate Ca^{2+} transient amplitude. While this study was unable to investigate the effect of TNF-α and IL-1β on I_{CaL}, previous work by Greensmith and Nirmalan (2013) found that in response to application of 50 ng/ml TNF-α in rat ventricular myocytes peak I_{CaL} reduced by 11 %. This is a minor effect and given that the I_{CaL} and resultant Ca influx are fundamentally similar in both rat (Greensmith & Nirmalan, 2013) and young sheep (Dibb et al., 2004) it is unlikely that an effect on I_{CaL} would contribute to the reduction in Ca^{2+} transient amplitude. For completeness, in future work it may be useful to characterise the effects of both cytokines on I_{CaL} in a large mammal model.

3.4.3 How do TNF-α and IL-1β alter SR Ca^{2+} content? Are the Ca^{2+} removal mechanisms affected?

SR Ca^{2+} content can be influenced by change to SERCA activity and change to RyR P_o. Rapid SERCA activity increases Ca^{2+} uptake resulting in increased SR Ca^{2+} content, while a decrease in SR Ca^{2+} content – as was identified in response to both cytokines – can be contributed to by reduced Ca^{2+} uptake as a result of deceased SERCA activity. Equally, RyR regulates Ca^{2+} release from the SR and thus can alter SR Ca^{2+} content (Bers, 2002).

At steady state, TNF-α did not alter the rate of intracellular calcium removal. $k_{sys,}$ k_{caff} and k_{SERCA} (and 90 - 10 % decay time) were all unchanged by TNF-α (Fig 3-6), suggesting NCX, and crucially, SERCA, are unaffected by TNF-α exposure. As such, it appears that an effect on SERCA, or indeed NCX is not responsible for the decrease of SR Ca^{2+} content. The fact that k_{SERCA} increased following TNF-α washout is surprising as this implies that here, SERCA

activity may be increased. Why this is the case, needs to be investigated further, however for all things being equal this ought to coincide with a modest increase of SR Ca^{2+} content (Bode et al., 2011). However, during washout, the decrease of SR Ca^{2+} produced by TNF-α was maintained adding further support to the suggestion that the decrease in SR Ca^{2+} content by TNF-α is not associated with change to the rate of SERCA-mediated Ca^{2+} removal. In other words, even *if* SERCA *is* increased during washout, the maintained reduction of SR Ca^{2+} (Fig 3-5) suggests that either (1) the effect of TNF-α on SERCA is uncoupled from that on SR and (2) something else must be responsible for the depletion of SR Ca^{2+}.

IL-1β increased the rate of intracellular Ca^{2+} removal (k_{sys}) which resulted from an increase of k_{caff} and ultimately an increase of k_{SERCA}. This suggests that the activity of NCX and SERCA are both increased by IL-1β. Again, this is an interesting phenomenon and the mechanism underlying this ought to be investigate further. However, in respect to SR Ca^{2+}, the effects of IL-1β may be more complex than those of TNF-α. For all things being equal, an increase of NCX activity could contribute to decreased SR Ca^{2+} (Shannon, Pogwizd, & Bers, 2003). Conversely, an increase in SERCA activity would increase SR Ca^{2+}. It may be therefore, that the effect of IL-1β on NCX is greater than that on SERCA thus contributing to a net decrease of SR Ca^{2+} content. However, given the relative contribution of NCX and SERCA to net Ca^{2+} removal (R. A. Bassani et al., 1992), and that that magnitude of effect on k_{SERCA} and k_{caff} is similar it is likely that as with TNF-α, another mechanism is primarily responsible for decreasing SR Ca^{2+}.

What is clear from both sets of data is SERCA activity is not *reduced* by either of the cytokines. To the contrary, most data suggests that SERCA activity is actually increased. This strongly suggests that something other than an effect on SERCA is responsible for the decrease of SR Ca^{2+} content.

One possible mechanism by which both TNF-α and IL-1β could reduce SR Ca^{2+} content is if they were to potentiate the RyR.

3.4.4 TNF-α and IL-1β produce and temporary potentiation of systolic Ca^{2+} – Could RyR sensitivity be increased?

SR Ca^{2+} is also influenced by RyR P_o. When RyR P_o is increased, so does diastolic SR Ca^{2+} leak leading to a reduced SR Ca^{2+} content (Belevych et al., 2007; Shannon et al., 2003). Luminal Ca^{2+} can also impact the RyR, as such reduced SR Ca^{2+} content would be expected to decrease RyR P_o (Ching et al., 2000).

A proportion of cytokine treated cells presented with an early potentiation of the Ca^{2+} transient and subsequent shortening in response to both cytokines (Fig 3-8). This agrees with findings in the work of Greensmith and Nirmalan (2013) which acknowledged a 1^{st} beat increase in Ca^{2+} transient amplitude in response to 50 ng/ml TNF-α in rat, but did not investigate further. The corresponding effects of these cytokines on shortening indicate that this early potentiation is a true physiological phenomenon, not a fluorescent artefact.

The effect of change to RyR P_o can cause only a brief change to Ca^{2+} transient amplitude (Trafford et al., 2000), therefore this initial 1-3 beat increase in Ca^{2+} amplitude is evidence to suggest increase in Ca^{2+} release from the SR through potentiation of the RyR. RyR regulates Ca^{2+} release from the SR, therefore this may account for the decrease in SR Ca^{2+} content during exposure, especially if, like caffeine (Greensmith et al., 2014), this Ca^{2+} release drives Ca^{2+} extrusion via NCX.

With both cytokines, there were also a proportion of cells which did not present with this initial increase in Ca^{2+} transient amplitude (Fig 3-9). The 24.07 % decrease in 1^{st} beat Ca^{2+} transient amplitude with IL-1β corresponds with the 23.63 % mean decrease identified at steady state, as shown in Fig 3-4A. This suggests that in this subgroup RyR potentiation may occur far more quickly, thus the final effect of IL-1β on systolic Ca^{2+} is rapid. Although I_{CaL} was not measured in this study, it is also possible that, in this sub-group of non-responders, these cytokines may be having a greater effect on LTCC, leading to decreased I_{CaL}, than that on RyR P_o.

While this temporary potentiation of systolic Ca^{2+} is indicative of increased RyR sensitivity, it is not definitive. As such chapter 4 will investigate this further.

3.4.5 Do TNF-α and IL-1β alter the relationship between cytoplasmic Ca^{2+} and sarcomere shortening?

TNF-α induced simultaneous decrease in both diastolic Ca^{2+} and resting sarcomere length by 4.35 ± 1.67 % and 0.46 ± 0.1 % respectively (Fig 3-2C and 3-2D), maintained following washout, indicates an increase in myofilament sensitivity to Ca^{2+}. After TNF-α washout, however the 16.79 ± 3.16 % decrease in Ca^{2+} transient amplitude was sustained, while sarcomere shortening was unchanged (Fig 3-2A and 3-2B). This could be used to further suggest increased myofilament sensitivity following washout, however it may also suggest that TNF-α reduced myofilament sensitivity, which was recovered with washout.

A potential change to myofilament sensitivity is also evident in IL-1β treated cells. Resting sarcomere length decreased by 0.76 ± 0.2 % while diastolic Ca^{2+} was unchanged, during both IL-1β application and washout (Fig 3-4C and 3-4D), and Ca^{2+} transient amplitude was decreased by 23.63 ± 6.61 % despite sarcomere shortening remaining unchanged, both of which could suggest increased sensitivity to Ca^{2+}. With washout, the effect on Ca^{2+} transient amplitude was maintained, however a 146.01 ± 59.32 % increase in sarcomere shortening occurred (Fig 3-4A and 3-4B). As with TNF-α, this could support reduced sensitivity to Ca^{2+}, recovered following IL-1β washout, or a direct increase in sensitivity to Ca^{2+} with washout.

This is evidence that some change to myofilament sensitivity may be occurring with TNF-α and IL-1β, however whether myofilament sensitivity is increased or decreased with exposure to these cytokines is still uncertain. This does, however, provide further cause to investigate the effects of both cytokines of myofilament sensitivity to Ca^{2+}. In addition, evidence supports that both cytokines may potentiate the RyR. The effects of TNF-α and IL-1β on RyR P_o and myofilament sensitivity to Ca^{2+} will be explored further in subsequent chapters.

Chapter 4

The effects of 50 ng/ml TNF-α and IL-1β on cardiac intracellular calcium waves

4.1 Introduction

4.1.1 Background to the effect of cytokines on RyR

Though the reduction in SR Ca^{2+} content by TNF-α and IL-1β identified in section 3.3.3, does not appear to be a consequence of SERCA inhibition, this may be the result of an increase in diastolic SR Ca^{2+} leak from the SR due to increased RyR P_o. SR Ca^{2+} leak is spontaneous release Ca^{2+} release from the SR via the RyR. Increased RyR P_o contributes to an increase in net diastolic Ca^{2+} leak from the SR. Increased leak leads to a reduction in SR Ca^{2+} content (Eisner, Kashimura, O'Neill, Venetucci, & Trafford, 2009).

Previous findings suggest there may be a role for increased SR Ca^{2+} release in sepsis. X. Zhu et al. (2005) found evidence of increased SR Ca^{2+} leak in a cecal ligation and puncture (CLP) model of sepsis, as Ca^{2+} spark frequency increased on time-dependent basis, indicating an effect on RyR P_o. Other studies suggest that this effect on RyR P_o may be due to the increased presence of proinflammatory cytokines in septic serum. In rat ventricular myocytes treated with TNF-α and IL-1β (0.05 and 2 ng/ml) for 3 hours, the frequency and duration of Ca^{2+} sparks increased, as did wave frequency when the cells were also exposed to high Ca^{2+} levels (Duncan et al., 2010). Similar effects on spontaneous Ca^{2+} release events – Ca^{2+} sparks and waves – were identified in atrial myocytes following 2 hour exposure to 0.05 ng/ml TNF-α (Zuo et al., 2018).

TNF-α is also elevated in other inflammatory conditions of the heart, such as in reperfusion injury following ischemia and post–myocardial infarction (Fauconnier et al., 2011; Y. Yang et al., 2014). Increased ROS production, particularly NO, promoted by TNF-α (10 ng/ml) treatment was associated with increased *S*-nitrosylation on the RyR, contributing to RyR P_o modulation (Fauconnier et al., 2011). The high levels of TNF-α in a post-myocardial infarction heart failure model have been associated with a reduced affinity of CaM binding to RyR (Y. Yang et al., 2014). RyR P_o is known to increase with less CaM binding (Balshaw, Xu, Yamaguchi, Pasek, & Meissner, 2001).

Although few studies have investigated the effect of IL-1β alone on RyR activity, IL-1β has been associated with arrhythmia, which can occur as a result of increased diastolic SR Ca^{2+} leak. IL-1β (10 ng/ml) promotes CaMKII oxidation and phosphorylation in cardiac strips from a diabetic model. CaMKII is a known modulator of RyR suggesting an indirect effect of IL-1β on RyR P_o (Monnerat et al., 2016).

However, previous studies suffer similar limitations to those described in chapter 3. Multiple experimental approaches were used; therefore, the effects of these cytokines were difficult to assimilate into a unified model. Furthermore, the previously described studies above investigating the effect of these cytokines on cardiac RyR, were all carried out in small mammal models; either rat (Duncan et al., 2010; Fauconnier et al., 2011; Y. Yang et al., 2014) or mice (Monnerat et al., 2016; Zuo et al., 2018), as opposed to in a large mammal model. This is important as there are differences in the binding affinities of RyR and their spatial density in different mammal species, which could affect overall activity (Bers, 1991).

In addition, these studies investigated effects on RyR and its modulators after prolonged (> 1 hour) exposure to one or both cytokines. Given that experiments of Fig 3-8 showed 1st beat potentiation of the Ca^{2+} transient (refer to section 3.3.5), implying that an effect on RyR activity may be more immediate than previously thought.

Given these limitations combined, there is a clear need to further investigate the effect of TNF-α and IL-1β on RyR function.

4.1.2 What are intracellular Ca^{2+} waves?

Ca^{2+} waves are multiple spontaneous diastolic Ca^{2+} release events from the SR which propagate across the myocyte to generate further Ca^{2+} release events. These Ca^{2+} release events are therefore also not uniformly distributed across the cell as would be expected in Ca^{2+} transient. The probability that a Ca^{2+} wave will occur is dependent on both the rate of SR Ca^{2+} loading and SR Ca^{2+} threshold, the latter of which is determined by RyR P_o. As such both increased SR Ca^{2+} uptake and increased RyR P_o can contribute to wave generation.

Increased RyR P_o generally cannot induce waves alone, however it can modulate the threshold for waves. If RyR P_o is increased the threshold would be reduced and therefore a small increase in SR Ca^{2+} content could evoke Ca^{2+} waves (Stokke et al., 2011; Venetucci, Trafford, & Eisner, 2007). If increased RyR P_o reduces the threshold beyond that of SR Ca^{2+} content, this will cause waves, as found in some ventricular arrhythmias and sudden cardiac death (Jiang et al., 2005). Equally if RyR P_o were to be reduced, the threshold for Ca^{2+} waves would become increased, therefore a large increase in SR Ca^{2+} content would be required to trigger Ca^{2+} release events and thus Ca^{2+} waves (Venetucci, Trafford, Diaz, O'Neill, & Eisner, 2006).

4.1.3 Experimental production of waves

Production of Ca^{2+} waves under experimental conditions can be carried out through either the RyR potentiated, increased SR Ca^{2+} content or a combination of both (Stokke et al., 2011; Venetucci et al., 2007). As this series of experiment was designed to measure the effect of TNF-α and IL-1β on RyR P_o through change to the SR Ca^{2+} threshold for waves, potentiation of the RyR independently in order to evoke waves would interfere with the results in response to both cytokines. Overloading the SR is therefore the most appropriate method of causing Ca^{2+} waves in this experiment.

There are multiple was of increasing SR Ca^{2+} content to meet the threshold and thus induce Ca^{2+} overload. A β-agonist could be used to increase SR Ca^{2+} loading, leading to the production of waves, however β-adrenergic stimulation is also known to impact RyR-mediated Ca^{2+} release in response to Ca^{2+} influx via the LTCC (Maxwell, Domeier, & Blatter, 2013; Zhou et al., 2009). Ouabain is a known Na^{+}-K^{+} ATPase inhibitor causing increased $[Na]_{i,}$ this in turn drives Ca^{2+} influx via reverse-phase NCX activity. The resulting elevation in $[Ca^{2+}]_i$ enhances SR Ca^{2+} loading, thus increasing SR Ca^{2+} content (Nishio et al., 2004). Increased $[Ca^{2+}]_o$ is able to steepen $[Ca^{2+}]$ gradients, facilitating non-specific Ca^{2+} influx and SR uptake, as well as SR Ca^{2+} leak (Bovo, Mazurek, Blatter, & Zima, 2011). A combination of both ouabain and high $[Ca^{2+}]_o$ could be used to further drive reverse-phase NCX activity and SR Ca^{2+} loading, ensuring production of waves for the given purpose of these experiments.

4.1.4 Aims

The aim of this experiment was to investigate the effects of TNF-α and IL-1β on (1) Ca^{2+} wave dynamics in a large mammal model and (2) any change to SR Ca^{2+} threshold for waves. This was in order to determine whether either cytokine had an effect on RyR potentiation.

4.2 Methods

4.2.1 Wave facilitation

As described in section 2.1.4 left ventricular myocytes from young control sheep were loaded with the ratiometric Ca^{2+} indicator Fura-2. The standard experimental solution given in section 2.2.1 was modified to include 5 mM extracellular Ca^{2+} and 0.3 mM Ouabain and so evoke spontaneous Ca^{2+} waves. These concentrations were optimised (see Fig 4-1) to produce a basal wave frequency of approximately 21 waves per minute. This meant that wave frequency was high enough to provide the required sensitivity to detect an effect if one was to occur but low enough to ensure each wave was a distinct event.

During a given experiment once wave frequency was stable, TNF-α and IL-1β were each applied individually at 50 ng/ml for 5 minutes prior to a 2 minute wash period.

4.2.2 Quantification of SR Ca^{2+} threshold for waves

In a similar protocol to that detailed in section 2.3.4, 20 mM caffeine was applied during a wave to indirectly measure SR Ca^{2+} content immediately prior to the wave. This determined the SR Ca^{2+} content required to reach the threshold causing a Ca^{2+} wave and therefore can be used to indicate the SR Ca^{2+} threshold for waves. The SR Ca^{2+} threshold indicates RyR P_o, and increased RyR P_o would be expected to reduce the threshold, while a decreased RyR P_o would be expected to raise the threshold (Stokke et al., 2011; Venetucci et al., 2007).

Caffeine potentiates the RyR, leading to Ca^{2+} release from the SR, as such it alters the SR threshold. This also contributes to a decrease in SR Ca^{2+} content to below the threshold, abolishing Ca^{2+} waves (Greensmith et al., 2014). To prevent caffeine impacting results through this independent effect on RyR and SR threshold, caffeine could only be applied at the end of an experiment. Some experiments were carried out solely on control waves, with caffeine application once a steady state had been reached. Of cells which received a cytokine treatment, after 5 minutes exposure, either caffeine was applied – thus the experiment was concluded – or the caffeine application followed a 2 minute washout period.

4.2.3 Analysis of Ca^{2+} waves

IonWizard files were exported as text files enabling them to be imported into Clampfit. Clampfit – while not designed for this specific purpose – has sophisticated event detection algorithms which are highly suitable for analysis of Ca^{2+} waves. The baseline of the Ca^{2+} signal was manually corrected using Clampfit, to allow measurement of Ca^{2+} wave amplitude and frequency.

A first marker was placed to indicate the baseline. As Ca^{2+} fluorescence moves in the positive direction during waves, only peaks moving in a positive direction were detected. A second marker just above the baseline and associated noise to indicate a threshold and by which only points that exceed beyond – ideally waves – would be detected. To further exclude any false peaks from being detected noise rejection generally initially set to ~50 ms. The noise rejection threshold did however often need to be altered in either direction, dependent on the volume of noise in the trace, while ensuring all true waves were detected. Using Clampfit event detection, the peak height of each wave was then automatically identified allowing the measurement of Ca^{2+} wave amplitude and instantaneous frequency, based on the time points at which these peaks occurred. If any signal interference remained despite implementation of these thresholds, noise effecting Ca^{2+} wave amp could be manually rejected and flagged as an incorrect amplitude value, therefore not interfering with results.

10 s averages were taken at the end of each 1 minute exposed to cytokine, and from the end of each 30 s interval during the washout period. Mean values were normalised to control. Data were analysed using a one-way repeated measures ANOVA.

4.3 Results

4.3.1 Optimisation of inducing waves in sheep myocytes

While other studies have implemented a similar method of evoking Ca^{2+} waves with ouabain and high $[Ca^{2+}]_o$, the sensitivity of Na^+/K^+- ATPase to ouabain varies between species, in particular large and small mammals (Blanco & Mercer, 1998). It was therefore important to reoptimize the method for use in sheep myocytes.

In control, a steady state wave frequency and amplitude was desired, in which there were gaps between waves greater than 1 second and Ca^{2+} wave amplitude was reasonably consistent. This was to allow any to change to frequency following the application of either cytokine. To determine how best to obtain this control wave frequency, a variety of ouabain and Ca^{2+} concentrations were tested.

The specimen record of Fig 4-1 shows the process by which the ouabain and Ca^{2+} concentration was optimised to provide a suitable basal wave frequency. As demonstrated by Fig 4-1A in most cases 0.1 mM ouabain and 5 mM Ca^{2+} did not provide sufficient SR Ca^{2+} overload to produce Ca^{2+} waves. As per Fig 4-1B Increasing $[Ca^{2+}]_o$ to 10 mM Ca^{2+}, did produce Ca^{2+} waves. However, those waves were not of consistent amplitude, presumably because wave frequency was so high that complete recovery between a given wave wasn't permitted, as such and as per Fig 4-1C, it was found that modulating ouabain concentration had a more subtle effect on frequency. After several iterations it was found that 0.3 mM ouabain and 5 mM Ca^{2+} could reliably evoke Ca^{2+} waves at the desired frequency (Fig 4-1D). Though Fig 4-1D provides a typical example, the baseline wave frequency did vary considerably between cells, but under no circumstance was wave frequency so high that the data could be not be used.

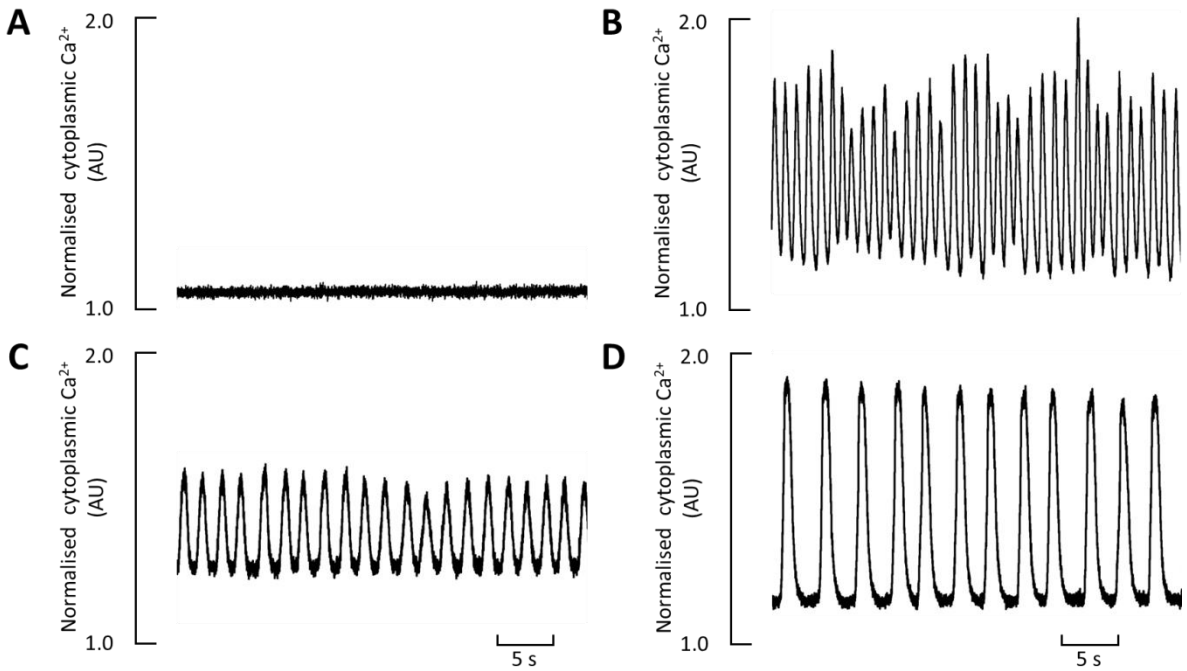

Figure 4-1. Specimen Ca^{2+} traces of cells exposed to different ouabain and Ca^{2+} concentrations. (A) 0.1 mM ouabain and 5 mM Ca^{2+}. (B) 0.1 mM ouabain and 10 mM Ca^{2+}. (C) 0.5 mM ouabain and 5 mM Ca^{2+}. (D) 0.3 mM ouabain and 5 mM Ca^{2+}.

4.3.2 The effect of 50 ng/ml TNF-α on intracellular Ca^{2+} wave amplitude and frequency

The specimen records of Fig 4-2 show an example of the time-dependent effect of TNF-α on Ca^{2+} wave amplitude and frequency. Fig 4-2A and 4-2B show typical original Ca^{2+} and sarcomere length records respectively. A time-dependent decrease in Ca^{2+} wave amplitude is clear and corresponds with a respective decrease in sarcomere shortening. Fig 4-2D provides example individual Ca^{2+} waves from the end of control, TNF-α and wash. As the effect on frequency isn't as obvious, Fig 4-2C provides the instantaneous frequency over the time course of the same experiment, again, a progressive increase is apparent. Fig 4-3 and Table 4-1 show the mean time-dependent decrease of Ca^{2+} wave amplitude and increase in frequency produced by TNF-α. On average, after 5 minutes of TNF-α exposure wave frequency was increased by 38.22 ± 8.11 % (n=22, p <0.001) whereas amplitude was

decreased by 46.13 ± 5.75 % (n=22, p <0.001). Neither the effect on frequency or amplitude reversed during the duration of the wash period.

Table 4-1: The effect of 50 ng/ml TNF-α on normalised Ca^{2+} wave amplitude and instantaneous wave frequency over time and with washout

Time (min)	Normalised Ca^{2+} amplitude (AU)	Normalised instantaneous frequency (AU)
Control	1 ± 0	1 ± 0
1	0.85 ± 0.04	1.08 ± 0.05
2	0.79 ± 0.05	1.16 ± 0.04
3	0.73 ± 0.05	1.28 ± 0.05
4	0.58 ± 0.04	1.4 ± 0.08
5	0.54 ± 0.06	1.38 ± 0.08
Wash (2 min)	0.45 ± 0.07	1.42 ± 0.15

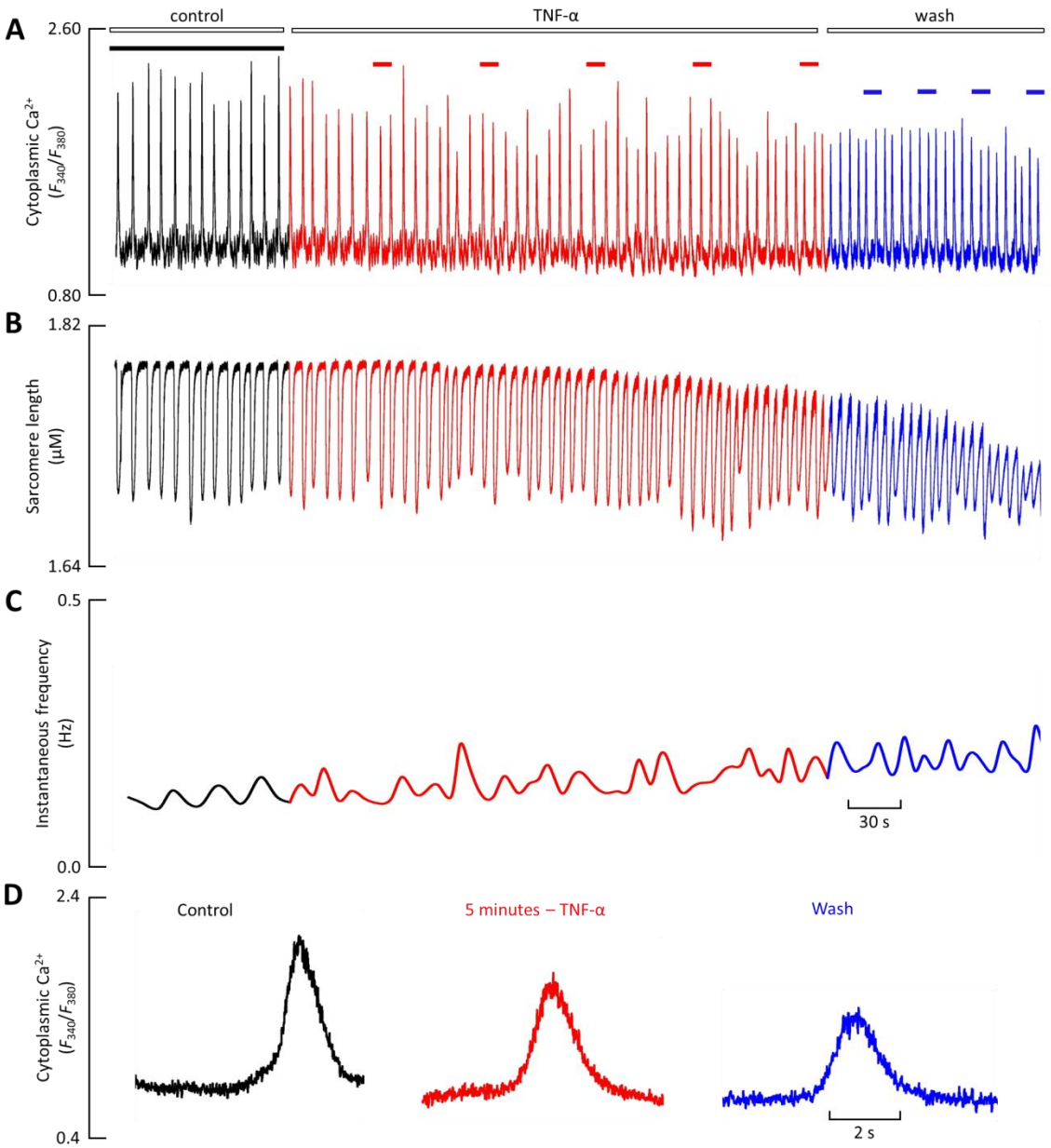

Figure 4-2. A specimen record of the effect of 50 ng/ml TNF-α [red] and washout [blue] wave dynamics, with averaged regions indicated. (A) specimen record showing Ca^{2+} waves. (B) specimen record showing sarcomere shortening. (C) specimen record showing change in the instantaneous frequency of Ca^{2+} waves (D) individual specimen waves from a control steady state period [black], 5 minutes of TNF-α exposure [red] and a 2 minute washout [blue]. The coloured lines above indicate the 10 s periods which were sampled and averaged, these were normalised to the control steady state indicated with the black line above.

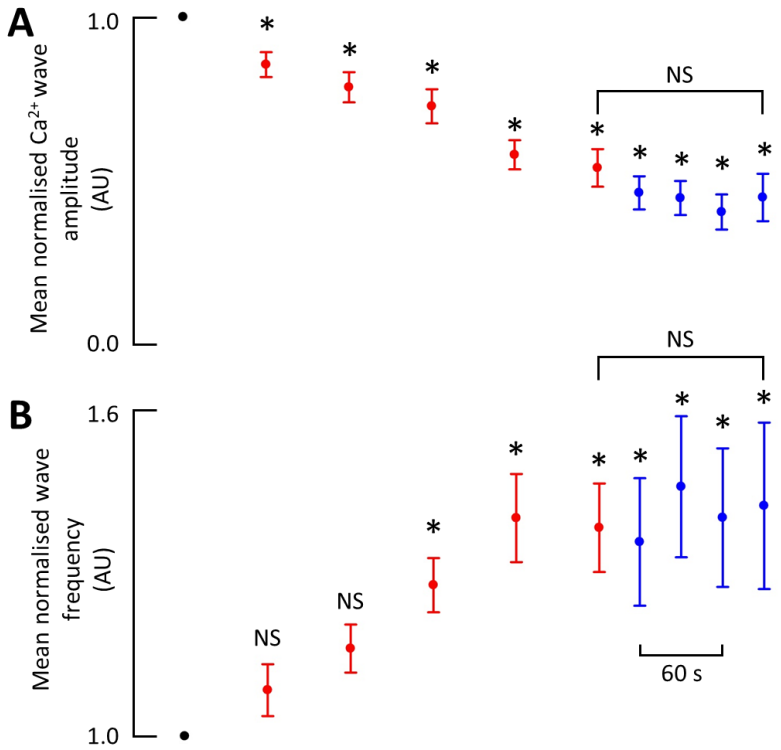

Figure 4-3. The effects of TNF-α [red] on Ca^{2+} wave dynamics in left ventricular myocytes from young control sheep over 5 minutes, and during a 2 minute washout [blue] (n = 33 cells from 10 animals). (A) mean Ca^{2+} wave amplitude. (B) mean wave frequency. 10 s periods were averaged at the end of each minute of cytokine application and each 30 s during washout. * indicates $p < 0.05$, NS denotes non-significance ($p > 0.05$).

4.3.3 The effect of 50 ng/ml IL-1β on intracellular Ca^{2+} wave amplitude and frequency

The specimen records of Fig 4-4 show an example of the time-dependent effect of IL-1β on Ca^{2+} wave amplitude and frequency. Fig 4-4A and 4-4B show typical original Ca^{2+} and sarcomere length records respectively. A time-dependent decrease in Ca^{2+} wave amplitude is clear and corresponds with a respective decrease in sarcomere shortening. Fig 4-4D provides example individual Ca^{2+} waves from the end of control, TNF-α and wash. As the effect on frequency is not as obvious, Fig 4-4C provides the instantaneous frequency over the time course of the same experiment, with an obvious progressive increase. Fig 4-5 and Table 4-2 show the mean time-dependent decrease of Ca^{2+} wave amplitude and frequency produced

by IL-1β. On average, after 5 minutes of IL-1β exposure the wave frequency was increased by 28.35 ± 11.35 % (n=32, p <0.001), whereas amplitude was decreased by 34.42 ± 6.82 % (n=32, p <0.001). As with TNF-α. neither the effect on frequency or amplitude reversed during the duration of the washout period.

Table 4-2: The effect of 50 ng/ml IL-1β on normalised Ca^{2+} wave amplitude and instantaneous wave frequency over time and with washout

Time (min)	Normalised Ca^{2+} amplitude (AU)	Normalised instantaneous frequency (AU)
Control	1 ± 0	1 ± 0
1	0.88 ± 0.05	1.07 ± 0.03
2	0.81 ± 0.06	1.14 ± 0.05
3	0.78 ± 0.06	1.13 ± 0.05
4	0.70 ± 0.06	1.16 ± 0.06
5	0.66 ± 0.07	1.28 ± 0.11
Wash (2 min)	0.59 ± 0.08	1.51 ± 0.13

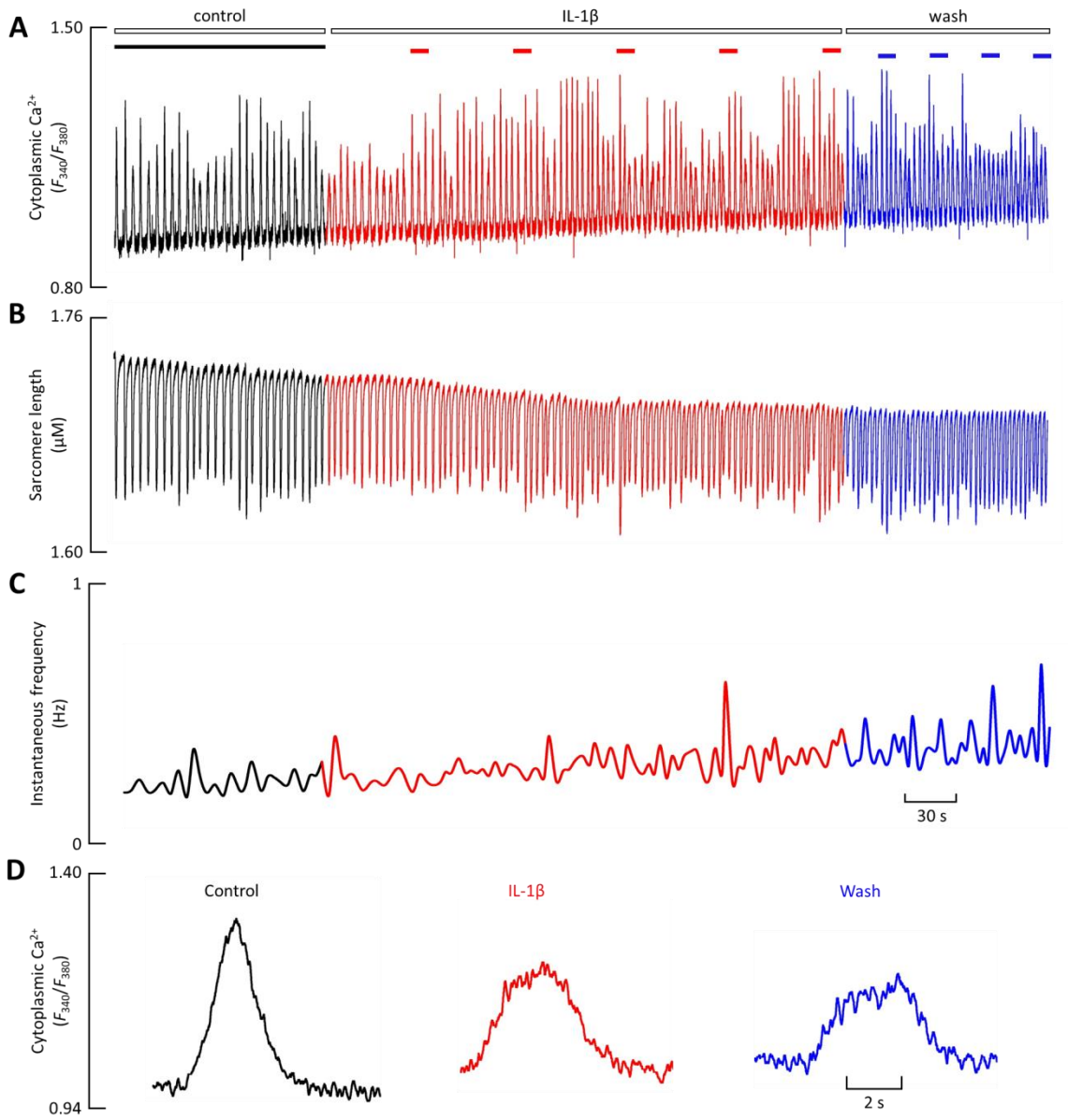

Figure 4-4. A specimen record of the effect of 50 ng/ml IL-1β [red] and washout [blue] wave dynamics, with averaged regions indicated. (A) specimen record showing Ca^{2+} waves. (B) specimen record showing sarcomere shortening. (C) specimen record showing change in the instantaneous frequency of Ca^{2+} waves (D) individual specimen waves from a control steady state period [black], 5 minutes of IL-1β exposure [red] and a 2 minute washout [blue]. The coloured lines above indicate the 10 s periods which were sampled and averaged, these were normalised to the control steady state indicated with the black line above.

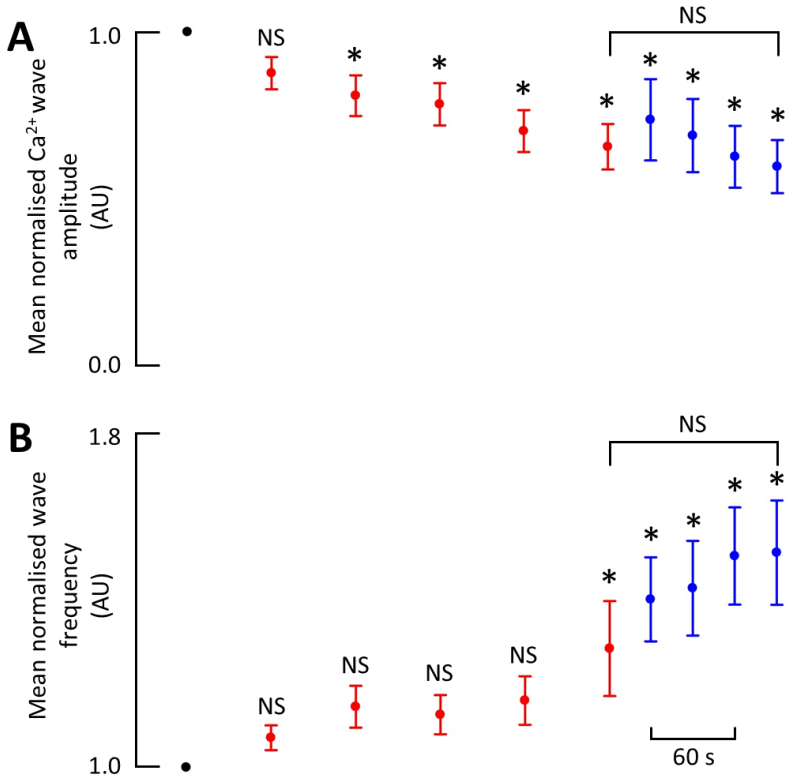

Figure 4-5. The effects of IL-1β [red] on Ca^{2+} wave dynamics in left ventricular myocytes from young control sheep over 5 minutes, and during a 2 minute washout [blue] (n = 39 cells from 7 animals). (A) mean Ca^{2+} wave amplitude. (B) mean wave frequency. 10 s periods were averaged at the end of each minute of cytokine application and each 30 s during washout. * indicates p <0.05, NS denotes non-significance (p >0.05).

4.3.4 The effect of TNF-α and IL-1β on SR Ca^{2+} content threshold for waves

The specimen records of Fig 4-6A and 4-6B show examples of the effect of TNF-α and IL-1β respectively on the amplitude of caffeine-evoked SR Ca^{2+} release. It is important to note that caffeine was applied during the onset of a Ca^{2+} wave and thus infers the SR Ca^{2+} threshold for that wave. With TNF-α on average (Fig 4-6C) caffeine-evoked Ca^{2+} wave amplitude decreased by 49.16 % (control; 1.66 ± 0.2 (n=12), TNF-α; 0.85 ± 0.11 (n=5) F_{340}/F_{380}, p = 0.021). Following washout this change was maintained (control; 1.66 ± 0.2 (n=12), washout; 0.77 ± 0.13 (n=6) F_{340}/F_{380}, p = 0.818).

On average (Fig 4-6D), with IL-1β the caffeine-evoked Ca^{2+} wave amplitude decreased by 52.94 % (control; 1.66 ± 0.2 (n=12), IL-1β; 0.78 ± 0.13 (n=13) F_{340}/F_{380}, p = 0.005). This caffeine-evoked Ca^{2+} transient amplitude was partially recovered with washout, which is not significantly different from both control (control; 1.66 ± 0.2 (n=12), washout; 1.29 ± 0.28 (n=8), F_{340}/F_{380}, p = 0.218) and following 5 minutes of IL-1β exposure (IL-1β; 0.78 ± 0.13 (n=13), washout; 1.29 ± 0.28 (n=8), F_{340}/F_{380}, p = 0.167).

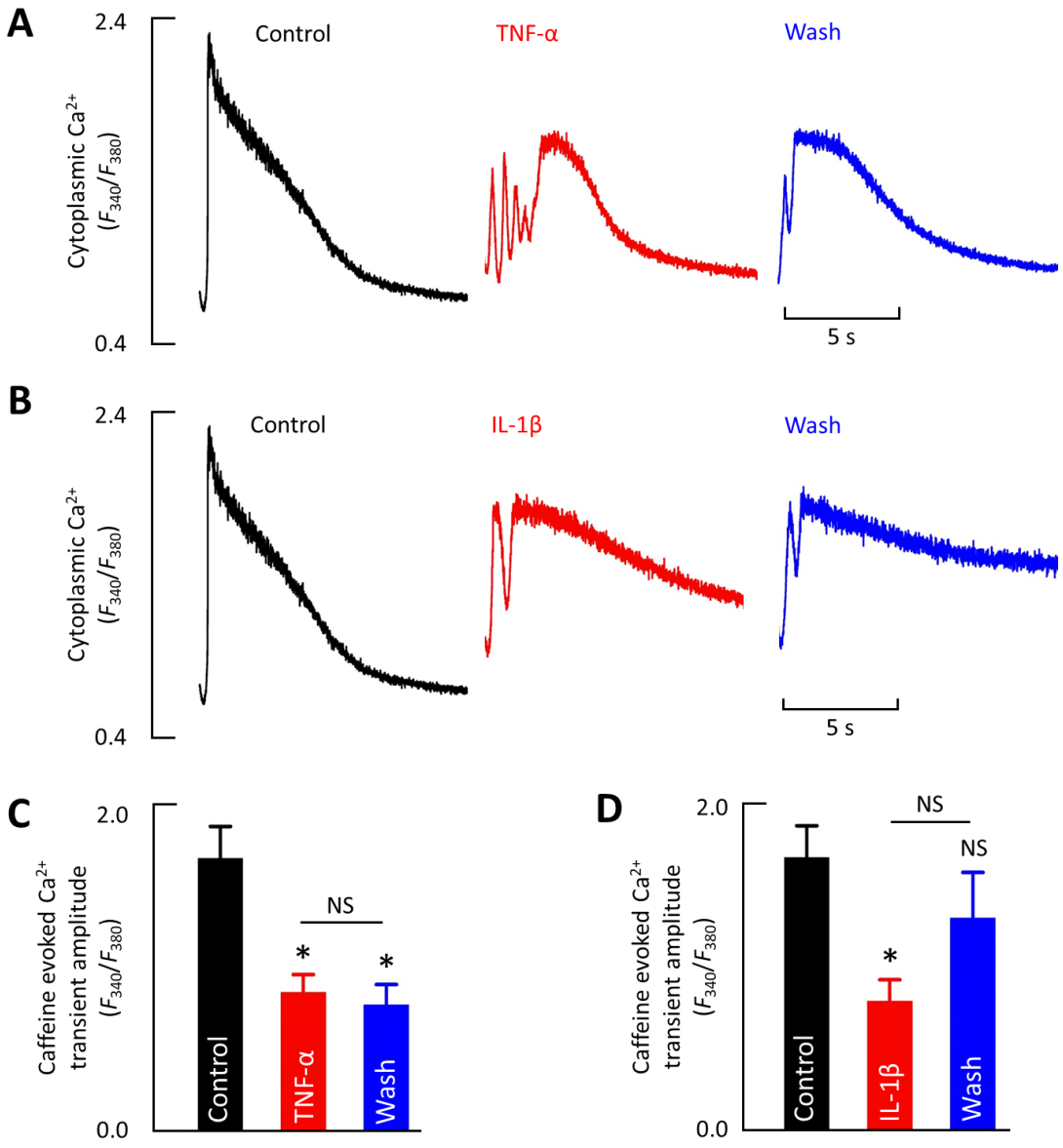

Figure 4-6. The effects of TNF-α and IL-1β on the SR Ca^{2+} threshold for waves. (A) specimen trace of caffeine application mid-wave in control conditions [black], with TNF-α [red] and wash [blue]. (B) specimen trace of caffeine application mid-wave in control conditions [black], with IL-1β [red] and wash [blue]. (C) mean caffeine-evoked Ca amplitude with TNF-α. (D) mean caffeine-evoked Ca^{2+} amplitude with IL-1β. * indicates $p < 0.05$, NS denotes non-significance ($p > 0.05$). (control, n = 12 cells from 4 animals; TNF-α, n = 5 cells from 3 animals; IL-1β, n = 13 cells from 5 animals; TNF-α washout, n = 6 cells from 4 animals; IL-1β washout, n = 8 cells from 5 animals).

4.4 Discussion

4.4.1 Does 50 ng/ml TNF-α and IL-1β potentiate the RyR?

Both TNF-α and IL-1β decreased mean Ca^{2+} wave amplitude and increased mean wave frequency (Fig 4-3 and 4-5). As decreased SR Ca^{2+} threshold occurs when a lower SR Ca^{2+} content is required before SR Ca^{2+} release, the SR Ca^{2+} content is lower and thus amplitude of Ca^{2+} released with each wave will also be reduced. Waves also occur more frequently when the threshold is reduced as rate of SR Ca^{2+} uptake is unchanged and a lower SR Ca^{2+} content threshold for waves can be met more promptly. The changes to both parameters therefore indicated a decrease in SR Ca^{2+} threshold for waves.

This was confirmed by the caffeine-evoked Ca^{2+} wave amplitude when applied mid-wave provided the SR Ca^{2+} content at the time of the wave, at the end of cytokine exposure this was reduced by 49.16 % and 52.94 % (Fig 4-6) with TNF-α and IL-1β respectively. As these waves occurred at lower SR Ca^{2+} contents, this further supports that both cytokines decreased SR Ca^{2+} threshold for waves. The SR Ca^{2+} threshold for waves is primarily determined by RyR P_o. The decrease in SR Ca^{2+} threshold, therefore suggests RyR P_o was elevated.

It should be noted that for a wave to occur SR Ca^{2+} content must be increased to that threshold; a concept that is important to understand the basis of certain arrhythmias (Venetucci et al., 2007). As the primary focus of these experiments were to measure SR Ca^{2+} threshold and therefore RyR P_o, not SR Ca^{2+} content, the experiment conditions provided initially forced SR Ca^{2+} content to meet the threshold. The above data supports that TNF-α and IL-1β decreased the SR Ca^{2+} threshold for waves in sheep myocytes, suggesting that both cytokines increase RyR P_o.

4.4.2 What is the underlying mechanism of increased RyR P_o with TNF-α and IL-1β?

RyR P_o can be Ca^{2+} dependent – with elevated SR Ca^{2+} or $[Ca^{2+}]_i$ contributing to elevated RyR P_o (Diaz, Trafford, O'Neill, & Eisner, 1997) – or Ca^{2+} independent. An example of a Ca^{2+} independent change to RyR P_o is caffeine, which potentiates the RyR (Greensmith et al., 2014).

In section 3.3.3, both cytokines were shown to reduce SR Ca^{2+} content. A reduction in SR Ca^{2+} content would be expected to decrease RyR P_o (Stokke et al., 2011) and thus increase the threshold for waves (Diaz et al., 1997). An increase in diastolic $[Ca^{2+}]_i$ could also elevate RyR P_o, however the experiments of sections 3.3.1 and 3.3.2 revealed that neither cytokine increased diastolic $[Ca^{2+}]_i$, but rather TNF-α caused a decrease in diastolic $[Ca^{2+}]_i$ and IL-1β had no effect. Given that changes to SR and cytoplasmic Ca^{2+} produced by TNF-α and IL-1β, if anything would decrease RyR P_o, it appears that effects of both cytokines must therefore increase RyR P_o directly as opposed to a Ca^{2+} dependent effect.

There are multiple other Ca^{2+} independent mechanisms of change to RyR P_o. TNF-α and IL-1β can both elevate mitochondrial ROS and activate ROS procuring enzymes such as NADPH oxidase (Nox) and xanthine oxidase. Acute cytokine exposure can lead to generation of ROS in a dose dependent and transient manner (Brandes, Weissmann, & Schroder, 2014; X. Chen et al., 2008; Fauconnier et al., 2011; D. Yang et al., 2007). Nox2 in particular is found in the sarcolemma, therefore sharing a close proximity to RyR, allowing local rises in ROS (Brandes et al., 2014).

Elevated NO production can also result from TNF-α and IL-1β exposure. With IL-1β, this rise in NO can occur due to activation of a myocardial L-arginine NO-pathway. The effects of TNF-α on negative inotropy have been attributed to NO production (Evans, Lewis, & Shah, 1993; Fauconnier et al., 2011; Finkel et al., 1992).

ROS and NO are capable of activating signalling pathways and proteins such as Ca^{2+}/calmodulin(CaM)-dependent protein kinase II (CaMKII) and CaM respectively, to

indirectly modulate RyR P_o, which if increased can contribute to SR Ca^{2+} leak (Ho et al., 2014; Okabe, Tsujimoto, & Kobayashi, 2000; Y. Yang et al., 2014). For instance, superoxide can initiate a signalling pathway involving CaM, Whilst CaM can both activate and inactivate RyR, dependent on concentration (Sigalas, Bent, Kitmitto, O'Neill, & Sitsapesan, 2009), CaM binding generally modulates Ca^{2+} release from the SR through reducing RyR P_o, acting as an inhibitor (Balshaw et al., 2001; Okabe et al., 2000). Low concentrations of superoxide can increase RyR P_o, while much higher concentrations (μM) can prevent CaM from inhibiting RyR entirely (Okabe et al., 2000). The resulting low CaM–RyR binding affinity can lead to severe ventricular arrhythmia (Y. Yang et al., 2014).

NO can drive CaMKII oxidation, contributing to increased CaMKII-dependent phosphorylation of RyR. RyR phosphorylation increases RyR P_o and thus Ca^{2+} spark frequency (Ho et al., 2014; Stokke et al., 2011). Prolonged (24 hour) IL-1β and (2 hour) TNF-α exposure have both been shown to promote CaMKII oxidation and phosphorylation of RyR in mice. This has been associated with arrhythmia (Monnerat et al., 2016; Zuo et al., 2018).

Duncan et al. (2010) found that combined application of both TNF-α and IL-1β had no effect on RyR potentiation in rat ventricular myocytes following permeabilisation. This suggests that a secondary mediator is involved in the effect on RyR which is able to accumulate in intact cells and required to do so for modulation to occur. Potential mediators could be ROS or NO, which can accumulate locally to RyR.

ROS and NO can also act directly on RyR, to modulate RyR P_o. Redox modifies the disulphide bonds between cysteine molecules. RyR contains many of these groups and therefore are sensitive to redox modification altering RyR P_o. ROS induced oxidation can increase the sensitivity of RyR to Ca^{2+} (Y. Yang et al., 2014; Zima & Blatter, 2006; Zissimopoulos & Lai, 2006). As such ROS, including superoxide and H_2O_2, can increase RyR P_o promoting Ca^{2+} release from the SR (Kaneko, Matsumoto, Hayashi, Kobayashi, & Yamazaki, 1994; Zima & Blatter, 2006).

NO is also capable of directly modulating cardiac RyR via covalent *S*-nitrosylation of reactive thiol residues within the RyR protein. The resulting conformational change increases RyR P_o

and as such the occurrence of spontaneous Ca^{2+} release events (Lim, Venetucci, Eisner, & Casadei, 2008).

In rat, TNF-α produced an increase in NO production altering RyR *S*-nitrosylation, known to increase RyR P_o and thus diastolic Ca^{2+} efflux from the SR (Fauconnier et al., 2011). Whilst NO-mediated *S*-nitrosylation increases RyR P_o, NO can also decrease RyR P_o when the level of PKA activation is high (Lim et al., 2008). This may be due to an overshadowing effect of PKA, which decreases Ca^{2+} release events (Valdivia et al., 1995).

Given the fairly fast effect on wave dynamics – with decreases in Ca^{2+} wave amplitude after only 1 and 2 minutes with TNF-α and IL-1β respectively – and the potentiation of the Ca^{2+} transient observed in section 3.X, the effect on RyR must be rapid. Local increases in ROS can NO occur rapidly, whereas pathways modifying RyR through phosphorylation are slow, taking a place over a number of minutes (Yoshida et al., 1992). The direct effects of ROS and NO are therefore the more likely mechanisms by which these cytokines could increase RyR P_o in sheep myocytes. The involvement of CaM and CaMKII in RyR modification cannot be entirely ruled out, especially due to the time-dependency of the effect.

4.4.3 Could the TNF-α and IL-1β induced increase in RyR P_o contribute to decrease of SR Ca^{2+}?

Change to RyR P_o alters the magnitude of spontaneous SR Ca^{2+} release; this therefore regulates SR Ca^{2+} content. Elevated RyR P_o increases SR Ca^{2+} leak and would be expected to reduce diastolic SR Ca^{2+} content. Caffeine – known to potentiate the RyR – has demonstrated that increased RyR P_o can decrease SR Ca^{2+} content. This reduction in SR Ca^{2+} content is known the then reduce the frequency of Ca^{2+} release events (Venetucci et al., 2007).

In the case of both cytokines, increased RyR P_o provides a cellular mechanism for diastolic SR Ca^{2+} leak and the subsequent decrease in SR Ca^{2+} content previously measured in section 3.3.3. Other studies which demonstrated reduced Ca^{2+} transient amplitude and SR Ca^{2+}

content in response to TNF-α and IL-1β, such as Greensmith and Nirmalan (2013) and Duncan et al. (2010) can also be attributed to RyR potentiation. Whilst the method used in this study can indicate change to RyR P_o, it cannot be used to quantify the extent of RyR P_o. Further experiments using confocal microscopy to measure the rate of Ca^{2+} sparks could be carried out to determine whether the elevation in RyR P_o with TNF-α and IL-1β can account entirely for the observed decrease in SR Ca^{2+} content. What is certain is that the increase in RyR P_o would contribute to reduced SR Ca^{2+} content.

4.4.4 The time-dependency and relative potency of the effect of TNF-α and IL-1β on RyR P_o

Over the 5 minute exposure periods with both cytokines, the effects on both Ca^{2+} wave amplitude and frequency changed on a time-dependent. This may indicate a level of time-dependency of the effect of TNF-α and IL-1β on RyR P_o. Whether or not these parameters would eventually reach a stable point beyond the 5 minute exposure time is undetermined. As the CLP-induced sepsis rat model studied by X. Zhu et al. (2005) also found a progressive increase in spontaneous Ca^{2+} release events over a 48 hour testing period, which – although cytokine concentrations were not measured assuming both cytokines were present in the septic serum – would suggest that the effects on RyR P_o are in fact time-dependent over a much longer time period.

This work also suggests that the changes in Ca^{2+} wave amplitude and frequency with TNF-α are more immediate than with IL-1β. At 1 minute in TNF-α, Ca^{2+} wave amplitude had reduced by 14.54 ± 3.8 %, whilst with IL-1β, Ca^{2+} wave amplitude was only significant decreased after 2 minutes of exposure by 19.07 ± 6.11 %. Similarly, while both cytokines increased wave frequency, this effect was only measured after 5 minutes exposure to IL-1β with a 28.35 ± 11.35 % increase in instant frequency. The equivalent increase in frequency (27.68 ± 4.97 %) was recorded at 3 minutes with TNF-α. This evidence suggests that the effect of IL-1β on RyR P_o is more latent and to a lesser extent than with TNF-α. It is possible that these cytokines alter RyR P_o through different mechanisms.

4.4.5 Are the effects of 50 ng/ml TNF-α and IL-1β on the RyR P_o reversible?

The TNF-α induced decrease in Ca^{2+} wave amplitude and increase in wave frequency were maintained with washout (Fig 4-3) and the effect of TNF-α on the SR Ca^{2+} threshold for waves was irreversible (Fig 4-6), suggesting RyR P_o did not recover to control levels or increase further during washout. This is supported by Fauconnier et al. (2011) who also found that RyR P_o was increased in response to ischemic reperfusion injury induced in rat, associated with elevated TNF-α levels. They found that the effect on RyR function was maintained a day later, once TNF-α levels had fallen.

During IL-1β washout, the reduction in Ca^{2+} wave amplitude and increase in wave frequency were maintained (Fig 4-5). The effect on the SR Ca^{2+} threshold for waves, however, appears to be partially recovered with washout, as the mean caffeine-evoked Ca^{2+} wave amplitude is between and not significant from both the control state and after IL-1β (Fig 4-6). IL-1β could act by a different mechanism with a higher reversibility. It is equally possible that the effect of IL-1β on the SR Ca^{2+} threshold for waves could have been completely reversed with a longer washout.

In summary, TNF-α and IL-1β decreased the SR Ca^{2+} threshold for waves, and therefore increased RyR P_o on a time dependent basis, with TNF-α acting more rapidly than IL-1β. The effect of TNF-α on RyR P_o was irreversible, whereas the effect caused by IL-1β showed signs of reversibility, with which complete reversibility may have been possible over a longer time period. Possible mechanisms for the effect of both cytokines include CaM and CaMKII-mediated phosphorylation of RyR and direct *S*-nitrosylation of RyR via NO. All these mechanisms can be promoted by elevated ROS and NO production as a result of increased cytokines, including TNF-α and IL-1β. Redox modification and *S*-nitrosylation appear to be the more likely mechanisms due to the speed of the effect observed, however the time-dependency could also suggest that there could be multiple mechanisms at play contributing to the overall effect on SR Ca^{2+} leak.

Chapter 5

The effects of 50 ng/ml TNF-α and IL-1β on myofilament sensitivity to Ca^{2+}

5.1 Introduction

The previous experiments described in chapter 3 suggested that TNF-α and IL-1β may alter myofilament sensitivity, however the precise nature of this effect was not clear. Certain observations suggested that myofilament sensitivity may be increased by both cytokines while others implied a decrease. There remained a clear need to investigate the effect of both cytokines on myofilament sensitivity more thoroughly.

5.1.1 Myofilament sensitivity

As described in section 1.2.8.1, the relationship between $[Ca^{2+}]_i$ and sarcomere shortening is sigmoidal. This relationship can shift in either direction, indicating an increase (left shift) or decrease (right shift) in myofilament sensitivity to Ca^{2+}. Myofilament sensitivity to Ca^{2+} determines the force of contracture at a given $[Ca^{2+}]_i$. Changes to myofilament sensitivity can occur as a result of altered rate of cross bridge cycling and the strength of cross bridges formed. A common target for alteration to myofilament sensitivity is TnC (Moss et al., 2004).

Myofilament sensitivity to Ca^{2+} is a powerful modulator of inotropy. If myofilament sensitivity is increased, a lower $[Ca^{2+}]_i$ is required for myofilament activation, positively effecting inotropy. Equally, with reduced myofilament sensitivity, myofilaments required higher $[Ca^{2+}]_i$ for activation, and so contractility at a given $[Ca^{2+}]_i$ is reduced.

An example of a compound which can modulate inotropy in this way is Levosimendan. At low concentrations Levosimendan binds with a high affinity to TnC accelerating the rate of cross bridge formation (Haikala, Levijoki, & Linden, 1995). This has a positive effect on inotropy, increasing the force of contraction without elevating $[Ca^{2+}]_i$ (Toller & Stranz, 2006).

5.1.2 Myofilament sensitivity in inflammatory disease

Decreased cardiac myofilament sensitivity has been identified in various models of sepsis and endotoxemia, including CLP and endotoxin injection. It is thought this phenomenon is mediated by NO and increased levels of PKA mediated phosphorylation of myofilament associated proteins (Y. Li, Ge, Peng, & Chen, 2013; Sips et al., 2013; Tavernier, Garrigue, Boulle, Vallet, & Adnet, 1998; Tavernier et al., 2001; Wu, Tang, & Liu, 2001). It is worth noting that these studies were carried out in a small mammal models, as such it is unknown whether the relationship between Ca^{2+} and contractility may be altered in a larger model. Also, whether the effect on myofilament sensitivity is directly associated with cytokines is undetermined.

In other conditions associated with inflammation in the heart, including end stage heart failure and post-myocardial infarction, myofilament Ca^{2+} sensitivity was increased. Reduced PKA mediated phosphorylation due to impaired β-adrenergic stimulation pathways was implicated (van der Velden, 2011; Venkataraman et al., 2013). As elevated proinflammatory cytokines would be expected in all the above-mentioned inflammatory heart conditions, whether they produce a positive or negative change to myofilament sensitivity, if any, is unknown.

5.1.3 The effects of cytokines on myofilament sensitivity

Previous work suggests cytokines can alter myofilament sensitivity, though work specifically related to cardiac muscle, and both TNF-α and IL-1β are limited. Furthermore, findings remain controversial.

In skeletal muscle, relatively high concentrations (500 ng/ml) TNF-α reduced myofilament calcium sensitivity which was shown to contribute to decreased contractile function in mice. It was theorised that ROS and NO may be involved (Reid, Lannergren, & Westerblad, 2002). However, in guinea-pig smooth muscle TNF-α increased the sensitivity of myofilaments to

Ca^{2+}, through phosphorylation of the myosin light chain (Parris, Cobban, Littlejohn, MacEwan, & Nixon, 1999).

Very few studies have measured the effect of cytokines applied directly to isolated ventricular myocytes. Here too exists considerable controversy. Goldhaber et al. (1996) found that relatively very high concentrations of TNF-α (10000 U/ml) could decrease the Ca^{2+} sensitivity of myofilaments in rabbit ventricular myocytes and attributed this to an effect on NO production. In those experiments, the effect on myofilament sensitivity was delayed (20 minutes) which is interesting given that the experiments of chapter 3 suggest that any effect on myofilament sensitivity appears to occur over much shorter periods (< 5 minutes). Whereas in rat ventricular myocytes, Duncan, Hopkins, and Harrison (2007) demonstrated no effect on myofilament sensitivity with TNF-α and IL-1β exposures lasting over an hour.

Overall, evidence supports the hypothesis that cytokines alter myofilament sensitivity, and this may account for impaired cardiac function in sepsis and other inflammatory heart diseases. While sepsis is associated with decreased myofilament Ca^{2+} sensitivity, the specific effects of TNF-α and IL-1β on myofilament sensitivity and whether these changes have a negative or positive inotropic effect remains unclear.

5.1.4 Aims

(1) Determine the effect of TNF-α and IL-1β exposure on myofilament sensitivity to Ca^{2+}

5.2 Methods

In order to measure an effect on myofilament sensitivity to Ca^{2+}, a parameter of contractility must be correlated with one of intracellular Ca^{2+}. Modulation of $[Ca^{2+}]_i$ allows $[Ca^{2+}]_i$ to become the independent variable. There are a number of ways to independently modulate $[Ca^{2+}]_i$, however they generally fall into one of two approaches; inducing physiological

changes to $[Ca^{2+}]_i$ – for example altering pacing frequency – or directly altering $[Ca^{2+}]_i$ through membrane permeabilisation. In this study, both approaches were used.

5.2.1 Modulation of intracellular calcium levels by change of pacing frequency

A standard pacing change protocol was applied to three groups of cells; untreated (exposed only to control solution, as detailed in section 2.2.1), 50 ng/ml TNF-α treated and 50 ng/ml IL-1β treated. The pacing protocol is demonstrated in Fig 5-1. Once a healthy pacing cell had been identified at 0.5 Hz, the stimulation frequency was then reduced to 0.1 Hz. Stimulation frequency was increased in a stepwise manner – through 0.5 Hz, 1 Hz and 2 Hz – to 3 Hz, and allowed to reach a new steady state at each frequency.

In cytokine-treated experiments, either TNF-α or IL-1β were applied through superfusion, as opposed to prior incubation. As such, in order to first confirm that a selected cell had basic contractile function, this was administered following a period of pacing at 0.5 Hz in control solution. Once a new steady state had formed with the cytokine, the pacing protocol continued.

An average of the final 5 Ca^{2+} beats were taken and analysed as per the protocol described in section 2.3. Mean values were normalised to control. The data from each cell was plotted both as diastolic Ca^{2+} against resting sarcomere length, and as the sarcomere length : diastolic Ca^{2+} against frequency. The relationship between end diastolic Ca^{2+} and sarcomere length were used to measure changes to myofilament sensitivity to Ca^{2+}, for the purpose of this experiment, as these parameters had the most stability (Wisloff et al., 2001). In both cases, the relationship between the two parameters was quantified using regression analysis. As the nature of the change was unclear, we used both single exponential, f = y0+a*exp(-b*x), and linear regression, f = y0+a*x. The values of the b and y0 coefficients were studied from the exponential and linear regressions respectively. Means were compared using a one-way ANOVA. When testing the effect of frequency on diastolic Ca^{2+} and shortening in control cells, the one-way ANOVA was followed by a Dunn's post-hoc test.

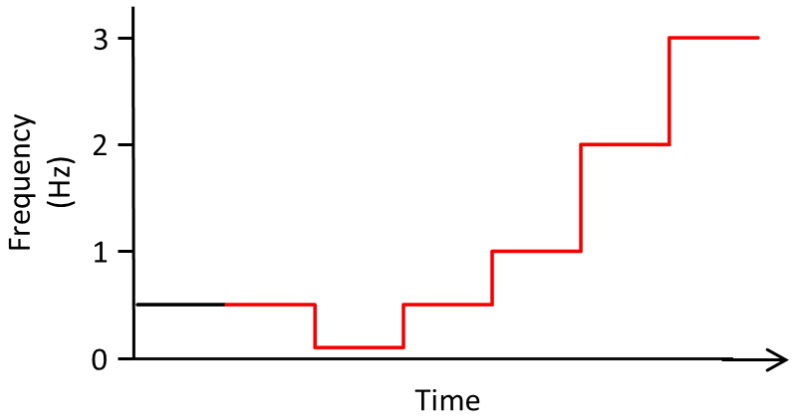

Figure 5-1. A diagram demonstrating the change in stimulation frequency of the time course of the experiment; highlighting the period over which the pacing cell was in control solution [black] and the period for which a cytokine treatment (if any) was applied [red].

5.2.2 Modulation of intracellular Ca^{2+} using permeabilisation.

Cells were permeabilised by superfusion with 20 µg / ml saponin in a Ca^{2+} free variation of the control solution described in section 2.2.1, for 60 – 90 s. The starting exposure time at the beginning of an experimental day was ~70 s, this exposure time was adapted throughout the day based on the success of the permeabilisation achieved in the previous experiment. This allowed for any variation in the initial membrane integrity following the isolation protocol and any further deterioration throughout the day.

Once permeabilised, resting sarcomere length was left to stabilise in a 0 Ca^{2+} control solution. In 50 ng/ml TNF-α and IL-1β treated cells, the cell was exposed for >100 seconds even if a steady state was reached prior to this, to allow time for any effect on myofilament sensitivity to Ca^{2+} to occur. 100 s was chosen as the minimum exposure period to each cytokine prior to an increase in $[Ca^{2+}]$, as this fell within the range of exposure times used in the experiments of chapter 3, in which a possible effect on myofilament sensitivity had been indicated.

In case the effect on myofilament sensitivity with these cytokines was time-dependent, the cell was exposed to each elevation in [Ca^{2+}] – 50 nM, 150 nM and 200 nM Ca^{2+} – for approximately 100 s. The experiment was ended early if the cell began to wave and data from that cell at the highest concentration tested could only be used if a steady state had been reached prior to the 1st wave. The resting sarcomere length during the last 10 s at each [Ca^{2+}] was measured using custom software (Greensmith, Eisner, & Nirmalan, 2010). If this 10 s period was unstable or in a constant state of decline, a point which best represented the sarcomere length over this period was measured. Mean sarcomere lengths measured at each [Ca^{2+}] were normalised to that measured in 0 Ca^{2+}. Data were analysed using a two-way ANOVA and subsequent individual comparisons were carried out through a Holm-Sidak post-hoc test.

Cells which survived exposure to 200 nM Ca^{2+} (at pH 7.34, as with all previous control solutions), were exposed to 100 s each to two further pH solutions. This resulted in a total of 3 pH control solutions – at pH 7.1, pH 7.34 and pH 7.6 – with a fixed Ca^{2+} concentration of 200 nM. The additional pH control solutions did not contain cytokines. This was designed as an supplementary control to determine whether the permeabilisation protocol was successful at allowing external application of Ca^{2+} to directly alter $[Ca^{2+}]_i$ and the resultant sarcomere shortening, as pH is known to alter myofilament sensitivity to Ca^{2+} (Orchard & Kentish, 1990).

5.3 Results

5.3.1 The effect of rate induced change to intracellular Ca^{2+} on sarcomere length in the presence of TNF-α and IL-1β

The absolute levels of systolic and diastolic intracellular Ca^{2+} and so force, are known to be dependent on stimulation frequency. The precise force (calcium)-frequency relationship is species dependent. In the majority of species including healthy humans, increased frequency is associated with a positive effect on both systolic and diastolic $[Ca^{2+}]_i$ and so sarcomere shortening (Bers, 2000; Gattoni et al., 2016; Varian & Janssen, 2007). For the purpose of this

experiment however, the nature of this relationship is not important. Rather, altering pacing frequency simply provides *a* physiological way to alter $[Ca^{2+}]_i$ levels in intact and fully functional cells and so provides a way to probe the relationship between $[Ca^{2+}]_i$ levels and sarcomere length.

The specimen records of Fig 5-2, 5-3 and 5-4 show examples of the effect of stimulation frequency on Ca^{2+} dynamics in untreated, TNF-α treated and IL-1β treated cells respectively. For each cell and at each frequency end diastolic Ca^{2+} and sarcomere length was measured. The mean normalised data from this analysis can be seen in Fig 5-5. It is clear from Fig 5-5A that the relationship between diastolic Ca^{2+} and sarcomere length is not altered by TNF-α or IL-1β. Whilst an exponential relationship would be expected, at lower frequencies this can appear linear (Varian & Janssen, 2007). As per section 5.2.1 the relationship was quantified using both linear and single exponential regression analysis on a cell by cell basis. On average, the slope of linear regression was unchanged between untreated cells (n=17) and those treated with TNF-α (n=10) and IL-1β (n=12) ($p = 0.658$) (Fig 5-5B). The mean rate constant of single exponential analysis was also unaffected in untreated (n=16), TNF-α (n=9) and IL-1β (n=12) treated cells ($p = 0.571$) (Fig 5-5C). This suggests that neither were altered by either cytokine.

The nature of the relationship between Ca^{2+} and sarcomere length carried between cells were not consistently described by linear or exponential regression, hence both methods were required. As such regression analysis was also performed on the relationship between rate and the ratio of end diastolic sarcomere length : Ca^{2+}. This too was unaffected by either cytokine, as no change was revealed between untreated (n=14), cells and those treated with TNF-α (n=9) and IL-1β (n=12) ($p = 0.238$) (Fig 5-6).

The specimen records of Fig 5-2A show examples of the effect of stimulation frequency on Ca^{2+} dynamics in untreated control cells. In control cells, on average stimulation frequency increased diastolic Ca^{2+} by 24.73 ± 6.43 % (n=19, $p < 0.05$) and 51.92 ± 11.53 % (n=12, $p < 0.05$) (Fig 5-2C) and 2 Hz and 3 Hz respectively. The lower stimulation frequencies – 0.1 Hz (n=22, $p > 0.05$) and 1 Hz (n=19, $p > 0.05$) – had no effect on diastolic Ca^{2+} levels.

The specimen records of Fig 5-2B show examples of the effect of stimulation frequency on contractility in untreated control cells. Increase in stimulation frequency decreases resting sarcomere length. When compared to that of 0.1 Hz, in control cells sarcomere length decreased by 0.71 ± 0.15 % (n=21, $p < 0.05$), 1.55 ± 0.29 % (n=19, $p < 0.05$), 3.08 ± 0.43 % (n=19, $p < 0.05$), 5.14 ± 0.51 % (n=12, $p < 0.05$) with 0.5 Hz, 1 Hz, 2 Hz and 3 Hz respectively (Fig 5-2D).

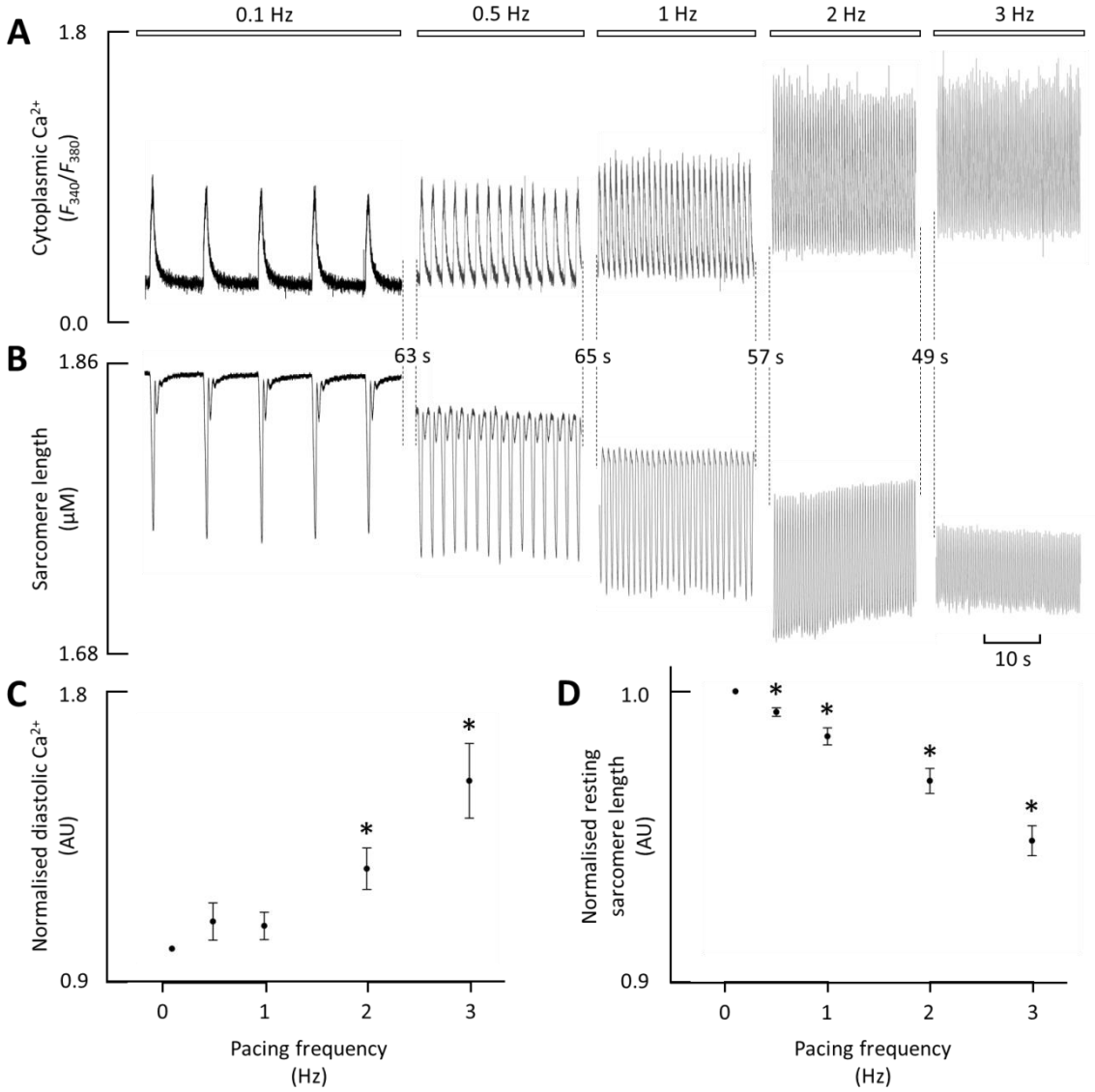

Figure 5-2. The influence of pacing frequency on Ca^{2+} dynamics and contractility in untreated control cells (n = 22 cells from 5 animals). (A) specimen record of change to systolic Ca^{2+} with change in frequency. (B) specimen record of change to contractility with change in frequency. (C) Mean diastolic [Ca^{2+}] at different pacing frequencies. (D) and resting sarcomere length at different pacing frequencies. * indicates $p < 0.05$, NS denotes non-significance ($p > 0.05$).

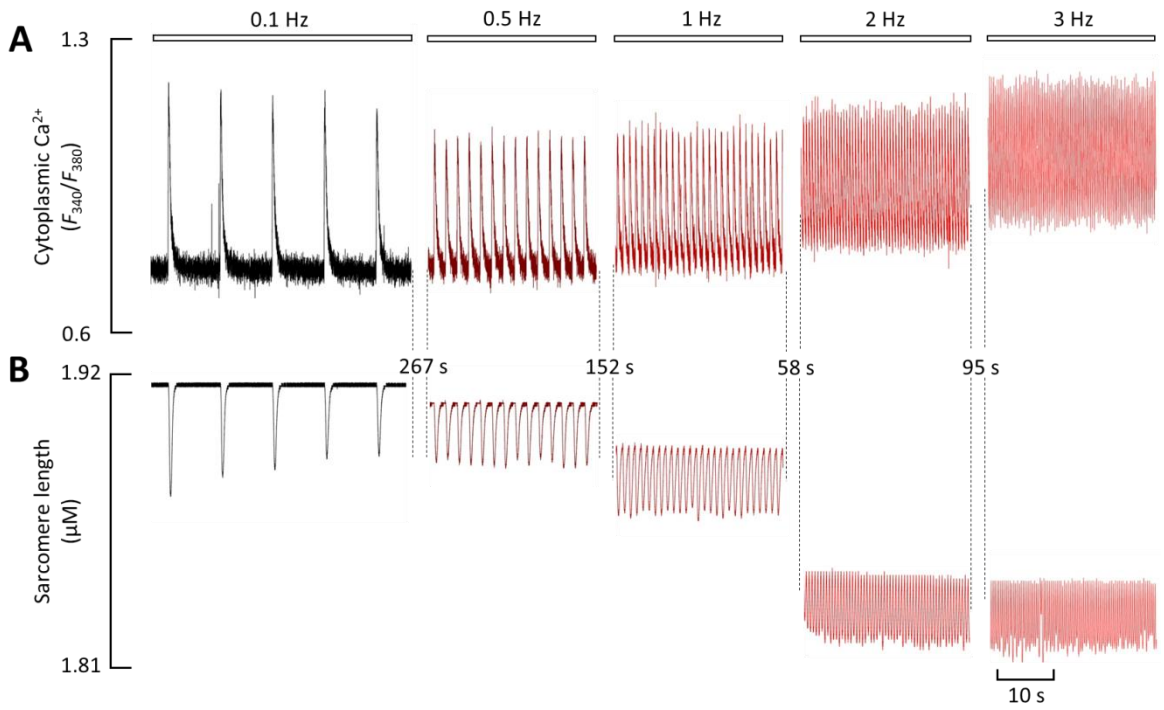

Figure 5-3. The influence of pacing frequency on Ca^{2+} dynamics and contractility in TNF-α treated cells. (A) specimen record of change to systolic Ca^{2+} with change in frequency. (B) specimen record of change to contractility with change in frequency.

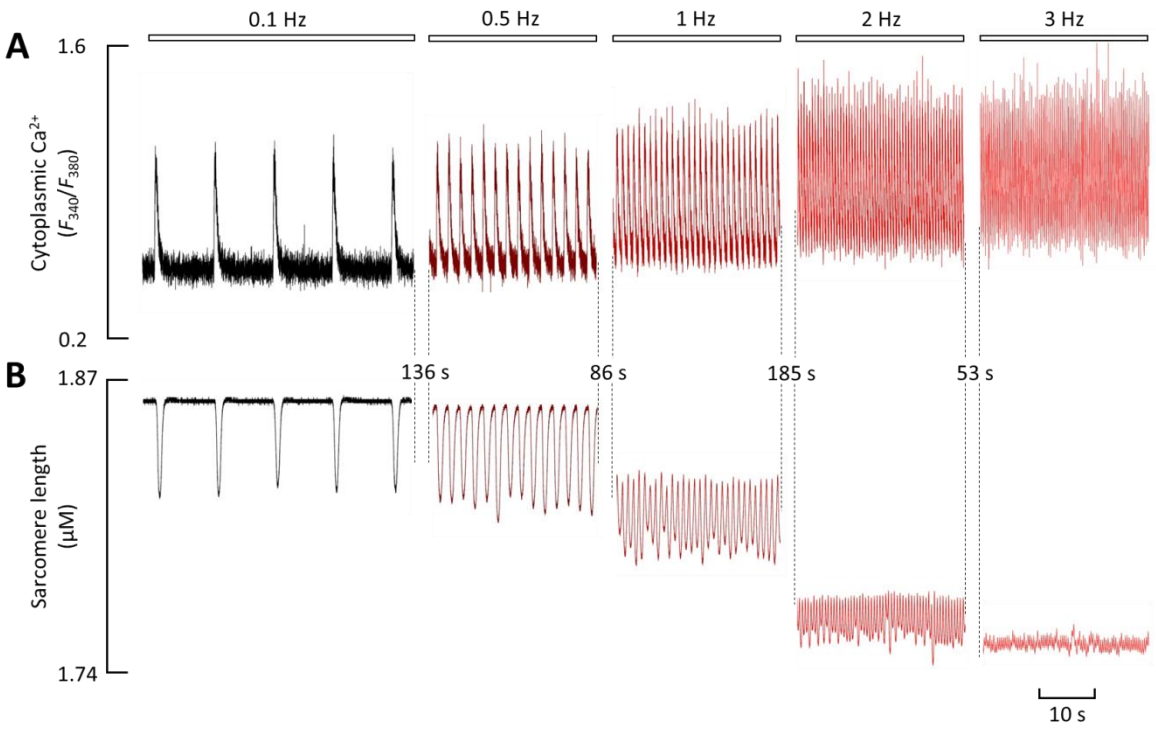

Figure 5-4. The influence of pacing frequency on Ca^{2+} dynamics and contractility in IL-1β treated cells. (A) specimen record of change to systolic Ca^{2+} with change in frequency. (B) specimen record of change to contractility with change in frequency.

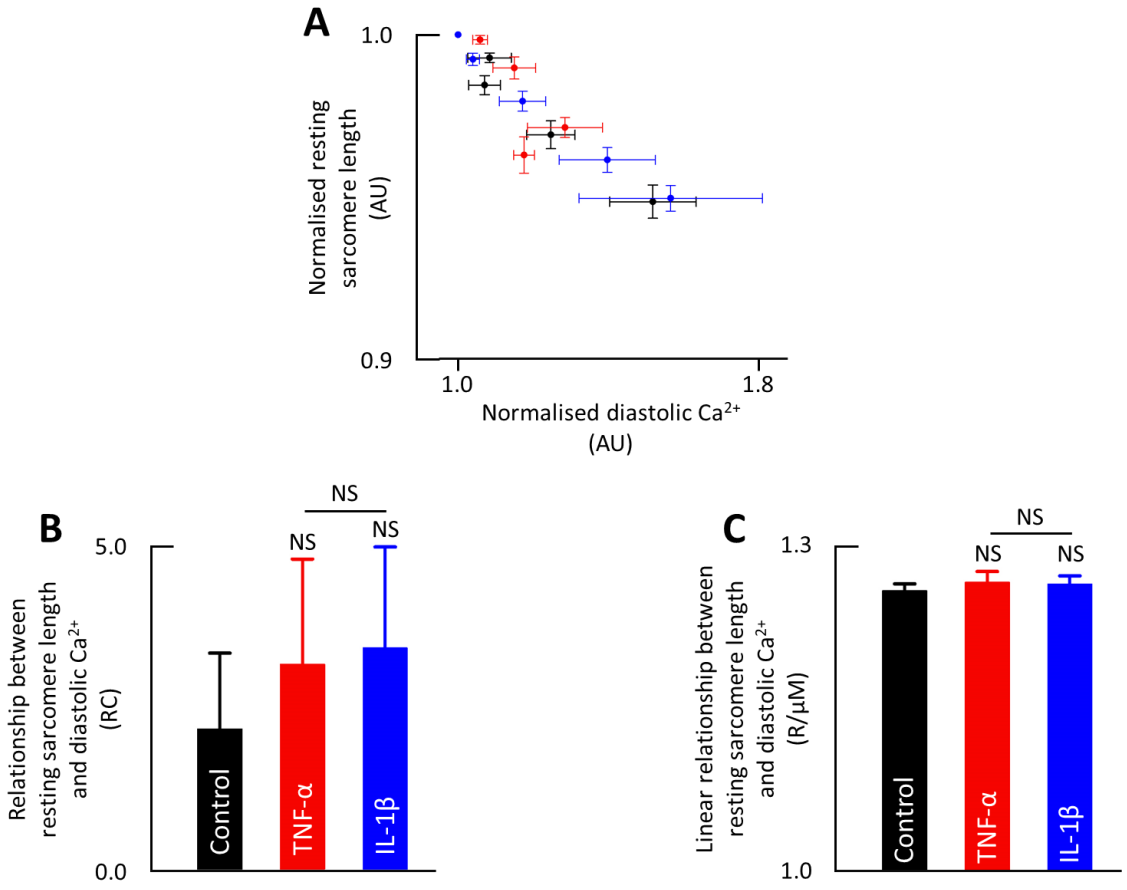

Figure 5-5. Mean data showing the relationship between resting sarcomere length and diastolic [Ca^{2+}] in untreated [black] (n = 22 cells from 5 animals), TNF-α treated [red] (n = 13 cells from 4 animals), and IL-1β treated [blue] (n = 12 cells from 4 animals) cells. (A) mean normalised resting sarcomere length plotted against mean normalised diastolic [Ca^{2+}]. (B) Mean rate constant of the curve relationship between resting sarcomere length and diastolic [Ca^{2+}]. (C) Mean change in diastolic [Ca^{2+}] with change in resting sarcomere length. * indicates $p < 0.05$, NS denotes non-significance ($p > 0.05$).

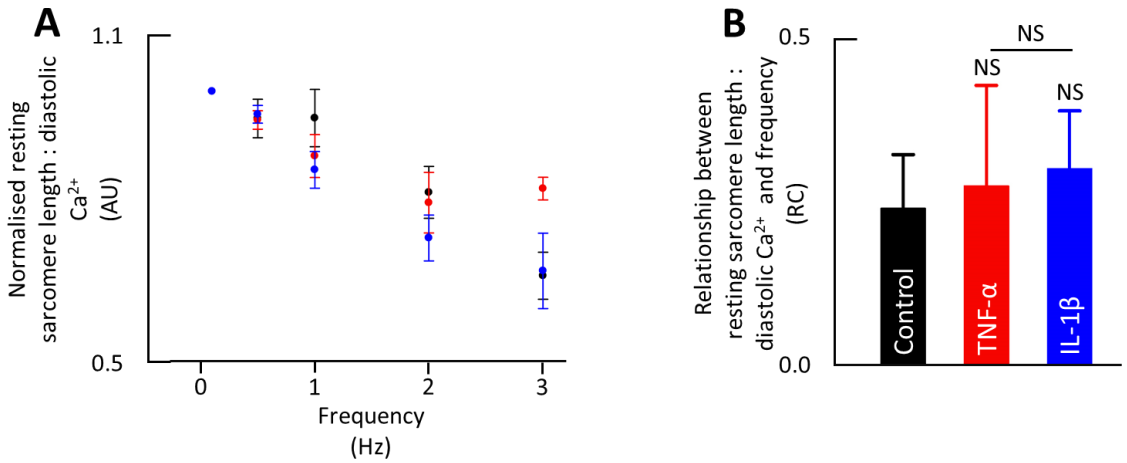

Figure 5-6. Mean data showing the relationship between the ratio of resting sarcomere length and diastolic [Ca^{2+}], and frequency in untreated [black], TNF-α treated [red], and IL-1β treated [blue] cells. (A) mean normalised resting sarcomere length ; diastolic [Ca^{2+}] against frequency. (B) mean rate constant of the curve relationship between the resting sarcomere length : diastolic [Ca^{2+}] and frequency. * indicates $p < 0.05$, NS denotes non-significance ($p > 0.05$).

5.3.2 The effect of TNF-α and IL-1β on the relationship between $[Ca^{2+}]_i$ and resting sarcomere length in permeabilised cells

Through the permeabilisation of myocytes it is possible to directly alter intracellular Ca^{2+} by introducing the cells to solutions of defined [Ca^{2+}]. This provides a more direct method of controlling intracellular calcium and so measures any change in myofilament sensitivity to Ca^{2+}. The range of [Ca^{2+}] in experimental solutions must be much lower than described in section 2.2.1 as the membrane and ion channels within no longer act as a selective barrier. Rather, internal Ca^{2+} will simply equilibrate with external. Though this manoeuvre alters cell function considerably, it has been used by others to isolate and specifically measure change to myofilament sensitivity to Ca^{2+} (Parris et al., 1999; Wisloff et al., 2001).

Fig 5-7A shows the result of this manoeuvre in untreated cells. A clear, response of sarcomere length to the range of calcium concentrations used is apparent. This

demonstrates that (1) the permeabilisation protocol is working, as without direct equilibration, such small changes of Ca^{2+} would not produce an effect and (2) the magnitude of sarcomere length change is great enough to provide sufficient sensitivity to detect an effect by cytokines if one were to exist.

The specimen record of Fig 5-7A, B and C show examples of the change of sarcomere length in response to change of $[Ca^{2+}]_i$ in untreated, TNF-α and IL-1β exposed cells. Fig 5-8 shows the mean relationship between $[Ca^{2+}]_i$ and sarcomere length and results of a two-way ANOVA. These data demonstrate two points. (1) sarcomere shortening in response to increased $[Ca^{2+}]_i$ is preserved in the presence of both cytokines. Although, (2) compared to control, that response is blunted by both TNF-α ($n=17$, $p = 0.003$) and IL-1β ($n=21$, $p<0.001$). In other words, in the presences of TNF-α and IL-1β the degree of shortening produced by any given $[Ca^{2+}]_i$ over the experimental range used is less. This is highlighted by the sarcomere length response to the highest concentration of Ca^{2+} used. In control cells, 200 nM Ca^{2+} produced a 2.25 ± 1.1 % ($n=8$) decrease in sarcomere length relative to 0 Ca^{2+}. In the presences of TNF-α and IL-1β, the same concentration of Ca^{2+} only produced a 0.64 ± 0.24 % ($n=6$) and 0.43 ± 0.13 % ($n=6$) decrease respectively. There was no difference in the magnitude of blunted response between cytokines ($p = 0.546$).

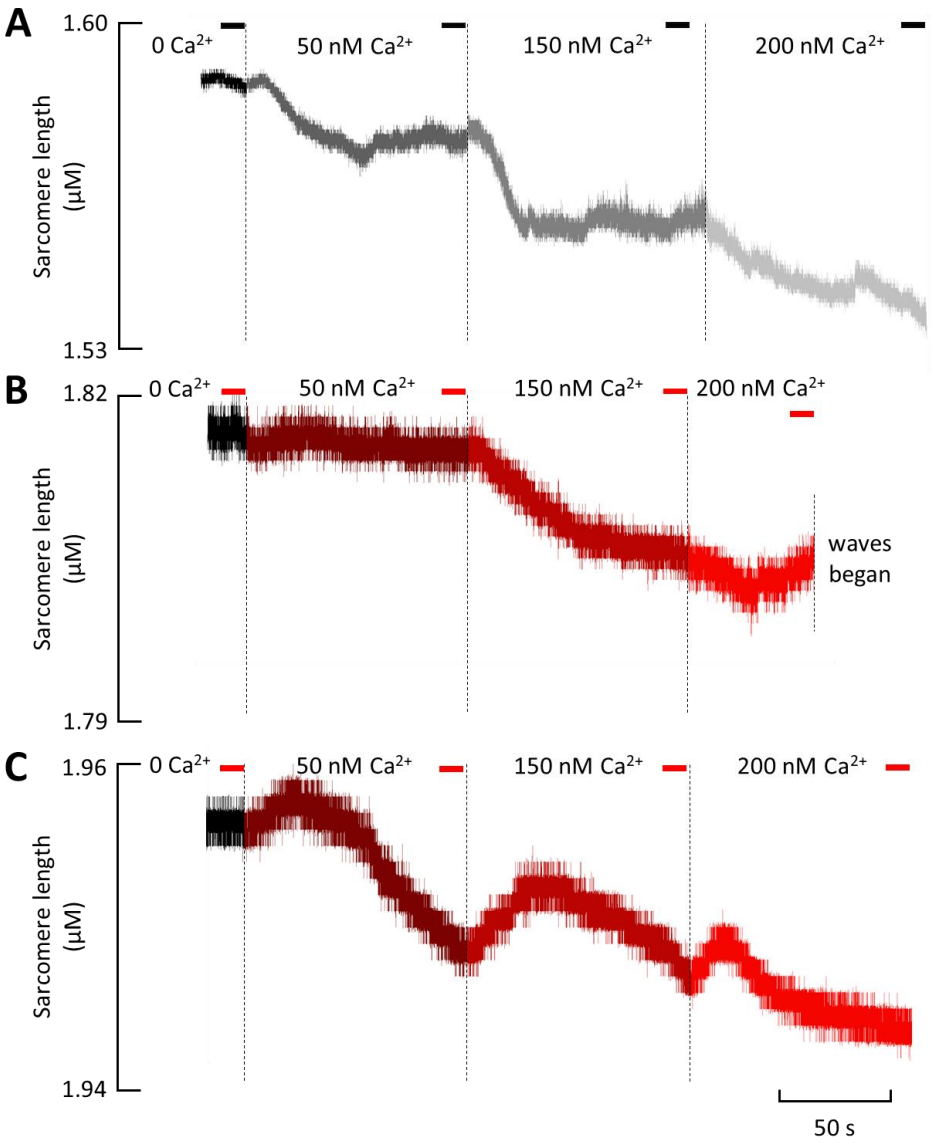

Figure 5-7. Specimen records demonstrating the change in resting sarcomere length in permeabilised cells with increasing [Ca^{2+}]. The bars above indicated the time period over which an average was taken. (A) in untreated control cells. (B) in 50 ng/ml TNF-α treated cells. (C) in 50 ng/ml IL-1β treated cells

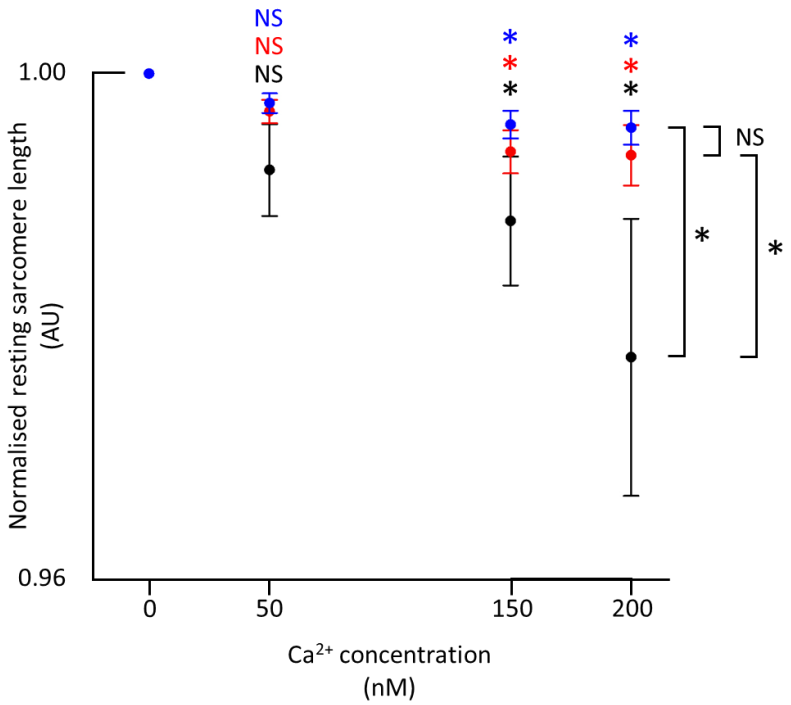

Figure 5-8. Mean resting sarcomere length at different [Ca^{2+}] in untreated control cells [black] (n = 17 cells from 5 animals), TNF-α treated cells [red] (n = 17 cells from 5 animals) and IL-1β treated cells [blue] (n = 21 cells from 7 animals). A two-way ANOVA revealed significance in the sarcomere length response with each [Ca^{2+}] [above], and the significance of the effect between untreated, TNF-α treated and IL-1β treated cells [right]. * indicates $p < 0.05$, NS denotes non-significance ($p > 0.05$).

5.3.3 Effects of acidity on myofilament sensitivity to Ca^{2+} with TNF-α and IL-1β

pH is known to alter myofilament sensitivity to Ca^{2+}, while retaining the sigmoidal relationship between [Ca^{2+}] and contractile force. pH interacts with troponin, altering the affinity of TnC for Ca^{2+} and its relationship with TnI. Acidosis reduces Ca^{2+} sensitivity, while increased pH increases Ca^{2+} sensitivity (Orchard & Kentish, 1990). Wisloff et al. (2001) used pH as a positive control in experiments measuring change to myofilament sensitivity to Ca^{2+} in permeabilised cells. In this study, we changed pH for two reasons. (1) In untreated cells, the change of pH served as a positive control to demonstrate we could detect a change to myofilament sensitivity to Ca^{2+} if one exists. (2) In treated cells, to determine if pH produced any further change myofilament sensitivity to Ca^{2+}. It was thought that the latter

experiments may provide addition support the experiments of section 5.3.2 and would highlight whether any myofilament sensitivity to Ca^{2+} reserve remained or if the effect had been saturated.

In untreated control cells, myofilament sensitivity to Ca^{2+} decreased with increased acidity, resulting in reduced shortening at a given $[Ca^{2+}]_i$ of 200 nM (Fig 5-9). With IL-1β, at any given pH the degree of shortening was reduced in comparison to control. However, the relationship between myofilament sensitivity to Ca^{2+} and pH appears to be at least partially lost. This is highlighted by the observation that similar magnitudes of shortening occur at each pH, with 0.48 ± 0.23 % (n=4), 0.43 ± 0.13 % (n=6), and 0.6 ± 0.27 % (n=3) reductions in sarcomere length from control at pH 7.1, 7.34 and 7.6 respectively.

With TNF-α, at pH 7.34, the change to sarcomere length is similar to that of IL-1β, decreasing by 0.64 ± 0.24 % (n=6). At pH 7.1 and 7.6 sarcomere shortening with TNF-α is increased in relation to control, with 3.53 ± 3.08 % (n=6) and 4.19 ± 2.97 % (n=6) decreases in resting sarcomere length at the set $[Ca^{2+}]$, however the relationship between myofilament sensitivity to Ca^{2+} and pH is maintained.

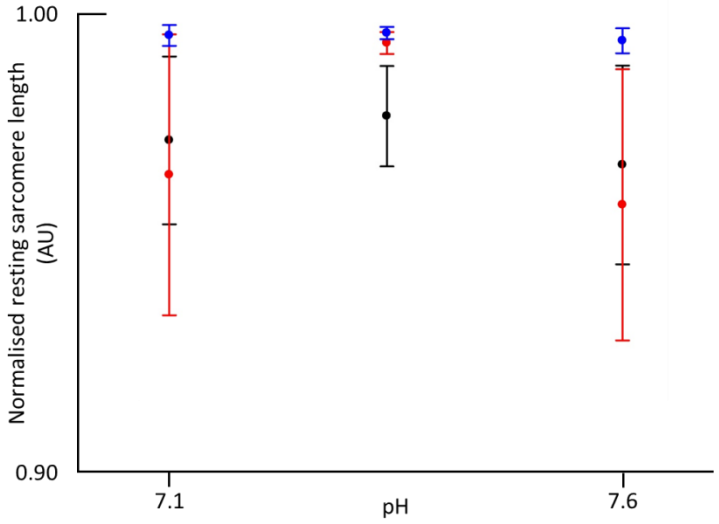

Figure 5-9. The mean resting sarcomere length at different acidities in untreated control cells [black] (n = 8 cells from 4 animals), TNF-α treated cells [red] (n = 6 cells from 5 animals) and IL-1β treated cells [blue] (n = 6 cells from 3 animals).

5.4 Discussion

5.4.1 Do TNF-α and IL-1β reduce myofilament sensitivity to Ca^{2+}?

Two experiments were used in an attempt to answer this question, both of which measured the relationship between change to sarcomere length with change to $[Ca^{2+}]_i$ physiologically. The first experiment modulated $[Ca^{2+}]_i$ physiologically using change to stimulation frequency. In the second experiment, permeabilisation of the cell membrane allowed $[Ca^{2+}]_i$ to be directly modulated through change in the $[Ca^{2+}]$ of solutions. In both cases, the resulting change to sarcomere length was measured.

5.4.1.1 Is the sarcomere length response to physiologically modulated $[Ca^{2+}]_i$ altered by TNF-α and IL-1β?

As introduced in 5.3.1, a change in stimulation frequency is known to alter $[Ca^{2+}]_i$ (Bers, 2000). Wisloff et al. (2001), Sips et al. (2013) and Reid et al. (2002) have used rate to produce

a change in Ca^{2+}, and so measure changes to myofilament sensitivity. As per Fig 5-2 and as expected, in sheep increasing pacing frequency increased diastolic $[Ca^{2+}]_i$ resulting in decreased resting sarcomere length. As such, we were able to compare the effects of both cytokines on the relationship between Ca^{2+} and sarcomere length.

According to Fig 5-5 and 5-6, it appears that neither TNF-α and IL-1β alter the relationship between Ca^{2+} increased by pacing frequency and sarcomere length. This observation alone suggests that neither TNF-α and IL-1β alter myofilament sensitivity.

As shown in Fig 5-2C, although 2 Hz and 3 Hz were able to increase diastolic Ca^{2+} considerably in the untreated sheep myocytes – by 24.73 ± 6.43 % and 51.92 ± 11.53 % respectively – the remaining lower frequencies were unable to alter diastolic Ca^{2+}. Similarly, while the entire rate spectrum tested was able to cause a significant decrease in sarcomere length, the magnitude of these changes ranged between 0.71 ± 0.15 % and 5.14 ± 0.51 % (Fig 5-2D). Given that the change to sarcomere length is so small over this range, the pacing frequency range used in this study to physiologically alter $[Ca^{2+}]_i$ may have been too narrow to provide sufficient sensitivity to detect an effect of either cytokine tested, should one exist. In rabbit – a small mammal model known to have a positive force-frequency relationship (Bers, 2000) – Varian and Janssen (2007) solely found significant changes in diastolic $[Ca^{2+}]_i$, at the higher frequencies tested (2 Hz and 3 Hz), this correlates with the findings in sheep (Fig 5-2C). It therefore is not surprising that over the range of frequencies used, the relationship between diastolic Ca^{2+} and sarcomere length appeared more linear. Similarly, in an endotoxin–administered model of sepsis, a decrease in diastolic Ca^{2+} and Ca^{2+} amplitude were found at 4 Hz, indicating a reduction in myofilament sensitivity to Ca^{2+} (Sips et al., 2013). In skeletal muscle fibres, Reid et al. (2002) 500 ng/ml TNF-α, a concentration 10 fold higher than used in this study, was shown not to affect contractile force at 1 and 10 Hz.

In comparison to the range of stimulation frequencies used in this study (0.1-3 Hz), Wisloff et al. (2001), Sips et al. (2013) and Reid et al. (2002) carried out tests over a much wider range of frequencies; 0.1-10 Hz, 1-4 Hz and 1-150 Hz. Whilst higher frequencies, such as 4 Hz and 5 Hz, were attempted in the sheep ventricular myocytes used in this study, the myocytes would not tolerate higher frequencies or could not maintain a steady state, therefore it was

not possible to reach or exceed a higher pacing frequency such as 10 Hz. A factor which may have contributed to the sheep myocytes inability to reach higher pacing frequencies, was the use of field stimulation as appose to patch clamping as a method of pacing cells. In addition, smaller mammal models, such as rat and mouse, are more tolerant to higher pacing frequencies, as their hearts naturally beat at a faster frequency than sheep.

There are disadvantages however, to using small mammal models in this experiment; their relationship between stimulation frequency and $[Ca^{2+}]_i$, and thus contractility, is biphasic. At lower stimulation frequencies – 0.5-1 Hz in rat and 1-2 Hz in mice – the force-frequency relationship is negative (Endoh, 2004; Gattoni et al., 2016). In sheep, there was a positive relationship between stimulation frequency and diastolic $[Ca^{2+}]_i$, and therefore resting cell length (Fig 5-2), this is therefore more clinically relevant to human studies (Bers, 2000; Gattoni et al., 2016).

Although other studies, such as Wisloff et al. (2001), have used this physiological method of adjusting $[Ca^{2+}]_i$ through change to stimulation frequency, in order to determine an effect on myofilament sensitivity to Ca^{2+}. More recent work by Varian and Janssen (2007) has indicated that, within the tested frequency range of 1-4 Hz, stimulation frequency can cause a decrease myofilament sensitivity to Ca^{2+} in rabbit. It is uncertain whether the effect of frequency on myofilament sensitivity to Ca^{2+} also exists in other species, however given that this would impact results, it may not necessarily be the most robust way to measure myofilament sensitivity.

Given the limitations in both the method and the rate spectrum achieved in a large mammal model, the changes of Ca^{2+} and sarcomere length produced by this range of frequencies may have been too small to reveal an effect on myofilament sensitivity to Ca^{2+}. As such, a more direct way of changing $[Ca^{2+}]_i$ was required.

5.4.1.2 Is the sarcomere length response to directly modulated $[Ca^{2+}]_i$ altered by TNF-α and IL-1β?

Both 50 ng/ml TNF-α and IL-1β individually decreased the extent of sarcomere shortening with stepwise increases in $[Ca^{2+}]$ when compared to untreated cells. At the highest concentration tested (200 nM Ca^{2+}) resting sarcomere length decreased by 2.25 ± 1.1 %, 0.64 ± 0.24 % and 0.43 ± 0.13 % in untreated, TNF-α treated and IL-1β treated cells respectively (Fig 5-8). This indicates a 71.56 % and 80.89 % reduction in the Ca^{2+} sensitivity of myofilament to with TNF-α and IL-1β. As there was no significant difference between the relationship between $[Ca^{2+}]$ and sarcomere length with TNF-α and IL-1β ($p = 0.546$), it is clear that both cytokines cause a similar effect on myofilament sensitivity to Ca^{2+}.

Despite the use of a 10 fold lower TNF-α concentration in this study, the effect of TNF-α was similar to that observed in mice skeletal muscle (Reid et al., 2002). This study also provides evidence that the decrease in myofilament sensitivity with TNF-α found by Goldhaber et al. (1996) in rabbit ventricular myocytes, is also a mechanism of decreased contractility in a large mammal model. Unlike the work of Goldhaber et al. (1996) however, which only identified an effect of Ca^{2+} sensitivity following ~20 minutes exposure to TNF-α, this study found evidence of decreased Ca^{2+} sensitivity over a much shorter time base (<10 mins).

The findings of this study also contradict that of Duncan et al. (2007), who found no change to myofilament sensitivity with prolonged TNF-α and IL-1β exposure in rat ventricular myocytes. As this study has identified that both TNF-α and IL-1β decrease Ca^{2+} sensitivity an overall larger decrease in Ca^{2+} sensitivity would be expected when both cytokines were administered together. Another possible explanation for the lack of an effect of these cytokines on myofilament sensitivity, may be a difference in activity in rat or an interaction between the cytokines which prevents an effect on myofilament sensitivity. Duncan et al. (2007) did however state that their method for detecting change to myofilament sensitivity may not have been sensitive enough to reveal a change, due to wide variation in the cells inotropic state initially.

5.4.2 How rapid are the effects of TNF-α and IL-1β on myofilament sensitivity to Ca^{2+}? – What is a possible mechanism for this change?

In endotoxemia, a condition associated with sepsis in which proinflammatory cytokines such as TNF-α and IL-1β would be expected to be elevated, there has been a reported time-dependent decrease in myofilament sensitivity to Ca^{2+} (Tavernier et al., 1998). Reid et al. (2002) later found that TNF-α could alter Ca^{2+} sensitivity on a time-dependent basis. This effect was gradual, with a ~4 % decrease in contractile force each hour.

Given the time allowed for steady state to be reach in 0 Ca^{2+} and the ~100 s exposure times in each [Ca^{2+}] used in this study, the overall cytokine exposure lasted for approximately 7-10 minutes. The length of exposure was much therefore much shorter than that used by Reid et al. (2002). At 200 nM Ca^{2+} – the final concentration introduced – the magnitude of sarcomere shortening had already been blunted with TNF-α. TNF-α caused a 0.64 ± 0.24 % decrease in sarcomere length, in comparison to the much larger 2.25 ± 1.1 % decrease in untreated cells. The effect on change to Ca^{2+} sensitivity therefore appears more rapid that suggested by Reid et al. (2002). A similar effect was observed in IL-1β treated cells where sarcomere shortening had also been blunted within the time course of the experiment, with only a 0.43 ± 0.13 % decrease in sarcomere shortening.

Previous work by Tavernier et al. (2001) indicated that increased phosphorylation, possibly by PKA, was the mechanism of decreased myofilament sensitivity to Ca^{2+} in a model of endotoxemia. PKA-mediates phosphorylation of cardiac myosin–binding protein C, this increases the rate of cross bridge detachment, therefore decreasing myofilament sensitivity (P. P. Chen, Patel, Rybakova, Walker, & Moss, 2010). TnI can also undergo phosphorylation via PKA, further contributing to decreased myofilament sensitivity to a smaller extent (M. Kumar et al., 2015). Wu et al. (2001) found that phosphorylation of TnI occurred in the earlier stages of sepsis – 9 hours following CLP – whereas during later phases, phosphorylation of myosin–binding protein C was predominant. Phosphorylation of these proteins can also be carried out by PKC. Phosphorylation is time-dependant, however phosphorylation of these proteins with PKA and PKC can increase over minutes (~2 min) exposure (Noland et al., 1995). This would be within the time course of this study, as >100 s

exposure to either cytokine was allowed prior to the first increase in [Ca^{2+}], in order to allow a steady state to be reached in 0 Ca^{2+}. Phosphorylation of these myofilament associated proteins could therefore be a possible mechanism of decreased myofilament sensitivity to Ca^{2+} with TNF-α and IL-1β.

Another possible mechanism of altered myofilament sensitivity to Ca^{2+} involves the direct effect of elevated NO and ROS production. In acute inflammation of the heart, NO and ROS have both been associated with reduced myofilament sensitivity to Ca^{2+} and impaired relaxation (Y. Li et al., 2013). In sepsis, *S*-nitrosylation of myofilament associated proteins is considered to be responsible for the decrease in myofilament sensitivity to Ca^{2+} (Sips et al., 2013). Excessive NO production can however limit ROS production and as such lead to increased myofilament sensitivity to Ca^{2+} (Ichinose et al., 2007).

5.4.3 Do the effects of TNF-α and IL-1β on myofilament sensitivity to Ca^{2+} alter with change to pH?

The expected relationship between pH and myofilament sensitivity to Ca^{2+} was found in untreated control cells, supporting that the permeabilisation method was effective and enabling control of intracellular [Ca^{2+}] and pH, and thus as a way of determining change to myofilament sensitivity.

When compared to the untreated cells, IL-1β reduced the change in sarcomere shortening achieved at all pH levels, at the given $[Ca^{2+}]_i$ of 200 nM. This supports the message of section 5.4.1.2 in that the decrease in myofilament sensitivity to Ca^{2+} with increased acidity is enhanced with IL-1β. IL-1β is therefore capable of reducing myofilament sensitivity to Ca^{2+} in sheep ventricular myocytes. With IL-1β, the degree of Ca^{2+} sensitivity also appeared to be less affected by increased acidity, resulting in a similar degree of shortening in all pH solutions used. This indicates that the pH dependency is partially lost in the presence of IL-1β. This loss of pH dependency suggests that the effect on myofilament sensitivity to Ca^{2+} caused by IL-1β is much greater than that of pH, and therefore IL-1β has already saturated

the effect on myofilament sensitivity to Ca^{2+}, resulting in no further influence by change in pH.

For economy reasons, TNF-α and IL-1β were left out of the pH solutions, with the exception of pH 7.34, which was the final solution used in the concentration curve above. This was carried out under the assumption that the effect of assumption that the effect of these cytokines on myofilament sensitivity would not readily wash out. As this experiment was measuring diastolic changes to sarcomere length, the assumption that the effect of TNF-α on myofilament sensitivity to Ca^{2+} would not readily reverse were based on the diastolic changes with TNF-α, shown in chapter 3. As per Fig 3-2C and 3-2D, the changes to both diastolic Ca^{2+} and resting sarcomere length with TNF-α were maintained with washout.

Over the pH range used, TNF-α appeared to cause an increase in myofilament sensitivity to Ca^{2+}. Sarcomere shortening was reduced when exposed to the pH 7.34 solution which did contain TNF-α – like IL-1β – indicating a reduction in Ca^{2+} sensitivity. The pH 7.1 and 7.6 solutions did not contain cytokines, and as such, mimics a washout step. The absence of cytokine from these solutions did not appear to affect the response to IL-1β, suggesting that the effect of IL-1β on myofilament sensitivity to Ca^{2+} was maintained following washout. With TNF-α washout, the effect on myofilament sensitivity to Ca^{2+} is shown to be far more readily reversible, restored to similar levels as untreated cells. This suggests that the effect of the cytokine is greater than that of pH following removal of TNF-α, and also that TNF-α has a higher reversibility than IL-1β.

A previous study by Goldhaber et al. (1996) investigated the possibility that TNF-α could alter myofilament sensitivity through a cytokine-induced change in pH. They found that change in pH was not the mechanism behind the TNF-α induced reduction of myofilament sensitivity in rabbit ventricular myocytes. This study further confirms the lack of involvement of pH, as both cytokines were demonstrated to have a much larger effect on myofilament sensitivity than pH.

Both TNF-α and IL-1β data supports a general reduction in myofilament sensitivity to Ca^{2+}, in which TNF-α had a higher level of reversibility.

5.4.4 Can the change to myofilament sensitivity to Ca^{2+} observed account for the changes to inotropy?

Other exogenous substances have been discovered with the ability to modulate myofilament sensitivity and alter inotropy. One such example is blebbistatin; a known Ca^{2+} desensitiser, which inhibits myosin-II ATPase to uncouple myofilament cross bridges in a dose dependent manner. In rat cardiac myocytes, Farman et al. (2008) found that 1 hour exposure to 0.5 µM blebbistatin almost completely abolished sarcomere shortening with no effect on Ca^{2+} transient amplitude. Blebbistatin can therefore be used as an example of how a Ca^{2+} desensitizer can reduce inotropy.

As per chapter 3, 50 ng/ml TNF-α reduced sarcomere shortening by 20.31 ± 7.58 % (Fig 3-2B), while IL-1β did not affect sarcomere shortening (Fig 3-4B). The effects with these cytokines on contractility are therefore weaker than the comparatively great levels of contractile inhibition with blebbistatin (Farman et al., 2008). As per section 5.3.2, both cytokines reduce myofilament sensitivity to Ca^{2+}, however as higher [Ca^{2+}] (150 nM and 200 nM) were able to cause a degree of sarcomere shortening (Fig 5-8), the ability of TNF-α and IL-1β to decrease in myofilament sensitivity is not as strong as that on blebbistatin. The reduced myofilament could contribute to loss of contractility, especially with the observed loss of contractility with TNF-α.

Chapter 6

The effect of TNF-α on Ca^{2+} handling and contractility in left ventricular myocytes from sheep with induced heart failure and those allowed to recover

6.1 Introduction

As was introduced in section 1.1.7, in heart failure, contractility is impaired, particularly in the left ventricle. This often leads to reduced fractional shortening and, as a result, reduces ejection fraction to less than 40 %. Cardiac output is therefore not easily maintained in heart failure, leading to hypoperfusion (Briston et al., 2011; Kemp & Conte, 2012; Mullens et al., 2008). As the heart cannot eject the same volume of blood, end-diastolic volume increases, as does end-systolic volume (Briston et al., 2011; Kemp & Conte, 2012).

Low cardiac output can promote cardiac remodelling. This helps the heart to maintain cardiac output and prevent hypoperfusion, but though increased cardiac workload. Resulting symptoms include dyspnea (laboured breathing) and tachycardia (Kemp & Conte, 2012). Due to the blunted force frequency relationship in the failing heart, tachycardia could worsen heart failure with a negative effect on inotropy (Lou, Janardhan, & Efimov, 2012; Mullens et al., 2008).

6.1.1 Altered Ca^{2+} handling in heart failure

This study is not attempting to characterise altered ECC in heart failure, as this has already been investigated using a robust and integrative approach (Briston et al., 2011). Alternatively, this study will explore the response of cells isolation from a heart failure model to TNF-α. It is therefore important to first understand perturbed Ca^{2+} handling in heart failure.

The Ca^{2+} transient amplitude decreased is reduced in heart failure, leading to reduced contractility. Whilst some studies have reported that SR Ca^{2+} content is reduced in heart failure (Lou et al., 2012; Phillips et al., 1998), Briston et al. (2011) reported that change to SR Ca^{2+} content may not be the primary cause of reduced Ca^{2+} release, rather decreased I_{CaL} could lead to reduced CICR by RyR. Equally, while RyR levels remain unchanged in heart failure, decreased fractional release via RyR means that I_{CaL} must be higher (Briston et al., 2011; Lou et al., 2012; Phillips et al., 1998). Impaired Ca^{2+} uptake by SERCA has been

implicated in the reduction to SR Ca^{2+} content (Lou et al., 2012). In heart failure resulting from ischemia, SERCA can be down-regulated, however in other forms and models of heart failure SERCA protein levels are unaffected (Briston et al., 2011; Lou et al., 2012).

There is conflicting evidence over whether PLN levels change in heart failure, with reports of down-regulated PLN in some cases of heart failure (Lou et al., 2012; Phillips et al., 1998). Down-regulation of PLN reduces the inhibition of SERCA, and therefore may be a compensatory mechanism to improve SR Ca^{2+} loading. There is however a reduced ability to modulate SR Ca^{2+} content with lower PLN, as such beat to beat variation in SR Ca^{2+} release and the resulting contractility, can lead to the occurrence of alternans (Phillips et al., 1998).

Decreased phosphorylation of PLN has also been reported in heart failure, contributing to reduced SR Ca^{2+} uptake by SERCA. The lower rate of Ca^{2+} removal contributes slower relaxation. It is thought than these effects on PLN and SERCA activity are mediated by levels of PKA and CaMKII. In some cases of heart failure, increased involvement of NCX in Ca^{2+} removal, results in overall rate of Ca^{2+} removal being unaffected, but lower diastolic Ca^{2+}. Heart failure cells are also less responsive to β-adrenergic stimulation (Briston et al., 2011; Lou et al., 2012; Phillips et al., 1998).

6.1.2 Cytokines in heart failure

TNF-α are increased in congestive heart failure and continue to increase with elevation in disease severity (Aukrust et al., 1999; Torre-Amione et al., 1996). Circulating plasma concentrations of TNF-α have been measured within a range of 0.5 – 32 pg/ml TNF-α in plasma in congestive heart failure by Testa et al. (1996) and 1.95-64 pg/ml by Torre-Amione et al. (1996). Other proinflammatory cytokines, including IL-1β and IL-6, become elevated in more advanced heart failure and anti-inflammatory cytokine levels can also be abnormal. Regardless of the cause of congestive heart failure, the cytokines present are similar (Aukrust et al., 1999; Testa et al., 1996; Torre-Amione et al., 1996). TNF-α has been associated with cardiac remodelling and left ventricular dysfunction, including depressed contractile function. In a heart failure model of mice where TNF-α production was up-

regulated, down-regulation of both SERCA and PLN occurred (Feldman et al., 2000; Torre-Amione et al., 1996)

Increased levels of soluble TNF-α receptors have been measured in association with heart failure, especially type 2 (p75) TNF-α receptors in more advanced heart failure. Soluble TNF-α receptors essentially competitively inhibit the effects of TNF-α as less is available to bind to membrane bound receptors capable of evoking a response. This could potentially reduce the effect of TNF-α in heart failure cells (Aukrust et al., 1999; Testa et al., 1996).

6.1.3 Recovery from heart failure

In some heart failure patients, treatment can improve and even, in some cases, fully restore cardiac function and reverse remodelling. In these individuals, mortality is lower than heart failure patients on a whole, however still elevated in comparison to healthy individuals (Nijst, Martens, & Mullens, 2017). It is therefore interesting to know whether such individuals remain susceptible to the effects of TNF-α, given that it is expected they would have already been exposed to elevated TNF-α previously in heart failure (Testa et al., 1996).

Many of the treatments used with heart failure are pharmaceutical, however cardiac resynchronization therapy (CRT) has also been shown to effectively improve cardiac function. CRT involves implantation of a pacemaker (sometimes accompanied by a defibrillator) to modify the pacing of the heart; to coordinate the pacing and thus contraction of the different myocardial chambers (Nijst et al., 2017).

Case studies involving heart failure patients treated with CRT, identified that improvements to myocardial function occurred which prolonged survival and reduced hospitalization. Following 3-4 months CRT, left ventricular ejection fraction have increased, allowing improved cardiac output. Left ventricular end-systolic volume and end-diastolic volume were both reduced, indicating decreased myocardial dilation. The proteins often down regulated in heart failure – SERCA, NCX, PLN, β1-adrenergic receptor – were up-regulated following

CRT treatment and restored to similar proportions as in health (Cleland et al., 2005; Mullens et al., 2008).

The heart failure recovery model used in this study mimics the effect on the heart once the factor causing heart failure – in this instance tachycardia – is removed. A similar canine model of congestive heart failure found that once tachypacing ceased, body weight, heart rate, respiratory rate and reduced ejection fraction were restored to their previous levels after a week. Myocardial dilation also recovered ~4 weeks following ceased tachycardia (Howard, Stopps, Moe, Gotlieb, & Armstrong, 1988). The model used in this study may bear some comparison with improved heart failure patients, especially those treated with CRT.

As above, cytokines are elevated in heart failure and involved in its pathogenesis. It is therefore fair to assume that both the heart failure model and recovery model cells have already been previously exposed to high levels of TNF-α.

This study will determine whether the effects of TNF-α on ECC in cells isolated from the heart failure and recovery models are similar to those in young control sheep. It is possible that the effects of TNF-α on the various measured parameters of ECC will become saturated in these experimental models or that the magnitude of the effects of TNF-α could be exacerbated, given that Ca^{2+} handling and contractility is already impaired in heart failure. As such, this could provide evidence as to whether patients with heart failure or in recovery would be as susceptible to the effects of TNF-α in the heart as healthy individuals.

6.1.4 Aims

(a) Determine the effects of 50 ng/ml TNF-α on left ventricular myocytes isolated from a tachypaced sheep model of heart failure
(b) Determine the effects of 50 ng/ml TNF-α on left ventricular myocytes isolated from an uncharacterised tachypaced sheep model of heart failure, allowed to recover for 5 weeks
(c) Investigate possible differences in the response to TNF-α, if any, between cells from these experimental models and that of a young control model.

6.2 Methods

6.2.1 Generation of the experimental models

The sheep used to generate both experimental models were age matched to that of the young control sheep used in the previous experiments (~18 months old). Heart failure was induced using tachypacing. Sheep were subjected to transvenous right ventricular tachypacing using a pacing lead – positioned at the right ventricular apex – and attached to a Medtronic Thera cardiac pacemaker, positioned in the cervical subcutaneous pocket. Following implantation of the pacemaker, ~10 days were allowed prior to pacemaker activation and thus onset of the tachypacing protocol, to enable animals to recover from the surgical procedure.

Hearts were paced at 210 beats per minute. The tachypacing protocol spanned over approximately 50 days, until the sheep presented with symptoms of heart failure, including lethargy, cachexia (weakness and muscle wasting) and dyspnoea. Echocardiography was carried out of conscious, unsedated animals, enabling alterations in fractional shortening to be assessed *in vivo*; this was used to determine end-stage heart failure. The animals were sacrificed once end-stage heart failure had been determined. Similar methods have been described and used by Briston et al. (2011), Dibb et al. (2009), Clarke et al. (2015) and Horn et al. (2012).

In order to confirm whether cells isolated from tachypaced sheep exhibited a heart failure-like phenotype, the raw k_{caff} values following control steady state (Fig 6-6B) were compared to that from young control animals (Fig 3-6B). k_{caff} was chosen because NCX activity is known to be decreased in heart failure, due to reduced NCX expression (Clarke et al, 2015). Furthermore, k_{caff} is unaffected by dye loading or calibration. k_{caff} was 28.81 % lower in cells from the tachypaced *heart failure* model than that of the young sheep control model ($p = 0.009$, unpaired t-test, young control sheep, 1.35 ± 0.13 F_{340}/F_{380}, $n = 15$; heart failure model, 0.96 ± 0.08 F_{340}/F_{380}, $n = 26$). Given that k_{caff} is significantly lower in the cells from the tachypaced model, this confirms that they were phenotypically heart failure in nature.

For the *recovery* heart failure model, the protocol was carried out as described above, however once severe heart failure had been induced, tachypacing was ceased. Animals were sacrificed following a period of 5 weeks, which allowed for recovery to occur if possible. While a similar canine model of heart failure and recovery has been studied by Howard et al. (1988) to determine changes to whole heart function *in vivo*, this model is currently uncharacterised on a cellular level.

All procedures carried out to generate these experimental models were done so in collaboration with the Trafford research group at the University of Manchester.

6.2.2 Experimental procedure

Cell isolation was carried out as described in section 2.1, from 2 experimental ovine models; tachypaced induced heart failure and following 5 weeks recovery. Data was recorded using Ionwizard software and measurements were taken as described in section 2.2. As per section 2.3.4, application of 10 mM caffeine was used to estimate SR Ca^{2+} content.

6.2.3 Analysis

As per section 2.3, the final 5 sweeps were averaged and values were normalised to control. Differences between control, TNF-α and wash state were compared using a one-way ANOVA. The normalised changes to each parameter with TNF-α and washout in both experimental models and the young control model used were also compared using a one-way ANOVA. Post-hoc tests were used to provide additional individual comparisons between the sub-groups.

In the figures comparing the data from the young control, heart failure and recovery sheep models, the data presented represents the normalised mean of a given parameter following TNF-α exposure or washout. All data for each cell were normalised to each cells' own control steady state value meaning all changes shown are relative. As previously described,

normalisation is useful given that this study is interested in the relative change to Ca^{2+}, as opposed to the absolute Ca^{2+} concentration.

6.3 Results

6.3.1 The effects of 50 ng/ml TNF-α on intracellular Ca^{2+} levels and contractility in heart failure sheep

The specimen records of Fig 6-1A and 6-1C show an example of the effect of TNF-α on Ca^{2+} dynamics in a heart failure model. On average, Ca^{2+} transient amplitude decreased by 21.08 ± 3.66 % with TNF-α (n=34, $p < 0.05$) (Fig 6-2A). Mean diastolic Ca^{2+} decreased by 3.19 ± 1.89 % with TNF-α (n=34, $p < 0.05$) (Fig 6-2C). Both changes to diastolic Ca^{2+} (n=32, $p < 0.05$) and Ca^{2+} transient amplitude (n=32, $p < 0.05$) were maintained during washout.

The specimen records of Fig 6-1B and 6-1D shows an example of the effect of TNF-α on contractility in a heart failure model. The mean resting sarcomere length decreased by 0.8 ± 0.2 % with TNF-α (n=25, $p < 0.05$), which was maintained following washout (n=24, $p < 0.05$) (Fig 6-2B). Sarcomere shortening unaffected by TNF-α application or washout (n=24, $p = 0.052$) (Fig 6-2D).

The specimen record of Fig 6-1E shows an example of the effect of TNF-α on rate of sarcomere shortening and relaxation in a heart failure model. Neither the rate of sarcomere shortening (n=20, $p = 0.457$) (Fig 6-2E), nor rate of sarcomere relaxation (n=21, $p = 0.100$) (Fig 6-2F) was affected by either TNF-α or washout.

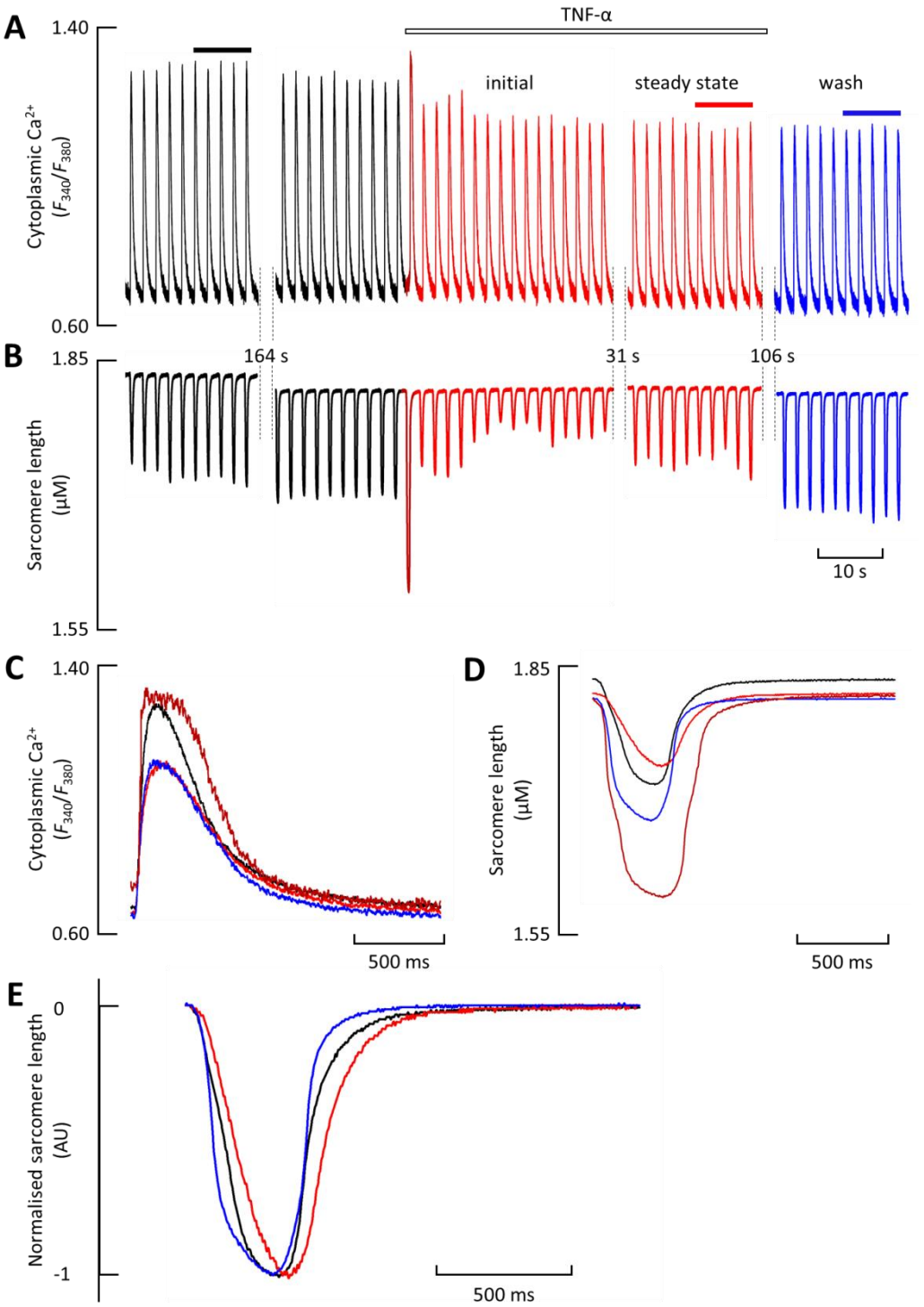

Figure 6-1. Specimen records of the effect of TNF-α on cytoplasmic Ca^{2+} and contractility in left ventricular myocytes from a sheep heart failure model. (A) specimen record showing Ca^{2+} transients. (B) specimen record showing sarcomere shortening. (C) specimen mean Ca^{2+} transients for the periods highlighted in A. (D) specimen mean sarcomere shortening traces for the periods highlighted in B. (E) specimen sarcomere shortening traces for the periods highlighted in B, with normalised diastolic and systolic levels.

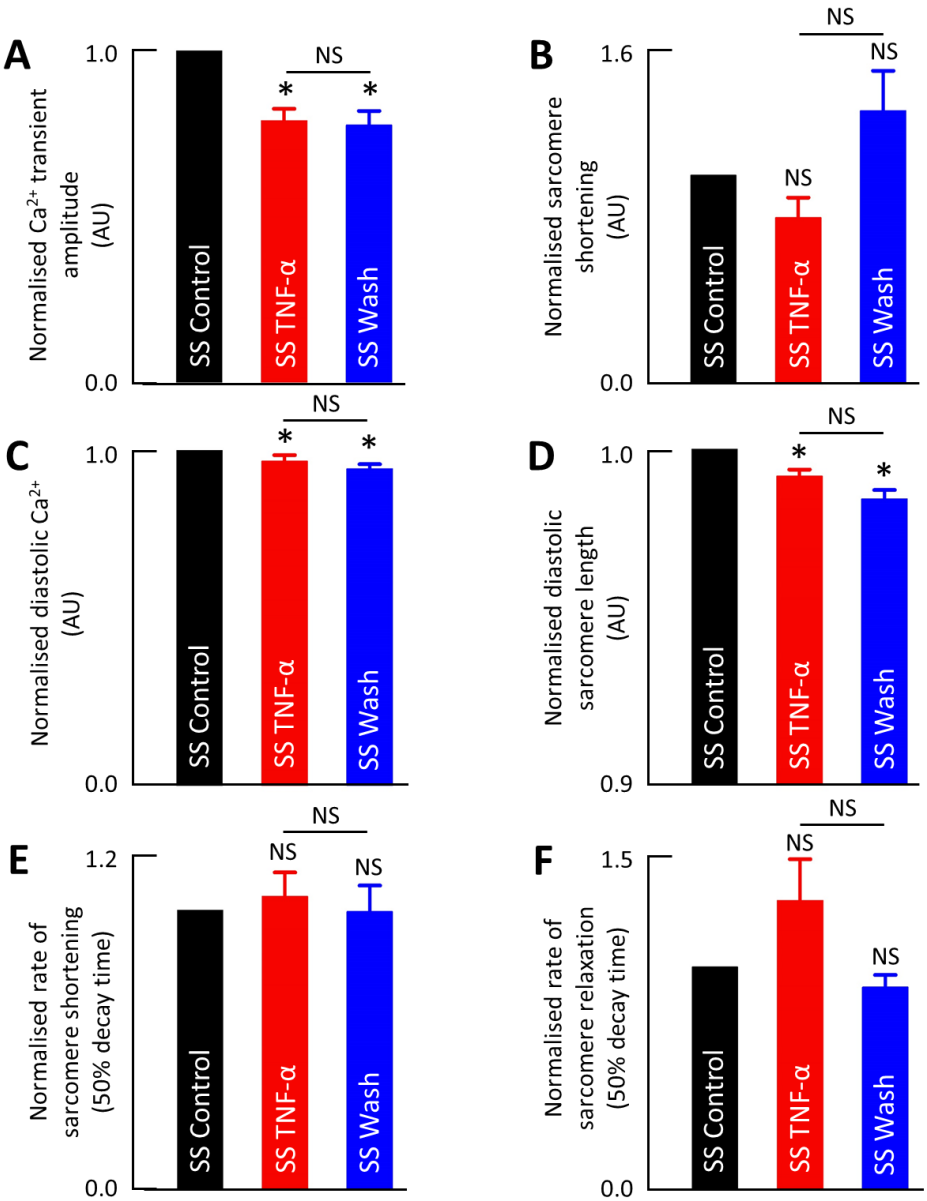

Figure 6-2. The effects of TNF-α and washout on cytoplasmic Ca^{2+} and contractility in left ventricular myocytes from a sheep heart failure model (n = 34 cells from 12 animals). (A) mean Ca^{2+} transient amplitude. (B) mean sarcomere shortening. (C) mean diastolic Ca^{2+}. (D) mean resting sarcomere length. (E) mean 50 % sarcomere shortening time. (F) mean 50 % sarcomere relaxation time. * indicates $p < 0.05$, NS denotes non-significance ($p > 0.05$), SS = steady state.

6.3.2 The effects of 50 ng/ml TNF-α on intracellular Ca^{2+} levels and contractility in heart failure recovery sheep

The specimen records of Fig 6-3A and 6-3C shows an example of the effect of TNF-α on Ca^{2+} dynamics in cells from heart failure recovery sheep. On average, diastolic Ca^{2+} was unchanged by TNF-α (n=25, p >0.05), but decreased by 1.42 ± 2.09 % during washout (n=24, p<0.05) (Fig 6-4C). Mean Ca^{2+} transient amplitude decreased by 16.09 ± 3.87 % with TNF-α (n=25, p <0.05) and was maintained during washout (n=24, p <0.05) (Fig 6-4A).

The specimen records of Fig 6-3B and 6-3D shows an example of the effect of TNF-α on contractility in cells from a heart failure recovery sheep. On average, resting sarcomere length decreased by 0.86 ± 0.2 % with TNF-α (n=20, p <0.05) and was maintained during washout (n=19, p <0.05) (Fig 6-4D). Sarcomere shortening decreased by 12.6 ± 6.9 % with TNF-α (n=20, p <0.05), maintained during washout (n=19, p <0.05) (Fig 6-4B).

The specimen record of Fig 6-3E demonstrates the effect of TNF-α on rate of relaxation and shortening in cells from a heart failure recovery sheep. Rate of sarcomere shortening unaffected by TNF-α and washout (n=20, p = 0.931) (Fig 6-4E), whilst rate of sarcomere relaxation was unaffected by TNF-α (n=20, p >0.05), but following washout the 50 % time of sarcomere relaxation decreased by 10.06 ± 3.5 % (n=19, p <0.05) (Fig 6-4F).

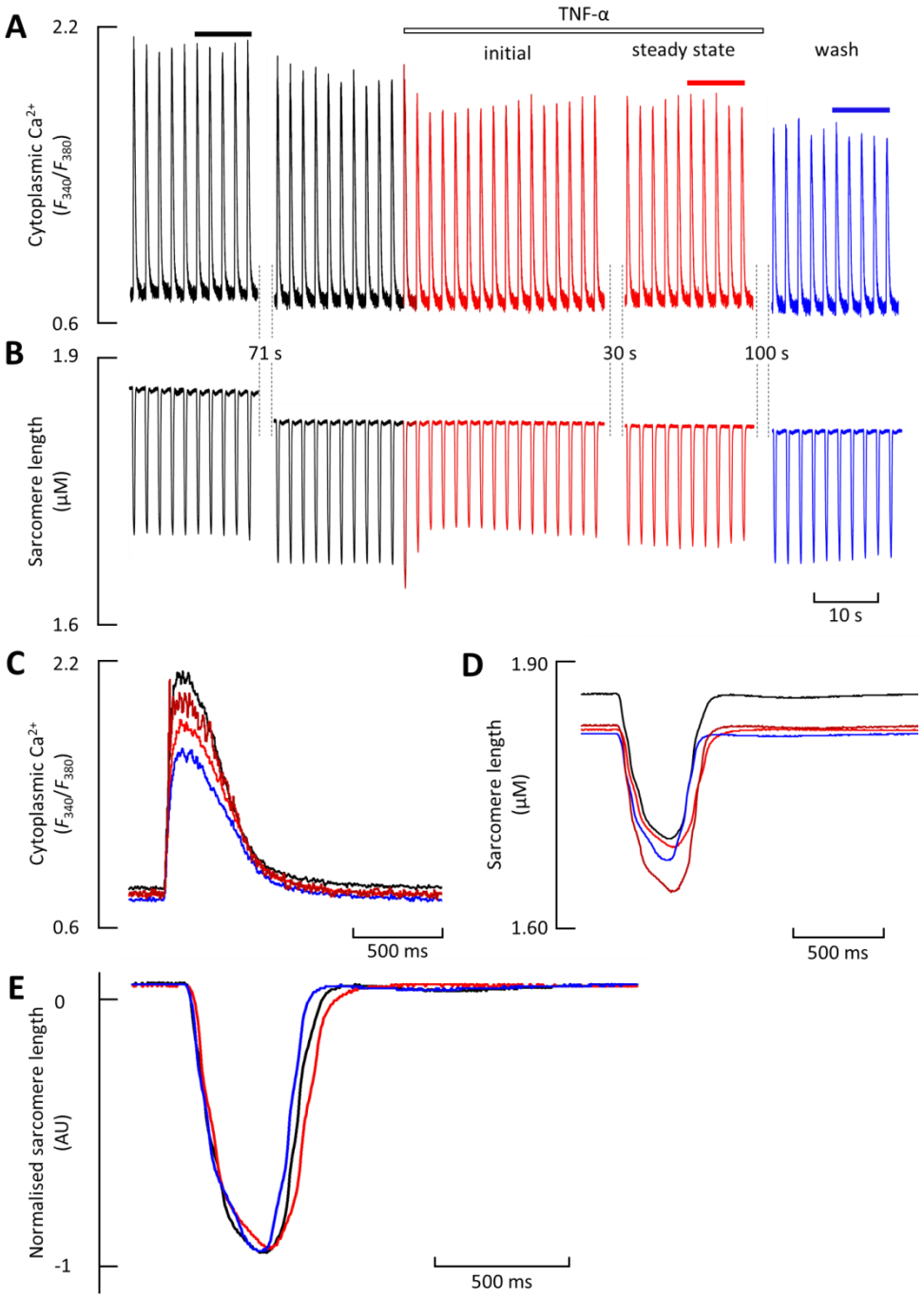

Figure 6-3. Specimen records of the effect of TNF-α on cytoplasmic Ca^{2+} and contractility in left ventricular myocytes from a sheep model allowed to recover from heart failure. (A) specimen record showing Ca^{2+} transients. (B) specimen record showing sarcomere shortening. (C) specimen mean Ca^{2+} transients for the periods highlighted in A. (D) specimen mean sarcomere shortening traces for the periods highlighted in B. (E) specimen sarcomere shortening traces for the periods highlighted in B, with normalised diastolic and systolic levels.

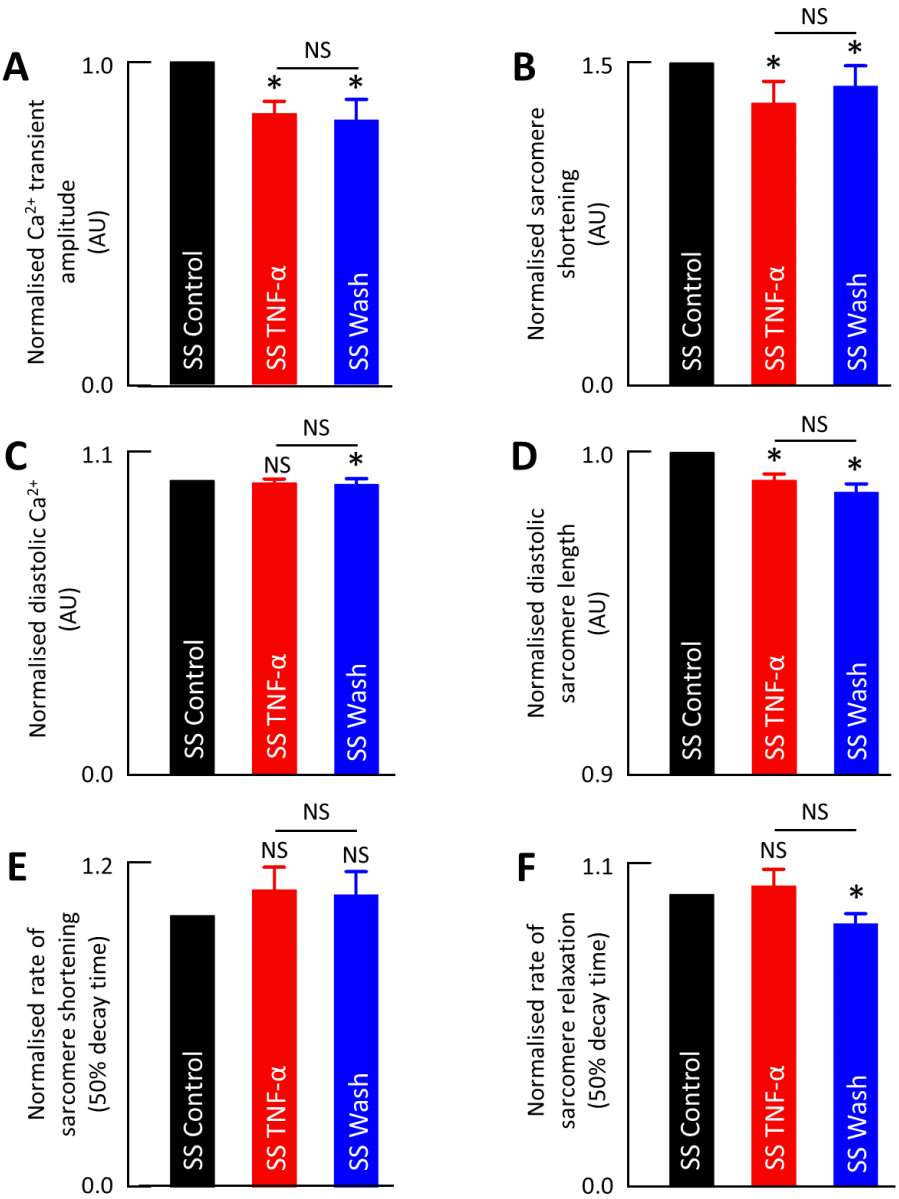

Figure 6-4. The effects of TNF-α and washout on cytoplasmic Ca^{2+} and contractility in left ventricular myocytes from a sheep model allowed to recover from heart failure (n = 25 cells from 4 animals). (A) mean Ca^{2+} transient amplitude. (B) mean sarcomere shortening. (C) mean diastolic Ca^{2+}. (D) mean resting sarcomere length. (E) mean 50 % sarcomere shortening time. (F) mean 50 % sarcomere relaxation time. * indicates $p < 0.05$, NS denotes non-significance ($p > 0.05$), SS = steady state.

6.3.3 The effect of TNF-α on SR Ca^{2+} content of both heart failure and recovery sheep

An example of the effect of TNF-α on caffeine evoked Ca^{2+} transient amplitude, thus SR Ca^{2+} content in cells from a heart failure model and heart failure recovery model, is shown in the specimen records of Fig 6-5A and Fig 6-5B respectively. On average, Ca^{2+} transient amplitude decreased by 19.62 ± 4.58 % (n=28, $p < 0.05$) (Fig 6-5C) and 24.13 ± 5.43 % (n=13, $p = 0.002$) (Fig 6-5D) with TNF-α in heart failure sheep and heart failure recovery sheep respectively. In both heart failure sheep (n=22, $p < 0.05$) and heart failure recovery sheep (n=13, $p < 0.001$) this was maintained following washout.

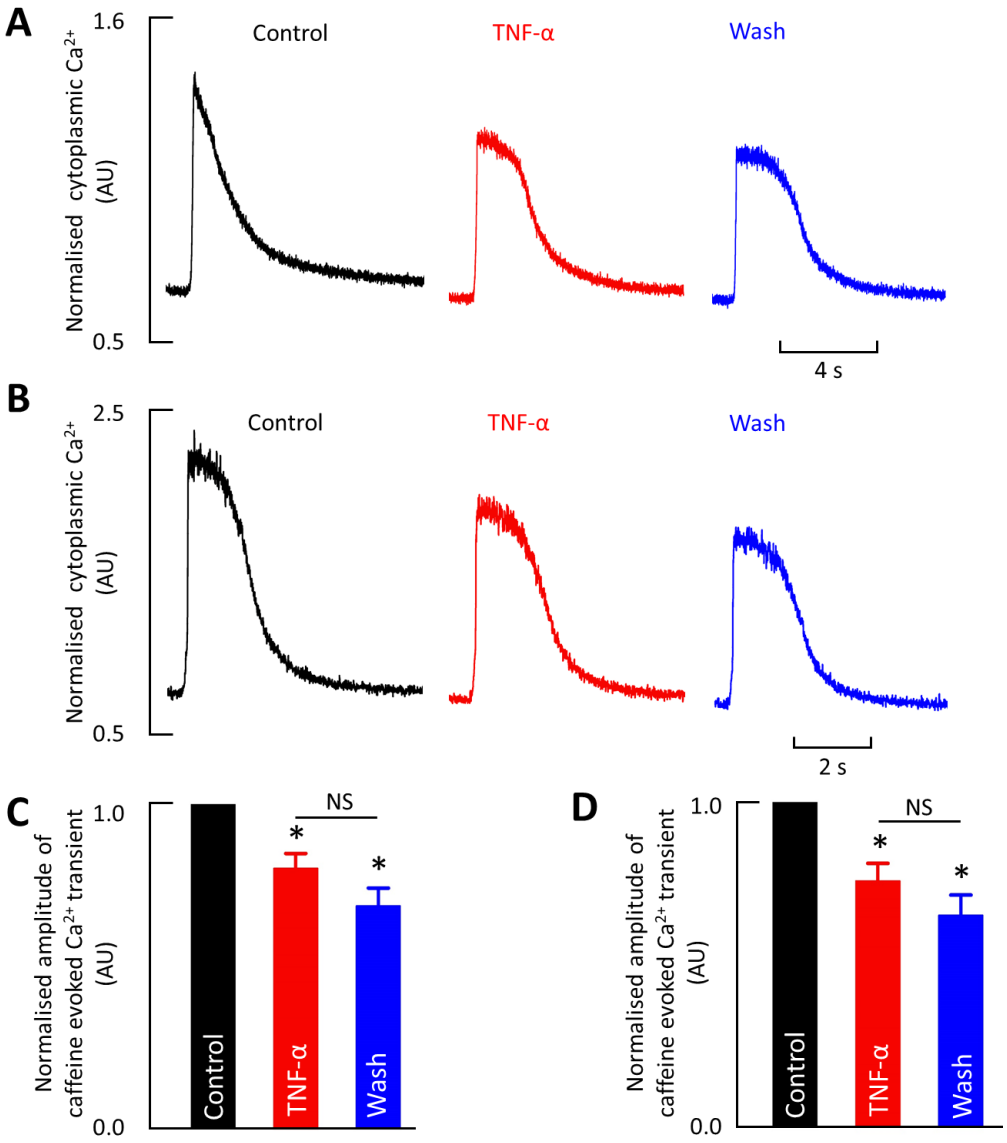

Figure 6-5. 10 mM caffeine evoked Ca^{2+} transient amplitudes in TNF-α treated cells from sheep models of heart failure (n = 28 cells from 10 animals) and heart failure recovery (n = 13 cells from 3 animals). (A) specimen record for caffeine evoked Ca^{2+} transient following control, cytokine and wash steady states in TNF-α treated cells from a heart failure model. (B) specimen record for caffeine evoked Ca^{2+} transient following control, cytokine and wash steady states in TNF-α treated cells from a heart failure recovery model. (C) mean caffeine evoked Ca^{2+} transients in TNF-α treated cells from a heart failure model. (D) mean caffeine evoked Ca^{2+} transients in TNF-α treated cells from a heart failure recovery model. * indicates $p < 0.05$, NS denotes non-significance ($p > 0.05$).

6.3.4 The effect of TNF-α on major Ca^{2+} removal mechanisms in heart failure and recovery sheep

The specimen records of Fig 6-6A and 6-6B shows an example of the effect of TNF-α on the rate of Ca^{2+} decay in normalised systolic Ca^{2+} transients (k_{sys}) and caffeine evoked Ca^{2+} transient (k_{caff}) in a cell from a heart failure model. No change to k_{sys} (n=34, p = 0.582) (Fig 6-6C), k_{caff} (n=25, p = 0.113) (Fig 6-6D) and k_{SERCA} (n=25, p = 0.491) (Fig 6-6E) were found with TNF-α or washout.

The specimen records of Fig 6-7A and 6-7B demonstrate the effect of TNF-α on rate of Ca^{2+} decay in normalised systolic Ca^{2+} transients (k_{sys}) and caffeine evoked Ca^{2+} transient (k_{caff}) in a cell from a heart failure recovery model. In heart failure recovery sheep, k_{sys} (n=25, p = 0.583) (Fig 6-7C), k_{caff} (n=12, p = 0.119) (Fig 6-7D) and k_{SERCA} (n=12, p = 0.469) (Fig 6-7E) were unaffected by TNF-α or washout.

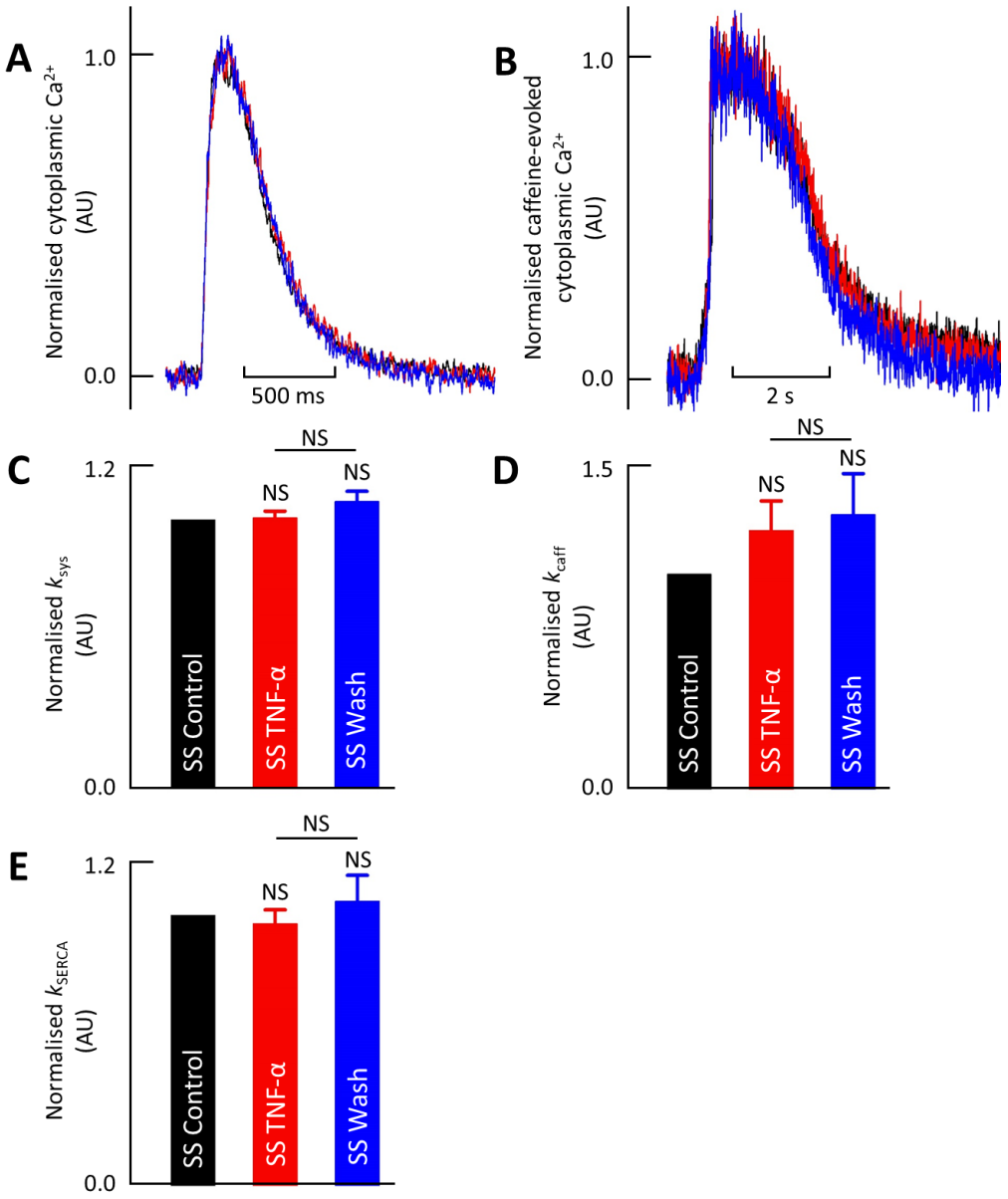

Figure 6-6. The effect of 50 ng/ml TNF-α on rate of Ca^{2+} removal in cells from a model of heart failure (n = 34 cells from 12 animals). (A) specimen trace of Ca^{2+} transients at control, TNF-α and washout steady state, with normalised diastolic and systolic levels. (B) specimen trace of caffeine-evoked Ca^{2+} transients at control, TNF-α and washout steady state, with normalised diastolic and systolic levels. (C) mean normalised k_{sys}. (D) mean normalised 90-10 % decay time of the Ca^{2+} transient. (E) mean normalised k_{caff}. (F) mean normalised k_{SERCA}. * indicates $p < 0.05$, NS denotes non-significance ($p > 0.05$), SS = steady state.

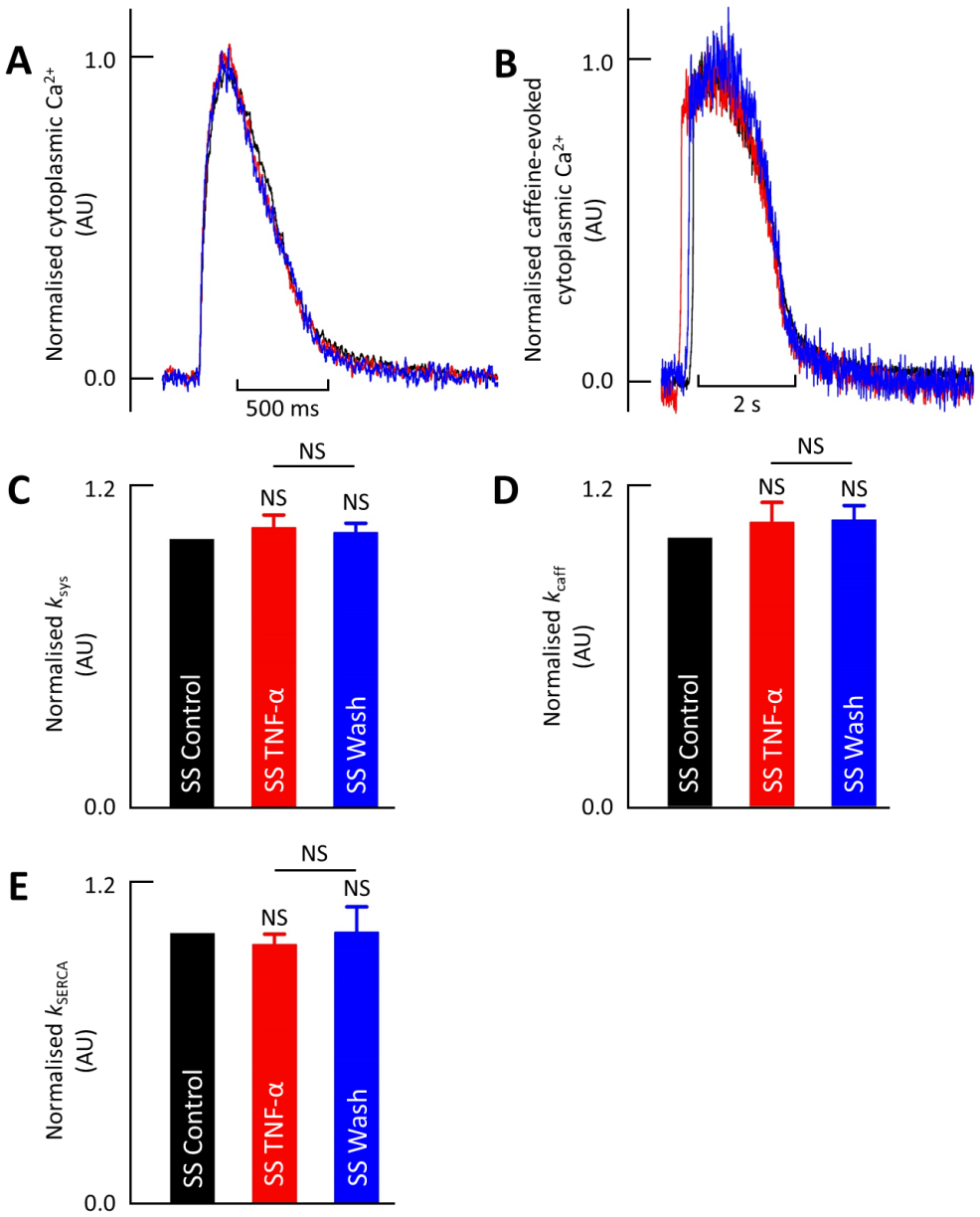

Figure 6-7. The effect of 50 ng/ml TNF-α on rate of Ca^{2+} removal in cells from a model of heart failure recovery (n = 25 cells from 4 animals). (A) specimen trace of Ca^{2+} transients at control, TNF-α and washout steady state, with normalised diastolic and systolic levels. (B) specimen trace of caffeine-evoked Ca^{2+} transients at control, TNF-α and washout steady state, with normalised diastolic and systolic levels. (C) mean normalised k_{sys}. (D) mean normalised 90-10 % decay time of the Ca^{2+} transient. (E) mean normalised k_{caff}. (F) mean normalised k_{SERCA}. * indicates $p < 0.05$, NS denotes non-significance ($p > 0.05$), SS = steady state.

6.3.5 The early effect of 50 ng/ml TNF-α on systolic Ca^{2+} in heart failure and recovery sheep

Preceding the decrease of systolic Ca^{2+} to a lower steady state in both the heart failure model (Fig 6-1 and 6-2) and the heart failure recovery model (Fig 6-3 and 6-4), certain cells TNF-α produced an early, short-lived potentiation of the Ca^{2+} transient amplitude lasting 1-3 beats. As with young control sheep, described in section 3.3.5, potentiation was defined as a greater than 10 % increase of systolic Ca^{2+} compared to control. Potentiation was observed in 44 % of heart failure cells and 48 % of heart failure recovery cells exposed to TNF-α.

An example of the effect of TNF-α on heart failure and recovery responders (presenting with 1^{st} beat potentiation) is demonstrated in the specimen records of Fig 6-8A and 6-8D respectively. In heart failure responders, TNF-α produced a 1^{st} beat mean increase in Ca^{2+} transient amplitude by 42.52 ± 12.34 % (n=15, $p < 0.05$) (Fig 6-8B), accompanied by a corresponding mean increase in sarcomere shortening by 76.21 ± 29.93 % (n=9, $p < 0.05$) (Fig 6-8C). In responders from the recovery model, TNF-α produced a similar 1^{st} beat mean increase in Ca^{2+} transient amplitude by 40.16 ± 9.81 % (n=12, $p < 0.05$) (Fig 6-8E), alongside an increase in sarcomere shortening by 94.49 ± 46.54 % (n=9, $p < 0.05$) (Fig 6-8F).

The specimen records of Fig 6-9A and 6-9D show the effect of TNF-α on heart failure and recovery non-responders (not presenting with potentiation). In non-responders from the heart failure model, TNF-α produced no immediate 1^{st} beat effect on either Ca^{2+} transient amplitude (n=19, $p > 0.05$) (Fig 6-9B), or sarcomere shortening (n=16, $p > 0.05$) (Fig 6-9C). At steady state, Ca^{2+} transient amplitude decreased by 28.57 ± 4.72 %. In non-responders from the recovery model, TNF-α produced no immediate effect on Ca^{2+} transient amplitude (n=13, $p > 0.05$), and sarcomere shortening (n=12, $p > 0.05$). At steady state Ca^{2+} transient amplitude was reduced by 23.32 ± 4.27 % (n=13, $p < 0.05$) (Fig 6-9E), coinciding with a mean decrease in sarcomere shortening by 14.84 ± 10.17 % (n=12, $p < 0.05$) (Fig 6-9F).

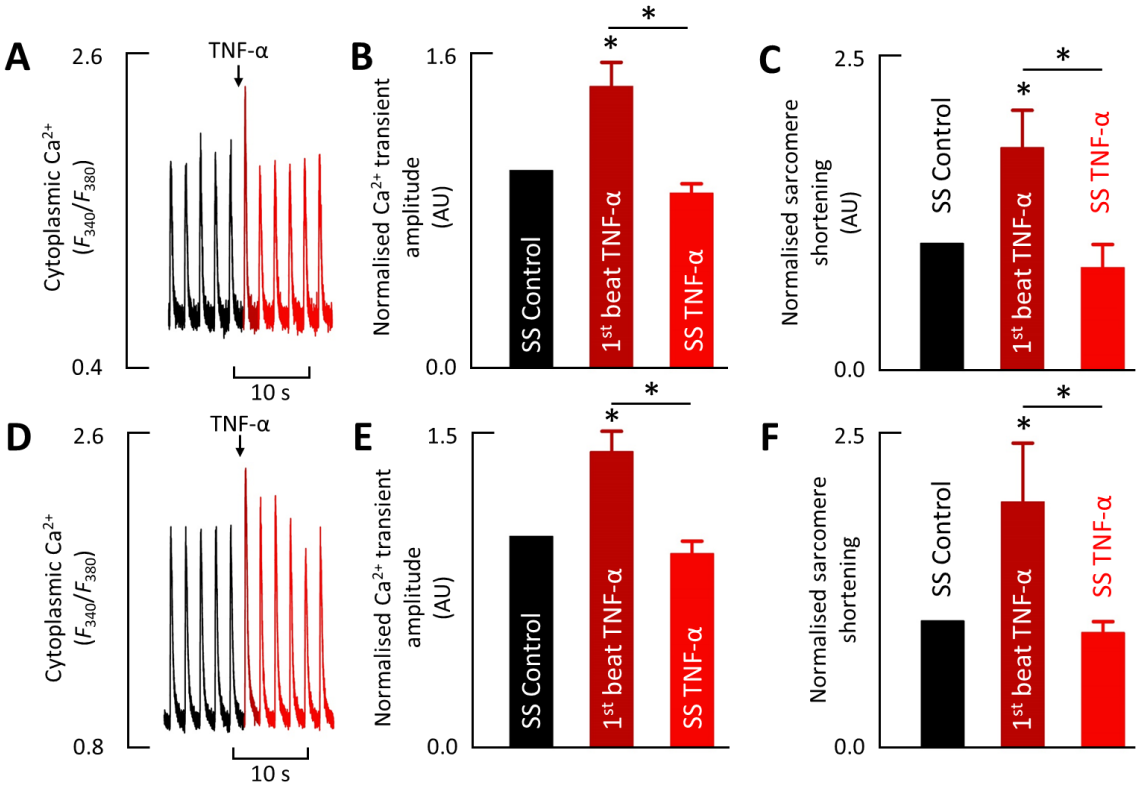

Figure 6-8. The effect of 50 ng/ml TNF-α on the 1st beat Ca^{2+} transient amplitude and contractility of cells from both models showing signs of RyR potentiation (A) specimen record showing Ca^{2+} transients from a heart failure model, immediately prior to [black], during [dark red] and following [red] 1st beat application of TNF-α. (B) mean normalised Ca^{2+} transient amplitude with 1st beat application of TNF-α in cells from a heart failure model (n = 15 cells from 7 animals). (C) mean normalised sarcomere shortening with 1st beat application of TNF-α in cells from a heart failure model. (D) specimen record showing Ca^{2+} transients from a heart failure recovery model, with 1st beat application of TNF-α, as labelled in A. (E) mean normalised Ca^{2+} transient amplitude with 1st beat application of TNF-α in cells from a heart failure recovery model (n = 12 cells from 4 animals). (F) mean normalised sarcomere shortening with 1st beat application of TNF-α in cells from a heart failure recovery model. * indicates $p < 0.05$, NS denotes non-significance ($p > 0.05$), SS = steady state.

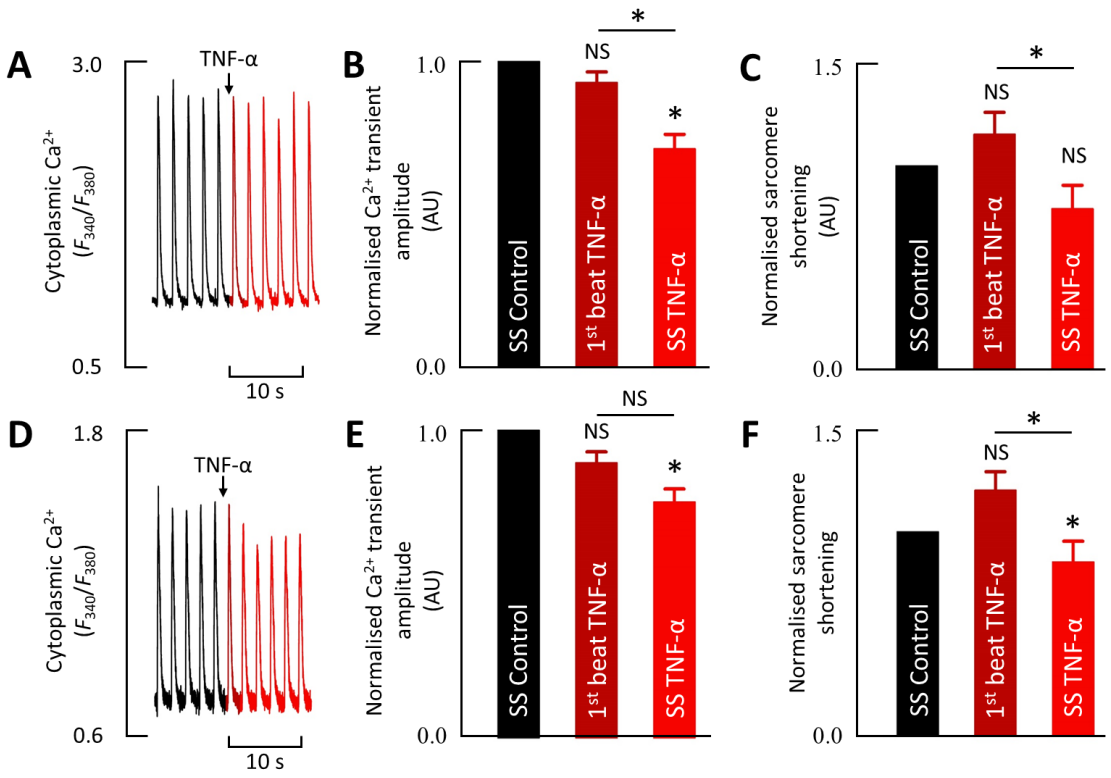

Figure 6-9. The effect of 50 ng/ml TNF-α on the 1st beat Ca^{2+} transient amplitude and contractility of cells from both models without signs of RyR potentiation (A) specimen record showing Ca^{2+} transients from a heart failure model, immediately prior to [black], during [dark red] and following [red] 1st beat application of TNF-α. (B) mean normalised Ca^{2+} transient amplitude with 1st beat application of TNF-α in cells from a heart failure model (n = 19 cells from 10 animals). (C) mean normalised sarcomere shortening with 1st beat application of TNF-α in cells from a heart failure model. (D) specimen record showing Ca^{2+} transients from a heart failure recovery model, with 1st beat application of TNF-α, as labelled in A. (E) mean normalised Ca^{2+} transient amplitude with 1st beat application of TNF-α in cells from a heart failure recovery model (n = 13 cells from 3 animals). (F) mean normalised sarcomere shortening with 1st beat application of TNF-α in cells from a heart failure recovery model. * indicates $p < 0.05$, NS denotes non-significance ($p > 0.05$), SS = steady state.

6.3.6 Differences in the magnitude of the effect of TNF-α on heart failure and recovery sheep in comparison to young control sheep

For all measured parameters, the histograms below show the values with TNF-α and washout normalised against control steady state (Fig 6-10 to 6-14), and therefore show the mean magnitude of the effect in each of the 3 models. This allows for direct comparison in the magnitude of the effects of TNF-α in young control sheep, the tachypaced sheep heart failure model, and 5 week recovery model.

Following TNF-α application to young control sheep, heart failure sheep and recovery sheep, there was no difference in the magnitude of change from control in Ca^{2+} transient amplitude ($p = 0.552$) (Fig 6-10A), diastolic Ca^{2+} ($p = 0.285$) (Fig 6-10C), sarcomere shortening ($p = 0.764$) (Fig 6-10B) and resting sarcomere length ($p = 0.298$) (Fig 6-10D). With TNF-α washout, there remained no difference in the magnitude of change to Ca^{2+} transient amplitude ($p = 0.324$) (Fig 6-11A), diastolic Ca^{2+} ($p = 0.627$) (Fig 6-11C), sarcomere shortening ($p = 0.157$) (Fig 6-11B) and resting sarcomere length ($p = 0.077$) (Fig 6-11D) between the different models used.

No difference was identified between the change to rate of sarcomere shortening ($p = 0.837$) (Fig 6-10E), or rate of sarcomere relaxation ($p = 0.261$) (Fig 6-10F), with TNF-α between the control and experimental models. This was also true following washout, where there was also no change to rate of sarcomere shortening ($p = 0.258$) (Fig 6-11E) or relaxation ($p = 0.185$) (Fig 6-11F).

The percentage change in caffeine-evoked Ca^{2+} transient amplitude ($p = 0.443$) with TNF-α was unchanged between the young control ($n=20$) and heart failure ($n=28$) and recovery ($n=13$) models (Fig 6-12A), nor did it change with washout ($p = 0.353$) (Fig 6-12B).

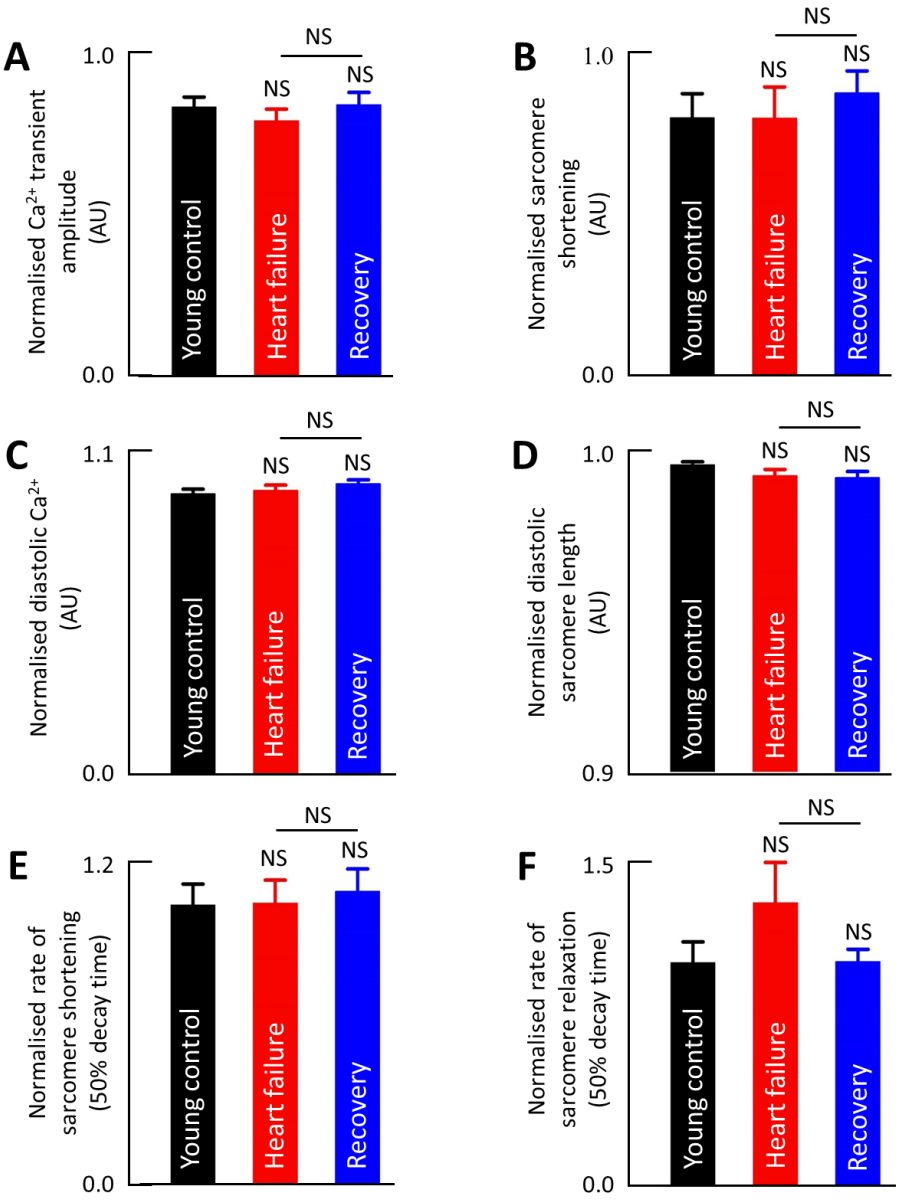

Figure 6-10. The comparative effect of 50 ng/ml TNF-α on Ca^{2+} dynamics and contractility in young control [black], heart failure [red] and heart failure recovery [blue] models. (A) mean normalised Ca^{2+} transient amplitude. (B) mean normalised sarcomere shortening. (C) mean normalised diastolic Ca^{2+}. (D) mean normalised resting sarcomere length. (E) mean normalised rate of sarcomere shortening. (F) mean normalised rate of sarcomere relaxation. * indicates $p < 0.05$, NS denotes non-significance ($p > 0.05$). Mean data presented has been previously normalised to its own control steady state, allowing comparison of the relative change to these parameters with TNF-α.

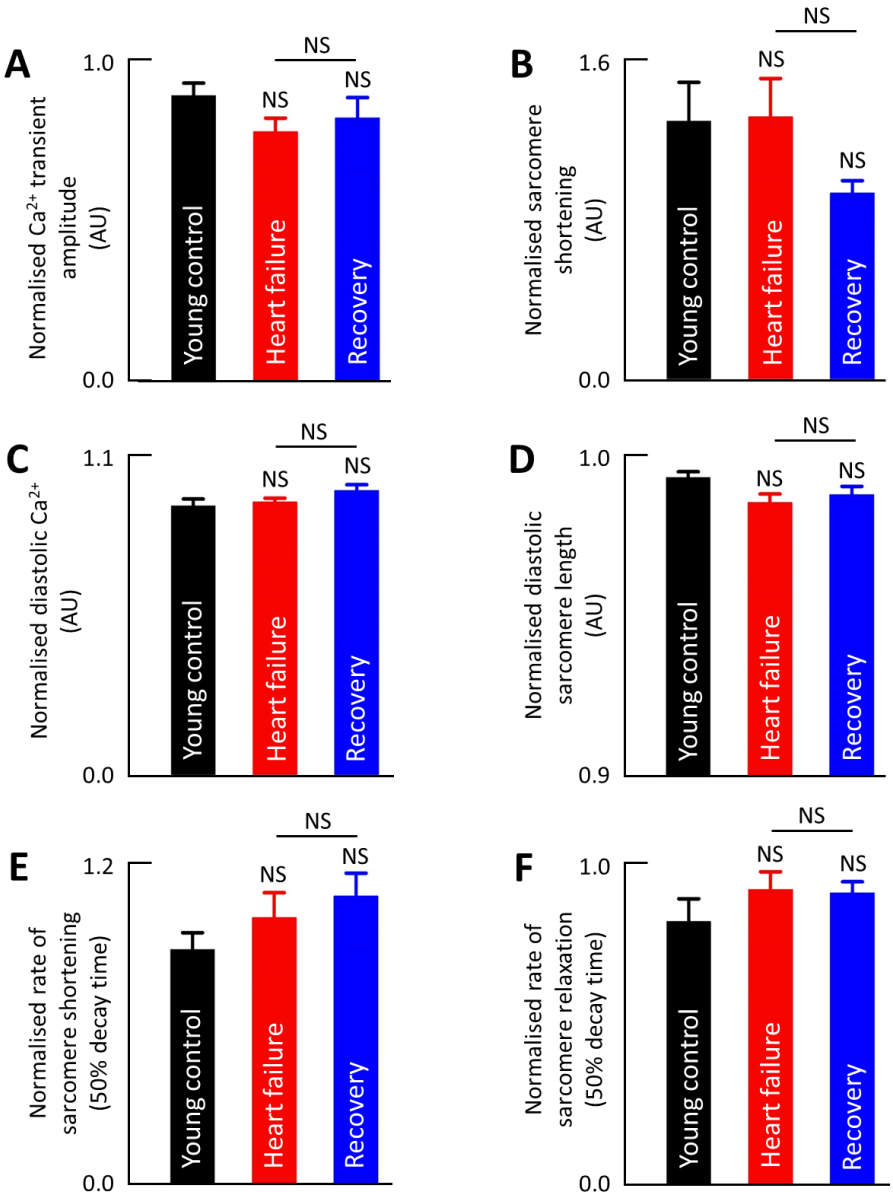

Figure 6-11. The comparative effect of TNF-α washout on Ca^{2+} dynamics and contractility in young control [black], heart failure [red] and heart failure recovery [blue] models. (A) mean normalised Ca^{2+} transient amplitude. (B) mean normalised sarcomere shortening. (C) mean normalised diastolic Ca^{2+}. (D) mean normalised resting sarcomere length. (E) mean normalised rate of sarcomere shortening. (F) mean normalised rate of sarcomere relaxation. * indicates $p < 0.05$, NS denotes non-significance ($p > 0.05$). Mean data presented has been previously normalised to its own control steady state, allowing comparison of the relative change to these parameters with washout.

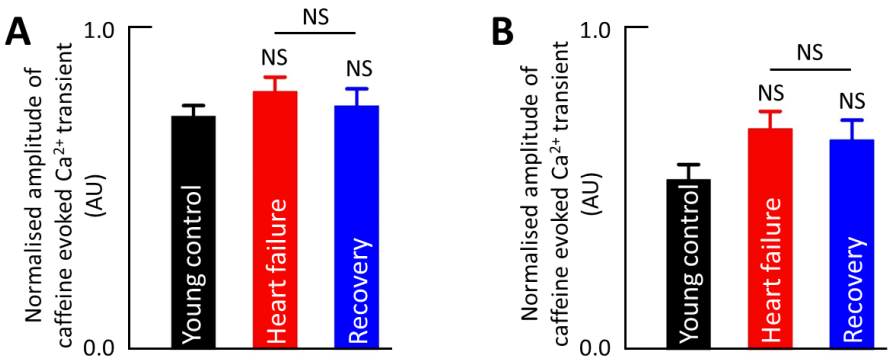

Figure 6-12. The comparative effect of TNF-α and washout on caffeine evoked Ca^{2+} transient amplitude in young control [black], heart failure [red] and heart failure recovery [blue] models. (A) mean normalised caffeine evoked Ca^{2+} transient amplitude with TNF-α. (B) mean normalised caffeine evoked Ca^{2+} transient amplitude with TNF-α washout. * indicates $p < 0.05$, NS denotes non-significance ($p > 0.05$). Mean data presented has been previously normalised to the amplitude of its own control caffeine-evoked Ca^{2+} transient, allowing comparison between the models, of relative change to these parameters.

The relative change to k_{sys} ($p = 0.943$) (Fig 6-13A) and k_{caff} ($p = 0.246$) (Fig 6-13C) produced by TNF-α application when compared to control steady state did not differ between the young control and disease models. Whilst k_{SERCA} did not alter significantly from control steady state in any model, the change in k_{SERCA} from control with TNF-α in young control sheep (n=11) was significantly different in both heart failure sheep (n=25, $p < 0.05$) and recovery sheep (n=12, $p<0.05$). The magnitude of change to k_{SERCA} produced by TNF-α did not differ between the heart failure sheep and recovery sheep ($p > 0.05$) (Fig 6-13E).

With TNF-α washout, there remained no difference in k_{sys} ($p = 0.671$) (Fig 6-13B) or k_{caff} ($p = 0.980$) (Fig 6-13D) between these models, or k_{SERCA} ($p > 0.05$) (Fig 6-13F) between the heart failure (n=20) when compared to both young control sheep (n=3) and recovery sheep (n=12). k_{SERCA} in recovery sheep is unchanged from control following TNF-α washout, this is different from that of young control sheep ($p < 0.05$) where k_{SERCA} increased by 91.67 ± 26.29 % with washout (Fig 6-13F).

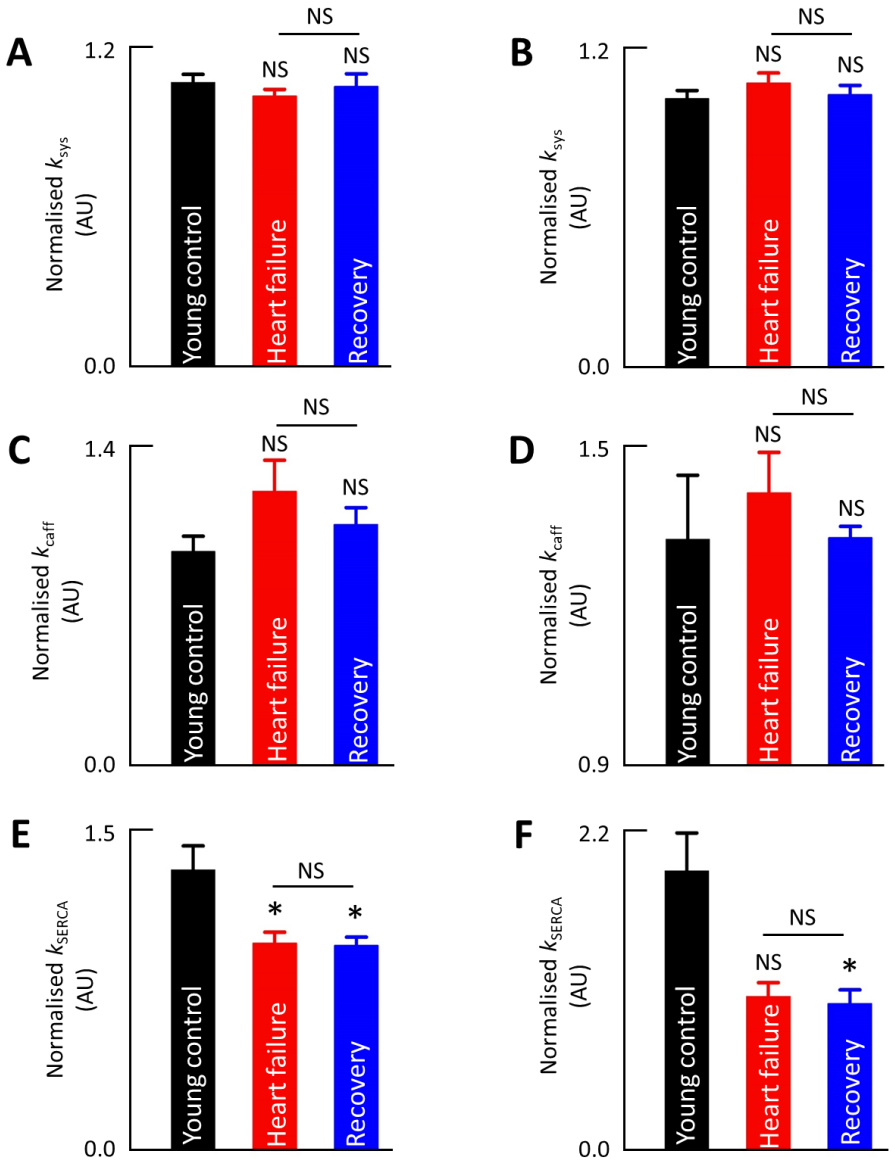

Figure 6-13. The comparative effects of TNF-α and washout on rate of Ca^{2+} removal in young control [black], heart failure [red] and heart failure recovery [blue] models. (A) mean normalised k_{sys} with TNF-α. (B) mean normalised k_{sys} with washout. (C) mean normalised k_{caff} with TNF-α. (D) mean normalised k_{caff} with washout. (E) mean normalised k_{SERCA} with TNF-α. (F) mean normalised k_{SERCA} with washout. * indicates $p < 0.05$, NS denotes non-significance ($p > 0.05$). Mean data presented has been previously normalised to its own control steady state, allowing comparison between the models, of relative change to these parameters.

The change to mean 1st beat change in Ca^{2+} transient amplitude with TNF-α in responders ($p = 0.189$) (Fig 6-14A) and non-responders ($p = 0.477$) (Fig 6-14C) was not different between

the young control, heart failure and recovery models. Similarly, the mean 1st beat change to sarcomere shortening in responders (p = 0.101) (Fig 6-14B) and non-responders (p = 0.091) (Fig 6-14D) with TNF-α did not differ between the models used.

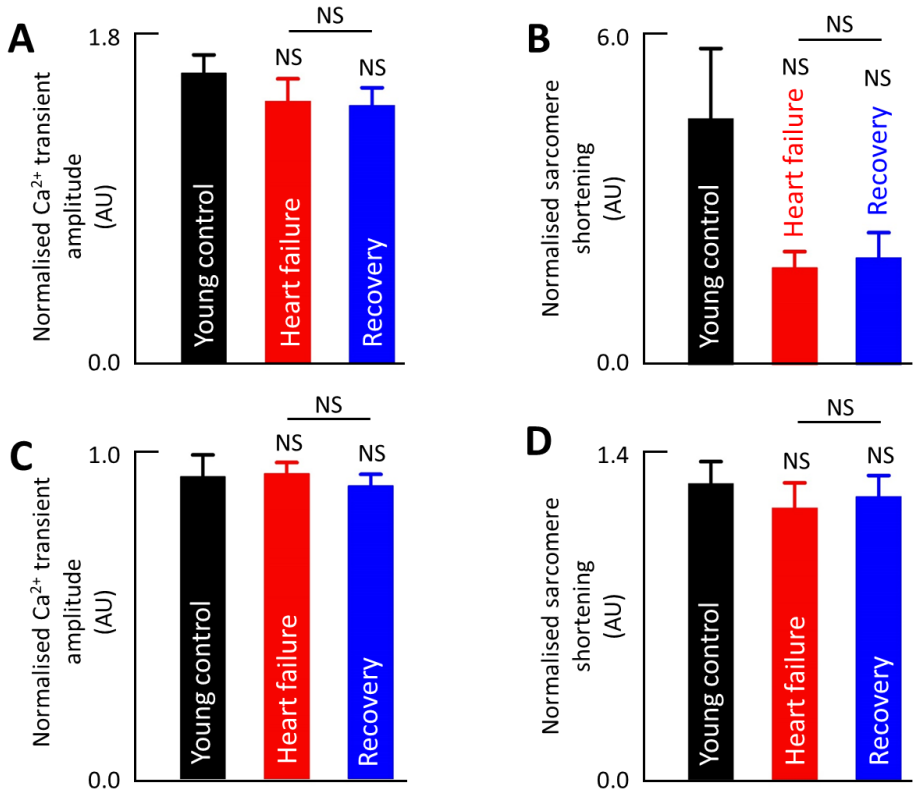

Figure 6-14. Comparisons between 1st beat responses to TNF-α. (A) mean Ca^{2+} transient amplitude in responders. (B) mean sarcomere shortening in responders. (C) mean Ca^{2+} transient amplitude in non-responders. (D) mean sarcomere shortening in non-responders. * indicates p <0.05, NS denotes non-significance (p >0.05). Mean data presented has been previously normalised to its own control steady state, allowing comparison of relative change to these parameters between the different models.

6.4 Discussion

6.4.1 Does acute exposure to 50 ng/ml TNF-α alter Ca^{2+} handling and contractility in the heart failure and recovery models?

In heart failure cells, TNF-α produced a maintained decrease in Ca^{2+} transient amplitude by 21.08 ± 3.66 % (Fig 6-2A), while sarcomere shortening was unchanged (Fig 6-2B). Although Briston et al. (2011) did not study change to contractility in heart failure, Ca^{2+} transient amplitude is already known to reduce, and this has been associated with elevated TNF-α levels (Feldman et al., 2000). The depressant effect of TNF-α on contractility may therefore have already been saturated by previous exposure TNF-α, prior to TNF-α exposure in experiments.

TNF-α also caused an irreversible decrease in diastolic Ca^{2+} by 3.19 ± 1.89 % in heart failure cells (Fig 6-2C). Diastolic Ca^{2+} is already reduced in heart failure (Briston et al., 2011), therefore it is interesting that TNF-α produces a further decrease in diastolic Ca^{2+} in heart failure cells, as this suggests that the effect on diastolic Ca^{2+} was not saturated by the effects of heart failure alone.

In recovery sheep cells, the 16.09 ± 3.87 % decrease in the Ca^{2+} transient produced by TNF-α was associated with a 12.6 ± 6.9 % decrease in sarcomere shortening, both of which were maintained with washout (Fig 6-4A and Fig 6-4B). Given the time allowed for recovery, any previous effect elevated circulating TNF-α could have had on contractility in heart failure may have been reversed. This is likely, as a canine model of tachycardia induced heart failure found improved contractility and a restored ejection fraction as week after pacing was ceased (Howard et al., 1988). In CRT treated heart failure patients, contractility and ejection fraction could also be improved following months of treatment (Cleland et al., 2005; Mullens et al., 2008). As contractility would be expected to be improved in the recovery model, the depressant effect of TNF-α on contractility would therefore no longer be saturated, and as in young control cells (Fig 3-2B), application of TNF-α in the experiment would be capable of reducing shortening.

TNF-α produced an irreversible 0.86 ± 0.2 % decrease in resting sarcomere in cells from the recovery model, however this was associated with no change to diastolic Ca^{2+}. However, during washout, diastolic Ca^{2+} did reduce by 1.42 ± 2.09 %. The changes in these parameters suggest that myofilament sensitivity to Ca^{2+} is elevated. As the recovery animals were paced to severe heart failure prior to the 5 weeks allowed for recovery, the effects of end-stage heart on myofilament sensitivity to Ca^{2+} may still be present (van der Velden, 2011).

In both the heart failure and recovery models, the rate of sarcomere shortening (Fig 6-2E and 6-4E) and rate of relaxation (Fig 6-2F and 6-4F) were unaltered by TNF-α. TNF-α washout produced a decrease by 10.06 ± 3.5 % of the 50 % decay time of sarcomere relaxation in cells from the recovery model, indicating that the rate of sarcomere relaxation increased. This is similar to the 18.92 ± 7.11 % decrease of the 50 % decay time of sarcomere relaxation, observed with TNF-α washout in young control cells (Fig 3-2F).

In heart failure reduced SERCA activity contributes to a lower rate of sarcomere relaxation (Lou et al., 2012). Heart failure cells are also less responsive to β-adrenergic stimulation, as such phosphorylation of PLN, therefore molecules such as PKA would not be capable of increasing SERCA activity and thus rate of Ca^{2+} removal to the same extent (Briston et al., 2011; Phillips et al., 1998). If the effect which TNF-α washout has on young control and recovery models is mediated by PLN phosphorylation, that could explain why the effect on increase is not observed in the heart failure model. This also suggest the impaired response to PLN phosphorylation, and thus modulation of SR Ca^{2+} content found in heart failure (Phillips et al., 1998), is restored in the recovery model. Phosphorylation of PLN occurs over a period of minutes, it is therefore possible that this is a gradual effect of TNF-α, only evident in washout. What contradicts phosphorylation of PLN, as a possible mechanism of increased rate of relaxation is that, unlike in young control cells, k_{SERCA} was not affected by TNF-α washout (Fig 6-7E). The contribution of NCX activity to Ca^{2+} removal increases in heart failure (Briston et al., 2011), and NCX is up-regulated in patients recovering from heart failure (Mullens et al., 2008). TNF-α or washout also had no effect on k_{caff} in recovery sheep. Increased SERCA or NCX activity cannot account for this increase in rate of relaxation in the recovery model, unless the changes are too small to detect.

6.4.2 How does 50 ng/ml TNF-α reduce Ca^{2+} transient amplitude in the heart failure and recovery models?

Ca^{2+} transient amplitude is primarily regulated by SR Ca^{2+} content and I_{CaL}. The latter was unable to be measured in this study, although Briston et al. (2011) found I_{CaL} to be reduced in heart failure. Although reduced I_{CaL} would be expected to decrease CICR, and thus blunt the Ca^{2+} transient amplitude, SR Ca^{2+} content has a larger role in modulation of Ca^{2+} release (Bers, 2002; Eisner, 2018).

As previously discussed, the relationship between SR Ca^{2+} content and Ca^{2+} transient amplitude is cubic (Trafford et al., 2000). In the heart failure model, TNF-α decreased SR Ca^{2+} content to 80.01 % of control (Fig 6-5C). As $(0.8001)^3$ = 0.5122, Ca^{2+} transient amplitude would be expected to decrease to 51.22 % of control. TNF-α only decreased Ca^{2+} transient amplitude to 78.39 % of control (Fig 6-5D). In the recovery model, TNF-α decreased SR Ca^{2+} content to 76.46 % of control. As $(0.7646)^3$ = 0.447, Ca^{2+} transient amplitude would be expected to decrease to 44.7 % of control with TNF-α. With TNF-α. Ca^{2+} transient amplitude decreased to only 82.95 % of control. As described in section 3.4.2, the method used to estimate SR Ca^{2+} content was through measuring the amplitude of caffeine evoked Ca^{2+} transients. TNF-α could have an effect on Ca^{2+} buffering, however the changes to SR Ca^{2+} content are large (decreasing by 19.62 ± 4.58 % and 24.13 ± 5.43 % in heart failure and recovery model cells respectively), therefore is it more likely that this is a true effect of TNF-α on SR Ca^{2+} content.

While reduced I_{CaL} could also contribute to reduced Ca^{2+} transient amplitude with TNF-α, in both models, the changes to SR Ca^{2+} content can account for the respective changes to Ca^{2+} transient amplitude alone.

6.4.3 How do TNF-α alter SR Ca^{2+} content in the heart failure and recovery models? Are the Ca^{2+} removal mechanisms affected?

The TNF-α evoked reduction in SR Ca^{2+} content, as recorded in heart failure and recovery models in section 3.4.2, could be altered by either a reduction in SERCA activity, thus SR Ca^{2+} uptake, or an increase in RyR P_o (Bers, 2002). First the effect of TNF-α on SERCA activity and other mechanisms of Ca^{2+} removal was explored in both experimental models.

TNF-α and washout produced no change in any mechanism of Ca^{2+} removal – k_{sys}, k_{caff} and k_{SERCA} – in both the heart failure and recovery models. Whilst some proteins associated with Ca^{2+} removal are down-regulated in heart failure (Mullens et al., 2008), Briston et al. (2011) reported no change to overall rate of Ca^{2+} removal in a similar heart failure model, due to compensatory increased contribution of NCX to Ca^{2+} removal. Mullens et al. (2008) suggested that down-regulated proteins associated with Ca^{2+} removal – such as SERCA and PLN – were up-regulated to control levels in patients in recovery from heart failure. As such, no prior effect on rate of Ca^{2+} removal would be anticipated in either the heart failure or recovery model. Changes in Ca^{2+} removal with TNF-α would not therefore be expected differ in the experimental models, from the young control model.

In young control cells k_{sys}, k_{caff} and k_{SERCA} were also unaffected by TNF-α, although with washout k_{SERCA} increased by 91.67 ± 26.29 % (Fig 3-6D to 3-6F). In heart failure cells, there was no such change to k_{SERCA}, this could be due to reduced PLN modulation of SERCA (Briston et al., 2011; Phillips et al., 1998). While this would not be expected to be the case in recovery cells, the restored levels of PLN and SERCA found by Mullens et al. (2008) in patients, were found following several months, which is much longer when compared to the period which the *recovery* model was allowed to recover (5 weeks). Any changes to protein regulation may have not occurred yet within that time.

As the activity of Ca^{2+} removal mechanisms were not affected by TNF-α in these experimental models, the change to SR Ca^{2+} content cannot be accounted for by reduced SR Ca^{2+} uptake. As has been shown to be the case for young control sheep (see chapter 4), TNF-α could also be increasing RyR P_o in these models, leading to increased SR Ca^{2+} leak.

6.4.4 TNF-α produces a temporary potentiation of systolic Ca^{2+} in the heart failure and recovery models – Could RyR sensitivity be increased?

Decreased SR Ca^{2+} content can be caused by SR Ca^{2+} leak as a result of increased RyR P_o (Belevych et al., 2007; Shannon et al., 2003). Of both the heart failure (Fig 6-8B) and recovery cells (Fig 6-8E), a proportion of cells presented with an immediate potentiation of systolic Ca^{2+}. This was accompanied by a single beat increase in sarcomere shortening (Fig 6-8C and 6-8D), indicating that this is a true phenomenon as opposed to a fluorescent artefact. Following this 1st beat potentiation of systolic Ca^{2+} in responder, a new lower Ca^{2+} transient amplitude steady state is reached. This produces a similar response to caffeine, known to potentiate RyR (Greensmith et al., 2014). This temporary potentiation is indicative of an increase in RyR P_o, suggesting that as with young control cells (chapter 4), RyR P_o is increased in heart failure and recovery cells in response to TNF-α.

In non-responders belonging to both the heart failure (Fig 6-9B) and recovery (Fig 6-9E) groups there was no 1st beat increase in systolic Ca^{2+} or sarcomere shortening. The depressant effect of TNF-α on Ca^{2+} amplitude may be more rapid in this subgroup.

As suggested in the young control animals, whilst the reduction in SR Ca^{2+} content can account for decreased systolic $[Ca^{2+}]_i$, an effect LTCC may also contribute, which may be more prominent in non-responders. In the heart failure and recovery models, the proportion of non-responders is far greater. In heart failure, RyR P_o would already be expected to be increased due to hyperphosphorylation, and I_{CaL} is known to decrease. The effect on TNF-α on further decreasing I_{CaL} may be greater than that on RyR P_o in these models. Prior hyperphosphorylation may have also saturated the effect on RyR P_o in some cells.

6.4.5 Does TNF-α alter the relationship between $[Ca^{2+}]_i$ and sarcomere length in the heart failure and recovery models?

In heart failure cells, TNF-α produced an irreversible decrease in Ca^{2+} transient amplitude by 21.08 ± 3.66 % (Fig 6-2A). Reduced systolic $[Ca^{2+}]_i$ would be expected to reduce the degree of

sarcomere shortening, as less Ca^{2+} is available to bind to myofilaments. With TNF-α, sarcomere shortening was unchanged (Fig 6-2B), despite the decrease in Ca^{2+} transient amplitude. This could indicate that in heart failure cells myofilament sensitivity to Ca^{2+} is increased with TNF-α. TNF-α also caused an irreversible decrease in both diastolic Ca^{2+} and resting sarcomere length by 3.19 ± 1.89 % and 0.8 ± 0.2 % respectively, in heart failure cells (Fig 6-2C and 6-2D). Once again, this could provide evidence that myofilament sensitivity to Ca^{2+} is increased. However, the effect on myofilament sensitivity could be an effect of heart failure as opposed to a result of TNF-α. Myofilament sensitivity to Ca^{2+} is already known to be increased at end-stage heart failure and may be a compensatory mechanism to help maintain cardiac output (van der Velden, 2011). In the model of heart failure used in this study, end-stage is the point at which the animals were sacrificed, thus myofilament sensitivity to Ca^{2+} may have be increased.

6.4.6 Is the magnitude of the effect of TNF-α different in heart failure and recovery?

Given that circulating TNF-α is elevated in heart failure and so it is assumed cells have been pre-exposed to TNF-α, this experiment aimed to determine whether cells from a model of heart failure had an altered response to TNF-α, and if this changed in that of a recovery model. If this was the case, this may suggest an increase or decrease in susceptibility of those with heart failure – or in recovery – to changes in cardiac function by TNF-α.

When comparing the responses of young control cells, heart failure model cells and recovery model cells to TNF-α, there no difference between the magnitude of change to diastolic and systolic Ca^{2+}, as well as that of the subsequent sarcomere shortening, with TNF-α (Fig 6-10) or washout (Fig 6-11). Nor was there a difference between the magnitude of decrease in SR Ca^{2+} content evoked by TNF-α, between the 3 models (Fig 6-12).

Although the magnitude of change to the overall rate of Ca^{2+} removal (k_{sys}) and rate of Ca^{2+} efflux (k_{caff}) – primarily via NCX – were not affected by TNF-α or washout, there was a

difference identified in k_{SERCA}, and thus change to SERCA activity, between the 3 models (Fig 6-13E and 6-13F).

Young sheep control cells treated with TNF-α did not have significantly altered k_{SERCA}, however k_{SERCA} at steady state in TNF-α was in between and not-significant from both control steady state and washout. In washout, k_{SERCA} did *significantly* increase by 91.67 ± 26.29 %, this could suggest that the effect on k_{SERCA} is gradual and that the method was not sensitive enough to detect any small increase in k_{SERCA} in TNF-α (Fig 3-6F). However, in both the heart failure (Fig 6-6E) and recovery (Fig 6-7E) models, neither TNF-α or washout produced a change in k_{SERCA}. As demonstrated in Fig 6-13E, k_{SERCA} is comparatively lower in both the heart failure and recovery models, when compared to the young control model. During TNF-α washout, k_{SERCA} remained significantly lower (Fig 6-13F) in cells from the recovery model.

Both CaMKII and PKA can modulate PLN through phosphorylation, this promotes PLN dissociation from SERCA, reversing its inhibitive effect on SERCA and increasing SERCA activity. This commonly occurs physiologically as part of a β-adrenergic response, although CaMKII and PKA activity can be raised in other circumstances also (Mattiazzi & Kranias, 2014). Effects resulting from phosphorylation tend to require several minutes before an effect is observed. As such – and considering the generally short cytokine exposure periods – the changes to $k_{SERCA,}$ and thus rate of Ca^{2+} uptake via SERCA, may have not become *statistically* evident until later, during the washout period.

In an ovine tachycardia induced heart failure model studied by Briston et al. (2011), isolated cells were less susceptible to changes evoked by a β-adrenergic response. In particular, it was found that phosphorylation of PLN was found to be reduced in the heart failure model. Any effect TNF-α, or rather washout, may be having on elevated $k_{SERCA,}$ is not found in either experimental model. This suggest that the effect of TNF-α on increased k_{SERCA} may be PKA or CaMKII mediated, further supporting why this is not found in heart failure.

Whilst there was no recorded difference between the magnitudes of 1^{st} beat increase in Ca^{2+} transient amplitude in the 3 models used (Fig 6-14A), potentiation was observed in a larger proportion of young control cells (71 %), when compared to that of heart failure cells (44 %)

and recovery cells (48 %). Fractional SR Ca^{2+} release is thought to be reduced in heart failure as a higher I_{CaL} is required to induce SR Ca^{2+} release (Phillips et al., 1998). Based on the previous experiments of this study (refer to chapter 4), TNF-α increases RyR P_o. If the RyR P_o in heart failure cells is lower than young control cells prior to TNF-α application, the increased RyR P_o with TNF-α may still be lower than that of young control cells. The threshold for potentiation of the Ca^{2+} transient would therefore be higher and fewer cells would be expected to reach it. It is unknown whether the RyR P_o would improve from heart failure in the recovery model, although the relative proportion of responders would indicate this not to be the case.

In summary, TNF-α decreases Ca^{2+} transient amplitude through a similar mechanism identified in young control cells (chapter 3); decreased SR Ca^{2+} content as a result of increased RyR P_o. The difference in the proportion of *responders* is lower in the heart failure and recovery models, which may be due to the reduction in RyR P_o found in heart failure. In the heart failure model, some of the effects on contractility appear to have been saturated, and thus cannot be depressed further with TNF-α. This may be due to the previous effects of elevated circulating TNF-α in heart failure. This saturation did not occur in recovery cells, suggesting that contractility was at least partially restored. There was some evidence of increased myofilament sensitivity in both models, however this may be produced by heart failure as opposed to TNF-α, especially given that TNF-α has been shown to reduce myofilament sensitivity in young control sheep. In addition, the small increase in SERCA activity observed with TNF-α washout in young control sheep appears to be mediated by phosphorylation of PLN, thus is not found in the other experimental models, as PLN phosphorylation is often decreased in heart failure, and doesn't appear to fully recover in the recovery model.

Chapter 7

General discussion

7.1 The effect of TNF-α and IL-1β on excitation-contraction coupling

7.1.1 The effect of TNF-α and IL-1β on global contractility

There is evidence that in models of bacteraemia – one cause of sepsis – there is a reduction in left ventricular contractile force generation of tension. This left ventricular dysfunction was found to be due to a circulating myocardial depressant substance, such as a cytokine (Gomez et al., 1990; Jha et al., 1993). The effect of TNF-α and IL-1β on contractility have been explored in isolated whole rat hearts, which were found to reduce cardiac contractility (Schulz et al., 1995). Even in isolated ventricular myocytes TNF-α has been associated with reduced cell shortening (Greensmith & Nirmalan, 2013).

In the young sheep used in this study, impaired contractility was also found with TNF-α, which reduced systolic sarcomere shortening by 20.31 ± 7.58 % (Fig 3-2B). Increased NO in response to TNF-α and IL-1β has been proposed as a mechanism for the reduction in contractility (Schulz et al., 1995). Unlike TNF-α, in young control sheep cells exposed to IL-1β there was no change to sarcomere shortening (Fig 3-4B), and as such IL-1β could not be directly associated with reduced contractility in sepsis.

TNF-α produced an irreversible decrease in resting sarcomere length by 0.46 ± 0.1 % in young control sheep (Fig 3-2D), this is surprising given that no diastolic dysfunction was observed by Greensmith and Nirmalan (2013) with TNF-α in rat myocytes, however this further highlights the importance of using a large mammal model. Duncan et al. (2010) also found no evidence of diastolic dysfunction with both TNF-α and IL-1β in rat ventricular myocytes. In sheep however, IL-1β irreversibly decreased resting sarcomere length by 0.76 ± 0.2 % (Fig 3-4D). In the case of both cytokines, these diastolic changes were small yet significant.

The rate of sarcomere shortening and relaxation was not altered by TNF-α or IL-1β in young control sheep. With IL-1β, this disagrees with the work of Radin et al. (2008) in rat ventricular myocytes, who found IL-1β reduced the rate of cell relaxation. Whilst redox signalling can promote PLN phosphorylation and thus increase the rate of Ca^{2+} removal and

thus relaxation (Ho et al., 2014), elevations in NO and ROS have also been associated with impaired relaxation in acute inflammation of the heart (Y. Li et al., 2013). The balance between NO and ROS production by these cytokines, and in these models, could determine the overall effect on rate of relaxation.

7.1.2 The effect of TNF-α and IL-1β on $[Ca^{2+}]_i$

Previous work by Greensmith and Nirmalan (2013) and Radin et al. (2008) has found that in rat ventricular myocytes, both TNF-α and IL-1β individually reduced systolic Ca^{2+}. This study found the same in sheep ventricular myocytes, with a 16.79 ± 3.16 % reduction in Ca^{2+} transient amplitude with TNF-α (Fig 3-2A) and a 23.63 ± 6.61 % decrease in Ca^{2+} transient amplitude with IL-1β (Fig 3-4A). While the decreased systolic Ca^{2+} with TNF-α can at least partially account for the reduced contraction, the decreased systolic Ca^{2+} with IL-1β cannot provide and explanation for why sarcomere shortening is unchanged, thus the mechanism of IL-1β may be more complex.

As with contractility, previous work in rat ventricular myocytes did not identify changes to diastolic $[Ca^{2+}]_i$ with TNF-α alone, or combined TNF-α and IL-1β treatment (Duncan et al., 2010; Greensmith & Nirmalan, 2013). This was also true for IL-1β, which did not alter diastolic Ca^{2+} in young control sheep (Fig 3-4C). TNF-α altered diastolic $[Ca^{2+}]_i$ in young control sheep, producing and irreversible decrease by 4.35 ± 1.67 % (Fig 3-2C).

7.1.3 The effect of TNF-α and IL-1β on SR Ca^{2+} content

Change to SR Ca^{2+} content can modulate systolic SR Ca^{2+} release and therefore alter Ca^{2+} transient amplitude at steady state, as not only does this affect the Ca^{2+} available for release, but also increased luminal $[Ca^{2+}]$ can elevate RyR P_o.

TNF-α decreased the caffeine evoked Ca^{2+} transient amplitude by 27.32 ± 3.41 % in young control cells (Fig 3-5C). This agrees with findings in rat ventricular myocytes, in which TNF-α

was also shown to decrease SR Ca^{2+} content (Greensmith & Nirmalan, 2013). Similarly, IL-1β also decreased the caffeine evoked Ca^{2+} transient amplitude by 41.39 ± 3.43 % (Fig 3-5D). All off the above effects were maintained in washout, thus the effect on SR Ca^{2+} content with both cytokines appears to be irreversible.

As calculated and discussed in sections 3.4.2 and 6.4.2, the cubic relationship between SR Ca^{2+} content and Ca^{2+} transient amplitude allowed prediction of the expected effect that the recorded change in SR Ca^{2+} content would have on systolic Ca^{2+} release, and thus Ca^{2+} transient amplitude. The change to SR Ca^{2+} content with both TNF-α and IL-1β could more than account for the decrease in Ca^{2+} transient amplitude. Given the large changes in caffeine-evoked Ca^{2+} transient amplitude, the expected reductions to systolic Ca^{2+}transient amplitude were actually greater than those achieved.

Caffeine was rapidly applied in order to indirectly measure SR Ca^{2+} content prior to and following treatment in all models used. Caffeine application increases RyR P_o in a Ca^{2+} independent manner. This RyR potentiation allows measurement of mass Ca^{2+} release from the SR, which is relative to SR Ca^{2+} content, although caffeine does not completely empty the SR. By using fluorescence to measure this Ca^{2+} release, only free cytoplasmic Ca^{2+} can bind to the fluorophores. Buffered Ca^{2+} is not detected. Furthermore, this sudden rise in $[Ca^{2+}]_i$ drives rapid Ca^{2+} extrusion, primarily via NCX, although PMCA may also contribute to a much smaller degree. This indirect method can therefore underestimate SR Ca^{2+} by approximately 25 %, and as a result SR Ca^{2+} content (J. W. Bassani, Bassani, & Bers, 1994). Furthermore, it does not take into account altered Ca^{2+} buffering. As use of the caffeine-evoked Ca^{2+} transient amplitude is more likely to underestimate SR Ca^{2+} content, the smaller than expected change to systolic Ca^{2+} transient amplitude could be due to underestimation of the Ca^{2+} release in systole, which would indicated Ca^{2+} buffering may be increased. Additionally, as contractile proteins within the myofilaments are also Ca^{2+} buffers, the decreased myofilament sensitivity to Ca^{2+} previously identified would be a mechanism for decreased Ca^{2+} buffering. Although Ca^{2+} buffering may be altered in response to both cytokines, the magnitude of the decrease to the caffeine-evoked Ca^{2+} transient amplitude is large. This indicates a true effect on SR Ca^{2+} content, as a change to Ca^{2+} buffering alone would not be able account fully for this change.

Patch clamping is another method which can more accurately determine SR Ca^{2+} content through measurement of the Ca^{2+} efflux following caffeine application. This method is not unaffected by Ca^{2+} buffering, due to its lack of sole reliance on Ca^{2+} inside the cell interacting with fluorophores. The resources and equipment required in order to patch clamp were unavailable, however use of fluorescent signals in response to caffeine application to estimate SR Ca^{2+} content is an accepted method in the field.

As both cytokines caused a reduction in SR Ca^{2+} content, this contradicts work of Jha et al. (1993), which recorded no change with septic serum. As the proportional concentrations of cytokines in this septic serum were unknown, the effect of other cytokines could have increased SR Ca^{2+} content, compensating for the decrease by TNF-α and IL-1β. Additionally, the activity of these cytokines when interacting with others is also unknown. This may also be the case in a study by Hobai, Edgecomb, LaBarge, and Colucci (2015), where no change in SR Ca^{2+} content was identified in rat ventricular myocytes treated with a mixture of LPS and multiple cytokines.

SR Ca^{2+} content is dependent on SR Ca^{2+} uptake by SERCA and Ca^{2+} release by RyR. Both TNF-α and IL-1β are known to promote ROS production (Brandes et al., 2014; X. Chen et al., 2008; Fauconnier et al., 2011; D. Yang et al., 2007) as well as reactive nitrogen species – such as NO – production (Evans et al., 1993; Finkel et al., 1992). This increase NO and redox signalling can in turn promote PKA activation (Beck et al., 2015; El-Ani et al., 2014).

ROS can decrease SR Ca^{2+} content (Ichinose et al., 2007) and NO can also contribute to decreased SR Ca^{2+} content through increasing RyR P_o, however the latter only occurs when PKA activation is low (Lim et al., 2008). With NO, the situation is more complex, as at high levels, NO can prevent further ROS production, leading to increased SR Ca^{2+} content (Ichinose et al., 2007).

The level of PKA activation can also determine the effect NO has on Ca^{2+} release, as PKA can also phosphorylate RyR, and at high levels of PKA activation, NO greatly reduces RyR P_o (Lim et al., 2008). PKA activation can also increase SERCA activity through phosphorylation of PLN (El-Ani et al., 2014).

The effect of increased ROS production on SR Ca^{2+} content must be greater than that of PKA activation for SR Ca^{2+} content to be reduced. Also, as the effect of ROS on RyR P_o is irreversible (Xu, Eu, Meissner, & Stamler, 1998), this mechanism could explain why the effect on SR Ca^{2+} content is maintained with washout. Although ROS activity is the most likely candidate, NO may also contribute to reduced SR Ca^{2+} content if PKA activation is low.

7.1.4 The effect of TNF-α and IL-1β on RyR P_o

Early and short-lived potentiation of systolic Ca^{2+} was observed in a proportion of cells isolated from young control sheep in response to both TNF-α and IL-1β, increasing by 57.75 ± 10.23 % and 51.72 ± 12.61 % respectively (Fig 3-8B and 3-8E). This was accompanied by a corresponding increase in sarcomere shortening (Fig 3-8C and 3-8F). While the magnitude of the increase in systolic Ca^{2+} was similar with both cytokines, this early potentiation was observed in a larger proportion of cells exposed to TNF-α (71 %), when compared to cells exposed to IL-1β (52 %). This may suggest that the effect of TNF-α on RyR P_o is more rapid.

This agrees with the findings of Greensmith and Nirmalan (2013) which acknowledged an early potentiation of the Ca^{2+} transient with 50 ng/ml TNF-α application in rat myocytes. This had not been further investigated in rat, however the simultaneous changes to Ca^{2+} and shortening in this study suggests that this is a true phenomenon, as opposed to a fluorescent artefact.

In non-responders, on average Ca^{2+} transient amplitude was either initially unaffected by cytokine application – in TNF-α treated cells (Fig 3-9B) – or immediately began to decrease; as with IL-1β treated cells (Fig 3-9E). This indicated that in this subgroup of cells the effect of both cytokines on decreased systolic Ca^{2+} was more rapid. This could also suggest that IL-1β has a more immediate effect on decreased systolic Ca^{2+}, whilst TNF-α has a more rapid, or possibly more potent effect on RyR.

TNF-α and IL-1β both decreased wave Ca^{2+} amplitude (Fig 4-3A and 4-5A), while simultaneously increasing wave frequency (Fig 4-3B and 4-5B) on a time-dependent basis.

This is indicative of reduced SR Ca^{2+} content threshold for waves and so increased RyR P_o. During wave experiments, ouabain and high $[Ca^{2+}]_o$ were used to artificially and perpetually increase SR Ca^{2+} to basal threshold SR Ca^{2+} content to produced waves. Under control conditions this produced waves at a frequency and amplitude that are proportional to rate Ca^{2+} entry and RyR P_o thence threshold SR Ca^{2+} content respectively (Diaz et al., 1997). This was then used to ascertain the effect of TNF-α and IL-1β wave dynamics; Ca^{2+} wave frequency and amplitude. Given the increase to frequency and decrease to amplitude, and that the rate of Ca^{2+} influx and SR Ca^{2+} uptake is presumably constant under these artificial conditions, any change to wave dynamics are as a result of change RyR P_o.

In the case of both cytokines, the data highly suggests RyR P_o is increased, as the SR Ca^{2+} threshold has clearly decreased. As demonstrated in figure 7-1, Ca^{2+} waves occur more frequently because at a constant rate of influx, threshold is reached more quickly, resulting in more waves occurring over the same period of time. As those waves occur at a lower SR Ca^{2+} content, the waves are smaller in amplitude (Bers, 1991).

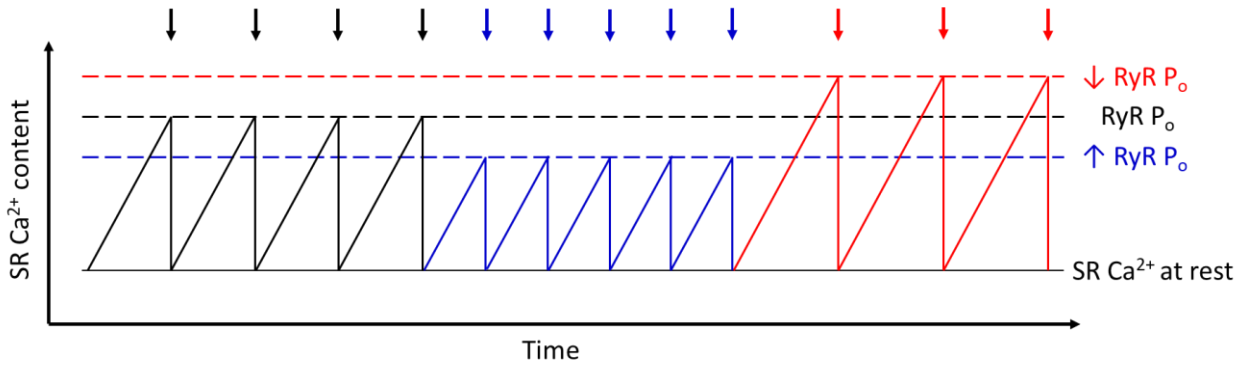

Figure 7-1. A diagram demonstrating the effect of increased [blue] and decreased [red] RyR P_o on the SR Ca^{2+} threshold for waves when Ca^{2+} influx and SR Ca^{2+} uptake are constant. Arrows above indicate the time points which a Ca^{2+} wave would be evoked.

Following 5 minutes cytokine treatment, wave frequency increased by 38.22 ± 8.11 % (Fig 3-3B) and amplitude decreased by 46.13 ± 5.75 % (Fig 3-3A) with TNF-α. IL-1β produced a 28.35 ± 11.35 % increase in wave frequency (Fig 3-5B) and 34.42 ± 6.82 % decrease in

amplitude (Fig 3-5A). This could indicate that the effect of TNF-α on RyR P_o is more rapid than IL-1β in young control cells, as the magnitude of change in both parameters is smaller with IL-1β over the same time period. In addition, significant changes to both parameters were observed at earlier time points with TNF-α. Comparisons in the degree of potency of these cytokines on RyR P_o must be interpreted with caution, as although the same concentration was used (50 ng/ml), the level of activity may differ.

The amplitude of caffeine-evoked SR Ca^{2+} release during the onset of a Ca^{2+} wave indicated the SR Ca^{2+} threshold at that point. After approximately 5 minutes exposure to TNF-α and IL-1β, the caffeine-evoked Ca^{2+} wave amplitude decreased by 49.16 % and 52.94 % respectively (Fig 4-6). This provides further supports that the SR threshold for waves is decreased with both cytokines. It is therefore possible to conclude that TNF-α and IL-1β increases RyR P_o and that this effect was time-dependent. This time-dependency of an effect on SR Ca^{2+} leak has also been identified in a CLP model of sepsis (X. Zhu et al., 2005).

Previous work in rat ventricular myocytes and mice atrial myocytes, identified a similar effect of TNF-α and IL-1β on increased frequency of spontaneous SR Ca^{2+} release events, such as Ca^{2+} sparks and waves, with prolonged exposure (2-3 hours) (Duncan et al., 2010; Zuo et al., 2018). While this study also indicates SR Ca^{2+} leak is increased via RyR in response to both cytokines, the early potentiation and cytokine exposure times used in these experiments – over minutes as opposed to hours – indicates an effect on RyR P_o may be more rapid than previously thought.

As previously discussed, both cytokines increase NO and ROS production. In myocardial dysfunction the levels of NO and ROS are imbalanced, and both are capable of interacting with the RyR (Hare & Stamler, 2005).

IL-1β is known to modulate contractility through activation of a myocardial L-arginine-NO pathway (Evans et al., 1993), while in isolated hamster muscular tissue TNF-a can also reversibly induce inotropy through increased NO (Finkel et al., 1992). Three forms of NO synthase which are found in cardiac myocytes are NOS1, NOS2 (iNOS) and NOS3 (eNOS) and both are responsible for production of the highly reactive free radical, NO (Hare & Stamler,

2005; Lim et al., 2008). Activation of NOS3 is more involved in physiological modulation of cardiac RyR, such as in response to stretch, aided by its proximity to LTCC (Hare & Stamler, 2005; Lim et al., 2008). NO derived from NOS2 is generally considered to be Ca^{2+}-independent as NOS2 is closely associated with high basal levels of Ca^{2+}/CaM, competitively inhibiting Ca^{2+} binding, unlike NOS1 and NOS3 (Hare & Stamler, 2005).

NO can directly modify cardiac RyR through *S*-nitrosylation, in which NO attaches covalently to reactive thiol residues, often within the amino acid cysteine (Hare & Stamler, 2005; Lim et al., 2008). RyR P_o increases with progressive *S*-nitrosylation of an increasing number of thiol sites on RyR, leading to increased Ca^{2+} spark frequency (Lim et al., 2008; Xu et al., 1998). ROS can also increase RyR P_o through oxidation of more than 7 thiols per RyR subunit (Xu et al., 1998). NO can also decrease RyR P_o when the level of PKA activation is high, however IL-1β mediated production of NO via NOS2 requires PKA activation (Lim et al., 2008; Oddis, Simmons, Hattler, & Finkel, 1996), therefore with IL-1β, when NO is high, so is PKA. This could explain why a lower proportion of cells presented with early potentiation of systolic Ca^{2+} than in TNF-α treated cells. A direct effect of elevated NO production may therefore not be the primary mechanism of the increased RyR P_o with IL-1β.

Another possible mechanism of RyR modulation is CaM mediated. The concentration of CaM can determine whether RyR is activated or inactivated (Sigalas et al., 2009), as can the binding affinity between CaM and RyR (Y. Yang et al., 2014). If 4 CaM bind to RyR this can greatly reduce cardiac RyR P_o through, inhibiting SR Ca^{2+} release (Balshaw et al., 2001). TNF-α is known to reduce the affinity of CaM binding to RyR, and as such increase RyR P_o (Balshaw et al., 2001; Y. Yang et al., 2014).

As previously mentioned, proinflammatory cytokines can activate ROS producing enzymes such as Nox (D. Yang et al., 2007). In addition to the direct effects of ROS on RyR, Nox is associated with redox signalling and can promote CaMKII oxidation (Ho et al., 2014). CaMKII oxidation contributes to increased phosphorylation of RyR. Previous work has implicated that IL-1β promotes CaMKII oxidation and thus phosphorylation of RyR (Monnerat et al., 2016). Although this phosphorylation of RyR by CaMKII would increase RyR P_o, it would cause only a brief increase in systolic Ca^{2+} (Eisner, George, Smith, Trafford, & Venetucci,

2010; Ho et al., 2014). This would mimic the 1st beat potentiation identified with both cytokines. That said, phosphorylation is slow when compared to redox signalling. Given that effect is rapid, as per the 1st beat potentiation of the Ca^{2+} transient, ROS or *S*-nitrosylation are more likely candidates for the early effects on RyR P_o. The elevation of ROS could contribute to CaMKII oxidation, and further elevation in RyR P_o, providing a possible mechanism for the time dependency of the cytokine's effects on RyR P_o.

7.1.5 The effect of TNF-α and IL-1β on I_{CaL}

Previous work has indicated that both TNF-α and IL-1β can produce small decreases in $I_{CaL.}$ at varying concentrations, although neither TNF-α or IL-1β alter LTCC expression (El Khoury et al., 2014). In rat myocytes exposed to a combination of LPS and various cytokines, including TNF and IL-1, Ca^{2+} influx via LTCC reduced by ~38 % (Hobai et al., 2015), although whether TNF and IL-1 were the active components on LTCC is unknown. Also, this effect could be greater than the individual effects of the cytokines, due to synergism. In rat ventricular myocytes, 50 ng/ml TNF-α reduced peak I_{CaL} by 11 % (Greensmith & Nirmalan, 2013), whilst in murine ventricular myocytes, the lower concentration of 30 pg/ml had no effect on I_{CaL} (El Khoury et al., 2014). In smooth muscle, the effect of TNF-α on reduced I_{CaL} was shown to be concentration dependent (Reyes-Garcia et al., 2016). 30 pg/ml IL-1β has also produced a 36 % reduced I_{CaL} by in murine ventricular myocytes (El Khoury et al., 2014).

While decreased I_{CaL} could theoretically contribute to reduction in Ca^{2+} transient amplitude, through decreasing CICR, the effects of these cytokines are fairly small. As the I_{CaL} and resultant Ca^{2+} influx are fundamentally similar in both rat (Greensmith & Nirmalan, 2013) and young sheep (Dibb et al., 2004), similar effects would be expected in sheep. In addition, the afore mentioned effects of these cytokines on SR Ca^{2+} content (section 7.1.3), are more likely to contribute to decreased Ca^{2+} transient amplitude.

7.1.6 The effect of TNF-α and IL-1β on SERCA activity

k_{SERCA} was unaffected by both TNF-α and IL-1β, thus indicating that SERCA activity was not altered by the presence of either cytokine. During washout, changes to k_{SERCA} were identified in the young control model only, with an increase of 91.67 ± 26.29 % in TNF-α treated cells (Fig 3-6F) and an increase of 78.26 ± 17.67 % in IL-1β treated cells (Fig 3-7F). The dynamics of this change with washout will be further discussed in section 7.2.3.

Modification to SERCA activity is regulated by PLN. When PLN is phosphorylated, SERCA activity and SR Ca^{2+} uptake are increased. Phosphorylation can take minutes before an effect is observed, and so it is possible that the effect recorded in washout may be the result of a prolonged effect of the cytokines and not a true effect of washout.

Elevated redox signaling via cytokine activated Nox stimulates CaMKII oxidation and CaMKII-mediated phosphorylation of PLN. TNF-α can also mediate increased PLN phosphorylation via PKA. Both mechanisms would increase SERCA activity (El-Ani et al., 2014; Ho et al., 2014).

If increased PLN phosphorylation were responsible for the effect on SERCA activity in response to both cytokines, the gradual change would only appear after several minutes; in washout, as found in these experiments. In addition, increased SERCA activity would not be expected to appear in the other experimental model as phosphorylation in heart failure is known to decrease (Briston et al., 2011; Lou et al., 2012; Phillips et al., 1998), this was also the case in the study (Fig 6-6E and 6-7E).

This data suggests that altered SERCA activity is not the cause for change in SR Ca^{2+} content produced cytokines, as even a gradual increase in SERCA activity would be expected to increase, not decrease SR Ca^{2+} uptake. This would also suggest that the effect on decreased SR Ca^{2+} content – most likely a result of increased SR Ca^{2+} leak via RyR, as previously discussed in section 7.1.4 – would be greater than the effect on SERCA activity and thus Ca^{2+} uptake.

7.1.7 The effect of TNF-α and IL-1β on sodium – calcium exchange

TNF-α had no effect on k_{caff} in cells isolated from young control sheep, and thus no effect on sarcolemmal Ca^{2+} efflux, in which NCX is the predominant method of Ca^{2+} removal. This method does not isolate Ca^{2+} removal via PMCA, however, the contribution of PMCA to Ca^{2+} removal in the heart is relatively small. Regardless, the collective pathways for Ca^{2+} extrusion appear to be unaffected by TNF-α. This supports the suggestion that TNF-α has no effect on the rate of Ca^{2+} removal by NCX.

Contrary to work by Radin et al. (2008) which suggested IL-1β reduced the rate of Ca^{2+} removal, this study found that in young sheep, IL-1β increased the overall rate of Ca^{2+} removal. With IL-1β, k_{sys} increased by 24.04 ± 6.5 %. Although the change to 90 - 10 % decay time of the Ca^{2+} transient with IL-1β was unchanged, this method of measurement may have not been sensitive enough to detect a small change. IL-1β increased k_{caff} by 29.47 ± 10.55 % (Fig 3-7E), indicating that IL-1β increased Ca^{2+} extrusion. The increase in the overall rate of Ca^{2+} removal is therefore most likely due to elevated NCX activity. This could provide a possible explanation for the small decrease in diastolic Ca^{2+} with IL-1β, as Ca^{2+} efflux would be more rapid, leading to lower $[Ca^{2+}]_i$.

7.1.8 The effect of TNF-α and IL-1β on myofilament sensitivity to Ca^{2+}

In the earlier experiments of chapter 3 there were indications that both TNF-α and IL-1β may have a positive effect on myofilament sensitivity to Ca^{2+}, due to the simultaneous changes in both diastolic Ca^{2+} and resting cell length with cytokine application. In the young control model, TNF-α produced an irreversible decrease in both diastolic Ca^{2+} and resting sarcomere length, and with IL-1β, diastolic Ca^{2+} was unaltered, while resting sarcomere length was irreversibly decreased. These diastolic changes while *significant*, were small, therefore use of them to infer the relationship between $[Ca^{2+}]_i$ and contractility must be interpreted with caution, especially as no diastolic dysfunction had been previously observed with TNF-α and IL-1β by Greensmith and Nirmalan (2013) and Duncan et al. (2010) in rat myocytes. These

changes did however give reason to investigate the effects of these cytokines on myofilament sensitivity to Ca^{2+} in young control sheep, through a more robust method.

Through measuring the degree of shortening in response to various elevations in $[Ca^{2+}]$ in permeabilised cells, the change in the relationship between $[Ca^{2+}]_i$ and contractility with TNF-α and IL-1β could be measured in a more robust way. The relationship between increased Ca^{2+} and reduced sarcomere length in permeabilised cells was blunted with both cytokines. This strongly suggests that both cytokines decreased myofilament sensitivity to Ca^{2+} (Fig 5-8). This agrees with the work of Goldhaber et al. (1996) which also identified that TNF-α reduced myofilament sensitivity to Ca^{2+} in rabbit cardiac myocytes. IL-1β also severely blunted the response of myofilaments to change in pH (Fig 5-9), suggesting that IL-1β may have saturated the effect on myofilament sensitivity to Ca^{2+}.

Both cytokines produced a depressed sarcomere shortening with increased $[Ca^{2+}]_i$ in permeabilised cells to a similar extent (Fig 5-8), suggesting they both have a similar degree of potency on myofilament sensitivity to Ca^{2+}. It is therefore possible that they may alter myofilament sensitive through the same or a similar mechanism. Goldhaber et al. (1996) has previously determined that the negative effect of TNF-α on myofilament sensitivity to Ca^{2+} was not primarily due to change to pH from TNF-α induced ROS production. Cytokine mediated elevation in NO and ROS production are a possible mechanism for decreased myofilament sensitivity to Ca^{2+} in acute myocardial inflammation (Y. Li et al., 2013). In a murine model of sepsis, *S*-nitrosylation of myofilament associated proteins by increased NO was associated with decreased myofilament sensitivity to Ca^{2+} leading to contractile dysfunction (Sips et al., 2013). Increased ROS production was also shown to decrease myofilament sensitivity to Ca^{2+} in a murine model of sepsis, however high NO levels can prevent the production of ROS through endotoxin-induced pathways (Ichinose et al., 2007), therefore NO has both a direct negative effect and indirect positive effect on myofilament sensitivity (Ichinose et al., 2007; Sips et al., 2013). *S*-nitrosylation through increased NO may not be the primary mechanism for the negative effect on myofilament sensitivity, as inhibition of NO production enzymes did not improve contractility in a rat model of endotoxemia. Another possible mechanism of decreased myofilament sensitivity is PKA-mediated phosphorylation of TnI (Tavernier et al., 2001). In both cardiac and non-cardiac

cells, cytokines – including TNF-α and IL-1β – have been shown to increase PKA activation, through NO and ROS signalling (Beck et al., 2015; El-Ani et al., 2014).

The negative effect on myofilament sensitivity appears to occur over a matter of minutes. In the experiments of chapter 5 changes to myofilament sensitivity were detected after more than 100 s exposure to the cytokines, and even then, the main differences were observed in 150 nM Ca^{2+}, after a further 100 s. PKA-mediated phosphorylation is therefore a possible mechanism for the decrease in myofilament sensitivity to Ca^{2+} with TNF-α and IL-1β. Elevated ROS production may also contribute to reduced myofilament sensitivity. While the reduction in contractility with TNF-α can be explained by the reduction in Ca^{2+} transient amplitude, both of these mechanisms could exacerbate myocardial depression.

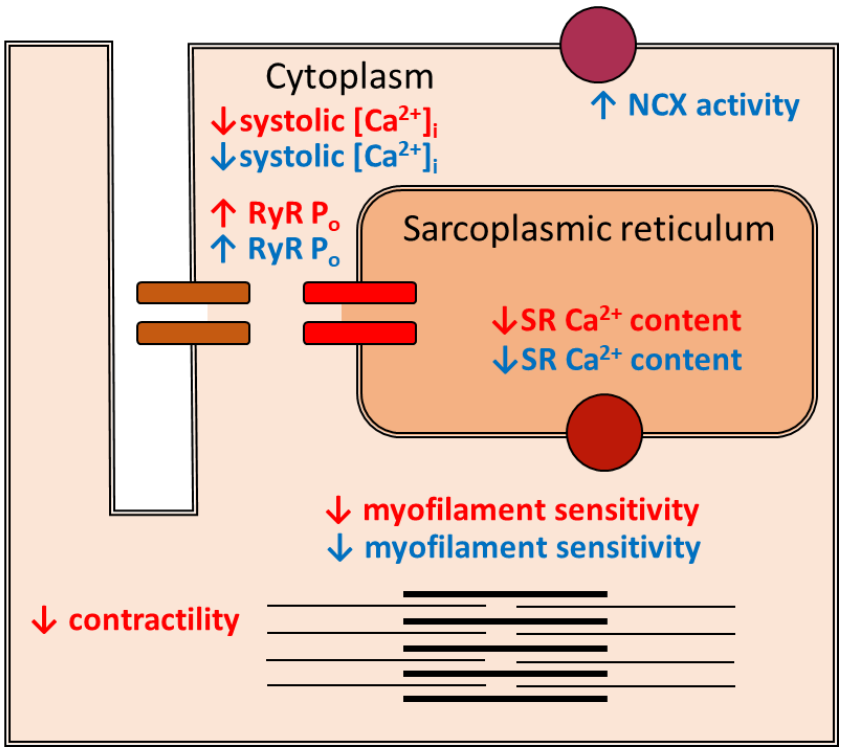

Figure 7-2. A diagram demonstrating the identified effects of 50 ng/ml TNF-α [red] and IL-1β [blue] on excitation-contraction coupling in left ventricular sheep myocytes. In the case of both cytokines increased RyR P_o provides a mechanism for the decrease in SR Ca^{2+} content, which leads to a reduction in systolic $[Ca^{2+}]_i$. Only with TNF-α did this reduced contractility. Both cytokines were shown to decrease myofilament sensitivity to Ca^{2+}.

7.2 Relative reversibility of TNF-α vs IL-1β

7.2.1 Intracellular Ca^{2+} and contractility

The effect of TNF-α on sarcomere shortening was completely reversed during washout, although systolic Ca^{2+} remained depleted. This suggests that the effect on contractility is readily reversible, however the effect on $[Ca^{2+}]_i$ is not. In IL-1β treated cells, no effect on contractility was found prior to washout, however as discussed in section 7.1.1, the 146.01 ± 59.32 % increase in sarcomere shortening recorded during washout (Fig 3-4B), may be a prolonged effect of IL-1β. If this is the case, the fact that the effect present during washout, implies that it is non-reversible. While both cytokines have non-reversible changes to $[Ca^{2+}]_i$, the effects of TNF-α on contractility appear to be more reality reversible that that of IL-1β.
With both TNF-α and IL-1β, any changes to rate of shortening and relaxation occurred during washout. During washout, the rate of sarcomere relaxation increased, as the 50 % decay time decreased by 18.92 ± 7.11 % (Fig 3-2F) and 50.46 ± 3.84 % (Fig 3-4F) in TNF-α and IL-1β respectively. During IL-1β washout, this was also accompanied by a decrease in the 50 % decay time of shortening by 28.54 ± 10.16 % (Fig 3-4E), suggesting that rate of shortening also increased. Once more, if these are prolonged effects of the cytokines, then they may be irreversible, or take longer to both appear and reverse than the time course of this study.

7.2.2 RyR P_o

As determined by the wave frequency and amplitude, the effects of both TNF-α (Fig 4-3) and IL-1β (Fig 4-5) on RyR P_o were non-reversible during the course of the experiment, no further effect on RyR P_o was observed. While the effect of TNF-α on the SR Ca^{2+} threshold was not reversible (Fig 4-6C), partial recovery of SR Ca^{2+} threshold was evident with washout in IL-1β treated cells. This was however not significant from both control and IL-1β (Fig 4-6D). What is certain is that the effect of IL-1β on SR Ca^{2+} threshold is not fully reversible during the 2 minute washout period. Further or complete recovery of SR Ca^{2+} threshold to control levels may have occurred over a longer washout in IL-1β treated cells.

The potential difference in reversibility of the effect on RyR P_o could be dependent on the mechanism by which it is altered. As the effect of ROS on RyR is irreversible (Xu et al., 1998), as were the effect of both cytokines on wave frequency and amplitude with washout (Fig 4-3 and 4-5), the early potentiation and more permanent effects could be attributed to direct ROS activity. RyR phosphorylation has also been suggested as a mechanism for altered RyR P_o. Phosphorylation is reversible, which could explain the partial recovery of the SR Ca^{2+} threshold with IL-1β washout (Fig 4-6).

7.2.3 Ca^{2+} removal

In IL-1β treated cells, k_{sys} increased by 80.54 ± 18.12 % greater than control during washout. This indicated an elevated rate of systolic Ca^{2+} removal with IL-1β washout, which was further confirmed by an 11.88 ± 9.41 % decrease in the 90 - 10 % decay time of the Ca^{2+} transient. As the increase in k_{SERCA} is only observed in washout – by 78.26 ± 17.67 % (Fig 3-7F) – NCX may be the predominant Ca^{2+} removal mechanism with IL-1β when overall Ca^{2+} removal is much lower. The increased involvement SERCA in Ca^{2+} removal may combine with the already established effect on increased NCX during washout, contributing to the greater overall rate of Ca^{2+} removal (Fig 3-7C).

TNF-α during washout k_{SERCA} increased by 91.67 ± 26.29 % (Fig 3-6F), as alluded to in section 7.1.6, this may also be a prolonged effect of the cytokine, due to the time required for phosphorylation to occur. This increase in SERCA activity did not, however, affect overall rate of Ca^{2+} removal, as k_{sys} was unaffected (Fig 3-6E). It appears that during washout rate of Ca^{2+} removal is more effected in IL-1β treated cells than those exposed to TNF-α.

With both cytokines, the increase in SERCA activity during washout had no effect on SR Ca^{2+} content and thus did not replenish SR Ca^{2+} content to control levels (Fig 3-5C and 3-5D). This may have been due to the maintained increase in RyR P_o with cytokine washout, having a greater effect on SR Ca^{2+} content than the effects on increased SR Ca^{2+} uptake.

7.2.4 Myofilament sensitivity to Ca^{2+}

The pH control experiment (Fig 5-9), gave some indication to the reversibility of the effects of TNF-α and IL-1β on myofilament sensitivity to Ca^{2+}, as cytokines were not present in the additional pH solutions, and therefore these solutions mimicked a washout protocol. Following this washout, the depressive effect of TNF-α on myofilament sensitivity to Ca^{2+} was restored to control-like levels (Fig 5-9). This could provide a mechanism for how contractility improves during washout despite the maintained decrease in Ca^{2+} transient amplitude (Fig 3-2A and 3-2B). With IL-1β, the blunted relationship between [Ca^{2+}] and shortening does not change during washout (Fig 5-9). Overall, this indicates that the effect of TNF-α on myofilament sensitivity to Ca^{2+} is more readily reversible than that of IL-1β.

7.3 The effect of TNF-α in heart failure and recovery

7.3.1 Does TNF-α alter ECC in models of heart failure and recovery?

In cells isolated from the recovery model, sarcomere shortening decreased by 12.6 ± 6.9 % (Fig 6-4B), however in cells isolated from the heart failure model, contractility was unaffected by TNF-α (Fig 6-2B). The altered contractility observed in the recovery model can be explained by the change in systolic Ca^{2+}, which decreased by 16.09 ± 3.87 % (Fig 6-4A). In the heart failure model, TNF-α also produced a decrease in Ca^{2+} transient amplitude, by 21.1 ± 3.66 % (Fig 6-2A), this can support that Ca^{2+} handling is impaired with TNF-α, but that systolic contractile function is not altered further. In both the heart failure and recovery models, the resting sarcomere length irreversibly decreased by 0.8 ± 0.2 % and 0.86 ± 0.2 % respectively with TNF-α (Fig 6-2D and 6-4D). This may be expected to contribute to further diastolic dysfunction in heart failure. TNF-α did not however alter the rate of sarcomere shortening and relaxation in both models.

In the heart failure model diastolic Ca^{2+} decreased by 3.19 ± 1.89 % but was not changed in the recovery model (Fig 6-2C and 6-4C). As k_{caff} was unaltered with TNF-α in either model (Fig 6-6E and 6-7E), this explains why diastolic Ca^{2+} is unaffected in the recover model but

not the decrease found in the heart failure model. This may indicate further dysfunction in the heart failure model with TNF-α.

In both the heart failure and recovery models, the caffeine evoked Ca^{2+} transient amplitude also decreased with TNF-α (Fig 6-5C and 6-5D). These changes produced by TNF-α to SR Ca^{2+} content in both models could more than account for decreased Ca^{2+} transient amplitudes. Whilst k_{SERCA} was unaffected by TNF-α in both models, and therefore a decreased rate of SR Ca^{2+} uptake is not responsible for the decrease in SR Ca^{2+} content.

Increased RyR P_o is a possible candidate for the mechanism behind decreased SR Ca^{2+} content. While this was not measured directly, the early potentiation of systolic Ca^{2+} identified in cells isolated from both experimental models (Fig 6-8B and 6-8E), provides evidence that RyR P_o may be increased. In TNF-α non-responders (Fig 6-9B and 6-9E), there was no immediate effect on Ca^{2+} transient amplitude, and so the effect on decreased systolic Ca^{2+} may have been predominant.

The experiments of chapter 6 also identified changes to diastolic function which could suggest myofilament sensitivity to Ca^{2+} was increased in the heart failure and recovery models with TNF-α. As in young control sheep, TNF-α was associated with a decrease in diastolic Ca^{2+} and resting sarcomere length. In the recovery model resting sarcomere length decreased with no change to diastolic Ca^{2+}. The magnitude of these changes was not different from those found in young control sheep, and thus these small changes must once again be taken with caution. Another aspect to consider is that both experimental models had at one point reached end-stage heart failure, in which myofilament sensitivity is already known to increase (van der Velden, 2011). Whether the effect on the relationship between diastolic Ca^{2+} and sarcomere length is due to TNF-α exposure or due solely to heart failure pathology is unknown. If the latter is the case, this could also suggest that the increased myofilament sensitivity to Ca^{2+} observed in end-stage heart failure remains following 5 weeks of recovery.

7.3.2 Does the magnitude of the effects of TNF-α differ in heart failure?

While contractility was unaffected by TNF-α in cells isolated from the heart failure model (Fig 6-2B), this was attributed to possible saturation of the effect on depressed contractility. The saturation of the effect on contractility was not observed in cells isolated from the recovery model, where sarcomere shortening decreased by a similar proportion to that of the young control model with TNF-α (Fig 6-4B and 6-10B).

The similar degrees of reduction to systolic Ca^{2+} in the experimental models and the young control sheep (Fig 6-10A) can be attributed to the similar magnitudes of decrease to the caffeine evoked Ca^{2+} transient amplitude (Fig 6-12). Although this suggests that the change to SR Ca^{2+} content produced by TNF-α did not alter between the models (Fig 6-12), RyR P_o may have been affected. The relative potency of TNF-α on RyR P_o between these models is fairly consistent, with 42.52 ± 12.34 % (Fig 6-8B) and 40.16 ± 9.81 % (Fig 6-8E) 1^{st} beat increases in Ca^{2+} transient amplitude in responders from the heart failure and recovery models respectively. The magnitude of these changes did not differ from those found in young control responders (Fig 6-14). Early potentiation of systolic Ca^{2+} was observed in 44.12 % of heart failure cells and 48 % of heart failure recovery cells exposed to TNF-α. This is a lower proportion than in young control cells (71 %), suggesting the effect of TNF-α on RyR P_o is far more rapid in young control sheep.

In section 7.1.4, it was suggested the RyR P_o could be altered by NO, ROS and phosphorylation. As RyR is already hyperphosphorylated in heart failure and the effects of further phosphorylation are minimal (Briston et al., 2011; Lou et al., 2012; Phillips et al., 1998), this could explain the small proportion of responders. Potentiation of systolic Ca^{2+} indicates that RyR P_o still occurs in heart failure with TNF-α. The mechanism behind this change could differ from the young control model. Y. Yang et al. (2014) found that in a rat heart failure model with high TNF-α levels the CaM–RyR binding affinity was decreased. This would increase RyR P_o. In the heart failure and recovery models, any change to RyR P_o could be contributed to or mediated by the altered affinity between CaM and RyR.

While k_{SERCA} did not differ significantly from control with TNF-α in all models (Fig 6-13E), there was a difference in k_{SERCA} between the 2 experimental models and control, but not between the heart failure and recovery models alone. This may suggest a subtle change in k_{SERCA} at TNF-α steady state that has not been detected in the young control model. This also provides further evidence that the 91.67 ± 0.26 % increase k_{SERCA} during TNF-α washout was not a true effect of washout, but rather a prolonged effect of cytokine exposure, as per section 7.1.6. k_{SERCA} was not altered by TNF-α or washout in either of the experimental models (Fig 6-6E and 6-7E). Overall, this suggests that SERCA activity gradually increases, initiated by TNF-α, in the young control model, and that due to the prolonged nature of this effect, this is identified in washout, but that in the heart failure and recovery models SERCA activity is unchanged. The mechanism behind the change in young control cells is likely mediated by PLN phosphorylation, inducing a slow increase in SERCA activity. The effect on SERCA may not be found in the heart failure cells as PLN phosphorylation is generally lower in heart failure (Briston et al., 2011; Lou et al., 2012; Phillips et al., 1998). This could also provide insight into the levels of PLN phosphorylation in the recovery model, which this lack of an effect on SERCA could suggest do not improve from heart failure with 5 weeks of recovery.

During TNF-α washout, the rate of sarcomere relaxation increases, as the 50 % decay time decreases by 18.92 ± 7.11 % (Fig 3-2F) and 10.06 ± 3.5 % (Fig 6-4F), in young control model and recovery model respectively. That of the heart failure model was not affected by washout (Fig 6-2F). Although overall Ca^{2+} removal (k_{sys}) was unchanged with TNF-α in all models tested, the previously discussed increase in SERCA activity (k_{SERCA}) may partially account for increased rate of relaxation in young control cells (Fig 3-6F). This could not account for improved relaxation in the recovery model. Phosphorylation of myofilament associated proteins could also alter rate of relaxation (Tavernier et al., 2001). If this is the mechanism of increased relaxation, the involvement of phosphorylation may support why this phenomenon is not found in the cells from the heart failure model. Improved rate of sarcomere relaxation could therefore be a compensatory mechanism in young control cells, which is lost in the heart failure model, but restored with 5 weeks recovery.

7.4 Clinical implications in sepsis

7.4.1 Do the effects of TNF-α and IL-1β provide a cellular basis for myocardial depression?

As discussed in sections 1.1.5 and 1.1.6, myocardial depression is a leading cause of death in sepsis. In myocardial depression, left ventricular contractility is reduced contributing to a reduction in LVEF by ~75 % and cardiac output. Ventricular dilation and loss of compliance are also present in myocardial depression; this along with increased end-diastolic volume can be compensatory mechanisms to help restore cardiac output (Ognibene et al., 1988; Parker et al., 1984; Parrillo, 1989).

With both TNF-α and IL-1β, systolic Ca^{2+} was reduced, providing further evidence of impaired Ca^{2+} handling in myocardial depression. In response to both cytokines, this decrease in systolic Ca^{2+} was mediated by reduced SR Ca^{2+} content due to elevated SR Ca^{2+} leak via RyR. Increased RyR P_o could provide a mechanism for the increased SR Ca^{2+} leak found in a CLP model of sepsis (X. Zhu et al., 2005).

The reduction in systolic Ca^{2+} produced by TNF-α, contributed to a 20.31 ± 7.58 % decrease in sarcomere shortening (Fig 3-2B); TNF-α could therefore provide a cellular basis for systolic dysfunction and may contribute in part to reduced left ventricular contractility in myocardial depression and other inflammatory conditions of the heart. Unlike TNF-α, IL-1β had no effect on sarcomere shortening (Fig 3-4B). As such, IL-1β cannot provide a cellular basis for loss of contractility and the resulting decrease in LVEF in sepsis but may contribute to diastolic dysfunction instead.

Both cytokines produced a small decrease in resting sarcomere length (Fig 3-2D and 3-4D), despite a decrease or lack of change to diastolic Ca^{2+} (Fig 3-2C and 3-4C). This shortened resting sarcomere length could provide a cellular basis for loss of compliance in myocardial depression, as these TNF-α and IL-1β treated myocytes show an inability to distend during diastole. This may also contribute to ventricle dilation, as the shorter resting sarcomere length would be expected to reduce the chamber size.

7.4.2 Restored function in survivors of sepsis

In survivors of sepsis, cardiac function is restored and thus symptoms of myocardial depression disappear. As discussed in section 1.1.6.2, a common LVEF is restored to 50 % during recovery from sepsis and full cardiac function is recovered following 10 – 28 days in survivors (Ognibene et al., 1988; Parker et al., 1984; Parrillo, 1989). Both cytokines could provide a mechanism for improved contractility in those recovering from myocardial depression, and thus at least partially restored LVEF. The TNF-α produced decrease in sarcomere shortening returned to control levels with washout in young control (Fig 3-2B), and although IL-1β did not affect shortening, sarcomere shortening increased with washout (Fig 3-4B). In patients with myocardial depression in sepsis, symptoms of myocardial depression are reversible over a number of days, whereas these effects took only minutes to take place. The washout phase of experiments in this study used solutions containing no cytokines, in physiological conditions the time taken for serum cytokine concentrations to drop may be much slower.

Even though resting sarcomere length remained decreased with cytokine washout, suggesting that some loss of compliance is still present, there is some evidence suggesting compliance may be beginning to improve with washout. In both TNF-α and IL-1β treated cells the rate of sarcomere relaxation increased during washout, with IL-1β the rate of both sarcomere shortening was also elevated. Improved relaxation would allow sarcomeres to distend more easily and aid both compliance and recovery from ventricular dilation. Improvements to diastolic function, such as increased compliance, may take longer to be restored than that of systolic function. In cells from the heart failure, rate of sarcomere relaxation did not increase with TNF-α washout. Recovery to this aspect of myocardial depression may not be as rapid or occur at all in heart failure patients.

7.4.3 Is there a cellular basis for the increased incidence of arrhythmias in sepsis

In early sepsis the likelihood of both atrial and ventricular arrhythmias increases especially in patients with low phosphate levels. The prevalence of ventricular fibrillation is also

particularly high in severe sepsis cases. This occurrence of arrhythmia in sepsis is indicative of high mortality (Schwartz et al., 2002; Shahreyar et al., 2018).

In chapter 4, the data suggests that TNF-α and IL-1β increase RyR P_o and this could account for negative inotropy. Increased RyR P_o is also pro-arrhythmogenic, however this requires a simultaneous increase of SR Ca^{2+} content (Venetucci et al., 2007). In other words, for arrhythmic evoking spontaneous Ca^{2+} release, though increasing RyR P_o may reduce the threshold for waves, that threshold must be met. Although TNF-α and IL-1β increased RyR P_o, both also reduced SR Ca^{2+} (Fig 3-5), the combined effect of which would be negatively arrhythmic.

Modulation of SERCA activity and RyR P_o can be mediated by phosphorylation, this is often associated with β-adrenergic stimulation. P_i can inhibit SERCA activity and increase SR Ca^{2+} leak from RyR (Smith, Duncan, Neary, Bruce, & Burton, 2000). Although this would be expected to lower the SR threshold for waves, the SR Ca^{2+} content would also be reduced beyond this point. If P_i is low, as with the patients with sepsis who have been identified as more prone to development of arrhythmia (Schwartz et al., 2002), this would promote SR Ca^{2+} uptake through PLN phosphorylation and decrease RyR P_o (Smith et al., 2000). Alone, the effects of low P_i would not induce waves, but would increase SR Ca^{2+} content. Given that both TNF-α and IL-1β increased RyR P_o, this would lower the threshold for waves, when combined with the increase in SR Ca^{2+} content, this would produce Ca^{2+} waves, providing a mechanism for arrhythmia is sepsis. *In vivo*, the effect on RyR P_o may become very important, as this *will* reduce the SR threshold for Ca^{2+} waves, however other factors could influence SR Ca^{2+} content. Spontaneous Ca^{2+} release would occur if the effect on RyR P_o is greater than that on depleted SR Ca^{2+} content. In addition, the situation is more complex in patients, as low phosphate or β-adrenergic stimulation would increase SR Ca^{2+} content. The combined effects of increased SR Ca^{2+} content and decreased threshold, lead to a much higher chance of arrhythmia. The effects of TNF-α on the dynamics of spontaneous Ca^{2+} release events is similar in atrial myocytes, and as such may also help explain the occurrence of atrial arrhythmias in sepsis (Zuo et al., 2018).

In the paced experiments of this study there was no evidence of arrhythmia, however no β-adrenergic substrates were applied to drive phosphorylation. As demonstrated with caffeine, which is also known to increase RyR P_o, spontaneous Ca^{2+} waves did not occur in the absence of β-adrenergic stimulation (Venetucci et al., 2007).

7.5 The cellular role of cytokines in clinical heart failure

As those with heart failure have pre-existing cardiac dysfunction and are likely to have had prior exposure to high levels of TNF-α, it was supposed that the effect of TNF-α may have different effects on ECC or alter the magnitude of these changes. One hypothesis was that some of the effects of TNF-α on ECC may be saturated in these experimental models.

Both CaMKII expression and ROS production are high in heart failure (Wagner et al., 2011). These were some of the common suggested mechanisms of cytokine mediated alteration for ECC, as such the effect on ECC may be expected to be greater in heart failure. That said, the elevation in both CaMKII and ROS in heart failure, may be greater than in healthy individuals, but equivalent to in those with sepsis. This may be the case as the magnitude of change produced by TNF-α was not different for the majority of parameters – including both diastolic and systolic Ca^{2+} – in the heart failure and recovery model. This suggested that the effects of TNF-α are not saturated in the heart failure or recover models, nor are they amplified. This indicates that even if cytokines were previously elevated in the heart failure model, Ca^{2+} handling can still be altered by subsequent exposure to TNF-α. There are however some small differences, which could alter the clinical response to elevated TNF-α in heart failure patients or those in recovery.

Diastolic Ca^{2+} is already decreased in heart failure, however this did not alter the magnitude of change to diastolic Ca^{2+} in the heart failure model, which irreversibly decreased by 3.19 ± 1.89 % with TNF-α (Fig 6-2C). In the cells from the recovery model, while washout produced a 1.42 ± 2.09 % decrease in diastolic Ca^{2+}, diastolic Ca^{2+} was unchanged by TNF-α itself (Fig 6-4C). This was unlike both control and heart failure cells, perhaps then given the previously

decreased diastolic Ca^{2+} in heart failure, the recovery model is less susceptible to changes alteration of diastolic Ca^{2+}.

In the young control cell, the depression of sarcomere shortening with TNF-α was restored to previous control levels washout, however in the cells from the recovery model, the 12.6 ± 6.9 % decrease with TNF-α was maintained (Fig 6-4B). The restored contractile function found in survivors of sepsis, following myocardial depression, therefore may not be found in patients in recovery from heart failure. Sarcomere shortening was unaffected by TNF-α application or washout in cells from the heart failure model (Fig 6-2D), despite the decrease in Ca^{2+} transient amplitude. It is proposed that the effect on sarcomere shortening has been saturated by previous exposure to TNF-α. Heart failure patients may be less susceptible to depressive effects of TNF-α upon re-exposure, but also show no sign of improved contractility with washout. Those with heart failure or in recovery would therefore be more susceptible to prolonged contractile dysfunction if they were to succumb to sepsis and the associated myocardial depression.

7.6 Implications for therapeutic approaches

One possible therapeutic approach when treating myocardial depression is to combat the cytokine evoked changes in ECC directly through administration of antibodies. As explained in section 1.3, TNF-α and IL-1β can bind to multiple receptors specifically, each producing different effects. For instance, TNF-α can bind to TNFR1, promoting cardiac remodelling, or bind to TNFR2, encouraging recovery and preventing damage which could further impair cardiac function. Similarly, IL-1β can self-regulate its own production and activity through binding to IL-1RII or IL-1RI (Idriss & Naismith, 2000; Kelly et al., 2010; Monden et al., 2007; Oppenheim et al., 1989; Subramaniam et al., 2004). There is some evidence that this course of treatment can improve ventricular function in severe sepsis, such as work by Vincent et al. (1992), who administered antibodies against TNF-α. One issue with this method is that in inhibiting the cytokines themselves, not only are the negative, cardiac remodelling pathways inhibited, but also those pathways which can prevent further cardiac dysfunction and those which aid the immune response against the pathogen causing sepsis.

Alternative therapeutic approaches involve prevention of the increased NO and ROS levels produced by these cytokines. It is thought that use of anti-oxidants and NOS inhibitors may aid treatment of sepsis and other inflammatory conditions, through preventing the direct effects of both NO and ROS, as well as indirect effects mediated by CaMKII and PKA activity (Beck et al., 2015).

Petros et al. (1994) used NG monomethyl-L-arginine – an NOS inhibitor – to treat hypotension in sepsis. While this course of treatment did have positive effects on cardiovascular function, such as elevated blood pressure, it also led to a further decrease in cardiac output. Whilst elevations in NO production with these cytokines may contribute myocardial depression, NO activity can be dependent on other components, such as PKA. In some cases, the effects of high NO may promote maintenance of cardiac output, thus inhibition of NOS may not always be beneficial.

Antioxidant supplementation has also been explored as a treatment to the negative effects of inflammation in sepsis and trauma conditions (Berger & Chiolero, 2007; Galley, Howdle, Walker, & Webster, 1997; Marik, Khangoora, Rivera, Hooper, & Catravas, 2017). Antioxidants prevent further ROS production and are often found naturally in serum of healthy individuals. Examples of antioxidants include N-acetyl-L-cysteine (NAC), selenium and various vitamins, including vitamin C (ascorbic acid). Of these, basal levels of both selenium and vitamin C are depressed in sepsis, so supplementation may be beneficial (Berger & Chiolero, 2007; Galley et al., 1997). Although NAC has not produced desired results in clinical trials alone, when combined treatment with selenium and vitamins, this was capable of preventing organ failure, improving both mortality and clinical outcome (Berger & Chiolero, 2007).

Vitamin C treatment also has also been effective at reducing the risk of multiple organ failure and improved cardiovascular function. While antioxidant treatment such as this can prevent further oxidation by ROS, it cannot affect oxidation which had already occurred (Galley et al., 1997; Marik et al., 2017). Early administration of antioxidants, as a preventive treatment in sepsis, may be able to perturb the myocardial depressant effects of both direct ROS activity and downstream effects like CaMKII oxidation. This would also not affect other signalling

carried out by the cytokine, which may be beneficial to recovery from both the infection and myocardial depression.

7.7 Limitations

Although all the methods used in this study allowed the individual effects of TNF-α and IL-1β to be categorised in a robust way, it would have been possible to gain some further insight into possible effects on I_{CaL} and NCX activity through use of patch clamping. This would also improve measurements of SR Ca^{2+} content, as it would not be influenced by Ca^{2+} buffering. However, the recorded changes to SR Ca^{2+} content in this study were considerable; as such any influence from Ca^{2+} buffering may be negligible. Unfortunately, the equipment required to patch clamp was not available.

7.8 Future work

This study characterised the individual effects of TNF-α and IL-1β on ECC, including the effects on RyR P_o and myofilament sensitivity to Ca^{2+}. The effects of these cytokines on RyR P_o, and so spontaneous SR Ca^{2+} release, can be investigated further through measurement of Ca^{2+} sparks using confocal microscopy. This could support the finding of this study, whilst also determining the magnitude of the effect on RyR P_o.

Future work will also investigate the mechanisms behind the identified effects on ECC. As previously discussed, the effects of these cytokines may be mediated by elevated ROS or NO production. Studies will be carried out to determine the magnitude of ROS and NO production in response to 50 ng/ml of each cytokine. This will support whether the concentrations of ROS and NO produced can contribute to the effects seen. On-going work within the laboratory group is being carried out to study whether the individual effects of TNF-α on myocytes can be limited through treatment with the known ROS inhibitor, NAC. Current results indicate that NAC may attenuate the effect of TNF-α on decreased cell

viability. Future work will explore whether this is also true for changes to Ca^{2+} handling and contractile function.

Previous studies have indicated that the effects of cytokines of myocardial contractility are dose dependent. Another next step would be to determine whether the same effects occur with TNF-α and IL-1β at clinical concentrations, and to what extent. The effects on ECC of other proinflammatory cytokines elevated in sepsis and other inflammatory conditions could also be characterised.

7.9 Summary

50 ng/ml TNF-α and IL-1β perturbed Ca^{2+} handing in sheep left ventricular myocytes. Both cytokines increased RyR P_o, which may provide a mechanism for the decreased SR Ca^{2+} content and systolic Ca^{2+} also identified. TNF-α produced a decrease in contractility, these changes may account for systolic dysfunction in myocardial depression, such as reduced ventricular contractility. Whilst IL-1β did not cause loss of contractility, there was some evidence of diastolic dysfunction with both cytokines, such as reduced resting sarcomere length; and reduced diastolic Ca^{2+} with TNF-α. This diastolic dysfunction has not been identified in many previous studies in small mammal models and could potentially contribute to diastolic dysfunction in myocardial depression, such as reduced compliance and ventricular dilation.

Both TNF-α and IL-1β decreased myofilament sensitivity to Ca^{2+}. This may have contributed to the reduced contractility in TNF-α treated cells, and may account for the muted response to changes in $[Ca^{2+}]_i$. Although many aspects of Ca^{2+} handling were not restored, with washout both cytokines either restored or increased contractility. This could explain the recovery of contractile function in survivors of sepsis and myocardial depression.

In work investigating the effect of TNF-α on cells isolated from models of heart failure and 5 week recovery, TNF-α was able to produce a similar effect on ECC. There was however some evidence indicating that the effect on contractility had already been saturated in the heart

failure model. The restored or improved contractility found in the young control models was also not replicated in either experimental model.

Chapter 8

Bibliography

Abernethy, A., Raza, S., Sun, J. L., Anstrom, K. J., Tracy, R., Steiner, J., . . . LeWinter, M. M. (2018). Pro-Inflammatory Biomarkers in Stable Versus Acutely Decompensated Heart Failure With Preserved Ejection Fraction. *J Am Heart Assoc, 7*(8). doi:10.1161/JAHA.117.007385

Acosta, C. D., Bhattacharya, S., Tuffnell, D., Kurinczuk, J. J., & Knight, M. (2012). Maternal sepsis: a Scottish population-based case-control study. *BJOG, 119*(4), 474-483. doi:10.1111/j.1471-0528.2011.03239.x

Acosta, C. D., Harrison, D. A., Rowan, K., Lucas, D. N., Kurinczuk, J. J., & Knight, M. (2016). Maternal morbidity and mortality from severe sepsis: a national cohort study. *BMJ Open, 6*(8), e012323. doi:10.1136/bmjopen-2016-012323

Agharazii, M., St-Louis, R., Gautier-Bastien, A., Ung, R. V., Mokas, S., Lariviere, R., & Richard, D. E. (2015). Inflammatory cytokines and reactive oxygen species as mediators of chronic kidney disease-related vascular calcification. *Am J Hypertens, 28*(6), 746-755. doi:10.1093/ajh/hpu225

Alkar, B. S., Mattsson, G., & Magnusson, P. (2018). Ischemic Cardiomyopathy: Contemporary Clinical Management. In A. Tsipis (Ed.), Current Perspectives on Cardiomyopathies. doi:10.5772/intechopen.76723

Amadou, A., Nawrocki, A., Best-Belpomme, M., Pavoine, C., & Pecker, F. (2002). Arachidonic acid mediates dual effect of TNF-alpha on Ca2+ transients and contraction of adult rat cardiomyocytes. *Am J Physiol Cell Physiol, 282*(6), C1339-1347. doi:10.1152/ajpcell.00471.2001

Archer, L. T., & Black, M. R. (1975). Myocardial failure with altered response to adrenaline in endotoxin shock. *Br J Pharmacol, 54*(2), 145-155.

Aukrust, P., Ueland, T., Lien, E., Bendtzen, K., Muller, F., Andreassen, A. K., . . . Gullestad, L. (1999). Cytokine network in congestive heart failure secondary to ischemic or idiopathic dilated cardiomyopathy. *Am J Cardiol, 83*(3), 376-382.

Baicu, S. C., & Taylor, M. J. (2002). Acid-base buffering in organ preservation solutions as a function of temperature: new parameters for comparing buffer capacity and efficiency. *Cryobiology, 45*(1), 33-48.

Balshaw, D. M., Xu, L., Yamaguchi, N., Pasek, D. A., & Meissner, G. (2001). Calmodulin binding and inhibition of cardiac muscle calcium release channel (ryanodine receptor). *J Biol Chem, 276*(23), 20144-20153. doi:10.1074/jbc.M010771200

Bassani, J. W., Bassani, R. A., & Bers, D. M. (1994). Relaxation in rabbit and rat cardiac cells: species-dependent differences in cellular mechanisms. *J Physiol, 476*(2), 279-293.

Bassani, J. W., Yuan, W., & Bers, D. M. (1995). Fractional SR Ca release is regulated by trigger Ca and SR Ca content in cardiac myocytes. *Am J Physiol, 268*(5 Pt 1), C1313-1319.

Bassani, R. A., Bassani, J. W., & Bers, D. M. (1992). Mitochondrial and sarcolemmal Ca2+ transport reduce [Ca2+]i during caffeine contractures in rabbit cardiac myocytes. *J Physiol, 453*, 591-608.

Bassani, R. A., & Bers, D. M. (1995). Rate of diastolic Ca release from the sarcoplasmic reticulum of intact rabbit and rat ventricular myocytes. *Biophys J, 68*(5), 2015-2022. doi:10.1016/S0006-3495(95)80378-4

Bean, B. P. (1989). Classes of calcium channels in vertebrate cells. *Annu Rev Physiol, 51*, 367-384. doi:10.1146/annurev.ph.51.030189.002055

Beck, K. F., Euler, J., Eisel, F., Beck, M., Kohler, Y., Sha, L. K., . . . Pfeilschifter, J. (2015). Cytokines induce protein kinase A-mediated signalling by a redox-dependent mechanism in rat renal mesangial cells. *Biochem Pharmacol, 93*(3), 362-369. doi:10.1016/j.bcp.2014.11.009

Belevych, A., Kubalova, Z., Terentyev, D., Hamlin, R. L., Carnes, C. A., & Gyorke, S. (2007). Enhanced ryanodine receptor-mediated calcium leak determines reduced sarcoplasmic reticulum calcium content in chronic canine heart failure. *Biophys J, 93*(11), 4083-4092. doi:10.1529/biophysj.107.114546

Berger, M. M., & Chiolero, R. L. (2007). Antioxidant supplementation in sepsis and systemic inflammatory response syndrome. *Crit Care Med, 35*(9 Suppl), S584-590. doi:10.1097/01.CCM.0000279189.81529.C4

Bers, D. M. (1991). *Excitation-contraction coupling and cardiac contractile force*. Dordrecht ; Boston: Kluwer.
Bers, D. M. (2000). Calcium fluxes involved in control of cardiac myocyte contraction. *Circ Res, 87*(4), 275-281.
Bers, D. M. (2002). Cardiac excitation-contraction coupling. *Nature, 415*(6868), 198-205. doi:10.1038/415198a
Betzenhauser, M. J., & Marks, A. R. (2010). Ryanodine receptor channelopathies. *Pflugers Arch, 460*(2), 467-480. doi:10.1007/s00424-010-0794-4
Biesmans, L., Macquaide, N., Heinzel, F. R., Bito, V., Smith, G. L., & Sipido, K. R. (2011). Subcellular heterogeneity of ryanodine receptor properties in ventricular myocytes with low T-tubule density. *PLoS One, 6*(10), e25100. doi:10.1371/journal.pone.0025100
Blake, P., Hasegawa, Y., Khosla, M. C., Fouad-Tarazi, F., Sakura, N., & Paganini, E. P. (1996). Isolation of "myocardial depressant factor(s)" from the ultrafiltrate of heart failure patients with acute renal failure. *ASAIO J, 42*(5), M911-915.
Blanco, G., & Mercer, R. W. (1998). Isozymes of the Na-K-ATPase: heterogeneity in structure, diversity in function. *Am J Physiol, 275*(5), F633-650. doi:10.1152/ajprenal.1998.275.5.F633
Blayney, L., Beck, K., MacDonald, E., D'Cruz, L., Nomikos, M., Griffiths, J., . . . Lai, F. A. (2013). ATP interacts with the CPVT mutation-associated central domain of the cardiac ryanodine receptor. *Biochim Biophys Acta, 1830*(10), 4426-4432. doi:10.1016/j.bbagen.2013.05.038
Bloom, M. W., Greenberg, B., Jaarsma, T., Januzzi, J. L., Lam, C. S. P., Maggioni, A. P., . . . Butler, J. (2017). Heart failure with reduced ejection fraction. *Nat Rev Dis Primers, 3*, 17058. doi:10.1038/nrdp.2017.58
Blum, A., & Miller, H. (2001). Pathophysiological role of cytokines in congestive heart failure. *Annu Rev Med, 52*, 15-27. doi:10.1146/annurev.med.52.1.15
Bode, E. F., Briston, S. J., Overend, C. L., O'Neill, S. C., Trafford, A. W., & Eisner, D. A. (2011). Changes of SERCA activity have only modest effects on sarcoplasmic reticulum Ca2+ content in rat ventricular myocytes. *J Physiol, 589*(Pt 19), 4723-4729. doi:10.1113/jphysiol.2011.211052
Bone, R. C., Balk, R. A., Cerra, F. B., Dellinger, R. P., Fein, A. M., Knaus, W. A., . . . Sibbald, W. J. (1992). Definitions for sepsis and organ failure and guidelines for the use of innovative therapies in sepsis. The ACCP/SCCM Consensus Conference Committee. American College of Chest Physicians/Society of Critical Care Medicine. *Chest, 101*(6), 1644-1655.
Boomer, J. S., To, K., Chang, K. C., Takasu, O., Osborne, D. F., Walton, A. H., . . . Hotchkiss, R. S. (2011). Immunosuppression in patients who die of sepsis and multiple organ failure. *JAMA, 306*(23), 2594-2605. doi:10.1001/jama.2011.1829
Borlaug, B. A., & Paulus, W. J. (2011). Heart failure with preserved ejection fraction: pathophysiology, diagnosis, and treatment. *Eur Heart J, 32*(6), 670-679. doi:10.1093/eurheartj/ehq426
Bossen, E. H., Sommer, J. R., & Waugh, R. A. (1981). Comparative stereology of mouse atria. *Tissue Cell, 13*(1), 71-77.
Bougle, A., & Duranteau, J. (2011). Pathophysiology of sepsis-induced acute kidney injury: the role of global renal blood flow and renal vascular resistance. *Contrib Nephrol, 174*, 89-97. doi:10.1159/000329243
Bouhemad, B., Nicolas-Robin, A., Arbelot, C., Arthaud, M., Feger, F., & Rouby, J. J. (2008). Isolated and reversible impairment of ventricular relaxation in patients with septic shock. *Crit Care Med, 36*(3), 766-774. doi:10.1097/CCM.0B013E31816596BC
Bovo, E., Mazurek, S. R., Blatter, L. A., & Zima, A. V. (2011). Regulation of sarcoplasmic reticulum Ca(2)(+) leak by cytosolic Ca(2)(+) in rabbit ventricular myocytes. *J Physiol, 589*(Pt 24), 6039-6050. doi:10.1113/jphysiol.2011.214171
Brady, A. J. (1991). Length dependence of passive stiffness in single cardiac myocytes. *Am J Physiol, 260*(4 Pt 2), H1062-1071. doi:10.1152/ajpheart.1991.260.4.H1062

Brandes, R. P., Weissmann, N., & Schroder, K. (2014). Nox family NADPH oxidases: Molecular mechanisms of activation. *Free Radic Biol Med, 76*, 208-226. doi:10.1016/j.freeradbiomed.2014.07.046

Brini, M., & Carafoli, E. (2011). The plasma membrane Ca(2)+ ATPase and the plasma membrane sodium calcium exchanger cooperate in the regulation of cell calcium. *Cold Spring Harb Perspect Biol, 3*(2). doi:10.1101/cshperspect.a004168

Briston, S. J., Caldwell, J. L., Horn, M. A., Clarke, J. D., Richards, M. A., Greensmith, D. J., . . . Trafford, A. W. (2011). Impaired beta-adrenergic responsiveness accentuates dysfunctional excitation-contraction coupling in an ovine model of tachypacing-induced heart failure. *J Physiol, 589*(Pt 6), 1367-1382. doi:10.1113/jphysiol.2010.203984

Bryant, D., Becker, L., Richardson, J., Shelton, J., Franco, F., Peshock, R., . . . Giroir, B. (1998). Cardiac failure in transgenic mice with myocardial expression of tumor necrosis factor-alpha. *Circulation, 97*(14), 1375-1381.

Buraei, Z., & Yang, J. (2010). The ss subunit of voltage-gated Ca2+ channels. *Physiol Rev, 90*(4), 1461-1506. doi:10.1152/physrev.00057.2009

Burton, J. O., Jefferies, H. J., Selby, N. M., & McIntyre, C. W. (2009). Hemodialysis-induced repetitive myocardial injury results in global and segmental reduction in systolic cardiac function. *Clin J Am Soc Nephrol, 4*(12), 1925-1931. doi:10.2215/CJN.04470709

Cailleret, M., Amadou, A., Andrieu-Abadie, N., Nawrocki, A., Adamy, C., Ait-Mamar, B., . . . Pecker, F. (2004). N-acetylcysteine prevents the deleterious effect of tumor necrosis factor-(alpha) on calcium transients and contraction in adult rat cardiomyocytes. *Circulation, 109*(3), 406-411. doi:10.1161/01.CIR.0000109499.00587.FF

Caride, A. J., Rega, A. F., & Garrahan, P. J. (1986). The reaction of Mg2+ with the Ca2+-ATPase from human red cell membranes and its modification by Ca2+. *Biochim Biophys Acta, 863*(2), 165-177.

Carswell, E. A., Old, L. J., Kassel, R. L., Green, S., Fiore, N., & Williamson, B. (1975). An endotoxin-induced serum factor that causes necrosis of tumors. *Proc Natl Acad Sci U S A, 72*(9), 3666-3670.

Chaudhry, H., Zhou, J., Zhong, Y., Ali, M. M., McGuire, F., Nagarkatti, P. S., & Nagarkatti, M. (2013). Role of cytokines as a double-edged sword in sepsis. *In Vivo, 27*(6), 669-684.

Chen, D., Assad-Kottner, C., Orrego, C., & Torre-Amione, G. (2008). Cytokines and acute heart failure. *Crit Care Med, 36*(1 Suppl), S9-16. doi:10.1097/01.CCM.0000297160.48694.90

Chen, P. P., Patel, J. R., Rybakova, I. N., Walker, J. W., & Moss, R. L. (2010). Protein kinase A-induced myofilament desensitization to Ca(2+) as a result of phosphorylation of cardiac myosin-binding protein C. *J Gen Physiol, 136*(6), 615-627. doi:10.1085/jgp.201010448

Chen, X., Andresen, B. T., Hill, M., Zhang, J., Booth, F., & Zhang, C. (2008). Role of Reactive Oxygen Species in Tumor Necrosis Factor-alpha Induced Endothelial Dysfunction. *Curr Hypertens Rev, 4*(4), 245-255.

Ching, L. L., Williams, A. J., & Sitsapesan, R. (2000). Evidence for Ca(2+) activation and inactivation sites on the luminal side of the cardiac ryanodine receptor complex. *Circ Res, 87*(3), 201-206.

Chousterman, B. G., Swirski, F. K., & Weber, G. F. (2017). Cytokine storm and sepsis disease pathogenesis. *Semin Immunopathol, 39*(5), 517-528. doi:10.1007/s00281-017-0639-8

Chung, J. H., Biesiadecki, B. J., Ziolo, M. T., Davis, J. P., & Janssen, P. M. (2016). Myofilament Calcium Sensitivity: Role in Regulation of In vivo Cardiac Contraction and Relaxation. *Front Physiol, 7*, 562. doi:10.3389/fphys.2016.00562

Clancy, D. J., Slama, M., Huang, S., Scully, T., McLean, A. S., & Orde, S. R. (2017). Detecting impaired myocardial relaxation in sepsis with a novel tissue Doppler parameter (septal e'/s'). *Crit Care, 21*(1), 175. doi:10.1186/s13054-017-1727-9

Clapham, D. E. (2007). Calcium signaling. *Cell, 131*(6), 1047-1058. doi:10.1016/j.cell.2007.11.028

Clarke, J. D., Caldwell, J. L., Horn, M. A., Bode, E. F., Richards, M. A., Hall, M. C., . . . Trafford, A. W. (2015). Perturbed atrial calcium handling in an ovine model of heart failure: potential roles for reductions in the L-type calcium current. *J Mol Cell Cardiol, 79*, 169-179. doi:10.1016/j.yjmcc.2014.11.017

Cleland, J. G., Daubert, J. C., Erdmann, E., Freemantle, N., Gras, D., Kappenberger, L., . . . Cardiac Resynchronization-Heart Failure Study, I. (2005). The effect of cardiac resynchronization on morbidity and mortality in heart failure. *N Engl J Med, 352*(15), 1539-1549. doi:10.1056/NEJMoa050496

Clowes, G. H., Jr., Vucinic, M., & Weidner, M. G. (1966). Circulatory and metabolic alterations associated with survival or death in peritonitis: clinical analysis of 25 cases. *Ann Surg, 163*(6), 866-885.

Collins, A., Somlyo, A. V., & Hilgemann, D. W. (1992). The giant cardiac membrane patch method: stimulation of outward Na(+)-Ca2+ exchange current by MgATP. *J Physiol, 454*, 27-57.

Combes, A., Frye, C. S., Lemster, B. H., Brooks, S. S., Watkins, S. C., Feldman, A. M., & McTiernan, C. F. (2002). Chronic exposure to interleukin 1beta induces a delayed and reversible alteration in excitation-contraction coupling of cultured cardiomyocytes. *Pflugers Arch, 445*(2), 246-256. doi:10.1007/s00424-002-0921-y

Cooper, P. J., Soeller, C., & Cannell, M. B. (2010). Excitation-contraction coupling in human heart failure examined by action potential clamp in rat cardiac myocytes. *J Mol Cell Cardiol, 49*(6), 911-917. doi:10.1016/j.yjmcc.2010.04.012

Court, O., Kumar, A., Parrillo, J. E., & Kumar, A. (2002). Clinical review: Myocardial depression in sepsis and septic shock. *Crit Care, 6*(6), 500-508.

Cunnion, R. E., Schaer, G. L., Parker, M. M., Natanson, C., & Parrillo, J. E. (1986). The coronary circulation in human septic shock. *Circulation, 73*(4), 637-644.

Dally, S., Bredoux, R., Corvazier, E., Andersen, J. P., Clausen, J. D., Dode, L., . . . Enouf, J. (2006). Ca2+-ATPases in non-failing and failing heart: evidence for a novel cardiac sarco/endoplasmic reticulum Ca2+-ATPase 2 isoform (SERCA2c). *Biochem J, 395*(2), 249-258. doi:10.1042/BJ20051427

Daniels, R., McNamara, G., Nutbeam, T., Fox, S., Sangan, V., Annekin, S., . . . Thakerar, V. (2017). *The sepsis manual* R. Daniels & T. Nutbeam (Eds.),

Daniels, R., Nutbeam, T., McNamara, G., & Galvin, C. (2011). The sepsis six and the severe sepsis resuscitation bundle: a prospective observational cohort study. *Emerg Med J, 28*(6), 507-512. doi:10.1136/emj.2010.095067

Delaloye, J., & Calandra, T. (2014). Invasive candidiasis as a cause of sepsis in the critically ill patient. *Virulence, 5*(1), 161-169. doi:10.4161/viru.26187

des Georges, A., Clarke, O. B., Zalk, R., Yuan, Q., Condon, K. J., Grassucci, R. A., . . . Frank, J. (2016). Structural Basis for Gating and Activation of RyR1. *Cell, 167*(1), 145-157 e117. doi:10.1016/j.cell.2016.08.075

Di Virgilio, F., Steinberg, T. H., & Silverstein, S. C. (1989). Organic-anion transport inhibitors to facilitate measurement of cytosolic free Ca2+ with fura-2. *Methods Cell Biol, 31*, 453-462.

Di Virgilio, F., Steinberg, T. H., Swanson, J. A., & Silverstein, S. C. (1988). Fura-2 secretion and sequestration in macrophages. A blocker of organic anion transport reveals that these processes occur via a membrane transport system for organic anions. *J Immunol, 140*(3), 915-920.

Diaz, M. E., Trafford, A. W., O'Neill, S. C., & Eisner, D. A. (1997). Measurement of sarcoplasmic reticulum Ca2+ content and sarcolemmal Ca2+ fluxes in isolated rat ventricular myocytes during spontaneous Ca2+ release. *J Physiol, 501 (Pt 1)*, 3-16.

Dibb, K. M., Clarke, J. D., Horn, M. A., Richards, M. A., Graham, H. K., Eisner, D. A., & Trafford, A. W. (2009). Characterization of an extensive transverse tubular network in sheep atrial myocytes and its depletion in heart failure. *Circ Heart Fail, 2*(5), 482-489. doi:10.1161/CIRCHEARTFAILURE.109.852228

Dibb, K. M., Rueckschloss, U., Eisner, D. A., Isenberg, G., & Trafford, A. W. (2004). Mechanisms underlying enhanced cardiac excitation contraction coupling observed in the senescent sheep myocardium. *J Mol Cell Cardiol, 37*(6), 1171-1181. doi:10.1016/j.yjmcc.2004.09.005

Dinarello, C. A. (2007). Historical insights into cytokines. *Eur J Immunol, 37 Suppl 1*, S34-45. doi:10.1002/eji.200737772

Dolara, P., Agresti, A., Giotti, A., & Pasquini, G. (1973). Effect of taurine on calcium kinetics of guinea-pig heart. *Eur J Pharmacol, 24*(3), 352-358.

Duncan, D. J., Hopkins, P. M., & Harrison, S. M. (2007). Negative inotropic effects of tumour necrosis factor-alpha and interleukin-1beta are ameliorated by alfentanil in rat ventricular myocytes. *Br J Pharmacol, 150*(6), 720-726. doi:10.1038/sj.bjp.0707147

Duncan, D. J., Yang, Z., Hopkins, P. M., Steele, D. S., & Harrison, S. M. (2010). TNF-alpha and IL-1beta increase Ca2+ leak from the sarcoplasmic reticulum and susceptibility to arrhythmia in rat ventricular myocytes. *Cell Calcium, 47*(4), 378-386. doi:10.1016/j.ceca.2010.02.002

Eck, M. J., & Sprang, S. R. (1989). The structure of tumor necrosis factor-alpha at 2.6 A resolution. Implications for receptor binding. *J Biol Chem, 264*(29), 17595-17605.

Eichacker, P. Q., Parent, C., Kalil, A., Esposito, C., Cui, X., Banks, S. M., . . . Natanson, C. (2002). Risk and the efficacy of antiinflammatory agents: retrospective and confirmatory studies of sepsis. *Am J Respir Crit Care Med, 166*(9), 1197-1205. doi:10.1164/rccm.200204-302OC

Eisner, D. A. (2018). Ups and downs of calcium in the heart. *J Physiol, 596*(1), 19-30. doi:10.1113/JP275130

Eisner, D. A., Choi, H. S., Diaz, M. E., O'Neill, S. C., & Trafford, A. W. (2000). Integrative analysis of calcium cycling in cardiac muscle. *Circ Res, 87*(12), 1087-1094.

Eisner, D. A., George, C. H., Smith, G. L., Trafford, A. W., & Venetucci, L. A. (2010). How does CaMKIIdelta phosphorylation of the cardiac ryanodine receptor contribute to inotropy? *Proc Natl Acad Sci U S A, 107*(31), E123; author reply E124. doi:10.1073/pnas.1008809107

Eisner, D. A., Kashimura, T., O'Neill, S. C., Venetucci, L. A., & Trafford, A. W. (2009). What role does modulation of the ryanodine receptor play in cardiac inotropy and arrhythmogenesis? *J Mol Cell Cardiol, 46*(4), 474-481. doi:10.1016/j.yjmcc.2008.12.005

El-Ani, D., Philipchik, I., Stav, H., Levi, M., Zerbib, J., & Shainberg, A. (2014). Tumor necrosis factor alpha protects heart cultures against hypoxic damage via activation of PKA and phospholamban to prevent calcium overload. *Can J Physiol Pharmacol, 92*(11), 917-925. doi:10.1139/cjpp-2014-0092

El Khoury, N., Mathieu, S., & Fiset, C. (2014). Interleukin-1beta reduces L-type Ca2+ current through protein kinase C activation in mouse heart. *J Biol Chem, 289*(32), 21896-21908. doi:10.1074/jbc.M114.549642

Endoh, M. (2004). Force-frequency relationship in intact mammalian ventricular myocardium: physiological and pathophysiological relevance. *Eur J Pharmacol, 500*(1-3), 73-86. doi:10.1016/j.ejphar.2004.07.013

Enriquez-Sarano, M., Rossi, A., Seward, J. B., Bailey, K. R., & Tajik, A. J. (1997). Determinants of pulmonary hypertension in left ventricular dysfunction. *J Am Coll Cardiol, 29*(1), 153-159.

Evans, H. G., Lewis, M. J., & Shah, A. M. (1993). Interleukin-1 beta modulates myocardial contraction via dexamethasone sensitive production of nitric oxide. *Cardiovasc Res, 27*(8), 1486-1490.

Fabiato, A., & Fabiato, F. (1978). Effects of pH on the myofilaments and the sarcoplasmic reticulum of skinned cells from cardiace and skeletal muscles. *J Physiol, 276*, 233-255.

Farajzadeh Valilou, S., Keshavarz-Fathi, M., Silvestris, N., Argentiero, A., & Rezaei, N. (2018). The role of inflammatory cytokines and tumor associated macrophages (TAMs) in microenvironment of pancreatic cancer. *Cytokine Growth Factor Rev, 39*, 46-61. doi:10.1016/j.cytogfr.2018.01.007

Farman, G. P., Tachampa, K., Mateja, R., Cazorla, O., Lacampagne, A., & de Tombe, P. P. (2008). Blebbistatin: use as inhibitor of muscle contraction. *Pflugers Arch, 455*(6), 995-1005. doi:10.1007/s00424-007-0375-3

Fauconnier, J., Meli, A. C., Thireau, J., Roberge, S., Shan, J., Sassi, Y., . . . Lacampagne, A. (2011). Ryanodine receptor leak mediated by caspase-8 activation leads to left ventricular injury after myocardial ischemia-reperfusion. *Proc Natl Acad Sci U S A, 108*(32), 13258-13263. doi:10.1073/pnas.1100286108

Fearnley, C. J., Roderick, H. L., & Bootman, M. D. (2011). Calcium signaling in cardiac myocytes. *Cold Spring Harb Perspect Biol, 3*(11), a004242. doi:10.1101/cshperspect.a004242

Feher, J. J. (1984). Unidirectional calcium and nucleotide fluxes in sarcoplasmic reticulum. I. Interpretation of flux ratios for different reaction schemes. *Biophys J, 45*(6), 1125-1133. doi:10.1016/S0006-3495(84)84260-5

Feldman, A. M., Combes, A., Wagner, D., Kadakomi, T., Kubota, T., Li, Y. Y., & McTiernan, C. (2000). The role of tumor necrosis factor in the pathophysiology of heart failure. *J Am Coll Cardiol, 35*(3), 537-544.

Fernandez-Sada, E., Torres-Quintanilla, A., Silva-Platas, C., Garcia, N., Willis, B. C., Rodriguez-Rodriguez, C., . . . Garcia-Rivas, G. (2017). Proinflammatory Cytokines Are Soluble Mediators Linked with Ventricular Arrhythmias and Contractile Dysfunction in a Rat Model of Metabolic Syndrome. *Oxid Med Cell Longev, 2017*, 7682569. doi:10.1155/2017/7682569

Fernandez, A., Tamayo, E., Heredia, M., Goncalves, L., Almansa, R., Gomez-Herreras, J. I., . . . Bermejo-Martin, J. F. (2013). IL-8 and mortality prediction in post-surgical septic shock. *APMIS, 121*(5), 463-465. doi:10.1111/apm.12010

Fill, M., & Copello, J. A. (2002). Ryanodine receptor calcium release channels. *Physiol Rev, 82*(4), 893-922. doi:10.1152/physrev.00013.2002

Filomatori, C. V., & Rega, A. F. (2003). On the mechanism of activation of the plasma membrane Ca2+-ATPase by ATP and acidic phospholipids. *J Biol Chem, 278*(25), 22265-22271. doi:10.1074/jbc.M302657200

Finkel, M. S., Oddis, C. V., Jacob, T. D., Watkins, S. C., Hattler, B. G., & Simmons, R. L. (1992). Negative inotropic effects of cytokines on the heart mediated by nitric oxide. *Science, 257*(5068), 387-389.

Fleischmann, C., Scherag, A., Adhikari, N. K., Hartog, C. S., Tsaganos, T., Schlattmann, P., . . . International Forum of Acute Care, T. (2016). Assessment of Global Incidence and Mortality of Hospital-treated Sepsis. Current Estimates and Limitations. *Am J Respir Crit Care Med, 193*(3), 259-272. doi:10.1164/rccm.201504-0781OC

Galley, H. F., Howdle, P. D., Walker, B. E., & Webster, N. R. (1997). The effects of intravenous antioxidants in patients with septic shock. *Free Radic Biol Med, 23*(5), 768-774.

Gattoni, S., Roe, A. T., Frisk, M., Louch, W. E., Niederer, S. A., & Smith, N. P. (2016). The calcium-frequency response in the rat ventricular myocyte: an experimental and modelling study. *J Physiol, 594*(15), 4193-4224. doi:10.1113/JP272011

Goldhaber, J. I., Kim, K. H., Natterson, P. D., Lawrence, T., Yang, P., & Weiss, J. N. (1996). Effects of TNF-alpha on [Ca2+]i and contractility in isolated adult rabbit ventricular myocytes. *Am J Physiol, 271*(4 Pt 2), H1449-1455. doi:10.1152/ajpheart.1996.271.4.H1449

Gomez, A., Wang, R., Unruh, H., Light, R. B., Bose, D., Chau, T., . . . Mink, S. (1990). hemofiltration reverses left ventricular dysfunction during sepsis in dogs. *Anesthesiology, 73*(4), 671-685.

Good, N. E., Winget, G. D., Winter, W., Connolly, T. N., Izawa, S., & Singh, R. M. (1966). Hydrogen ion buffers for biological research. *Biochemistry, 5*(2), 467-477.

Greensmith, D. J. (2014). Ca analysis: an Excel based program for the analysis of intracellular calcium transients including multiple, simultaneous regression analysis. *Comput Methods Programs Biomed, 113*(1), 241-250. doi:10.1016/j.cmpb.2013.09.004

Greensmith, D. J., Eisner, D. A., & Nirmalan, M. (2010). The effects of hydrogen peroxide on intracellular calcium handling and contractility in the rat ventricular myocyte. *Cell Calcium, 48*(6), 341-351. doi:10.1016/j.ceca.2010.10.007

Greensmith, D. J., Galli, G. L., Trafford, A. W., & Eisner, D. A. (2014). Direct measurements of SR free Ca reveal the mechanism underlying the transient effects of RyR potentiation under physiological conditions. *Cardiovasc Res, 103*(4), 554-563. doi:10.1093/cvr/cvu158

Greensmith, D. J., & Nirmalan, M. (2013). The effects of tumor necrosis factor-alpha on systolic and diastolic function in rat ventricular myocytes. *Physiol Rep, 1*(4), e00093. doi:10.1002/phy2.93

Grynkiewicz, G., Poenie, M., & Tsien, R. Y. (1985). A new generation of Ca2+ indicators with greatly improved fluorescence properties. *J Biol Chem, 260*(6), 3440-3450.

Gullestad, L., Ueland, T., Vinge, L. E., Finsen, A., Yndestad, A., & Aukrust, P. (2012). Inflammatory cytokines in heart failure: mediators and markers. *Cardiology, 122*(1), 23-35. doi:10.1159/000338166

Gyorke, S., & Fill, M. (1993). Ryanodine receptor adaptation: control mechanism of Ca(2+)-induced Ca2+ release in heart. *Science, 260*(5109), 807-809.

Haikala, H., Levijoki, J., & Linden, I. B. (1995). Troponin C-mediated calcium sensitization by levosimendan accelerates the proportional development of isometric tension. *J Mol Cell Cardiol, 27*(10), 2155-2165.

Hanft, L. M., Korte, F. S., & McDonald, K. S. (2008). Cardiac function and modulation of sarcomeric function by length. *Cardiovasc Res, 77*(4), 627-636. doi:10.1093/cvr/cvm099

Hansen, S. H., Andersen, M. L., Birkedal, H., Cornett, C., & Wibrand, F. (2006). The important role of taurine in oxidative metabolism. *Adv Exp Med Biol, 583*, 129-135.

Hardaway, R. M., Williams, C. H., & Vasquez, Y. (2001). Disseminated intravascular coagulation in sepsis. *Semin Thromb Hemost, 27*(6), 577-583. doi:10.1055/s-2001-18863

Hare, J. M., & Stamler, J. S. (2005). NO/redox disequilibrium in the failing heart and cardiovascular system. *J Clin Invest, 115*(3), 509-517. doi:10.1172/JCI24459

Hattori, M., Yamazaki, M., Ohashi, W., Tanaka, S., Hattori, K., Todoroki, K., . . . Hattori, Y. (2016). Critical role of endogenous histamine in promoting end-organ tissue injury in sepsis. *Intensive Care Med Exp, 4*(1), 36. doi:10.1186/s40635-016-0109-y

Head, D. L., & Yankeelov, J. A., Jr. (1976). The effect of calcium chloride on the activity and inhibition of bacterial collagenase. *Int J Pept Protein Res, 8*(2), 155-165.

Hilgemann, D. W., Matsuoka, S., Nagel, G. A., & Collins, A. (1992). Steady-state and dynamic properties of cardiac sodium-calcium exchange. Sodium-dependent inactivation. *J Gen Physiol, 100*(6), 905-932.

Ho, H. T., Liu, B., Snyder, J. S., Lou, Q., Brundage, E. A., Velez-Cortes, F., . . . Gyorke, S. (2014). Ryanodine receptor phosphorylation by oxidized CaMKII contributes to the cardiotoxic effects of cardiac glycosides. *Cardiovasc Res, 101*(1), 165-174. doi:10.1093/cvr/cvt233

Hobai, I. A., Edgecomb, J., LaBarge, K., & Colucci, W. S. (2015). Dysregulation of intracellular calcium transporters in animal models of sepsis-induced cardiomyopathy. *Shock, 43*(1), 3-15. doi:10.1097/SHK.0000000000000261

Animals (Scientific Procedures) Act, (1986).

Horn, M. A., Graham, H. K., Richards, M. A., Clarke, J. D., Greensmith, D. J., Briston, S. J., . . . Trafford, A. W. (2012). Age-related divergent remodeling of the cardiac extracellular matrix in heart failure: collagen accumulation in the young and loss in the aged. *J Mol Cell Cardiol, 53*(1), 82-90. doi:10.1016/j.yjmcc.2012.03.011

Hoshino, A., Takenaka, H., Mizukoshi, O., Imanishi, J., Kishida, T., & Tovey, M. G. (1983). Effect of anti-interferon serum of influenza virus infection in mice. *Antiviral Res, 3*(1), 59-65.

Howard, R. J., Stopps, T. P., Moe, G. W., Gotlieb, A., & Armstrong, P. W. (1988). Recovery from heart failure: structural and functional analysis in a canine model. *Can J Physiol Pharmacol, 66*(12), 1505-1512.

Huxley, A. F., & Niedergerke, R. (1954). Structural changes in muscle during contraction; interference microscopy of living muscle fibres. *Nature, 173*(4412), 971-973.

Huxley, H., & Hanson, J. (1954). Changes in the cross-striations of muscle during contraction and stretch and their structural interpretation. *Nature, 173*(4412), 973-976.

Ichinose, F., Buys, E. S., Neilan, T. G., Furutani, E. M., Morgan, J. G., Jassal, D. S., . . . Bloch, K. D. (2007). Cardiomyocyte-specific overexpression of nitric oxide synthase 3 prevents myocardial dysfunction in murine models of septic shock. *Circ Res, 100*(1), 130-139. doi:10.1161/01.RES.0000253888.09574.7a

Idriss, H. T., & Naismith, J. H. (2000). TNF alpha and the TNF receptor superfamily: structure-function relationship(s). *Microsc Res Tech, 50*(3), 184-195. doi:10.1002/1097-0029(20000801)50:3<184::AID-JEMT2>3.0.CO;2-H

Ing, D. J., Zang, J., Dzau, V. J., Webster, K. A., & Bishopric, N. H. (1999). Modulation of cytokine-induced cardiac myocyte apoptosis by nitric oxide, Bak, and Bcl-x. *Circ Res, 84*(1), 21-33.

Jacob, R., Dierberger, B., & Kissling, G. (1992). Functional significance of the Frank-Starling mechanism under physiological and pathophysiological conditions. *Eur Heart J, 13 Suppl E*, 7-14.

Jayasinghe, I., Crossman, D., Soeller, C., & Cannell, M. (2012). Comparison of the organization of T-tubules, sarcoplasmic reticulum and ryanodine receptors in rat and human ventricular myocardium. *Clin Exp Pharmacol Physiol, 39*(5), 469-476. doi:10.1111/j.1440-1681.2011.05578.x

Jerin, A., Pozar-Lukanovic, N., Sojar, V., Stanisavljevic, D., Paver-Erzen, V., & Osredkar, J. (2003). Balance of pro- and anti-inflammatory cytokines in liver surgery. *Clin Chem Lab Med, 41*(7), 899-903. doi:10.1515/CCLM.2003.136

Jha, P., Jacobs, H., Bose, D., Wang, R., Yang, J., Light, R. B., & Mink, S. (1993). Effects of E. coli sepsis and myocardial depressant factor on interval-force relations in dog ventricle. *Am J Physiol, 264*(5 Pt 2), H1402-1410. doi:10.1152/ajpheart.1993.264.5.H1402

Jiang, D., Wang, R., Xiao, B., Kong, H., Hunt, D. J., Choi, P., . . . Chen, S. R. (2005). Enhanced store overload-induced Ca2+ release and channel sensitivity to luminal Ca2+ activation are common defects of RyR2 mutations linked to ventricular tachycardia and sudden death. *Circ Res, 97*(11), 1173-1181. doi:10.1161/01.RES.0000192146.85173.4b

Jones, C., & Griffiths, R. D. (2013). Mental and physical disability after sepsis. *Minerva Anestesiol, 79*(11), 1306-1312.

Ju, Y. K., & Allen, D. G. (1999). How does beta-adrenergic stimulation increase the heart rate? The role of intracellular Ca2+ release in amphibian pacemaker cells. *J Physiol, 516 (Pt 3)*, 793-804.

Kalin, A., Acosta, C., Kurinczuk, J. J., Brocklehurst, P., & Knight, M. (2015). Severe sepsis in women with group B Streptococcus in pregnancy: an exploratory UK national case-control study. *BMJ Open, 5*(10), e007976. doi:10.1136/bmjopen-2015-007976

Kaneko, M., Matsumoto, Y., Hayashi, H., Kobayashi, A., & Yamazaki, N. (1994). Oxygen free radicals and calcium homeostasis in the heart. *Mol Cell Biochem, 139*(1), 91-100.

Kaur, K., Sharma, A. K., Dhingra, S., & Singal, P. K. (2006). Interplay of TNF-alpha and IL-10 in regulating oxidative stress in isolated adult cardiac myocytes. *J Mol Cell Cardiol, 41*(6), 1023-1030. doi:10.1016/j.yjmcc.2006.08.005

Kelly, M. L., Wang, M., Crisostomo, P. R., Abarbanell, A. M., Herrmann, J. L., Weil, B. R., & Meldrum, D. R. (2010). TNF receptor 2, not TNF receptor 1, enhances mesenchymal stem cell-mediated cardiac protection following acute ischemia. *Shock, 33*(6), 602-607. doi:10.1097/SHK.0b013e3181cc0913

Kemp, C. D., & Conte, J. V. (2012). The pathophysiology of heart failure. *Cardiovasc Pathol, 21*(5), 365-371. doi:10.1016/j.carpath.2011.11.007

Kimchi, A., Ellrodt, A. G., Berman, D. S., Riedinger, M. S., Swan, H. J., & Murata, G. H. (1984). Right ventricular performance in septic shock: a combined radionuclide and hemodynamic study. *J Am Coll Cardiol, 4*(5), 945-951.

Kivisto, T., Makiranta, M., Oikarinen, E. L., Karhu, S., Weckstrom, M., & Sellin, L. C. (1995). 2,3-Butanedione monoxime (BDM) increases initial yields and improves long-term survival of isolated cardiac myocytes. *Jpn J Physiol, 45*(1), 203-210.

Klabunde, R. E., & Coston, A. F. (1995). Nitric oxide synthase inhibition does not prevent cardiac depression in endotoxic shock. *Shock, 3*(1), 73-78.

Kranias, E. G., & Hajjar, R. J. (2012). Modulation of cardiac contractility by the phospholamban/SERCA2a regulatome. *Circ Res, 110*(12), 1646-1660. doi:10.1161/CIRCRESAHA.111.259754

Kumar, A., Kumar, A., Paladugu, B., Mensing, J., & Parrillo, J. E. (2007). Transforming growth factor-beta1 blocks in vitro cardiac myocyte depression induced by tumor necrosis factor-alpha, interleukin-1beta, and human septic shock serum. *Crit Care Med, 35*(2), 358-364. doi:10.1097/01.CCM.0000254341.87098.A4

Kumar, A., Thota, V., Dee, L., Olson, J., Uretz, E., & Parrillo, J. E. (1996). Tumor necrosis factor alpha and interleukin 1beta are responsible for in vitro myocardial cell depression induced by human septic shock serum. *J Exp Med, 183*(3), 949-958.

Kumar, M., Govindan, S., Zhang, M., Khairallah, R. J., Martin, J. L., Sadayappan, S., & de Tombe, P. P. (2015). Cardiac Myosin-binding Protein C and Troponin-I Phosphorylation Independently Modulate Myofilament Length-dependent Activation. *J Biol Chem, 290*(49), 29241-29249. doi:10.1074/jbc.M115.686790

Lacinova, L., & Hofmann, F. (2005). Ca2+- and voltage-dependent inactivation of the expressed L-type Ca(v)1.2 calcium channel. *Arch Biochem Biophys, 437*(1), 42-50. doi:10.1016/j.abb.2005.02.025

Lanner, J. T., Georgiou, D. K., Joshi, A. D., & Hamilton, S. L. (2010). Ryanodine receptors: structure, expression, molecular details, and function in calcium release. *Cold Spring Harb Perspect Biol, 2*(11), a003996. doi:10.1101/cshperspect.a003996

Larsson, H. P. (2010). How is the heart rate regulated in the sinoatrial node? Another piece to the puzzle. *J Gen Physiol, 136*(3), 237-241. doi:10.1085/jgp.201010506

Lee, Y. C., Hsiao, C. Y., Hung, M. C., Hung, S. C., Wang, H. P., Huang, Y. J., & Wang, J. T. (2016). Bacteremic Urinary Tract Infection Caused by Multidrug-Resistant Enterobacteriaceae Are Associated With Severe Sepsis at Admission: Implication for Empirical Therapy. *Medicine (Baltimore), 95*(20), e3694. doi:10.1097/MD.0000000000003694

Levitsky, D. O., Benevolensky, D. S., Levchenko, T. S., Smirnov, V. N., & Chazov, E. I. (1981). Calcium-binding rate and capacity of cardiac sarcoplasmic reticulum. *J Mol Cell Cardiol, 13*(9), 785-796.

Levitsky, D. O., Fraysse, B., Leoty, C., Nicoll, D. A., & Philipson, K. D. (1996). Cooperative interaction between Ca2+ binding sites in the hydrophilic loop of the Na(+)-Ca2+ exchanger. *Mol Cell Biochem, 160-161*, 27-32.

Levy, M. M., Fink, M. P., Marshall, J. C., Abraham, E., Angus, D., Cook, D., . . . Sccm/Esicm/Accp/Ats/Sis. (2003). 2001 SCCM/ESICM/ACCP/ATS/SIS International Sepsis Definitions Conference. *Crit Care Med, 31*(4), 1250-1256. doi:10.1097/01.CCM.0000050454.01978.3B

Li, K. L., Methawasin, M., Tanner, B. C. W., Granzier, H. L., Solaro, R. J., & Dong, W. J. (2018). Sarcomere length-dependent effects on Ca(2+)-troponin regulation in myocardium expressing compliant titin. *J Gen Physiol*. doi:10.1085/jgp.201812218

Li, L., Chen, L., Zhang, W., Liao, Y., Chen, J., Shi, Y., & Luo, S. (2017). Serum cytokine profile in patients with breast cancer. *Cytokine, 89*, 173-178. doi:10.1016/j.cyto.2015.12.017

Li, X., Eschun, G., Bose, D., Jacobs, H., Yang, J. J., Light, R. B., & Mink, S. N. (1998). Histamine H3 activation depresses cardiac function in experimental sepsis. *J Appl Physiol (1985), 85*(5), 1693-1701. doi:10.1152/jappl.1998.85.5.1693

Li, Y., Ge, S., Peng, Y., & Chen, X. (2013). Inflammation and cardiac dysfunction during sepsis, muscular dystrophy, and myocarditis. *Burns Trauma, 1*(3), 109-121. doi:10.4103/2321-3868.123072

Liang, S. Y. (2016). Sepsis and Other Infectious Disease Emergencies in the Elderly. *Emerg Med Clin North Am, 34*(3), 501-522. doi:10.1016/j.emc.2016.04.005

Lim, G., Venetucci, L., Eisner, D. A., & Casadei, B. (2008). Does nitric oxide modulate cardiac ryanodine receptor function? Implications for excitation-contraction coupling. *Cardiovasc Res, 77*(2), 256-264. doi:10.1093/cvr/cvm012

Lin, G. L., McGinley, J. P., Drysdale, S. B., & Pollard, A. J. (2018). Epidemiology and Immune Pathogenesis of Viral Sepsis. *Front Immunol, 9*, 2147. doi:10.3389/fimmu.2018.02147

Liu, S. J., Zhou, W., & Kennedy, R. H. (1999). Suppression of beta-adrenergic responsiveness of L-type Ca2+ current by IL-1beta in rat ventricular myocytes. *Am J Physiol, 276*(1), H141-148. doi:10.1152/ajpheart.1999.276.1.H141

Locke, F. S. (1895). Towards the Ideal Artificial Circulating Fluid for the Isolated Frog's Heart: Preliminary Communication. *J Physiol, 18*(4), 332-333.

Lopez-Castejon, G., & Brough, D. (2011). Understanding the mechanism of IL-1beta secretion. *Cytokine Growth Factor Rev, 22*(4), 189-195. doi:10.1016/j.cytogfr.2011.10.001

Lou, Q., Janardhan, A., & Efimov, I. R. (2012). Remodeling of calcium handling in human heart failure. *Adv Exp Med Biol, 740*, 1145-1174. doi:10.1007/978-94-007-2888-2_52

Maass, D. L., White, J., & Horton, J. W. (2002). IL-1beta and IL-6 act synergistically with TNF-alpha to alter cardiac contractile function after burn trauma. *Shock, 18*(4), 360-366.

MacLean, L. D., Mulligan, W. G., McLean, A. P., & Duff, J. H. (1967). Patterns of septic shock in man--a detailed study of 56 patients. *Ann Surg, 166*(4), 543-562.
MacLennan, D. H., Kimura, Y., & Toyofuku, T. (1998). Sites of regulatory interaction between calcium ATPases and phospholamban. *Ann N Y Acad Sci, 853*, 31-42.
Mann, D. L., & Young, J. B. (1994). Basic mechanisms in congestive heart failure. Recognizing the role of proinflammatory cytokines. *Chest, 105*(3), 897-904.
Mannick, J. A., Rodrick, M. L., & Lederer, J. A. (2001). The immunologic response to injury. *J Am Coll Surg, 193*(3), 237-244.
Marik, P. E., Khangoora, V., Rivera, R., Hooper, M. H., & Catravas, J. (2017). Hydrocortisone, Vitamin C, and Thiamine for the Treatment of Severe Sepsis and Septic Shock: A Retrospective Before-After Study. *Chest, 151*(6), 1229-1238. doi:10.1016/j.chest.2016.11.036
Markel, T. A., Crisostomo, P. R., Wang, M., Herrmann, J. L., Abarbanell, A. M., & Meldrum, D. R. (2007). Right ventricular TNF resistance during endotoxemia: the differential effects on ventricular function. *Am J Physiol Regul Integr Comp Physiol, 293*(5), R1893-1897. doi:10.1152/ajpregu.00359.2007
Martin, G. S., Mannino, D. M., & Moss, M. (2006). The effect of age on the development and outcome of adult sepsis. *Crit Care Med, 34*(1), 15-21.
Mattiazzi, A., & Kranias, E. G. (2014). The role of CaMKII regulation of phospholamban activity in heart disease. *Front Pharmacol, 5*, 5. doi:10.3389/fphar.2014.00005
Maurer, M. S., Spevack, D., Burkhoff, D., & Kronzon, I. (2004). Diastolic dysfunction: can it be diagnosed by Doppler echocardiography? *J Am Coll Cardiol, 44*(8), 1543-1549. doi:10.1016/j.jacc.2004.07.034
Maxwell, J. T., Domeier, T. L., & Blatter, L. A. (2013). beta-adrenergic stimulation increases the intra-SR Ca termination threshold for spontaneous Ca waves in cardiac myocytes. *Channels (Austin), 7*(3), 206-210. doi:10.4161/chan.24173
McDonald, T. F., Cavalie, A., Trautwein, W., & Pelzer, D. (1986). Voltage-dependent properties of macroscopic and elementary calcium channel currents in guinea pig ventricular myocytes. *Pflugers Arch, 406*(5), 437-448.
McTiernan, C. F., Lemster, B. H., Frye, C., Brooks, S., Combes, A., & Feldman, A. M. (1997). Interleukin-1 beta inhibits phospholamban gene expression in cultured cardiomyocytes. *Circ Res, 81*(4), 493-503.
Meierhenrich, R., Schutz, W., & Gauss, A. (2008). [Left ventricular diastolic dysfunction. Implications for anesthesia and critical care]. *Anaesthesist, 57*(11), 1053-1068. doi:10.1007/s00101-008-1457-0
Mera, S., Tatulescu, D., Cismaru, C., Bondor, C., Slavcovici, A., Zanc, V., . . . Oltean, M. (2011). Multiplex cytokine profiling in patients with sepsis. *APMIS, 119*(2), 155-163. doi:10.1111/j.1600-0463.2010.02705.x
Milani-Nejad, N., & Janssen, P. M. (2014). Small and large animal models in cardiac contraction research: advantages and disadvantages. *Pharmacol Ther, 141*(3), 235-249. doi:10.1016/j.pharmthera.2013.10.007
Miura, Y., & Kimura, J. (1989). Sodium-calcium exchange current. Dependence on internal Ca and Na and competitive binding of external Na and Ca. *J Gen Physiol, 93*(6), 1129-1145.
Mohseny, A. B., van Velze, V., Steggerda, S. J., Smits-Wintjens, V. E. H. J., Bekker, V., & Lopriore, E. (2018). Late-onset sepsis due to urinary tract infection in very preterm neonates is not uncommon. *European Journal of Pediatrics, 177*(1), 33-38. doi:10.1007/s00431-017-3030-9
Monden, Y., Kubota, T., Inoue, T., Tsutsumi, T., Kawano, S., Ide, T., . . . Sunagawa, K. (2007). Tumor necrosis factor-alpha is toxic via receptor 1 and protective via receptor 2 in a murine model of myocardial infarction. *Am J Physiol Heart Circ Physiol, 293*(1), H743-753. doi:10.1152/ajpheart.00166.2007
Monnerat, G., Alarcon, M. L., Vasconcellos, L. R., Hochman-Mendez, C., Brasil, G., Bassani, R. A., . . . Medei, E. (2016). Macrophage-dependent IL-1beta production induces cardiac arrhythmias in diabetic mice. *Nat Commun, 7*, 13344. doi:10.1038/ncomms13344

Moss, R. L., Razumova, M., & Fitzsimons, D. P. (2004). Myosin crossbridge activation of cardiac thin filaments: implications for myocardial function in health and disease. *Circ Res, 94*(10), 1290-1300. doi:10.1161/01.RES.0000127125.61647.4F

Mullens, W., Bartunek, J., Tang, W. H., Delrue, L., Herbots, L., Willems, R., . . . Vanderheyden, M. (2008). Early and late effects of cardiac resynchronization therapy on force-frequency relation and contractility regulating gene expression in heart failure patients. *Heart Rhythm, 5*(1), 52-59. doi:10.1016/j.hrthm.2007.09.009

Muller-Werdan, U., Engelmann, H., & Werdan, K. (1998). Cardiodepression by tumor necrosis factor-alpha. *Eur Cytokine Netw, 9*(4), 689-691.

Naik, E., & Dixit, V. M. (2011). Mitochondrial reactive oxygen species drive proinflammatory cytokine production. *J Exp Med, 208*(3), 417-420. doi:10.1084/jem.20110367

Neco, P., Rose, B., Huynh, N., Zhang, R., Bridge, J. H., Philipson, K. D., & Goldhaber, J. I. (2010). Sodium-calcium exchange is essential for effective triggering of calcium release in mouse heart. *Biophys J, 99*(3), 755-764. doi:10.1016/j.bpj.2010.04.071

Neri, M., Riezzo, I., Pomara, C., Schiavone, S., & Turillazzi, E. (2016). Oxidative-Nitrosative Stress and Myocardial Dysfunctions in Sepsis: Evidence from the Literature and Postmortem Observations. *Mediators Inflamm, 2016*, 3423450. doi:10.1155/2016/3423450

Neumann, F. J., Ott, I., Gawaz, M., Richardt, G., Holzapfel, H., Jochum, M., & Schomig, A. (1995). Cardiac release of cytokines and inflammatory responses in acute myocardial infarction. *Circulation, 92*(4), 748-755.

Ngoc, P. L., Gold, D. R., Tzianabos, A. O., Weiss, S. T., & Celedon, J. C. (2005). Cytokines, allergy, and asthma. *Curr Opin Allergy Clin Immunol, 5*(2), 161-166.

Nguyen, T., Cao, L. B., Tran, M., & Movahed, A. (2013). Biventricular pulsus alternans: An echocardiographic finding in patient with pulmonary embolism. *World J Clin Cases, 1*(5), 162-165. doi:10.12998/wjcc.v1.i5.162

Nijst, P., Martens, P., & Mullens, W. (2017). Heart Failure with Myocardial Recovery - The Patient Whose Heart Failure Has Improved: What Next? *Prog Cardiovasc Dis, 60*(2), 226-236. doi:10.1016/j.pcad.2017.05.009

Nishio, M., Ruch, S. W., Kelly, J. E., Aistrup, G. L., Sheehan, K., & Wasserstrom, J. A. (2004). Ouabain increases sarcoplasmic reticulum calcium release in cardiac myocytes. *J Pharmacol Exp Ther, 308*(3), 1181-1190. doi:10.1124/jpet.103.060004

Noland, T. A., Jr., Guo, X., Raynor, R. L., Jideama, N. M., Averyhart-Fullard, V., Solaro, R. J., & Kuo, J. F. (1995). Cardiac troponin I mutants. Phosphorylation by protein kinases C and A and regulation of Ca(2+)-stimulated MgATPase of reconstituted actomyosin S-1. *J Biol Chem, 270*(43), 25445-25454.

Nowycky, M. C., Fox, A. P., & Tsien, R. W. (1985). Three types of neuronal calcium channel with different calcium agonist sensitivity. *Nature, 316*(6027), 440-443.

Oddis, C. V., Simmons, R. L., Hattler, B. G., & Finkel, M. S. (1996). Protein kinase A activation is required for IL-1-induced nitric oxide production by cardiac myocytes. *Am J Physiol, 271*(1 Pt 1), C429-434. doi:10.1152/ajpcell.1996.271.1.C429

Odeh, M. (1993). Tumor necrosis factor-alpha as a myocardial depressant substance. *Int J Cardiol, 42*(3), 231-238.

Ognibene, F. P., Parker, M. M., Natanson, C., Shelhamer, J. H., & Parrillo, J. E. (1988). Depressed left ventricular performance. Response to volume infusion in patients with sepsis and septic shock. *Chest, 93*(5), 903-910.

Okabe, E., Tsujimoto, Y., & Kobayashi, Y. (2000). Calmodulin and cyclic ADP-ribose interaction in Ca2+ signaling related to cardiac sarcoplasmic reticulum: superoxide anion radical-triggered Ca2+ release. *Antioxid Redox Signal, 2*(1), 47-54. doi:10.1089/ars.2000.2.1-47

Opal, S. M., Garber, G. E., LaRosa, S. P., Maki, D. G., Freebairn, R. C., Kinasewitz, G. T., . . . Bernard, G. R. (2003). Systemic host responses in severe sepsis analyzed by causative microorganism and treatment effects of drotrecogin alfa (activated). *Clin Infect Dis, 37*(1), 50-58. doi:10.1086/375593

Oppenheim, J. J., Matsushima, K., Yoshimura, T., Leonard, E. J., & Neta, R. (1989). Relationship between interleukin 1 (IL1), tumor necrosis factor (TNF) and a neutrophil attracting peptide (NAP-1). *Agents Actions, 26*(1-2), 134-140.

Orchard, C. H., & Kentish, J. C. (1990). Effects of changes of pH on the contractile function of cardiac muscle. *Am J Physiol, 258*(6 Pt 1), C967-981. doi:10.1152/ajpcell.1990.258.6.C967
Ozaki, K., & Leonard, W. J. (2002). Cytokine and cytokine receptor pleiotropy and redundancy. *J Biol Chem, 277*(33), 29355-29358. doi:10.1074/jbc.R200003200
Paiva, C. N., & Bozza, M. T. (2014). Are reactive oxygen species always detrimental to pathogens? *Antioxid Redox Signal, 20*(6), 1000-1037. doi:10.1089/ars.2013.5447
Parker, M. M., Shelhamer, J. H., Bacharach, S. L., Green, M. V., Natanson, C., Frederick, T. M., . . . Parrillo, J. E. (1984). Profound but reversible myocardial depression in patients with septic shock. *Ann Intern Med, 100*(4), 483-490.
Parker, M. M., Suffredini, A. F., Natanson, C., Ognibene, F. P., Shelhamer, J. H., & Parrillo, J. E. (1989). Responses of Left-Ventricular Function in Survivors and Nonsurvivors of Septic Shock. *Journal of Critical Care, 4*(1), 19-25. doi:Doi 10.1016/0883-9441(89)90087-7
Parrillo, J. E. (1989). The cardiovascular pathophysiology of sepsis. *Annu Rev Med, 40*, 469-485. doi:10.1146/annurev.me.40.020189.002345
Parrillo, J. E., Burch, C., Shelhamer, J. H., Parker, M. M., Natanson, C., & Schuette, W. (1985). A circulating myocardial depressant substance in humans with septic shock. Septic shock patients with a reduced ejection fraction have a circulating factor that depresses in vitro myocardial cell performance. *J Clin Invest, 76*(4), 1539-1553. doi:10.1172/JCI112135
Parrillo, J. E., Parker, M. M., Natanson, C., Suffredini, A. F., Danner, R. L., Cunnion, R. E., & Ognibene, F. P. (1990). Septic shock in humans. Advances in the understanding of pathogenesis, cardiovascular dysfunction, and therapy. *Ann Intern Med, 113*(3), 227-242.
Parris, J. R., Cobban, H. J., Littlejohn, A. F., MacEwan, D. J., & Nixon, G. F. (1999). Tumour necrosis factor-alpha activates a calcium sensitization pathway in guinea-pig bronchial smooth muscle. *J Physiol, 518 (Pt 2)*, 561-569.
Pelzmann, B., Schaffer, P., Bernhart, E., Lang, P., Machler, H., Rigler, B., & Koidl, B. (1998). L-type calcium current in human ventricular myocytes at a physiological temperature from children with tetralogy of Fallot. *Cardiovasc Res, 38*(2), 424-432.
Peng, W., Shen, H., Wu, J., Guo, W., Pan, X., Wang, R., . . . Yan, N. (2016). Structural basis for the gating mechanism of the type 2 ryanodine receptor RyR2. *Science, 354*(6310). doi:10.1126/science.aah5324
Peterson, B. Z., DeMaria, C. D., Adelman, J. P., & Yue, D. T. (1999). Calmodulin is the Ca2+ sensor for Ca2+ -dependent inactivation of L-type calcium channels. *Neuron, 22*(3), 549-558.
Petros, A., Lamb, G., Leone, A., Moncada, S., Bennett, D., & Vallance, P. (1994). Effects of a nitric oxide synthase inhibitor in humans with septic shock. *Cardiovasc Res, 28*(1), 34-39.
Philipson, K. D., Bersohn, M. M., & Nishimoto, A. Y. (1982). Effects of pH on Na+-Ca2+ exchange in canine cardiac sarcolemmal vesicles. *Circ Res, 50*(2), 287-293.
Phillips, R. M., Narayan, P., Gomez, A. M., Dilly, K., Jones, L. R., Lederer, W. J., & Altschuld, R. A. (1998). Sarcoplasmic reticulum in heart failure: central player or bystander? *Cardiovasc Res, 37*(2), 346-351.
Piacentino, V., 3rd, Weber, C. R., Chen, X., Weisser-Thomas, J., Margulies, K. B., Bers, D. M., & Houser, S. R. (2003). Cellular basis of abnormal calcium transients of failing human ventricular myocytes. *Circ Res, 92*(6), 651-658. doi:10.1161/01.RES.0000062469.83985.9B
Picht, E., Zima, A. V., Shannon, T. R., Duncan, A. M., Blatter, L. A., & Bers, D. M. (2011). Dynamic calcium movement inside cardiac sarcoplasmic reticulum during release. *Circ Res, 108*(7), 847-856. doi:10.1161/CIRCRESAHA.111.240234
Pierrakos, C., Attou, R., Decorte, L., Kolyviras, A., Malinverni, S., Gottignies, P., . . . De Bels, D. (2014). Transcranial Doppler to assess sepsis-associated encephalopathy in critically ill patients. *BMC Anesthesiol, 14*, 45. doi:10.1186/1471-2253-14-45
Potz, B. A., Sellke, F. W., & Abid, M. R. (2016). Endothelial ROS and Impaired Myocardial Oxygen Consumption in Sepsis-induced Cardiac Dysfunction. *J Intensive Crit Care, 2*(1).
Qiu, P., Cui, X., Sun, J., Welsh, J., Natanson, C., & Eichacker, P. Q. (2013). Antitumor necrosis factor therapy is associated with improved survival in clinical sepsis trials: a meta-analysis. *Crit Care Med, 41*(10), 2419-2429. doi:10.1097/CCM.0b013e3182982add

Qiu, Y., Liao, R., & Zhang, X. (2009). Impedance-based monitoring of ongoing cardiomyocyte death induced by tumor necrosis factor-alpha. *Biophys J, 96*(5), 1985-1991. doi:10.1016/j.bpj.2008.11.036

Radin, M. J., Holycross, B. J., Dumitrescu, C., Kelley, R., & Altschuld, R. A. (2008). Leptin modulates the negative inotropic effect of interleukin-1beta in cardiac myocytes. *Mol Cell Biochem, 315*(1-2), 179-184. doi:10.1007/s11010-008-9805-6

Ramirez, R. J., Sah, R., Liu, J., Rose, R. A., & Backx, P. H. (2011). Intracellular [Na(+)] modulates synergy between Na(+)/Ca (2+) exchanger and L-type Ca (2+) current in cardiac excitation-contraction coupling during action potentials. *Basic Res Cardiol, 106*(6), 967-977. doi:10.1007/s00395-011-0202-z

Raper, R. F., & Fisher, M. M. (1988). Profound reversible myocardial depression after anaphylaxis. *Lancet, 1*(8582), 386-388.

Reddy, L. G., Jones, L. R., Pace, R. C., & Stokes, D. L. (1996). Purified, reconstituted cardiac Ca2+-ATPase is regulated by phospholamban but not by direct phosphorylation with Ca2+/calmodulin-dependent protein kinase. *J Biol Chem, 271*(25), 14964-14970.

Reid, M. B., Lannergren, J., & Westerblad, H. (2002). Respiratory and limb muscle weakness induced by tumor necrosis factor-alpha: involvement of muscle myofilaments. *Am J Respir Crit Care Med, 166*(4), 479-484. doi:10.1164/rccm.2202005

Reyes-Garcia, J., Flores-Soto, E., Solis-Chagoyan, H., Sommer, B., Diaz-Hernandez, V., Garcia-Hernandez, L. M., & Montano, L. M. (2016). Tumor Necrosis Factor Alpha Inhibits L-Type Ca(2+) Channels in Sensitized Guinea Pig Airway Smooth Muscle through ERK 1/2 Pathway. *Mediators Inflamm, 2016*, 5972302. doi:10.1155/2016/5972302

Ringer, S. (1883). A third contribution regarding the Influence of the Inorganic Constituents of the Blood on the Ventricular Contraction. *J Physiol, 4*(2-3), 222-225.

Rohr, S. (2004). Role of gap junctions in the propagation of the cardiac action potential. *Cardiovasc Res, 62*(2), 309-322. doi:10.1016/j.cardiores.2003.11.035

Rousseau, E., Smith, J. S., Henderson, J. S., & Meissner, G. (1986). Single channel and 45Ca2+ flux measurements of the cardiac sarcoplasmic reticulum calcium channel. *Biophys J, 50*(5), 1009-1014. doi:10.1016/S0006-3495(86)83543-3

Rozanski, G. J., & Witt, R. C. (1994). IL-1 inhibits beta-adrenergic control of cardiac calcium current: role of L-arginine/nitric oxide pathway. *Am J Physiol, 267*(5 Pt 2), H1753-1758. doi:10.1152/ajpheart.1994.267.5.H1753

Santana, L. F., Cheng, E. P., & Lederer, W. J. (2010). How does the shape of the cardiac action potential control calcium signaling and contraction in the heart? *J Mol Cell Cardiol, 49*(6), 901-903. doi:10.1016/j.yjmcc.2010.09.005

Sasaguri, K., Yamaguchi, K., Nakazono, T., Mizuguchi, M., & Irie, H. (2016). Sepsis patients' renal manifestation on contrast-enhanced CT. *Clin Radiol, 71*(6), 617 e611-617. doi:10.1016/j.crad.2016.02.018

Sawai, N., Kita, M., Kodama, T., Tanahashi, T., Yamaoka, Y., Tagawa, Y., . . . Imanishi, J. (1999). Role of gamma interferon in Helicobacter pylori-induced gastric inflammatory responses in a mouse model. *Infect Immun, 67*(1), 279-285.

Scheinert, R. B., Asokan, A., Rani, A., Kumar, A., Foster, T. C., & Ormerod, B. K. (2015). Some hormone, cytokine and chemokine levels that change across lifespan vary by cognitive status in male Fischer 344 rats. *Brain Behav Immun, 49*, 216-232. doi:10.1016/j.bbi.2015.06.005

Schillinger, W., Fiolet, J. W., Schlotthauer, K., & Hasenfuss, G. (2003). Relevance of Na+-Ca2+ exchange in heart failure. *Cardiovasc Res, 57*(4), 921-933.

Schramm, P., Klein, K. U., Falkenberg, L., Berres, M., Closhen, D., Werhahn, K. J., . . . Engelhard, K. (2012). Impaired cerebrovascular autoregulation in patients with severe sepsis and sepsis-associated delirium. *Crit Care, 16*(5), R181. doi:10.1186/cc11665

Schreur, K. D., & Liu, S. (1997). Involvement of ceramide in inhibitory effect of IL-1 beta on L-type Ca2+ current in adult rat ventricular myocytes. *Am J Physiol, 272*(6 Pt 2), H2591-2598. doi:10.1152/ajpheart.1997.272.6.H2591

Schulz, R., Nava, E., & Moncada, S. (1992). Induction and potential biological relevance of a Ca(2+)-independent nitric oxide synthase in the myocardium. *Br J Pharmacol, 105*(3), 575-580.
Schulz, R., Panas, D. L., Catena, R., Moncada, S., Olley, P. M., & Lopaschuk, G. D. (1995). The role of nitric oxide in cardiac depression induced by interleukin-1 beta and tumour necrosis factor-alpha. *Br J Pharmacol, 114*(1), 27-34.
Schwartz, A., Gurman, G., Cohen, G., Gilutz, H., Brill, S., Schily, M., . . . Shoenfeld, Y. (2002). Association between hypophosphatemia and cardiac arrhythmias in the early stages of sepsis. *Eur J Intern Med, 13*(7), 434.
Seo, S. H., & Webster, R. G. (2002). Tumor necrosis factor alpha exerts powerful anti-influenza virus effects in lung epithelial cells. *J Virol, 76*(3), 1071-1076.
Shahreyar, M., Fahhoum, R., Akinseye, O., Bhandari, S., Dang, G., & Khouzam, R. N. (2018). Severe sepsis and cardiac arrhythmias. *Ann Transl Med, 6*(1), 6. doi:10.21037/atm.2017.12.26
Shane, A. L., Sanchez, P. J., & Stoll, B. J. (2017). Neonatal sepsis. *Lancet, 390*(10104), 1770-1780. doi:10.1016/S0140-6736(17)31002-4
Shannon, T. R., Pogwizd, S. M., & Bers, D. M. (2003). Elevated sarcoplasmic reticulum Ca2+ leak in intact ventricular myocytes from rabbits in heart failure. *Circ Res, 93*(7), 592-594. doi:10.1161/01.RES.0000093399.11734.B3
Shaw, R. M., & Colecraft, H. M. (2013). L-type calcium channel targeting and local signalling in cardiac myocytes. *Cardiovasc Res, 98*(2), 177-186. doi:10.1093/cvr/cvt021
Sheka, A. C., Tevis, S., & Kennedy, G. D. (2016). Urinary tract infection after surgery for colorectal malignancy: risk factors and complications. *Am J Surg, 211*(1), 31-39. doi:10.1016/j.amjsurg.2015.06.006
Sheu, C. C., Gong, M. N., Zhai, R., Chen, F., Bajwa, E. K., Clardy, P. F., . . . Christiani, D. C. (2010). Clinical characteristics and outcomes of sepsis-related vs non-sepsis-related ARDS. *Chest, 138*(3), 559-567. doi:10.1378/chest.09-2933
Shigekawa, M., Finegan, J. A., & Katz, A. M. (1976). Calcium transport ATPase of canine cardiac sarcoplasmic reticulum. A comparison with that of rabbit fast skeletal muscle sarcoplasmic reticulum. *J Biol Chem, 251*(22), 6894-6900.
Shinagawa, Y., Satoh, H., & Noma, A. (2000). The sustained inward current and inward rectifier K+ current in pacemaker cells dissociated from rat sinoatrial node. *J Physiol, 523 Pt 3*, 593-605.
Sibbald, W. J., Paterson, N. A., Holliday, R. L., Anderson, R. A., Lobb, T. R., & Duff, J. H. (1978). Pulmonary hypertension in sepsis: measurement by the pulmonary arterial diastolic-pulmonary wedge pressure gradient and the influence of passive and active factors. *Chest, 73*(5), 583-591.
Sigalas, C., Bent, S., Kitmitto, A., O'Neill, S., & Sitsapesan, R. (2009). Ca(2+)-calmodulin can activate and inactivate cardiac ryanodine receptors. *Br J Pharmacol, 156*(5), 794-806. doi:10.1111/j.1476-5381.2008.00092.x
Singer, M., Deutschman, C. S., Seymour, C. W., Shankar-Hari, M., Annane, D., Bauer, M., . . . Angus, D. C. (2016). The Third International Consensus Definitions for Sepsis and Septic Shock (Sepsis-3). *JAMA, 315*(8), 801-810. doi:10.1001/jama.2016.0287
Sips, P. Y., Irie, T., Zou, L., Shinozaki, S., Sakai, M., Shimizu, N., . . . Ichinose, F. (2013). Reduction of cardiomyocyte S-nitrosylation by S-nitrosoglutathione reductase protects against sepsis-induced myocardial depression. *Am J Physiol Heart Circ Physiol, 304*(8), H1134-1146. doi:10.1152/ajpheart.00887.2012
Skayian, Y., & Kreydiyyeh, S. I. (2006). Tumor necrosis factor alpha alters Na+-K+ ATPase activity in rat cardiac myocytes: involvement of NF-kappaB, AP-1 and PGE2. *Life Sci, 80*(2), 173-180. doi:10.1016/j.lfs.2006.08.037
Smith, G. L., Duncan, A. M., Neary, P., Bruce, L., & Burton, F. L. (2000). P(i) inhibits the SR Ca(2+) pump and stimulates pump-mediated Ca(2+) leak in rabbit cardiac myocytes. *Am J Physiol Heart Circ Physiol, 279*(2), H577-585. doi:10.1152/ajpheart.2000.279.2.H577
Smith, G. L., & Eisner, D. A. (2019). Calcium Buffering in the Heart in Health and Disease. *Circulation, 139*(20), 2358-2371. doi:10.1161/CIRCULATIONAHA.118.039329

Solaro, R. J., Moir, A. J., & Perry, S. V. (1976). Phosphorylation of troponin I and the inotropic effect of adrenaline in the perfused rabbit heart. *Nature, 262*(5569), 615-617.
Spudich, J. A. (2001). The myosin swinging cross-bridge model. *Nat Rev Mol Cell Biol, 2*(5), 387-392. doi:10.1038/35073086
Stamm, C., Cowan, D. B., Friehs, I., Noria, S., del Nido, P. J., & McGowan, F. X., Jr. (2001). Rapid endotoxin-induced alterations in myocardial calcium handling: obligatory role of cardiac TNF-alpha. *Anesthesiology, 95*(6), 1396-1405.
Stokke, M. K., Briston, S. J., Jolle, G. F., Manzoor, I., Louch, W. E., Oyehaug, L., . . . Sjaastad, I. (2011). Ca(2+) wave probability is determined by the balance between SERCA2-dependent Ca(2+) reuptake and threshold SR Ca(2+) content. *Cardiovasc Res, 90*(3), 503-512. doi:10.1093/cvr/cvr013
Stoll, B. J., Hansen, N., Fanaroff, A. A., Wright, L. L., Carlo, W. A., Ehrenkranz, R. A., . . . Poole, W. K. (2002). Late-onset sepsis in very low birth weight neonates: the experience of the NICHD Neonatal Research Network. *Pediatrics, 110*(2 Pt 1), 285-291.
Subramaniam, S., Stansberg, C., & Cunningham, C. (2004). The interleukin 1 receptor family. *Dev Comp Immunol, 28*(5), 415-428. doi:10.1016/j.dci.2003.09.016
Suelter, C. H., & DeLuca, M. (1983). How to prevent losses of protein by adsorption to glass and plastic. *Anal Biochem, 135*(1), 112-119.
Sugishita, K., Kinugawa, K., Shimizu, T., Harada, K., Matsui, H., Takahashi, T., . . . Kohmoto, O. (1999). Cellular basis for the acute inhibitory effects of IL-6 and TNF- alpha on excitation-contraction coupling. *J Mol Cell Cardiol, 31*(8), 1457-1467. doi:10.1006/jmcc.1999.0989
Suleiman, M. S., Rodrigo, G. C., & Chapman, R. A. (1992). Interdependence of intracellular taurine and sodium in guinea pig heart. *Cardiovasc Res, 26*(9), 897-905.
Takahashi, A., Camacho, P., Lechleiter, J. D., & Herman, B. (1999). Measurement of intracellular calcium. *Physiol Rev, 79*(4), 1089-1125. doi:10.1152/physrev.1999.79.4.1089
Takenaka, H., Adler, P. N., & Katz, A. M. (1982). Calcium fluxes across the membrane of sarcoplasmic reticulum vesicles. *J Biol Chem, 257*(21), 12649-12656.
Tatsumi, T., Matoba, S., Kawahara, A., Keira, N., Shiraishi, J., Akashi, K., . . . Nakagawa, M. (2000). Cytokine-induced nitric oxide production inhibits mitochondrial energy production and impairs contractile function in rat cardiac myocytes. *J Am Coll Cardiol, 35*(5), 1338-1346.
Tavernier, B., Garrigue, D., Boulle, C., Vallet, B., & Adnet, P. (1998). Myofilament calcium sensitivity is decreased in skinned cardiac fibres of endotoxin-treated rabbits. *Cardiovasc Res, 38*(2), 472-479.
Tavernier, B., Mebazaa, A., Mateo, P., Sys, S., Ventura-Clapier, R., & Veksler, V. (2001). Phosphorylation-dependent alteration in myofilament ca2+ sensitivity but normal mitochondrial function in septic heart. *Am J Respir Crit Care Med, 163*(2), 362-367. doi:10.1164/ajrccm.163.2.2002128
Teparrukkul, P., Hantrakun, V., Day, N. P. J., West, T. E., & Limmathurotsakul, D. (2017). Management and outcomes of severe dengue patients presenting with sepsis in a tropical country. *PLoS One, 12*(4), e0176233. doi:10.1371/journal.pone.0176233
Testa, M., Yeh, M., Lee, P., Fanelli, R., Loperfido, F., Berman, J. W., & LeJemtel, T. H. (1996). Circulating levels of cytokines and their endogenous modulators in patients with mild to severe congestive heart failure due to coronary artery disease or hypertension. *J Am Coll Cardiol, 28*(4), 964-971.
Thakur, A., Xue, M., Stapleton, F., Lloyd, A. R., Wakefield, D., & Willcox, M. D. (2002). Balance of pro- and anti-inflammatory cytokines correlates with outcome of acute experimental Pseudomonas aeruginosa keratitis. *Infect Immun, 70*(4), 2187-2197.
Thomas, M. J., Sjaastad, I., Andersen, K., Helm, P. J., Wasserstrom, J. A., Sejersted, O. M., & Ottersen, O. P. (2003). Localization and function of the Na+/Ca2+-exchanger in normal and detubulated rat cardiomyocytes. *J Mol Cell Cardiol, 35*(11), 1325-1337.
Thum, T., & Borlak, J. (2001). Butanedione monoxime increases the viability and yield of adult cardiomyocytes in primary cultures. *Cardiovasc Toxicol, 1*(1), 61-72.
Toller, W. G., & Stranz, C. (2006). Levosimendan, a new inotropic and vasodilator agent. *Anesthesiology, 104*(3), 556-569.

Torre-Amione, G., Kapadia, S., Benedict, C., Oral, H., Young, J. B., & Mann, D. L. (1996). Proinflammatory cytokine levels in patients with depressed left ventricular ejection fraction: a report from the Studies of Left Ventricular Dysfunction (SOLVD). *J Am Coll Cardiol, 27*(5), 1201-1206. doi:10.1016/0735-1097(95)00589-7

Trafford, A. W., Diaz, M. E., & Eisner, D. A. (1999). A novel, rapid and reversible method to measure Ca buffering and time-course of total sarcoplasmic reticulum Ca content in cardiac ventricular myocytes. *Pflugers Arch, 437*(3), 501-503. doi:10.1007/s004240050808

Trafford, A. W., Diaz, M. E., O'Neill, S. C., & Eisner, D. A. (2002). Integrative analysis of calcium signalling in cardiac muscle. *Front Biosci, 7*, d843-852.

Trafford, A. W., Diaz, M. E., Sibbring, G. C., & Eisner, D. A. (2000). Modulation of CICR has no maintained effect on systolic Ca2+: simultaneous measurements of sarcoplasmic reticulum and sarcolemmal Ca2+ fluxes in rat ventricular myocytes. *J Physiol, 522 Pt 2*, 259-270.

Treinys, R., & Jurevicius, J. (2008). L-type Ca2+ channels in the heart: structure and regulation. *Medicina (Kaunas), 44*(7), 491-499.

Tsao, C. M., Ho, S. T., & Wu, C. C. (2015). Coagulation abnormalities in sepsis. *Acta Anaesthesiol Taiwan, 53*(1), 16-22. doi:10.1016/j.aat.2014.11.002

Tschope, C., Kherad, B., Klein, O., Lipp, A., Blaschke, F., Gutterman, D., . . . Van Linthout, S. (2019). Cardiac contractility modulation: mechanisms of action in heart failure with reduced ejection fraction and beyond. *Eur J Heart Fail, 21*(1), 14-22. doi:10.1002/ejhf.1349

Tsujino, M., Hirata, Y., Imai, T., Kanno, K., Eguchi, S., Ito, H., & Marumo, F. (1994). Induction of nitric oxide synthase gene by interleukin-1 beta in cultured rat cardiocytes. *Circulation, 90*(1), 375-383.

Tunwell, R. E., Wickenden, C., Bertrand, B. M., Shevchenko, V. I., Walsh, M. B., Allen, P. D., & Lai, F. A. (1996). The human cardiac muscle ryanodine receptor-calcium release channel: identification, primary structure and topological analysis. *Biochem J, 318 (Pt 2)*, 477-487.

Vaccines against influenza WHO position paper - November 2012. (2012). *Wkly Epidemiol Rec, 87*(47), 461-476.

Valdivia, H. H., Kaplan, J. H., Ellis-Davies, G. C., & Lederer, W. J. (1995). Rapid adaptation of cardiac ryanodine receptors: modulation by Mg2+ and phosphorylation. *Science, 267*(5206), 1997-2000.

van der Velden, J. (2011). Diastolic myofilament dysfunction in the failing human heart. *Pflugers Arch, 462*(1), 155-163. doi:10.1007/s00424-011-0960-3

van Dillen, J., Zwart, J., Schutte, J., & van Roosmalen, J. (2010). Maternal sepsis: epidemiology, etiology and outcome. *Curr Opin Infect Dis, 23*(3), 249-254. doi:10.1097/QCO.0b013e328339257c

van Heerebeek, L., Borbely, A., Niessen, H. W., Bronzwaer, J. G., van der Velden, J., Stienen, G. J., . . . Paulus, W. J. (2006). Myocardial structure and function differ in systolic and diastolic heart failure. *Circulation, 113*(16), 1966-1973. doi:10.1161/CIRCULATIONAHA.105.587519

van Weerd, J. H., & Christoffels, V. M. (2016). The formation and function of the cardiac conduction system. *Development, 143*(2), 197-210. doi:10.1242/dev.124883

Varian, K. D., & Janssen, P. M. (2007). Frequency-dependent acceleration of relaxation involves decreased myofilament calcium sensitivity. *Am J Physiol Heart Circ Physiol, 292*(5), H2212-2219. doi:10.1152/ajpheart.00778.2006

Varro, A., Negretti, N., Hester, S. B., & Eisner, D. A. (1993). An estimate of the calcium content of the sarcoplasmic reticulum in rat ventricular myocytes. *Pflugers Arch, 423*(1-2), 158-160.

Vendome, J., Posy, S., Jin, X., Bahna, F., Ahlsen, G., Shapiro, L., & Honig, B. (2011). Molecular design principles underlying beta-strand swapping in the adhesive dimerization of cadherins. *Nat Struct Mol Biol, 18*(6), 693-700. doi:10.1038/nsmb.2051

Venetucci, L. A., Trafford, A. W., Diaz, M. E., O'Neill, S. C., & Eisner, D. A. (2006). Reducing ryanodine receptor open probability as a means to abolish spontaneous Ca2+ release and increase Ca2+ transient amplitude in adult ventricular myocytes. *Circ Res, 98*(10), 1299-1305. doi:10.1161/01.RES.0000222000.35500.65

Venetucci, L. A., Trafford, A. W., & Eisner, D. A. (2007). Increasing ryanodine receptor open probability alone does not produce arrhythmogenic calcium waves: threshold sarcoplasmic reticulum calcium content is required. *Circ Res, 100*(1), 105-111. doi:10.1161/01.RES.0000252828.17939.00

Venkataraman, R., Baldo, M. P., Hwang, H. S., Veltri, T., Pinto, J. R., Baudenbacher, F. J., & Knollmann, B. C. (2013). Myofilament calcium de-sensitization and contractile uncoupling prevent pause-triggered ventricular tachycardia in mouse hearts with chronic myocardial infarction. *J Mol Cell Cardiol, 60*, 8-15. doi:10.1016/j.yjmcc.2013.03.022

Vincent, J. L., Bakker, J., Marecaux, G., Schandene, L., Kahn, R. J., & Dupont, E. (1992). Administration of anti-TNF antibody improves left ventricular function in septic shock patients. Results of a pilot study. *Chest, 101*(3), 810-815.

Vugia, D. J., Kiehlbauch, J. A., Yeboue, K., N'Gbichi, J. M., Lacina, D., Maran, M., . . . et al. (1993). Pathogens and predictors of fatal septicemia associated with human immunodeficiency virus infection in Ivory Coast, west Africa. *J Infect Dis, 168*(3), 564-570.

Wagner, S., Ruff, H. M., Weber, S. L., Bellmann, S., Sowa, T., Schulte, T., . . . Maier, L. S. (2011). Reactive oxygen species-activated Ca/calmodulin kinase IIdelta is required for late I(Na) augmentation leading to cellular Na and Ca overload. *Circ Res, 108*(5), 555-565. doi:10.1161/CIRCRESAHA.110.221911

Walpoth, B. N., & Erman, B. (2015). Regulation of ryanodine receptor RyR2 by protein-protein interactions: prediction of a PKA binding site on the N-terminal domain of RyR2 and its relation to disease causing mutations. *F1000Res, 4*, 29. doi:10.12688/f1000research.5858.1

Wang, W., Falk, S. A., Jittikanont, S., Gengaro, P. E., Edelstein, C. L., & Schrier, R. W. (2002). Protective effect of renal denervation on normotensive endotoxemia-induced acute renal failure in mice. *Am J Physiol Renal Physiol, 283*(3), F583-587. doi:10.1152/ajprenal.00270.2001

Warrick, H. M., & Spudich, J. A. (1987). Myosin structure and function in cell motility. *Annu Rev Cell Biol, 3*, 379-421. doi:10.1146/annurev.cb.03.110187.002115

Wheeler, A. P., & Bernard, G. R. (2007). Acute lung injury and the acute respiratory distress syndrome: a clinical review. *Lancet, 369*(9572), 1553-1564. doi:10.1016/S0140-6736(07)60604-7

Wimsatt, D. K., Hohl, C. M., Brierley, G. P., & Altschuld, R. A. (1990). Calcium accumulation and release by the sarcoplasmic reticulum of digitonin-lysed adult mammalian ventricular cardiomyocytes. *J Biol Chem, 265*(25), 14849-14857.

Wisloff, U., Loennechen, J. P., Falck, G., Beisvag, V., Currie, S., Smith, G., & Ellingsen, O. (2001). Increased contractility and calcium sensitivity in cardiac myocytes isolated from endurance trained rats. *Cardiovasc Res, 50*(3), 495-508.

Wu, L. L., Tang, C., & Liu, M. S. (2001). Altered phosphorylation and calcium sensitivity of cardiac myofibrillar proteins during sepsis. *Am J Physiol Regul Integr Comp Physiol, 281*(2), R408-416. doi:10.1152/ajpregu.2001.281.2.R408

Xu, L., Eu, J. P., Meissner, G., & Stamler, J. S. (1998). Activation of the cardiac calcium release channel (ryanodine receptor) by poly-S-nitrosylation. *Science, 279*(5348), 234-237.

Yang, D., Elner, S. G., Bian, Z. M., Till, G. O., Petty, H. R., & Elner, V. M. (2007). Pro-inflammatory cytokines increase reactive oxygen species through mitochondria and NADPH oxidase in cultured RPE cells. *Exp Eye Res, 85*(4), 462-472. doi:10.1016/j.exer.2007.06.013

Yang, Y., Guo, T., Oda, T., Chakraborty, A., Chen, L., Uchinoumi, H., . . . Bers, D. M. (2014). Cardiac myocyte Z-line calmodulin is mainly RyR2-bound, and reduction is arrhythmogenic and occurs in heart failure. *Circ Res, 114*(2), 295-306. doi:10.1161/CIRCRESAHA.114.302857

Yates, J. C., & Dhalla, N. S. (1975). Structural and functional changes associated with failure and recovery of hearts after perfusion with Ca2+-free medium. *J Mol Cell Cardiol, 7*(2), 91-103.

Yokoyama, T., Vaca, L., Rossen, R. D., Durante, W., Hazarika, P., & Mann, D. L. (1993). Cellular basis for the negative inotropic effects of tumor necrosis factor-alpha in the adult mammalian heart. *J Clin Invest, 92*(5), 2303-2312. doi:10.1172/JCI116834

Yoshida, A., Takahashi, M., Imagawa, T., Shigekawa, M., Takisawa, H., & Nakamura, T. (1992). Phosphorylation of ryanodine receptors in rat myocytes during beta-adrenergic stimulation. *J Biochem, 111*(2), 186-190.
Zahradnikova, A., & Zahradnik, I. (2012). Construction of calcium release sites in cardiac myocytes. *Front Physiol, 3*, 322. doi:10.3389/fphys.2012.00322
Zahradnikova, A., Zahradnik, I., Gyorke, I., & Gyorke, S. (1999). Rapid activation of the cardiac ryanodine receptor by submillisecond calcium stimuli. *J Gen Physiol, 114*(6), 787-798.
Zhang, G. J., & Adachi, I. (1999). Serum interleukin-6 levels correlate to tumor progression and prognosis in metastatic breast carcinoma. *Anticancer Res, 19*(2B), 1427-1432.
Zheng, S. X., Vrindts, Y., Lopez, M., De Groote, D., Zangerle, P. F., Collette, J., . . . Reginster, J. Y. (1997). Increase in cytokine production (IL-1 beta, IL-6, TNF-alpha but not IFN-gamma, GM-CSF or LIF) by stimulated whole blood cells in postmenopausal osteoporosis. *Maturitas, 26*(1), 63-71.
Zhong, J., Adams, H. R., & Rubin, L. J. (1997). Cytosolic Ca2+ concentration and contraction-relaxation properties of ventricular myocytes from Escherichia coli endotoxemic guinea pigs: effect of fluid resuscitation. *Shock, 7*(5), 383-388.
Zhou, P., Zhao, Y. T., Guo, Y. B., Xu, S. M., Bai, S. H., Lakatta, E. G., . . . Wang, S. Q. (2009). Beta-adrenergic signaling accelerates and synchronizes cardiac ryanodine receptor response to a single L-type Ca2+ channel. *Proc Natl Acad Sci U S A, 106*(42), 18028-18033. doi:10.1073/pnas.0906560106
Zhu, W., Varga, Z., & Silva, J. R. (2016). Molecular motions that shape the cardiac action potential: Insights from voltage clamp fluorometry. *Prog Biophys Mol Biol, 120*(1-3), 3-17. doi:10.1016/j.pbiomolbio.2015.12.003
Zhu, X., Bernecker, O. Y., Manohar, N. S., Hajjar, R. J., Hellman, J., Ichinose, F., . . . Schmidt, U. (2005). Increased leakage of sarcoplasmic reticulum Ca2+ contributes to abnormal myocyte Ca2+ handling and shortening in sepsis. *Crit Care Med, 33*(3), 598-604.
Zilberberg, M. D., Nathanson, B. H., Sulham, K., Fan, W., & Shorr, A. F. (2017). Carbapenem resistance, inappropriate empiric treatment and outcomes among patients hospitalized with Enterobacteriaceae urinary tract infection, pneumonia and sepsis. *BMC Infect Dis, 17*(1), 279. doi:10.1186/s12879-017-2383-z
Zima, A. V., & Blatter, L. A. (2006). Redox regulation of cardiac calcium channels and transporters. *Cardiovasc Res, 71*(2), 310-321. doi:10.1016/j.cardiores.2006.02.019
Zimmermann, N., Boknik, P., Gams, E., Gsell, S., Jones, L. R., Maas, R., . . . Scholz, H. (1996). Mechanisms of the contractile effects of 2,3-butanedione-monoxime in the mammalian heart. *Naunyn Schmiedebergs Arch Pharmacol, 354*(4), 431-436.
Zissimopoulos, S., & Lai, F. A. (2006). Redox regulation of the ryanodine receptor/calcium release channel. *Biochem Soc Trans, 34*(Pt 5), 919-921. doi:10.1042/BST0340919
Zuo, S., Li, L. L., Ruan, Y. F., Jiang, L., Li, X., Li, S. N., . . . Ma, C. S. (2018). Acute administration of tumour necrosis factor-alpha induces spontaneous calcium release via the reactive oxygen species pathway in atrial myocytes. *Europace, 20*(8), 1367-1374. doi:10.1093/europace/eux271